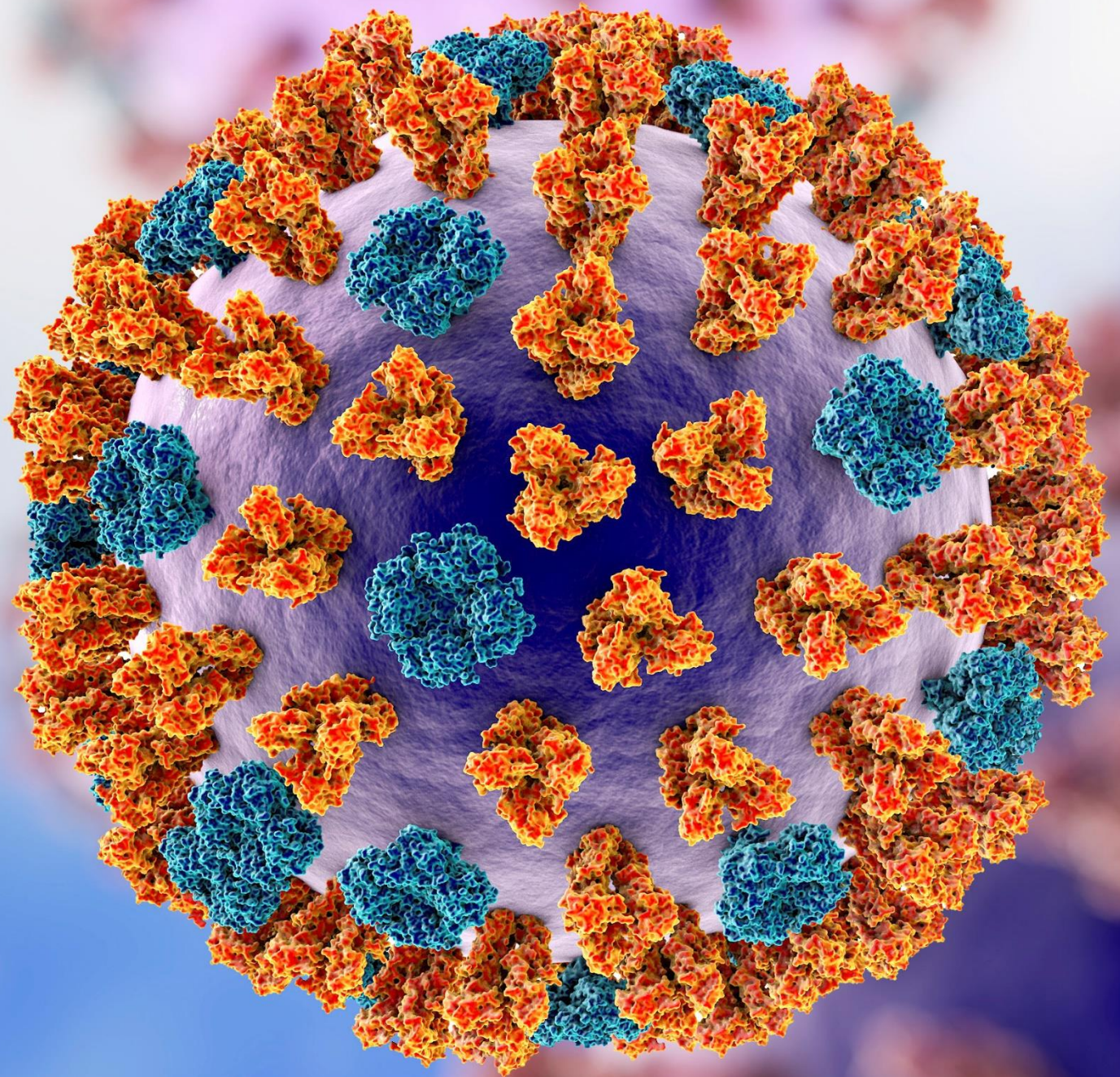


# Functional Crosstalk between Influenza A Virus Hemagglutinin and Neuraminidase



*Wenjuan Du*

**Functional crosstalk between influenza A virus  
hemagglutinin and neuraminidase**

**Wenjuan Du**

Cover art: 123RF.COM

Layout and design: Wenjuan Du

Print: <https://proefschrift-aio.nl/>

Printing of this thesis was sponsored by the department of  
“Biomolecular Health Sciences”, Utrecht.

Copyright: Wenjuan Du, 2020. All rights reserved.

# **Functional crosstalk between influenza A virus hemagglutinin and neuraminidase**

Functionele samenspraak tussen influenza A virus hemagglutinine  
en neuraminidase

(met een samenvatting in het Nederlands)

## **Proefschrift**

ter verkrijging van de graad van doctor aan de Universiteit Utrecht op gezag van de  
rector magnificus, prof.dr.H.R.B.M. Kummeling, ingevolge het besluit van het college  
voor promoties in het openbaar te verdedigen op  
donderdag 22 oktober 2020 des middags te 12.45 uur

door

**Wenjuan Du**

geboren op 10 september 1988 te Shandong, China

**Promotor:**

Prof. dr. F.J.M. van Kuppeveld

**Copromotoren:**

Dr. C.A.M. de Haan

Dr. E. de Vries

Wenjuan Du was financially supported by China Scholarship Council (CSC).

# Contents

## Introduction

Chapter 1	General introduction	<b>1</b>
-----------	----------------------	----------

## Experimental work

Chapter 2	Substrate binding by the second sialic acid-binding site of influenza A virus N1 neuraminidase contributes to enzymatic activity	<b>33</b>
Chapter 3	The 2 <sup>nd</sup> sialic acid-binding site of influenza A virus neuraminidase is an important determinant of the hemagglutinin-neuraminidase-receptor balance	<b>63</b>
Chapter 4	Mutation of the second sialic acid-binding site of influenza A virus neuraminidase drives compensatory mutations in hemagglutinin	<b>103</b>
Chapter 5	Analysis of pandemic influenza A(H1N1) virus neuraminidase evolution reveals entanglement of different phenotypes	<b>135</b>

## Discussion

Interlude	Tuning influenza A virus HA-NA balance to the receptor repertoire	<b>169</b>
Chapter 6	Influenza A virus hemagglutinin–neuraminidase–receptor balance: preserving virus motility	<b>173</b>
Chapter 7	Second sialic acid-binding site of influenza A virus neuraminidase: binding receptors for efficient release	<b>195</b>

## Summaries

Summary in English		
Nederlandse samenvatting		

## Miscellaneous

Acknowledgements		
Curriculum Vitae		
List of publications		





# **Chapter 1**

## **General Introduction**

Influenza A viruses (IAVs) are animal viruses with high zoonotic potential that infect a wide range of hosts, including humans, wild birds, poultry, pigs, horses, dogs and marine mammals (1). They cause a huge economic burden and major public health problems (2). In humans, IAVs cause seasonal epidemics and occasional pandemics (3). The pandemics resulted from animal influenza viruses that crossed the species barrier and acquired the capacity to transmit between humans (4).

IAV represents a paradigm for an emerging virus. A large and antigenically diverse reservoir of IAVs exists in wild aquatic birds, in which the infection is normally asymptomatic (5, 6). The virus appears to be fully adapted to these reservoir species. Avian influenza viruses circulating in aquatic birds provide all genetic diversity needed for the emergence of pandemic and/or epidemic viruses in humans as well as other mammalian species, including domestic animals. For instance, avian IAVs can be transmitted to domestic birds, like chickens and ducks, thereby causing severe disease and huge economic losses. Avian IAVs can also be transmitted to pigs, which may act as a “mixing vessel” by supporting reassortment of genes from different IAVs, which may result in an antigenic shift (7). Both pigs and domestic birds can further spread influenza viruses to humans, occasionally causing pandemics.

IAVs are members of the family *Orthomyxoviridae*, a group of enveloped viruses carrying a segmented negative-sense single-stranded RNA genome (8). Influenza viruses are classified into four distinct genera (A, B, C and D) based on antigenic differences in their nucleoprotein and matrix protein. Members of the three main genera (A, B, C) infect humans and influenza D virus has been found to infect cattle, goats and pigs (9). IAVs are classified further according to genetic and antigenic properties of the major surface glycoproteins hemagglutinin (HA) and neuraminidase (NA). To date, 18 HA and 11 NA subtypes have been identified (7). All subtypes were found in aquatic birds except for the H17N10 and H18N11, which only were detected in bats (10-12). Influenza viruses are named according to the following procedure: genus (e.g., A, B, C, D)/host origin (except for viruses isolated from humans)/geographical location of isolation/strain number/year of virus collection, followed by virus subtype between brackets, for example influenza A/Hongkong/1/1968 (H3N2).

In little more than the last 100 years, several pandemics were recorded: the 1918 H1N1 Spanish pandemic, the 1957 H2N2 Asian pandemic, the 1968 H3N2 Hong Kong pandemic, the 1977 H1N1 Russian pandemic, and the 2009 H1N1 pandemic (H1N1pdm09). The 1918 pandemic, which is the worst in recorded history, killed up to 50 million people worldwide (13). As no IAVs isolated before 1918 are currently available, the origin of this pandemic, including timing of its appearance in humans and the involvement of potential intermediate hosts, remains unanswered (14). The 1957 H2N2 virus caused approximately 2 million deaths globally (15). This virus resulted from the reassortment of

human H1N1 and avian H2N2 IAVs viruses and replaced the H1N1 virus (16). Like the pandemic virus that preceded it, the 1968 H3N2 virus was generated by a reassortment event, this time between the circulating human H2N2 virus and an avian H3 IAV (17). This pandemic was mild in its mortality impact due to the retention of previously circulating N2 NA (18). The H3N2 virus quickly became endemic and replaced the previous H2N2 virus. It has now been circulating globally for 52 years. The 1977 H1N1 pandemic virus was a descendent of the 1918 H1N1 virus that had been absent from circulation for 20 years (15). Remarkably, the virus that reappeared more resembled the H1N1 virus from 1950 than that from 1957 when H1N1 disappeared (19). As it is unlikely that this virus was maintained in the field for more than 20 years without accumulation of mutations, the 1977 pandemic possibly was the result of a laboratory accident (20). In general, the disease caused by this pandemic was mild and almost entirely restricted to persons <25 years old due to the absence of H1N1 virus infection in humans after 1957. H1N1pdm09 which caused the first IAV pandemic of the 21<sup>st</sup> century was derived from two unrelated swine H1N1 viruses, one of them a “classical” swine derivative of the 1918 human virus and the other belonging to the European avian-like H1N1 lineage (21). The H1N1pdm09 replaced the pre-2009 H1N1 seasonal virus.

Viruses from various other influenza subtypes (H5, H7, H9) have sporadically infected humans but these have not become established in humans (22-26). The H5N1 avian influenza virus that was detected in Hongkong in 1997 has frequently been reported to infect humans and to cause serious disease. Since 1997, H5N1 strains continued to circulate in China. Since 2003, H5N1 viruses have spread to different parts of Asia, Africa, and Europe causing epizootics (27). As of January 2020, a total of 861 human cases has been confirmed with H5N1 virus infection, among which 455 died (28). The H5N1 virus has, however, not yet acquired the ability to efficiently transmit from humans to humans. In 2013, three cases of human infection with a previously undescribed H7N9 virus were reported in China (29). These were followed by five epidemic waves of human H7N9 infections, which resulted in more than one thousand deaths (30, 31). Most of these cases occurred due to the direct or indirect contact with infected poultry. In March 1999, two cases of human infection with H9N2 in Hong Kong were reported (26, 32). H9N2 viruses are currently widespread in poultry and obtained mutations in HA that increased binding to human type receptors (33, 34). Human infections with H9N2 viruses have been infrequently reported (35, 36), but epidemiological studies suggest that they may occur more frequently than currently recognized (37).

### **I) IAV genome and virion**

Influenza viruses contain a negative-sense RNA genome consisting of eight segments in influenza A and B viruses and seven segments in influenza C and D viruses (Fig 1A). Each segment encodes one or two major viral proteins. In all species, each viral RNA (vRNA) genome segment forms viral

ribonucleoprotein (vRNP) complexes in which the 5' and 3' termini of the vRNA are associated with a RNA-dependent RNA polymerase (RdRP), while the rest of the vRNA binds to oligomers of the nucleoprotein (NP) encoded by RNA segment 5, forming a double-helical rod-like structure (38). Influenza RdRP is a heterotrimer consisting of the proteins polymerase basic 1 (PB1), PB2, and polymerase acidic (PA) (P3 in influenza C and D viruses), which are encoded by the three largest RNA genome segments (Fig. 1A) (39-41). The RdRP is responsible for replication and transcription of vRNA genomes. RNA segments 4 and 6 encode viral surface glycoproteins haemagglutinin (HA), which is responsible for binding to sialic-acid (SIA) containing-receptors, and neuraminidase (NA), which functions as a receptor-destroying enzyme facilitating virion release from decoy receptors and the cell surface as well as preventing virion aggregation RNA segments 7 and 8 encode two proteins. Segment 7 encodes nonstructural protein NS1 and nuclear export protein (NEP; also known as NS2) while segment 8 encodes matrix protein (M1) and membrane protein (M2). NS1 protein is a virulence factor that antagonizes the host innate immune response in infected cells (42, 43). The M1 protein forms a scaffold underneath the membranous envelope of the influenza virion. The M2 protein forms a tetrameric ion channel that, together with HA and NA glycoproteins, is anchored in the virion envelope.

Influenza viruses display enveloped, pleiomorphic virions with diverse morphologies, ranging from spherical to filamentous (Fig 1B). While laboratory-adapted strains of influenza virus are usually spherical with 100 to 120 nm diameters, clinical isolates displays varied morphologies (44). They can be spheres with 100-120 nm diameters, slightly filamentous with diameters of ~90 nm and lengths of 120-200 nm or extended filaments with lengths ranging to over 30 000 nm (45). Remarkably, when clinical isolates are passaged in chicken eggs or cell culture, the filamentous phenotype are lost. The role of filaments in IAV infection is understudied and remains poorly understood (44, 46).

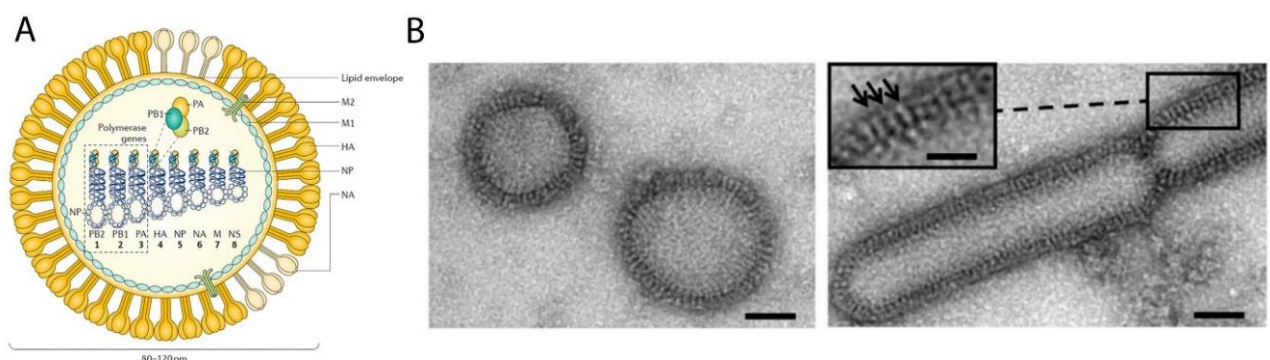


**Fig 1. IAV particle.** (A) Schematic picture of an IAV particle. The viral envelope contains two surface glycoproteins, HA and NA, which are encoded by gene segments 4 and 6, respectively. IAV particle contains 8 gene segments. Each gene segment encodes one or two major proteins. All the genomic RNA

segments are bound with NPs that are encoded by segment 5 to form vRNPs. Each vRNP is bound by a single polymerase complex comprised by PB1, PB2 and PA, which are encoded by the three largest genome segments. RNA segments 7 and 8 encode more than one protein, being M1 and M2 or NS1 and NEP (also known as NS2). The M1 protein underlies the viral envelope while the M2 protein, an ion channel, is embedded within the viral envelope. The figure was taken from (2). (B) Electron micrograph of negatively-stained IAV particles. A/Victoria/3/75 (H3N2) viruses display spherical (left) and filamentous (right) morphologies. Scale bars, 50 nm. Individual glycoproteins on the virion surface are indicated with arrows in the inset on the right (scale bar, 25 nm). The figure was taken from (198).

## II) IAV life cycle

**Attachment and entry:** Virus infection is initiated by the attachment of virus through HA binding to SIA-containing glycans on the cell surface (Fig 2). Upon virus binding, the virus is internalized via different receptor-mediated endocytosis pathways including macropinocytosis and clathrin-mediated endocytosis (47, 48). The lower pH within the endosome triggers an irreversible conformational change in HA, resulting in the insertion of a hydrophobic fusion peptide of HA into the endosomal membrane and subsequent fusion of the viral envelope with the endosomal membrane (49, 50). The influx of proton and potassium ions through the ion channel M2 acidifies the virion interior and causes the dissociation of M1 from vRNP, releasing the vRNPs into cytoplasm upon fusion (51, 52).

**Genome replication and transcription:** The vRNPs are subsequently transported into the nucleus of infected cells where they are transcribed through the enzymatic activities of the viral polymerase complex associated to the vRNPs (Fig 2). Transcription is a primer-dependent process that involves the production of 5' capped and 3' polyadenylated mRNA molecules using the vRNA segments as templates (39, 41). Unlike the RNA polymerase from the non-segmented negative-sense RNA viruses, influenza virus RNA polymerase is not able to synthesize and methylate cap structures. So influenza virus acquires capped oligomers from the 5' end of nascent host mRNAs by a process known as cap-snatching (53). The resulting capped RNA fragments are then used as primers to initiate synthesis of viral mRNAs, after which the viral mRNAs are exported into the cytoplasm for translation into viral proteins. The translation of the viral mRNAs occurs either at cytosolic ribosomes (for PB1, PB2, PA, NP, NS1, NS2, and M1) or endoplasmic reticulum (ER)-associated ribosomes (for the membrane proteins HA, NA, and M2) (54). In contrast to viral transcription, replication is independent of primers and occurs through a complementary RNA (cRNA) replicative intermediate and requires newly synthesized polymerase complex as well as the presence of NP (55, 56).

**Assembly and budding:** During vRNA replication, vRNPs are produced by binding of vRNAs to NP and polymerase complex (Fig 2). With the support of NS2 and M1, which are imported into the nucleus

after their synthesis, the vRNPs are exported into the cytoplasm (57, 58). It is proposed that the M1 may function as an adaptor protein linking NS2 to vRNPs. Upon arrival in the cytoplasm, the vRNPs are transported toward the plasma membrane for viral assembly by the association with Rab11-positive recycling endosomes (59). Rab11 binds to the viral polymerase PB2 subunit, potentially playing a role in a quality control mechanism that makes sure that new virions incorporate vRNPs carrying a polymerase. HA, NA, and M2 are co-translationally inserted into the ER membrane, after which they are modified by enzymes from both ER and Golgi. The mature membrane proteins HA, NA, and M2 are then transported to the apical plasma membrane. vRNPs bound with M1 bud from the plasma membrane where HA, NA, and M2 are located (60). NA facilitates newly assembled virion release by removing SIAs on the cell surface, thereby preventing newly assembled virions from sticking at the cell surface as well as preventing virion aggregation (61, 62).

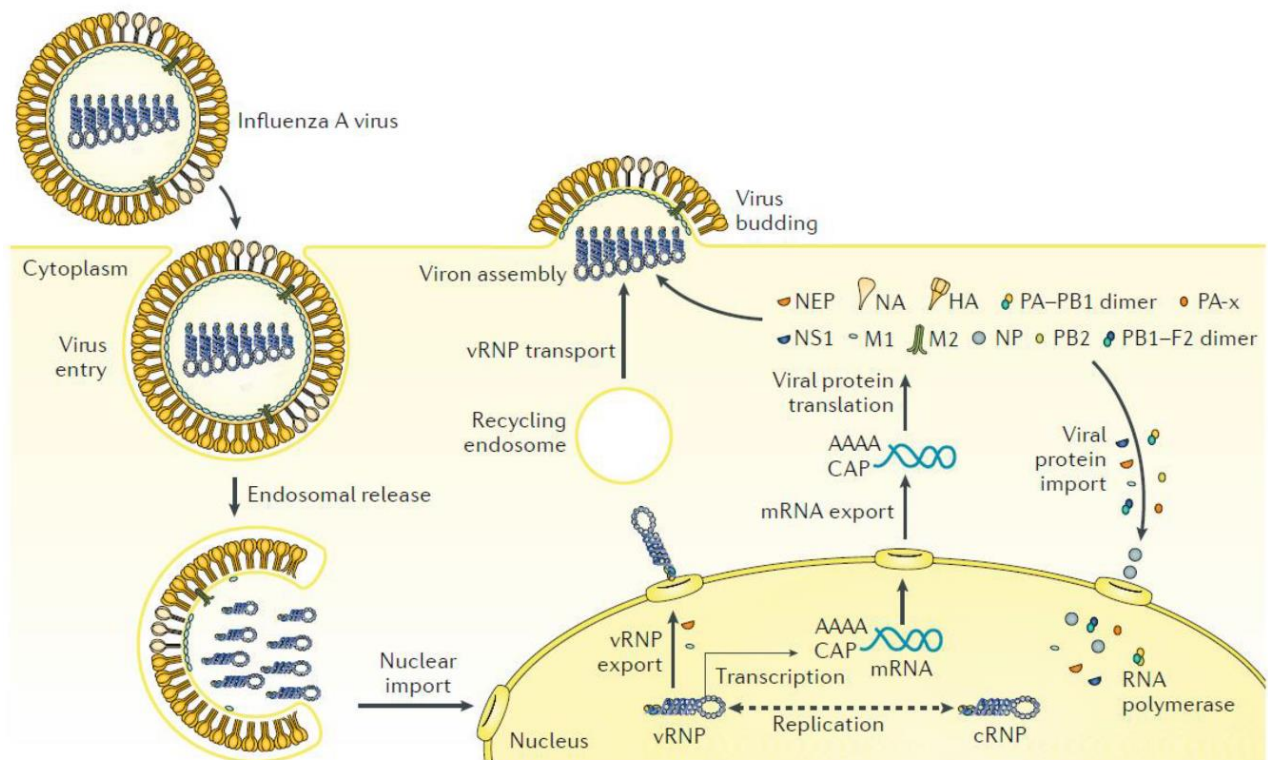


**Fig 2. IAV life cycle.** IAV infection starts with the attachment of HA to SIA receptors on the cell surface. The virus is internalized via receptor-mediated endocytosis. Low pH-triggered conformational changes in HA causes fusion of viral and endosomal membranes, resulting in the release of vRNPs into the cytoplasm. Subsequently, viral genomes are transported to the nucleus of the host cell for transcription of mRNA and replication through a positive-sense complementary RNP (cRNP) intermediate. Viral mRNAs are exported to the cytoplasm for translation into viral proteins. The structural proteins are assembled into new virions together with the newly synthesized vRNPs at the cell membrane. The newly generated progeny virus is released by budding. The figure was taken from (2).

### III) HA glycoprotein

HA is the most abundant protein on the surface of the virion, and functions as the receptor binding and virus-cell fusion protein. HA subtypes are divided into two groups based on sequence comparisons and structural characteristics. Group 1 includes subtypes H1, H2, H5, H6, H8, H9, H11, H12, H13, H16, H17, and H18, and Group 2 is composed of subtypes H3, H4, H14, H7, H15 and H10 (12). The first crystal structure of the ectodomain of HA was determined in 1983 (63). These and other studies showed HA exists as a membrane-anchored homotrimer (Fig. 3A), and that the HA trimer protrudes approximately 135 Å from the membrane. Each protomer can be divided into two domains: the membrane-distal globular head domain (HA1), which contains the receptor binding site (RBS), and the membrane-proximal stem domain (HA2). The RBS forms a shallow pocket. The 130 loop (residues 133-138), the 190 helix (residues 190-198) and the 220 loop (residues 220-229) form the edges of RBS whereas four highly conserved residues form the base (Tyr98, Trp153, His183 and Tyr195; H3 numbering) (Fig 3A) (64).

HA is translated as an fusion incompetent precursor, termed HA0 (65). To achieve fusion competence, HA0 must be cleaved into HA1 and HA2 subunits, which remain linked by disulfide bonds (66, 67). Cleavage occurs at monobasic or multibasic cleavage sites. Multibasic sites are commonly found in chicken-adapted IAVs (of H5 and H7 subtype), which are referred as highly pathogenic viruses. Multibasic cleavage sites are cleaved by furin (68). Furin is ubiquitously expressed (69), which may explain why avian IAVs with multibasic cleavage sites are generally more pathogenic. By contrast, HAs of human or low pathogenic avian IAVs usually carry a monobasic cleavage site, which has been proposed to be processed by different proteases present in the human or avian respiratory and enteric tract (70, 71). HA2 carries the hydrophobic fusion peptide at its N-terminus, which -following cleavage- inserts firmly into a pocket near the axis of the trimer (72). Exposure to low pH in endosomes causes conformational transitions of HA2, leading to insertion of the fusion peptide in the endosomal membrane and the fusion of viral and cell membranes (67, 73). The pH threshold for HA2 conformational changes differs for avian and human viruses (74-77), with human viruses generally displaying a lower activation pH threshold.

Influenza virus infection requires binding of HA to cell surface-exposed SIAs on the host cell surface. The linkage of the terminal SIA to the penultimate galactose occurs at carbon 3 or 6, generating  $\alpha$ 2,3- and  $\alpha$ 2,6-linked SIA isomers, respectively (Fig 3B) (78). Avian influenza virus prefers binding to  $\alpha$ 2,3-linked SIAs that are dominant in the avian gut while human influenza virus prefers binding to  $\alpha$ 2,6-linked SIAs that are dominant in the human upper respiratory tract (79, 80). The explanation for the

distinct binding specificity between avian and human viruses has been achieved from the crystal structures of the HA-receptor complex. The RBS of the avian HA optimally accommodates the  $\alpha$ 2,3-linked SIA, which adopts a thin and straight trans conformation whereas the RBS of human HA is wider resulting in the accommodation of the more bulky cis conformation adopted by  $\alpha$ 2,6-linked SIAs (81, 82). Just a few well-characterized amino acid substitutions in the HA RBS of avian viruses are sufficient to change the receptor binding specificity, for instance, E190D/G225D for H1 HA, and Q226L/G228S for H3 and H5 HAs (83). Of note, more recently it has become apparent that the apparent absolute dichotomy in the binding preference of human and avian IAVs is a gross oversimplification of HA specificity and that the HA binding properties of human (and also avian) isolates can differ considerably (84-88).

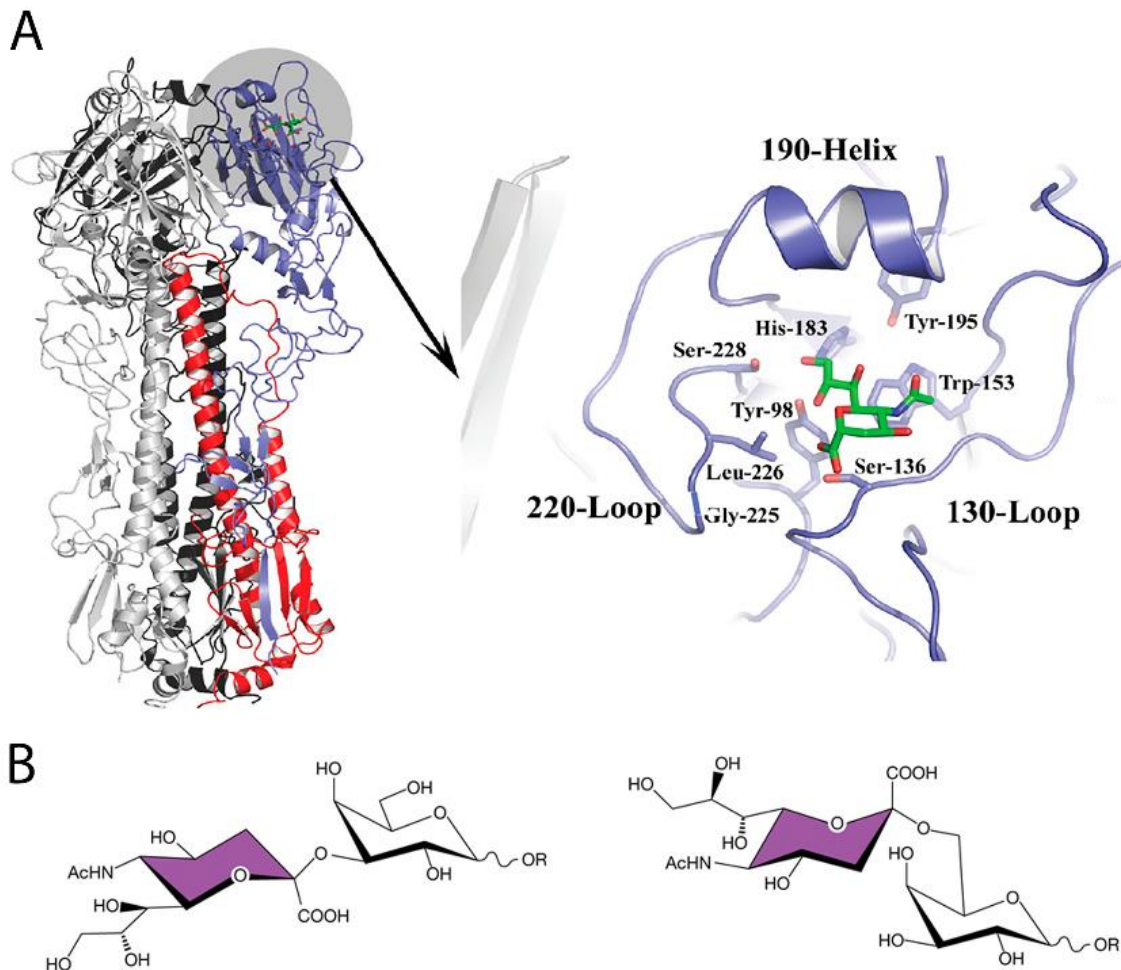


**Fig 3. HA structures and SIAs linkages.** (A) Crystal structure of an HA trimer. Trimeric HA is shown in cartoon representation, with one protomer colored grey, another black, and the third shown in blue (HA1) and red (HA2). The RBS for one protomer shown in blue is highlighted by the grey circle, and this region with magnification is shown in the right panel. Three structural features and conserved residues (H3 numbering) in the binding pocket are labeled. SIA is displayed in stick representation (oxygen in red;



nitrogen in blue; carbon in green). The figure was taken from (163). (B)  $\alpha$ 2,3- and  $\alpha$ 2,6-linked SIA. The terminal SIA is linked to the penultimate galactose via carbon 3 (left) or 6 (right), generating  $\alpha$ 2,3- and  $\alpha$ 2,6-linked SIA. The figure was taken from (150).

#### IV) NA glycoprotein

The NA exists as a homotetramer. Each polypeptide encompasses about 470 amino acids and forms four distinct domains: the N-terminal cytoplasmic tail, the transmembrane region, the thin stalk and the catalytic head (Fig 4A). NA accounts for approximately 10-20% of the total glycoproteins on the virion surface and there are about 40-50 NA spikes compared to 300-400 HA spikes on an average sized virion of 120 nm (89). Depending on filamentous or spherical virion morphology, cryo-electron tomography studies have shown that the NAs can exist as local clusters on the virion surface or as individual spikes isolated by HA spikes (90). Just as for HA, also NAs subtypes can be clustered into two phylogenetic groups. Group I includes N1, N4, N5 and N8 subtypes, while group II includes N2, N3, N6, N7 and N9 subtypes.

##### 1) Cytoplasmic tail & Transmembrane domain

The N-terminal cytoplasmic domain consists of six amino acids: MNPQK. This sequence is almost 100 % conserved in all IAVs, suggesting a critical role of this region in virus replication (91). IAV engineered to carry a NA without the cytoplasmic tail could still be rescued though with a significantly attenuated phenotype (92). Of note, site-specific mutations in this domain resulted in reduced virus titer and altered virus morphology (93-95). It has been postulated that the change in virus morphology and reduction in yield of viruses lacking the cytoplasmic domain may result from the loss of interaction with the M1 protein, thereby affecting the efficiency of virion budding (94, 95). However, the role of the tail domain in packing the surface NA into virions remains unclear.

The N-terminal hydrophobic transmembrane domain (TMD) of the type II transmembrane NA, which generally consists of residues 7-29, is variable between subtypes. In all subtypes, however, it's predicted to form an alpha helix (91, 96). The TMD is required for the transport of NA from ER to the apical surface, as well as for the interaction with lipid rafts (97). Single amino acid substitutions within the TMD can result in altered architecture in the anchoring signal peptide, which may block transport to the plasma membrane (98). The N-terminal amino acids 1 to 74, which covers the cytoplasmic tail, the TMD and part of the stalk region, are sufficient to confer cell membrane localization and NA tetramerization (99-101). The interaction between the TMDs of the NA tetramer depends on polar residues and their positioning with respect to the helix and the membrane bilayer (100).

## **2) Stalk**

A thin stalk domain with variable length and sequence is located between the transmembrane and head domain. Even with this variability, all NA stalks among different NA subtypes share some structural features, like at least one cysteine residue and a predicted glycosylation site (91, 96). The cysteine residue may result in the formation of a NA dimers by disulfide-bonding (91). The glycosylation site is a determinant of virulence, as the loss of this site resulted in enhanced virulence in mice for both 2009 pandemic H1N1 and H7N9 (102).

It has been reported extensively that NA stalk truncations are associated with the adaptation of avian IAVs from wild aquatic birds to domestic poultry (103-106). A decreased stalk length has been shown to negatively affect NA activity of virions (107-110). An explanation for this effect is that the limited height of NA, flanked by a high number of HAs, hinders access of NA to SIA receptors (111, 112). Moreover, it seems that NA stalk length is also involved in virulence in mammalian models of infection (113). For instance, the H1N1pdm09 carrying a NA stalk truncation caused higher lethality in mice and virulence in ferrets than the wild type virus (102).

## **3) Head domain and catalytic site**

The first crystal structure of this domain was reported in 1983 for IAVs (89) and in 1992 for influenza B virus (IBV) (114). Currently, the crystal structures of head domains have been determined for all IAV (115-119) and IBV NA subtypes (114). The structure shows that all NA heads form a box-shaped structure consisting of four protomers (Fig 4B). The tetrameric form of NA is absolutely required for NA enzymatic activity (120). Each protomer folds as a six-bladed propeller structure, with each blade carrying four anti-parallel  $\beta$ -sheets that are stabilized by disulfide bonds and connected by loops with variable length. A catalytic site is located on the surface of each monomer and is directed sideward, a property that facilitates NA cleavage of SIAs from nearby membrane glycoproteins (114, 121). These catalytic sites form a large cavity through charged residues in the pocket and around the rim (119, 121). The NA active site comprises an inner shell and an outer shell. The inner shell is made up by eight highly conserved residues that contact the SIAs directly: Arg118, Asp151, Arg152, Arg224, Glu276, Arg292, Arg371, and Tyr406 (N2 numbering), while the outer shell is responsible for structural stability and includes residues that are regarded as framework residues: Glu119, Arg156, Trp178, Ser179, Asp198, Ile222, Glu227, Glu277, Asn294 (114, 121). The active site is highly conserved in both avian and human IAVs, making it an ideal target for drug inhibition. Arg151 and Arg152 in the catalytic site are part of the “150 loop” that consists of residues 147-152. Interestingly, most group I NAs have an additional cavity close to the 150-loop (150-cavity), but this cavity has not been observed in group II NAs (115). The cavity is created by the movement of the 150-loop upon conformational change when the active site binds to substrate. The H1N1pdm09 N1 doesn't seem to have the 150-cavity, which is similar to

the group II NAs (117, 122). It's postulated that due to the low flexibility of H1N1pdm09 N1 and group II NAs, the open 150-loop conformation is rarely seen in the static crystal structure (122). The 150-cavity is proposed to be a good target for group I NA inhibitors (115).

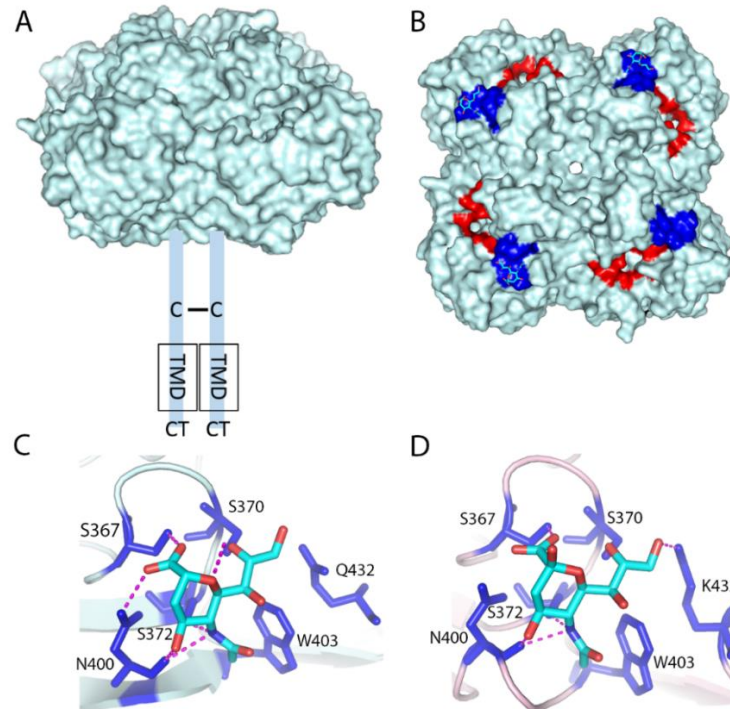


**Fig 4. NA structure.** (A) Schematic representation of NA structure. NA exists as a homo-tetramer of four identical subunits. Each subunit consists of a cytoplasmic tail (CT), transmembrane domain (TMD), stalk and head domain. The presence of a Cys residue in the stalk domain may enable the formation of a disulfide-bond between two monomers (C—C). (B) Crystal structure of the head domain of the NA from A/R/1/5+/1957(H2N2) (PDB ID: 4H53) (118), shown as tetramer with the surface representation. The active site and 2SBS are colored red and blue, respectively. SIA bound to the 2SBS is shown as sticks (oxygen in red; nitrogen in blue; carbon in cyan). The complex of the 2SBS with Neu5Ac for N2 (PDB ID: 4H53) (C) and N9 (D) from A/tern/Australia/G70C/75 (PDB ID:1MWE) (126). Neu5Ac is shown as sticks (oxygen in red; nitrogen in blue; carbon in cyan). Residues in the 2SBS that directly contact with Neu5Ac are shown in blue and their numbering is indicated. Hydrogen bonds are shown as dashed magenta lines. The figures are made by Pymol.

#### 4) The second sialic acid-binding site (2SBS)

Hemagglutination activity of NA was first shown in 1984 for N9 (123). The NA enzymatic activity was inhibited by an inhibitor binding in its active site, but the hemadsorption activity was not. Some of the amino acid residues responsible for hemadsorption were identified by sequencing the monoclonal escape mutants of N9 NA that lost this activity, concluding that enzymatic and hemadsorption activities

of NA are associated with two separate sites on N9 NA head (124). Upon transferring these amino acids by site-directed mutagenesis into N2 NA, hemagglutination was observed as well for N2 (125). The first structural evidence of the existence of a hemadsorption site (also referred to 2SBS) was resolved in 1997 by solving the crystal structure of N9 in complex with two SIAs bound to the catalytic site and the 2SBS (126). The 2SBS is adjacent to the catalytic site which forms a deep pocket (Fig. 4B)(118, 126-129). The 2SBS, forming a shallow pocket, consists of three loops - the 370 loop, 400 loop and 430 loop - containing the SIAs contacting residues: Ser367, Ser370, Ser372, Asn400, Trp403, and Lys432 (Fig 4C-D). The SIA-contact residues in the 2SBS, particularly in the 370 and 400 loops, appear to be highly conserved in avian influenza viruses, while this conservation is invariably lost in human influenza viruses (126, 127), indicating the 2SBS may have important biological functions for virus replication in birds. Disruption of the 2SBS negatively affected virus replication in chicken embryo fibroblast cultures, however, replication in Peking ducks was not affected (130). While this may indicate the 2SBS not important for virus replication *in vivo*, it should be noted that the viruses used in this study have mismatched HA and NA, which may affect the apparent importance of the 2SBS for replication. Uhlenborff and coworkers (127) showed that N2 viruses with and without the hemadsorption activities displayed similar activity against monovalent substrates, while higher enzymatic activity against multivalent substrate was observed for virus with hemagglutination activity. More recently, a functional 2SBS was shown to contribute to NA activity of N9 of recent H7N9 viruses (129). Glycan array analysis of N9 revealed that the 2SBS displays preferred binding to  $\alpha$  2,3-linked sialosides and weak or no binding to  $\alpha$  2,6-linked sialosides (129). The presence of a functional 2SBS presumably enhances NA enzymatic activity against multivalent substrate by bringing the substrate closer to the NA active site (127, 129). Until now, binding of SIA to the 2SBS has been demonstrated using X-ray crystallography for N2, N5, N6, and N9 (118, 126, 131) and by saturation-transfer difference (STD) NMR for N1 (128). Using STD NMR, binding of  $\alpha$ 2,3-sialyllactose to avian IAV derived N1 was shown to be much stronger than to N1 of H1N1pdm09 (128), in agreement with the latter protein containing a mutation in the 2SBS.

### **5) NA enzymatic activity & substrate specificity**

The receptor-destroying activity of influenza virus NA was first demonstrated by Hirst (132), and the “split product” was later identified as N-acetylneuraminic acid (Neu5Ac), one of the SIAs (133). The catalytic mechanism of NA has not been completely understood but is proposed to start with the binding of substrate to the active site (134, 135). This step involves salt-bridge formation between the carboxylate of the SIA and the three arginine residues at positions 118, 292 and 371, resulting in translocation of carboxylate from the axial position into a pseudo-equatorial position. In the next step, the transition-state intermediate is formed, which involves proton donation from solvent. Asp151,

Arg152 and Glu277 are proposed to contribute to the stability of the cationic intermediate. Subsequently, the transition-state intermediate covalently binds to the hydroxyl group of Tyr406. Finally, cleavage takes place, leading to the release of Neu5Ac in an  $\alpha$ -anomeric conformation, followed by conversion into a  $\beta$ -anomeric state (96). The optimal pH range for NA cleavage activity supposedly is 5.5-6.5 (136, 137). Low pH stability of NA activity may enhance viral replication in vitro and has been proposed to contribute to the spread of pandemic viruses (138, 139). The presence of  $\text{Ca}^{2+}$  is pivotal for NA thermostability and enzymatic activity (140, 141). There is a conserved calcium binding site in each NA protomer of all known type A and B NAs formed by residues Asp293, Gly297, Asp324, Tyr347 and two water molecules (142). Depending on the NA subtype, up to 3 calcium binding sites per subunit of each tetramer are observed (115, 116, 143).

Compared with the well-characterized HA binding specificity, studies on the NA substrate specificity are limited. All IAV NA proteins prefer cleavage of  $\alpha 2,3$  over  $\alpha 2,6$  sialosides, regardless whether they are derived from avian or human viruses. Human viruses, however, are generally relatively better at cleaving  $\alpha 2,6$  SIAs than avian viruses (144, 145). NA specificity thus appears to contrast the apparent preference of HA of human viruses for  $\alpha 2,6$  sialylated glycans (146, 147). The specificity of NA nevertheless evolves with time for human viruses, resulting in increased cleavage of  $\alpha 2,6$ -linked SIAs (146-148). A single Ile275Val substitution in human N2 was shown to result in increased cleavage of  $\alpha 2,6$ -linked SIAs, and Val at position 275 was maintained in all later human viruses (146).

## V) IAV (decoy) receptors

SIAs are a family of nine-carbon monosaccharides that serve as terminal residues of carbohydrate chains on membrane-anchored glycoproteins, glycolipids and secreted glycoproteins among others at mucosal surfaces (149). Common SIAs present in mammals are N-acetylneuraminic acid (Neu5Ac) and N-glycolylneuraminic acid (Neu5Gc) (149, 150) (Fig 5A). Neu5Gc has been found in pigs, horses, and monkeys, but humans, dogs, ferrets as well as most bird species do not express Neu5Gc (151, 152). Sialoglycans, which are abundantly displayed on cell surfaces, play important roles in cell signaling, development, and host-pathogen interactions. Glycans contain a variety of internal sugars, linkages, and branching patterns resulting in hundreds of different SIA-containing oligosaccharides. Proteins contain N- and O-linked glycans. N-linked glycosylation refers to the addition of an oligosaccharide to an Asn residue of a protein within the consensus sequence Asn-X-Ser/Thr (X is any amino acid except Pro). N-glycans shares a common core sequence  $\text{Man}_3\text{GlcNAc}_2$  (153). This common sequence can be extended by different types of oligosaccharides with variable length, leading to three classes of N-linked oligosaccharides: "oligomannose", "complex", and "hybrid" (Fig. 5B). O-linked glycosylation is characterized by the attachment of GalNAc to the hydroxyl of Ser or Thr residues of a protein (154). There is a wide variety of O-glycans with eight different core structures. Each core can be extended by

the addition of sugar residues forming linear or branched chains. Compared to N-linked glycans, O-linked glycans are normally shorter and less complex. Mucins carry a great number of O-glycans with four major core structures (cores 1 to 4) (Fig. 5C). Core 1 and 2 structures are found in both glycoproteins and mucins produced by different cell types while core 3 and 4 structures are restricted to mucins and glycoproteins in gastrointestinal and bronchial tissues.

It is not known whether binding to specific sialoglycoproteins or -lipids is required for virus endocytic uptake and infection. Mouse cells deficient in the production of glycolipids can be infected efficiently with human H3N2 virus, suggesting the sialylated glycolipids are not essential for H3N2 virus infection (155). In the absence of sialylated N-glycans, efficient virus entry can also still occur (48) presumably via binding of IAV to O-linked glycans and/or glycolipids. Macropinocytic uptake of virus particles was, however, reduced in these cells indicating the importance of N-glycans therefor (48). N-glycans did not appear to be required for clathrin-mediated endocytosis. An important role for N-glycans in IAV entry is supported by the observation that human H3N2 and H1N1 viruses efficiently bind to bi-antennary glycans containing multiple LacNAc repeats (87)(Fig. 5B). Interestingly, older H3N2 strains can also bind to shorter monoantennary glycans. More recent H3 isolates display, however, relatively weak and inconsistent binding to these glycans (88, 156).

Before viruses can bind to the functional receptors at the cell surface of the epithelial cells of the respiratory tract they must first traverse the overlying mucus layer. This mucosal barrier act as the first line of defense against IAV infection. The mucus layer forms a gel-like barrier and exists in two parts: a more viscous mucus gel layer on top of a less viscous periciliary liquid layer (PCL), into which the cilia protrude (157). Mucins, the main constituents of mucus, includes two types: secreted mucins and membrane-tethered mucins (158). Mucins are one of the largest macromolecules encoded in mammalian cells with the size of 200 kDa to 200 MDa and form a mesh. Mucins are heavily glycosylated, mainly containing O-glycans ending in SIAs (159). The densely sialylated mucins can function as decoy ligands for IAVs. Viruses somehow need to be able to prevent being captured and to move through mucus to reach the underlying cells (160, 161). Pathogens that are immobilized within mucus are steadily being transported towards the pharynx where they can be cleared. Of note, exosomes present in mucus, which are secreted by human airway epithelial cells and contain both  $\alpha$ 2,3- and  $\alpha$ 2,6-linked SIAs, can also function as decoys for IAVs (162).

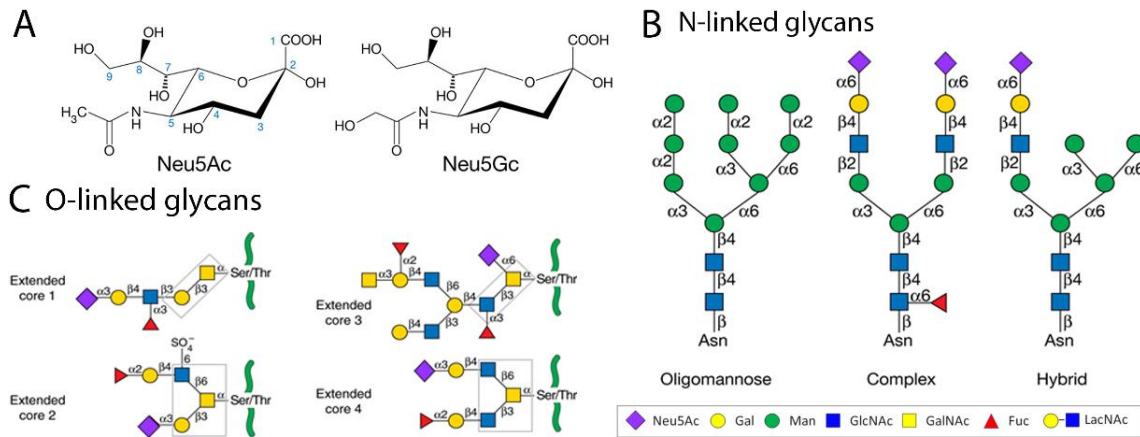


**Fig 5. Types of SIAs and glycan structures.** (A) SIAs are a family of nine-carbon monosaccharides. All SIA family members carry a glycerol-like side chain (C7 to C9) but vary in the side chain attached to C5. Common SIAs found in mammals are Neu5Ac and Neu5Gc. The C5 carbon in Neu5Ac is modified with an N-acetyl group, which can be further hydroxylated resulting in the formation of Neu5Gc. The figure was taken from (150). (B) Types of N-glycans. There are three general types of N-glycans in eukaryote glycoproteins. All N-glycans share the common core  $\text{Man}_3\text{GlcNAc}_2\text{Asn}$ . Complex N-glycans can accommodate up to six branches initiated by GlcNAc and each can be elongated with  $\text{Gal}\beta 1-4\text{GlcNAc}$  (LacNAc) repeats. The figure was adapted from (153). (C) Major core structures of O-linked glycans. Mucins contain complex O-GalNAc glycans with different cores identified by gray boxes. All four core structures (in boxes) may be elongated, branched, and terminated with Fuc or SIA. Green lines indicate the protein backbone. Purple diamond: Neu5Ac; yellow circle: galactose; green circle: mannose; blue square: N-acetylglucosamine; yellow square: N-acetylglactosamine. The figure was adapted from (154).

## VI) HA-NA-receptor balance

HA binding to SIAs receptors on target cells is required to initiate virus infection, whereas the NA cleaves SIAs from both the HA and cell surface, thereby facilitating newly assembled virus release and promoting virus spreading to other cells. Considering the apparently opposite functions of HA and NA, it is reasonable to assume a delicate balance must exist between HA and NA for optimal virus replication (163, 164). If the HA binding and NA cleavage are mismatched, for instance when the sialidase activity of NA is suboptimal, virus may remain bound by non-functional decoy receptors on the cell surface and get stuck, blocking virus binding to functional receptors (112). NA with low enzymatic activity may also result in the lack of release of newly assembled virion from the cell surface

due to the binding of HA to SIAs that haven't been cleaved by NA. Alternatively, if the sialidase activity of NA is too strong compared to HA binding, SIAs may be removed from functional receptors on the cell surface before HA binding, resulting in reduced virus entry and replication (112).

The HA-NA balance probably is also critical for the ability of viruses to traverse the mucus layer overlaying the epithelial cells of the respiratory tract (160). The HA-NA balance must be adjusted as such that the virus is able to adhere to mucus long enough to allow virus entry into the mucus layer. Viruses that bind too tightly to SIAs will probably go through the mucus barrier very slowly, and will possibly be unable to reach the epithelial cell surface before mucociliary clearance (161). On the other hand, viruses able to move through the mucus layer should have an HA-NA balance that allows these viruses to stably attach to the surface of the underlying epithelium resulting in their endocytic uptake. Thus, the HA-NA balance of IAVs should be adjusted to allow penetration of the mucus layer as well as endocytic uptake in epithelial cells (161, 165).

When viruses cross the host species barrier and encounter a host that displays a novel sialic acid repertoire in mucus and on the cell surface, the HA-NA balance of these viruses needs to be readjusted for efficient replication and transmission to occur. So, when avian IAV crosses the species barrier to adapt to mammals, the receptor binding specificity of HA changes from  $\alpha$ 2,3-linked SIAs to  $\alpha$ 2,6-linked SIAs (166), which is subsequently thought to drive alterations in the substrate specificity of NA. For example, with time the NA activity in human H2N2 and H3N2 viruses increased for  $\alpha$ 2,6-linked SIAs, presumably to match the altered HA binding specificity (146, 147). The HA-NA balance is also thought to differ between human and swine viruses as was demonstrated by analysis of the HA and NA activities of H1N1pdm09 and related swine viruses. HA of swine viruses displayed a higher affinity for a broad range of glycans than the pandemic H1, while these viruses had similar NA activities. The HA-NA balance observed for H1N1pdm09 appeared similar to the balance of a previous pandemic IAV, indicating this balance is optimal for influenza virus adaptation to humans (167). Of note, however, these results should be cautiously interpreted as the HA-NA balance was studied using recombinant proteins and not in the context of virus particles.

The HA-NA balance of H1N1pdm09 was also shown to play a critical role in transmission via respiratory droplets in ferrets (168). The introduction of NA from a 2009 pandemic virus into a swine H1N2 virus increased respiratory-droplet transmissibility in ferrets. This can be explained by the higher NA enzymatic activity of the pandemic virus than that of swine virus, as the HAs of these two viruses displayed similar receptor-binding specificity and affinity for  $\alpha$ 2,6-linked SIAs. Apparently, the HA-NA balance of the chimeric swine virus was better adapted for transmission between ferrets than the wild type swine virus.



The HA-NA balance required for optimal replication appears to differ between viruses derived from different avian species. Adaptation of viruses from aquatic birds to domestic poultry is commonly accompanied with a deletion in the NA stalk (103-105). As mentioned above, the decreased stalk length has negative effect on NA activity. The acquisition of an additional N-glycan on the HA head domain is another featured evolutionary change in chicken-adapted avian influenza viruses. This glycan decreases HA binding avidity to SIAs receptors by steric hindrance (169). The additional glycosylation of HA and a shortened NA stalk are common features for chicken H5 and H7 IAVs (169, 170), which likely result in an altered HA-NA balance in adaptation to a new host (111).

A readjustment of the functional HA-NA balance may be required when NA activity is altered by selection of mutations that confer resistance to antiviral drugs (NA inhibitors). These substitutions often decrease NA activity altering the HA-NA balance (171-173). The HA-NA balance may be restored by the selection of substitutions in NA, which increase NA activity again, or in HA, which result in lower affinity for SIA receptors (174, 175). Of note, antibody-driven antigenic variation of HA, which may result in altered HA-receptor binding, may in turn also select for mutations that decrease NA activity and result in NA antigenic variation and even in the acquisition of drug resistance (176). Possibly, a similar mechanism may explain why pre-2009 seasonal H1N1 viruses acquired drug resistance mutations in NA (177).

## **VII) Analysis of HA-NA balance.**

There is no standard way to evaluate the HA-NA balance. The most common way is to study HA and NA protein activity and specificity separately by using either recombinant proteins or virus particles. There is limited methodology to study the balance between the HA and NA activities in context of virus particles.

### **1) Analysis of HA and NA protein activities separately**

Solid phase binding assays, including glycoprotein and glycan binding assays, are the most commonly used methods to quantify HA binding affinity and specificity (178). Glycoproteins or glycans are immobilized on surfaces, after which HA proteins or viruses are used to detect binding to these surfaces. These solid phase-based binding assays are good ways to study HA protein binding specificity towards  $\alpha$ 2,3-linked or  $\alpha$ 2,6-linked glycan structures and can accommodate many structurally defined glycans. When using recombinant HA protein, HA is generally pre-complexed with antibody to increase binding avidity and for detection purposes. However, the application of complexation with antibody is artificial and little informative about the binding of virus particles. Furthermore, surfaces densely coated with a unique synthetic glycan are not representative for the receptor-containing surfaces that viruses are confronted with *in vivo* (179).

The most commonly used substrate to characterize the NA enzymatic activity is the small fluorogenic substrate 4-methylumbelliferyl-N-acetylneuraminic acid (MUNANA) (180). The NA cleavage of this small molecule results in the release of fluorescent 4-methylumbelliferone (4-MU). Another small, soluble compound is the chemiluminescent NA-Star substrate (181). The main drawback of these assays is that the monovalent substrates are not representative of the multivalent sialosides that virus encounters *in vivo*. Additionally, it is not informative about the cleavage preference of NA for  $\alpha$ 2,3- or  $\alpha$ 2,6-linked SIAs. To solve this, several other assays have been applied to explore NA substrate specificity, such as STD-NMR (145) and enzyme-linked lectin assays (ELLAs) (167, 182-184). In ELLAs, glycoprotein-coated surfaces or glycan arrays are incubated with NA proteins or virus particles, after which the NA activity is detected by lectins that specifically recognize sialylated or non-sialylated glycotopes. Decreased or increased binding of these lectins is used to quantify NA activity and allows to determine NA cleavage specificity by using lectins specifically recognizing  $\alpha$ 2,3- or  $\alpha$ 2,6-linked SIAs.

The separate analysis of HA and NA activity of proteins or virus particles is informative, but does not necessarily reflect the genuine HA-NA balance of virus particles. For instance, the HA-NA balance of virus particles is not solely determined by the HA and NA proteins *per se*, but also by their incorporation levels and spatial organization in virus particles. To complicate matters further, the presence of HA in the virion may enhance NA enzymatic activity against multivalent substrates (185, 186). The importance of receptor-binding by HA for NA activity probably also partly explains why HA-specific antibodies can block NA activity by limiting the interactions of virions with SIA-containing surfaces (187).

## **2) HA-NA balance of virus particles:**

In 1942, the hemagglutination assay was developed. In this assay the agglutination of red blood cells (RBC) is observed resulting from crosslinking of RBCs by HA proteins on virus particles (188). While this assay is informative on the virus-binding properties, it may also be used to study the HA-NA balance. The HA-NA balance is reflected by the difference in or loss of hemagglutination by incubation at 37°C compared to hemagglutination conducted at 4°C. The difference is explained by NA being inactive and active at 4°C and at 37°C, respectively. The use of erythrocytes from different species may be informative about the HA-NA balance for different types of receptor (189). However, structural diversity and identity of glycans on RBCs are not well-defined, which limit the application of this method.

Recently, Sakai and coworkers developed a new assay to study virus motility on a receptor-coated surface using fluorescent labeled virus (190, 191) and fluorescence imaging microscopy. IAV and ICV migration pattern could be monitored and was proposed that virus mobility depends on the balance

between HA binding and NA activity. However, via this method it is relatively difficult to quantify and categorize virus movement patterns and to determine the correlation between virus movement and the HA-NA balance.

We and others (185, 192) developed a kinetic assay based on biolayer-interferometry (BLI) to analyze the HA-NA balance of virus particles (Fig 6). BLI is a label-free technology for measuring biomolecular interactions (193) and has been used extensively throughout the studies described in this thesis. It is an optical technique based on light intensity interference (194). Interference changes between the intensities of the reflected light beams are used to measure changes in the molecular layer immobilized on the sensor surface. In this assay, synthetic glycans or glycoproteins receptors are immobilized on the sensor surface, followed by analysis of binding and release of virus particle to the receptors in time.

Using BLI, we previously showed that virus binding is proportional to the number of virus particles present when NA activity is inhibited (185). This underscores the importance of accurate determination of virus particle numbers in virus stocks that are compared. Furthermore, even while individual HA-receptor interactions are very weak (mM range) (195-197), viruses are immobilized on the sensor surface in the absence of NA activity (Fig 6A). This is explained by multivalent binding between virus particles and the receptor-coated BLI-sensor surface. Low activity NA also contributed to binding of virions to the sensors. In the presence of NA activity, viruses bound on SIA-containing sensors move on the sensor surface thereby cleaving SIAs until the receptor density is sufficiently decreased to allow virus dissociation. The rate of virus release from the sensor surface reflects the HA-NA balance (Fig 6B). Virus self-elution is faster when HA binds with lower affinity or when NA is more active. Virus self-elution is slower when HA binds with higher affinity or when NA is less active. Thus, BLI allows a qualitative and quantitative analysis of the HA-NA-receptor balance.

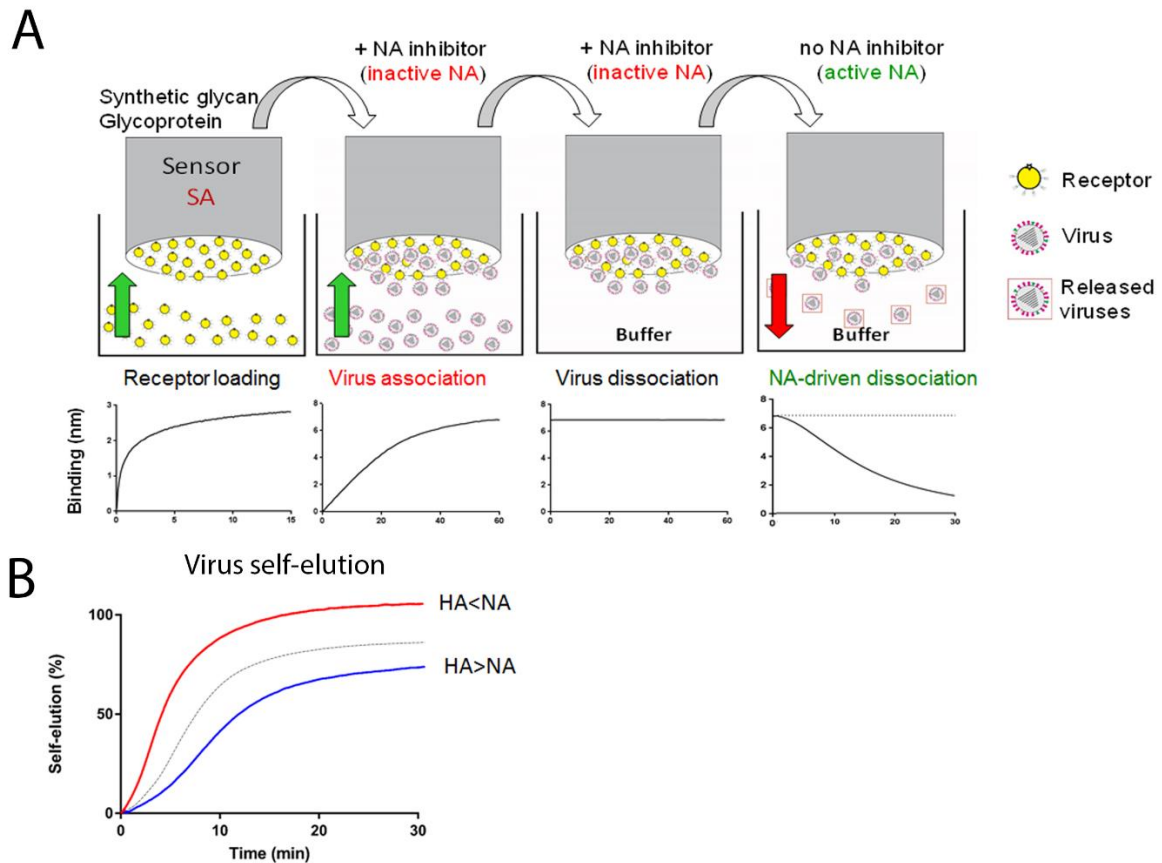


**Fig 6. (A) Schematic diagram of BLI assay.** Biotinylated IAV receptors (synthetic glycans or glycoproteins) are loaded to a streptavidin (SA)-containing biosensor surface, resulting in a receptor loading curve. X-axis depicts time, Y-axis the binding level. Subsequently, the receptor-bound sensor is moved to a well containing viruses in the presence of NA inhibitor, generating a virus association curve. When the virus-bound sensor is moved to a well containing no free virus particles, but NA inhibitor only, there is no virus dissociation. However, when the NA inhibitor is removed, NA-driven dissociation occurs. (B) NA-driven dissociation normalized to the virus association level is used to graph virus self-elution. Virus self-elution reflects the HA-NA balance. When HA and NA are in balance a certain self-elution curve is observed (grey dashed line). If HA has a lower avidity and/or NA has a higher enzymatic activity, the virus will show faster self-elution (HA<NA; red solid line). On the other hand, if HA has a higher avidity and/or NA has a lower enzymatic activity, the virus will show slower self-elution (HA>NA; blue solid line). The figure is based on (185).

**VII) Outline of this thesis:**

As HA and NA proteins have apparent opposite functions, it is widely accepted that the activities of HA and NA must be in delicate balance to allow efficient virus entry, replication, and transmission. Compared to the well-characterized role of HA during this process, much less is known about the contribution of NA, including its 2SBS. **The importance of the 2SBS for NA activity and the HA-NA balance of virus particles is the main topic of this thesis.** We first analyzed the role of the 2SBS in enzymatic activity of N1 using a recombinant protein approach (**chapter 2**). We showed that the 2SBS in avian N1 proteins is an important determinant of NA activity and contributes to virus replication. Next, we analyzed the contribution of the 2SBS to the HA-NA balance in the context of virus particles using biolayer interferometry analyses of N2-containing viruses (**chapter 3**). Our results indicate that the 2SBS is an important determinant of the HA-NA-receptor balance and virus replication. The importance the 2SBS was shown to depend on the specific HA protein with which NA is combined. Subsequently, we analyzed whether mutation of the 2SBS may select for mutations in HA to restore the HA-NA balance of H5N1 virus (**chapter 4**). This was indeed shown to occur. All mutations in HA that were selected decreased receptor binding to avian-type receptors, while one also resulted in increased binding to human-type receptors. The observation that mutations of the 2SBS may result in evolution of viruses with increased binding to human-type receptors and hence zoonotic potential, was underscored by phylogenetic analysis of H9N2 viruses. The evolution of N1 of H1N1pdm09 virus was studied upon the emergence of this virus in the human population (**chapter 5**). The results indicate a key role for residue 432 in the 2SBS in NA activity and antigenicity and suggest that entanglement of NA phenotypes may be an important factor in NA evolution. The results furthermore indicate that the HA-NA balance of virus particles may also be significantly affected by changes in the incorporation of NA in virions. The importance of the HA-NA balance for virus mobility is discussed in detail in **chapter 6**, while the importance of the 2SBS for this balance is discussed in **chapter 7**.

**References**

1. Medina RA, García-Sastre A. 2011. Influenza A viruses: new research developments. *Nature Reviews Microbiology* 9:590-603.
2. Krammer F, Smith GJD, Fouchier RAM, Peiris M, Kedzierska K, Doherty PC, Palese P, Shaw ML, Treanor J, Webster RG, García-Sastre A. 2018. Influenza. *Nature Reviews Disease Primers* 4:3.
3. Molinari NA, Ortega-Sanchez IR, Messonnier ML, Thompson WW, Wortley PM, Weintraub E, Bridges CB. 2007. The annual impact of seasonal influenza in the US: measuring disease burden and costs. *Vaccine* 25:5086-96.
4. Taubenberger JK, Kash JC. 2010. Influenza virus evolution, host adaptation, and pandemic formation. *Cell Host Microbe* 7:440-51.
5. Webster RG, Bean WJ, Gorman OT, Chambers TM, Kawaoka Y. 1992. Evolution and ecology of influenza A viruses. *Microbiological reviews* 56:152-179.
6. Long JS, Mistry B, Haslam SM, Barclay WS. 2019. Host and viral determinants of influenza A virus species specificity. *Nature Reviews Microbiology* 17:67-81.
7. Gamblin SJ, Skehel JJ. 2010. Influenza hemagglutinin and neuraminidase membrane glycoproteins. *The Journal of biological chemistry* 285:28403-28409.
8. Lamb R, Krug R. 2001. *Orthomyxoviridae: The Viruses and Their Replication*. Fields Virology Volume 1 1.
9. Zhai S-L, Zhang H, Chen S-N, Zhou X, Lin T, Liu R, Lv D-H, Wen X-H, Wei W-K, Wang D, Li F. 2017. Influenza D Virus in Animal Species in Guangdong Province, Southern China. *Emerging infectious diseases* 23:1392-1396.
10. Ciminski K, Thamamongood T, Zimmer G, Schwemmler M. 2017. Novel insights into bat influenza A viruses. *The Journal of general virology* 98:2393-2400.
11. Tong S, Li Y, Rivallier P, Conrardy C, Castillo DAA, Chen L-M, Recuenco S, Ellison JA, Davis CT, York IA, Turmelle AS, Moran D, Rogers S, Shi M, Tao Y, Weil MR, Tang K, Rowe LA, Sammons S, Xu X, Frace M, Lindblade KA, Cox NJ, Anderson LJ, Rupprecht CE, Donis RO. 2012. A distinct lineage of influenza A virus from bats. *Proceedings of the National Academy of Sciences* 109:4269.
12. Tong S, Zhu X, Li Y, Shi M, Zhang J, Bourgeois M, Yang H, Chen X, Recuenco S, Gomez J, Chen L-M, Johnson A, Tao Y, Dreyfus C, Yu W, McBride R, Carney PJ, Gilbert AT, Chang J, Guo Z, Davis CT, Paulson JC, Stevens J, Rupprecht CE, Holmes EC, Wilson IA, Donis RO. 2013. New World Bats Harbor Diverse Influenza A Viruses. *PLOS Pathogens* 9:e1003657.
13. Johnson NP, Mueller J. 2002. Updating the accounts: global mortality of the 1918-1920 "Spanish" influenza pandemic. *Bull Hist Med* 76:105-15.
14. Smith GJD, Bahl J, Vijaykrishna D, Zhang J, Poon LLM, Chen H, Webster RG, Peiris JSM, Guan Y. 2009. Dating the emergence of pandemic influenza viruses. *Proceedings of the National Academy of Sciences of the United States of America* 106:11709-11712.
15. Kilbourne ED. 2006. Influenza pandemics of the 20th century. *Emerging infectious diseases* 12:9-14.
16. Scholtissek C, Rohde W, Von Hoyningen V, Rott R. 1978. On the origin of the human influenza virus subtypes H2N2 and H3N2. *Virology* 87:13-20.
17. Kawaoka Y, Krauss S, Webster RG. 1989. Avian-to-human transmission of the PB1 gene of influenza A viruses in the 1957 and 1968 pandemics. *Journal of virology* 63:4603-4608.
18. Kilbourne ED. 1997. Perspectives on Pandemics: A Research Agenda. *The Journal of Infectious Diseases* 176:S29-S31.
19. Nakajima K, Desselberger U, Palese P. 1978. Recent human influenza A (H1N1) viruses are closely related genetically to strains isolated in 1950. *Nature* 274:334-339.
20. Rozo M, Gronvall GK. 2015. The Reemergent 1977 H1N1 Strain and the Gain-of-Function Debate. *mBio* 6:e01013-15.
21. Garten RJ, Davis CT, Russell CA, Shu B, Lindstrom S, Balish A, Sessions WM, Xu X, Skepner E, Deyde V, Okomo-Adhiambo M, Gubareva L, Barnes J, Smith CB, Emery SL, Hillman MJ, Rivallier

- P, Smagala J, de Graaf M, Burke DF, Fouchier RAM, Pappas C, Alpuche-Aranda CM, López-Gatell H, Olivera H, López I, Myers CA, Faix D, Blair PJ, Yu C, Keene KM, Dotson PD, Jr., Boxrud D, Sambol AR, Abid SH, St George K, Bannerman T, Moore AL, Stringer DJ, Blevins P, Demmler-Harrison GJ, Ginsberg M, Kriner P, Waterman S, Smole S, Guevara HF, Belongia EA, Clark PA, Beatrice ST, Donis R, et al. 2009. Antigenic and genetic characteristics of swine-origin 2009 A(H1N1) influenza viruses circulating in humans. *Science (New York, NY)* 325:197-201.
22. Kandun IN, Wibisono H, Sedyaningsih ER, Yusharmen, Hadisoedarsuno W, Purba W, Santoso H, Septiawati C, Tresnaningsih E, Heriyanto B, Yuwono D, Harun S, Soeroso S, Giriputra S, Blair PJ, Jeremijenko A, Kosasih H, Putnam SD, Samaan G, Silitonga M, Chan KH, Poon LL, Lim W, Klimov A, Lindstrom S, Guan Y, Donis R, Katz J, Cox N, Peiris M, Uyeki TM. 2006. Three Indonesian clusters of H5N1 virus infection in 2005. *N Engl J Med* 355:2186-94.
  23. Wang H, Feng Z, Shu Y, Yu H, Zhou L, Zu R, Huai Y, Dong J, Bao C, Wen L, Wang H, Yang P, Zhao W, Dong L, Zhou M, Liao Q, Yang H, Wang M, Lu X, Shi Z, Wang W, Gu L, Zhu F, Li Q, Yin W, Yang W, Li D, Uyeki TM, Wang Y. 2008. Probable limited person-to-person transmission of highly pathogenic avian influenza A (H5N1) virus in China. *The Lancet* 371:1427-1434.
  24. Qi X, Qian YH, Bao CJ, Guo XL, Cui LB, Tang FY, Ji H, Huang Y, Cai PQ, Lu B, Xu K, Shi C, Zhu FC, Zhou MH, Wang H. 2013. Probable person to person transmission of novel avian influenza A (H7N9) virus in Eastern China, 2013: epidemiological investigation. *Bmj* 347:f4752.
  25. Gao R, Cao B, Hu Y, Feng Z, Wang D, Hu W, Chen J, Jie Z, Qiu H, Xu K, Xu X, Lu H, Zhu W, Gao Z, Xiang N, Shen Y, He Z, Gu Y, Zhang Z, Yang Y, Zhao X, Zhou L, Li X, Zou S, Zhang Y, Li X, Yang L, Guo J, Dong J, Li Q, Dong L, Zhu Y, Bai T, Wang S, Hao P, Yang W, Zhang Y, Han J, Yu H, Li D, Gao GF, Wu G, Wang Y, Yuan Z, Shu Y. 2013. Human infection with a novel avian-origin influenza A (H7N9) virus. *N Engl J Med* 368:1888-97.
  26. Peiris M, Yuen KY, Leung CW, Chan KH, Ip PLS, Lai RWM, Orr WK, Shortridge KF. 1999. Human infection with influenza H9N2. *The Lancet* 354:916-917.
  27. Guan Y, Smith GJD. 2013. The emergence and diversification of panzootic H5N1 influenza viruses. *Virus Research* 178:35-43.
  28. World, Health, Organizatio. Cumulative number of confirmed human cases of avian influenza A(H5N1) reported to WHO, 2003-2020. [https://www.who.int/influenza/human\\_animal\\_interface/H5N1\\_cumulative\\_table\\_archives/en/](https://www.who.int/influenza/human_animal_interface/H5N1_cumulative_table_archives/en/).
  29. Gao R, Cao B, Hu Y, Feng Z, Wang D, Hu W, Chen J, Jie Z, Qiu H, Xu K, Xu X, Lu H, Zhu W, Gao Z, Xiang N, Shen Y, He Z, Gu Y, Zhang Z, Yang Y, Zhao X, Zhou L, Li X, Zou S, Zhang Y, Li X, Yang L, Guo J, Dong J, Li Q, Dong L, Zhu Y, Bai T, Wang S, Hao P, Yang W, Zhang Y, Han J, Yu H, Li D, Gao GF, Wu G, Wang Y, Yuan Z, Shu Y. 2013. Human Infection with a Novel Avian-Origin Influenza A (H7N9) Virus. *New England Journal of Medicine* 368:1888-1897.
  30. Iuliano AD, Jang Y, Jones J, Davis CT, Wentworth DE, Uyeki TM, Roguski K, Thompson MG, Gubareva L, Fry AM, Burns E, Trock S, Zhou S, Katz JM, Jernigan DB. 2017. Increase in Human Infections with Avian Influenza A(H7N9) Virus During the Fifth Epidemic - China, October 2016-February 2017. *MMWR Morbidity and mortality weekly report* 66:254-255.
  31. Li C, Chen H. 2020. H7N9 Influenza Virus in China. *Cold Spring Harbor Perspectives in Medicine* doi:10.1101/cshperspect.a038349.
  32. Lin YP, Shaw M, Gregory V, Cameron K, Lim W, Klimov A, Subbarao K, Guan Y, Krauss S, Shortridge K, Webster R, Cox N, Hay A. 2000. Avian-to-human transmission of H9N2 subtype influenza A viruses: Relationship between H9N2 and H5N1 human isolates. *Proceedings of the National Academy of Sciences* 97:9654.
  33. Matrosovich MN, Krauss S, Webster RG. 2001. H9N2 Influenza A Viruses from Poultry in Asia Have Human Virus-like Receptor Specificity. *Virology* 281:156-162.
  34. Neumann G, Kawaoka Y. 2015. Transmission of influenza A viruses. *Virology* 479-480:234-246.
  35. Saito T, Lim W, Suzuki T, Suzuki Y, Kida H, Nishimura S-I, Tashiro M. 2001. Characterization of a human H9N2 influenza virus isolated in Hong Kong. *Vaccine* 20:125-133.

36. Butt KM, Smith GJD, Chen H, Zhang LJ, Leung YHC, Xu KM, Lim W, Webster RG, Yuen KY, Peiris JSM, Guan Y. 2005. Human infection with an avian H9N2 influenza A virus in Hong Kong in 2003. *Journal of clinical microbiology* 43:5760-5767.
37. Li C, Chen H. 2014. Enhancement of Influenza Virus Transmission by Gene Reassortment, p 185-204. *In* Compans RW, Oldstone MBA (ed), *Influenza Pathogenesis and Control - Volume I* doi:10.1007/82\_2014\_389. Springer International Publishing, Cham.
38. Engelhardt OG, Smith M, Fodor E. 2005. Association of the influenza A virus RNA-dependent RNA polymerase with cellular RNA polymerase II. *Journal of virology* 79:5812-5818.
39. Fodor E, Te Velhuis AJW. 2019. Structure and Function of the Influenza Virus Transcription and Replication Machinery. *Cold Spring Harb Perspect Med* doi:10.1101/cshperspect.a038398.
40. Walker AP, Fodor E. 2019. Interplay between Influenza Virus and the Host RNA Polymerase II Transcriptional Machinery. *Trends Microbiol* 27:398-407.
41. Pflug A, Lukarska M, Resa-Infante P, Reich S, Cusack S. 2017. Structural insights into RNA synthesis by the influenza virus transcription-replication machine. *Virus Research* 234:103-117.
42. Rajsbaum R, Albrecht RA, Wang MK, Maharaj NP, Versteeg GA, Nistal-Villán E, García-Sastre A, Gack MU. 2012. Species-Specific Inhibition of RIG-I Ubiquitination and IFN Induction by the Influenza A Virus NS1 Protein. *PLOS Pathogens* 8:e1003059.
43. Hayman A, Comely S, Lackenby A, Hartgroves LCS, Goodbourn S, McCauley JW, Barclay WS. 2007. NS1 proteins of avian influenza A viruses can act as antagonists of the human alpha/beta interferon response. *Journal of virology* 81:2318-2327.
44. Dadonaite B, Vijayakrishnan S, Fodor E, Bhella D, Hutchinson EC. 2016. Filamentous influenza viruses. *Journal of General Virology* 97:1755-1764.
45. Vijayakrishnan S, Loney C, Jackson D, Suphamungmee W, Rixon FJ, Bhella D. 2013. Cryotomography of budding influenza A virus reveals filaments with diverse morphologies that mostly do not bear a genome at their distal end. *PLoS pathogens* 9:e1003413-e1003413.
46. Badham MD, Rossman JS. 2016. Filamentous Influenza Viruses. *Current Clinical Microbiology Reports* 3:155-161.
47. Chu VC, Whittaker GR. 2004. Influenza virus entry and infection require host cell N-linked glycoprotein. *Proceedings of the National Academy of Sciences of the United States of America* 101:18153-18158.
48. de Vries E, de Vries RP, Wienholts MJ, Floris CE, Jacobs M-S, van den Heuvel A, Rottier PJM, de Haan CAM. 2012. Influenza A virus entry into cells lacking sialylated N-glycans. *Proceedings of the National Academy of Sciences of the United States of America* 109:7457-7462.
49. Ni F, Chen X, Shen J, Wang Q. 2014. Structural insights into the membrane fusion mechanism mediated by influenza virus hemagglutinin. *Biochemistry* 53:846-854.
50. Ruigrok RW, Aitken A, Calder LJ, Martin SR, Skehel JJ, Wharton SA, Weis W, Wiley DC. 1988. Studies on the structure of the influenza virus haemagglutinin at the pH of membrane fusion. *J Gen Virol* 69 ( Pt 11):2785-95.
51. Martin K, Helenius A. 1991. Nuclear transport of influenza virus ribonucleoproteins: The viral matrix protein (M1) promotes export and inhibits import. *Cell* 67:117-130.
52. Stauffer S, Feng Y, Nebioglu F, Heilig R, Picotti P, Helenius A. 2014. Stepwise Priming by Acidic pH and a High K<sup>+</sup> Concentration Is Required for Efficient Uncoating of Influenza A Virus Cores after Penetration. *Journal of Virology* 88:13029.
53. Plotch SJ, Bouloy M, Ulmanen I, Krug RM. 1981. A unique cap(m7GpppXm)-dependent influenza virion endonuclease cleaves capped RNAs to generate the primers that initiate viral RNA transcription. *Cell* 23:847-858.
54. York A, Fodor E. 2013. Biogenesis, assembly, and export of viral messenger ribonucleoproteins in the influenza A virus infected cell. *RNA biology* 10.
55. Jorba N, Coloma R, Ortín J. 2009. Genetic trans-complementation establishes a new model for influenza virus RNA transcription and replication. *PLoS pathogens* 5:e1000462-e1000462.



56. York A, Hengrung N, Vreede FT, Huiskonen JT, Fodor E. 2013. Isolation and characterization of the positive-sense replicative intermediate of a negative-strand RNA virus. *Proceedings of the National Academy of Sciences of the United States of America* 110:E4238-E4245.
57. Shimizu T, Takizawa N, Watanabe K, Nagata K, Kobayashi N. 2011. Crucial role of the influenza virus NS2 (NEP) C-terminal domain in M1 binding and nuclear export of vRNP. *FEBS Lett* 585:41-6.
58. Akarsu H, Burmeister WP, Petosa C, Petit I, Muller CW, Ruigrok RW, Baudin F. 2003. Crystal structure of the M1 protein-binding domain of the influenza A virus nuclear export protein (NEP/NS2). *Embo j* 22:4646-55.
59. Amorim MJ, Bruce EA, Read EKC, Foeglein Á, Mahen R, Stuart AD, Digard P. 2011. A Rab11- and Microtubule-Dependent Mechanism for Cytoplasmic Transport of Influenza A Virus Viral RNA. *Journal of Virology* 85:4143.
60. Chen BJ, Leser GP, Morita E, Lamb RA. 2007. Influenza Virus Hemagglutinin and Neuraminidase, but Not the Matrix Protein, Are Required for Assembly and Budding of Plasmid-Derived Virus-Like Particles. *Journal of Virology* 81:7111.
61. Burnet FM, McCrea JF, Anderson SG. 1947. Mucin as Substrate of Enzyme Action by Viruses of the Mumps Influenza Group. *Nature* 160:404-405.
62. Basak S, Tomana M, Compans RW. 1985. Sialic acid is incorporated into influenza hemagglutinin glycoproteins in the absence of viral neuraminidase. *Virus Research* 2:61-68.
63. Wilson IA, Skehel JJ, Wiley DC. 1981. Structure of the haemagglutinin membrane glycoprotein of influenza virus at 3 Å resolution. *Nature* 289:366-373.
64. Skehel JJ, Wiley DC. 2000. Receptor Binding and Membrane Fusion in Virus Entry: The Influenza Hemagglutinin. *Annual Review of Biochemistry* 69:531-569.
65. Smrt ST, Lorieau JL. 2017. Membrane Fusion and Infection of the Influenza Hemagglutinin, p 37-54. *In* Atassi MZ (ed), *Protein Reviews: Volume 18* doi:10.1007/5584\_2016\_174. Springer Singapore, Singapore.
66. Huang RTC, Rott R, Klenk H-D. 1981. Influenza viruses cause hemolysis and fusion of cells. *Virology* 110:243-247.
67. Ivanovic T, Choi JL, Whelan SP, van Oijen AM, Harrison SC. 2013. Influenza-virus membrane fusion by cooperative fold-back of stochastically induced hemagglutinin intermediates. *eLife* 2:e00333.
68. Stieneke-Gröber A, Vey M, Angliker H, Shaw E, Thomas G, Roberts C, Klenk HD, Garten W. 1992. Influenza virus hemagglutinin with multibasic cleavage site is activated by furin, a subtilisin-like endoprotease. *The EMBO journal* 11:2407-2414.
69. Schalken JA, Roebroek AJ, Oomen PP, Wagenaar SS, Debruyne FM, Bloemers HP, Van de Ven WJ. 1987. fur gene expression as a discriminating marker for small cell and nonsmall cell lung carcinomas. *J Clin Invest* 80:1545-9.
70. Böttcher E, Matrosovich T, Beyerle M, Klenk H-D, Garten W, Matrosovich M. 2006. Proteolytic Activation of Influenza Viruses by Serine Proteases TMPRSS2 and HAT from Human Airway Epithelium. *Journal of Virology* 80:9896.
71. Chaipan C, Kobasa D, Bertram S, Glowacka I, Steffen I, Solomon Tsegaye T, Takeda M, Bugge TH, Kim S, Park Y, Marzi A, Pöhlmann S. 2009. Proteolytic Activation of the 1918 Influenza Virus Hemagglutinin. *Journal of Virology* 83:3200.
72. Chen J, Lee KH, Steinhauer DA, Stevens DJ, Skehel JJ, Wiley DC. 1998. Structure of the Hemagglutinin Precursor Cleavage Site, a Determinant of Influenza Pathogenicity and the Origin of the Labile Conformation. *Cell* 95:409-417.
73. Das DK, Govindan R, Nikic-Spiegel I, Krammer F, Lemke EA, Munro JB. 2018. Direct Visualization of the Conformational Dynamics of Single Influenza Hemagglutinin Trimers. *Cell* 174:926-937 e12.
74. Di Lella S, Herrmann A, Mair CM. 2016. Modulation of the pH Stability of Influenza Virus Hemagglutinin: A Host Cell Adaptation Strategy. *Biophys J* 110:2293-2301.

75. DuBois RM, Zaraket H, Reddivari M, Heath RJ, White SW, Russell CJ. 2011. Acid stability of the hemagglutinin protein regulates H5N1 influenza virus pathogenicity. *PLoS Pathog* 7:e1002398.
76. Russell CJ. 2014. Acid-Induced Membrane Fusion by the Hemagglutinin Protein and Its Role in Influenza Virus Biology, p 93-116. *In* Compans RW, Oldstone MBA (ed), *Influenza Pathogenesis and Control - Volume I* doi:10.1007/82\_2014\_393. Springer International Publishing, Cham.
77. Galloway SE, Reed ML, Russell CJ, Steinhauer DA. 2013. Influenza HA Subtypes Demonstrate Divergent Phenotypes for Cleavage Activation and pH of Fusion: Implications for Host Range and Adaptation. *PLOS Pathogens* 9:e1003151.
78. Traving C, Schauer R. 1998. Structure, function and metabolism of sialic acids. *Cellular and Molecular Life Sciences CMLS* 54:1330-1349.
79. Shinya K, Ebina M, Yamada S, Ono M, Kasai N, Kawaoka Y. 2006. Influenza virus receptors in the human airway. *Nature* 440:435-436.
80. van Riel D, Munster VJ, de Wit E, Rimmelzwaan GF, Fouchier RAM, Osterhaus ADME, Kuiken T. 2007. Human and Avian Influenza Viruses Target Different Cells in the Lower Respiratory Tract of Humans and Other Mammals. *The American Journal of Pathology* 171:1215-1223.
81. Shi Y, Wu Y, Zhang W, Qi J, Gao GF. 2014. Enabling the 'host jump': structural determinants of receptor-binding specificity in influenza A viruses. *Nature Reviews Microbiology* 12:822-831.
82. Lipsitch M, Barclay W, Raman R, Russell CJ, Belser JA, Cobey S, Kason PM, Lloyd-Smith JO, Maurer-Stroh S, Riley S, Beauchemin CA, Bedford T, Friedrich TC, Handel A, Herfst S, Murcia PR, Roche B, Wilke CO, Russell CA. 2016. Viral factors in influenza pandemic risk assessment. *eLife* 5:e18491.
83. Matrosovich M, Tuzikov A, Bovin N, Gambaryan A, Klimov A, Castrucci M, Donatelli I, Kawaoka Y. 2000. Early Alterations of the Receptor-Binding Properties of H1, H2, and H3 Avian Influenza Virus Hemagglutinins after Their Introduction into Mammals. *Journal of virology* 74:8502-12.
84. Liu Y, Childs RA, Matrosovich T, Wharton S, Palma AS, Chai W, Daniels R, Gregory V, Uhlenendorff J, Kiso M, Klenk H-D, Hay A, Feizi T, Matrosovich M. 2010. Altered Receptor Specificity and Cell Tropism of D222G Hemagglutinin Mutants Isolated from Fatal Cases of Pandemic A(H1N1) 2009 Influenza Virus. *Journal of Virology* 84:12069.
85. Childs RA, Palma AS, Wharton S, Matrosovich T, Liu Y, Chai W, Campanero-Rhodes MA, Zhang Y, Eickmann M, Kiso M, Hay A, Matrosovich M, Feizi T. 2009. Receptor-binding specificity of pandemic influenza A (H1N1) 2009 virus determined by carbohydrate microarray. *Nature Biotechnology* 27:797-799.
86. Gulati S, Smith DF, Cummings RD, Couch RB, Griesemer SB, St. George K, Webster RG, Air GM. 2013. Human H3N2 Influenza Viruses Isolated from 1968 To 2012 Show Varying Preference for Receptor Substructures with No Apparent Consequences for Disease or Spread. *PLOS ONE* 8:e66325.
87. Peng W, de Vries RP, Grant OC, Thompson AJ, McBride R, Tsogtbaatar B, Lee PS, Razi N, Wilson IA, Woods RJ, Paulson JC. 2017. Recent H3N2 Viruses Have Evolved Specificity for Extended, Branched Human-type Receptors, Conferring Potential for Increased Avidity. *Cell host & microbe* 21:23-34.
88. Lin YP, Xiong X, Wharton SA, Martin SR, Coombs PJ, Vachieri SG, Christodoulou E, Walker PA, Liu J, Skehel JJ, Gamblin SJ, Hay AJ, Daniels RS, McCauley JW. 2012. Evolution of the receptor binding properties of the influenza A(H3N2) hemagglutinin. *Proceedings of the National Academy of Sciences* 109:21474.
89. Varghese JN, Laver WG, Colman PM. 1983. Structure of the influenza virus glycoprotein antigen neuraminidase at 2.9 Å resolution. *Nature* 303:35-40.
90. Harris A, Cardone G, Winkler DC, Heymann JB, Brecher M, White JM, Steven AC. 2006. Influenza virus pleiomorphy characterized by cryoelectron tomography. *Proceedings of the National Academy of Sciences* 103:19123.
91. Blok J, Air GM. 1982. Variation in the membrane-insertion and "stalk" sequences in eight subtypes of influenza type A virus neuraminidase. *Biochemistry* 21:4001-4007.

92. García-Sastre A, Palese P. 1995. The cytoplasmic tail of the neuraminidase protein of influenza A virus does not play an important role in the packaging of this protein into viral envelopes. *Virus Research* 37:37-47.
93. Bilsel P, Castrucci MR, Kawaoka Y. 1993. Mutations in the cytoplasmic tail of influenza A virus neuraminidase affect incorporation into virions. *Journal of virology* 67:6762-6767.
94. Jin H, Leser GP, Zhang J, Lamb RA. 1997. Influenza virus hemagglutinin and neuraminidase cytoplasmic tails control particle shape. *The EMBO journal* 16:1236-1247.
95. Barman S, Adhikary L, Chakrabarti AK, Bernas C, Kawaoka Y, Nayak DP. 2004. Role of transmembrane domain and cytoplasmic tail amino acid sequences of influenza a virus neuraminidase in raft association and virus budding. *Journal of virology* 78:5258-5269.
96. Air GM. 2012. Influenza neuraminidase. *Influenza Other Respir Viruses* 6:245-56.
97. Barman S, Nayak DP. 2000. Analysis of the Transmembrane Domain of Influenza Virus Neuraminidase, a Type II Transmembrane Glycoprotein, for Apical Sorting and Raft Association. *Journal of Virology* 74:6538.
98. Ernst AM, Zacherl S, Herrmann A, Hacke M, Nickel W, Wieland FT, Brugger B. 2013. Differential transport of Influenza A neuraminidase signal anchor peptides to the plasma membrane. *FEBS Lett* 587:1411-7.
99. Kundu A, Jabbar MA, Nayak DP. 1991. Cell surface transport, oligomerization, and endocytosis of chimeric type II glycoproteins: role of cytoplasmic and anchor domains. *Molecular and Cellular Biology* 11:2675.
100. Nordholm J, da Silva DV, Damjanovic J, Dou D, Daniels R. 2013. Polar residues and their positional context dictate the transmembrane domain interactions of influenza A neuraminidases. *J Biol Chem* 288:10652-60.
101. da Silva DV, Nordholm J, Madjo U, Pfeiffer A, Daniels R. 2013. Assembly of subtype 1 influenza neuraminidase is driven by both the transmembrane and head domains. *J Biol Chem* 288:644-53.
102. Park S, Il Kim J, Lee I, Bae JY, Yoo K, Nam M, Kim J, Sook Park M, Song KJ, Song JW, Kee SH, Park MS. 2017. Adaptive mutations of neuraminidase stalk truncation and deglycosylation confer enhanced pathogenicity of influenza A viruses. *Sci Rep* 7:10928.
103. Blumenkrantz D, Roberts KL, Shelton H, Lycett S, Barclay WS. 2013. The Short Stalk Length of Highly Pathogenic Avian Influenza H5N1 Virus Neuraminidase Limits Transmission of Pandemic H1N1 Virus in Ferrets. *Journal of Virology* 87:10539.
104. Sun Y, Tan Y, Wei K, Sun H, Shi Y, Pu J, Yang H, Gao GF, Yin Y, Feng W, Perez DR, Liu J. 2013. Amino Acid 316 of Hemagglutinin and the Neuraminidase Stalk Length Influence Virulence of H9N2 Influenza Virus in Chickens and Mice. *Journal of Virology* 87:2963.
105. Bi Y, Xiao H, Chen Q, Wu Y, Fu L, Quan C, Wong G, Liu J, Haywood J, Liu Y, Zhou B, Yan J, Liu W, Gao GF. 2015. Changes in the length of the neuraminidase stalk region impacts H7N9 virulence in mice. *Journal of Virology* doi:10.1128/JVI.02553-15:JVI.02553-15.
106. Hoffmann TW, Munier S, Larcher T, Soubieux D, Ledevin M, Esnault E, Tourdes A, Croville G, Guérin JL, Quéré P, Volmer R, Naffakh N, Marc D. 2012. Length variations in the NA stalk of an H7N1 influenza virus have opposite effects on viral excretion in chickens and ducks. *Journal of virology* 86:584-588.
107. Els MC, Air GM, Murti KG, Webster RG, Laver WG. 1985. An 18-amino acid deletion in an influenza neuraminidase. *Virology* 142:241-247.
108. Castrucci MR, Kawaoka Y. 1993. Biologic importance of neuraminidase stalk length in influenza A virus. *Journal of virology* 67:759-764.
109. Matsuoka Y, Swayne DE, Thomas C, Rameix-Welti M-A, Naffakh N, Warnes C, Altholtz M, Donis R, Subbarao K. 2009. Neuraminidase stalk length and additional glycosylation of the hemagglutinin influence the virulence of influenza H5N1 viruses for mice. *Journal of virology* 83:4704-4708.

110. Bender C, Hall H, Huang J, Klimov A, Cox N, Hay A, Gregory V, Cameron K, Lim W, Subbarao K. 1999. Characterization of the Surface Proteins of Influenza A (H5N1) Viruses Isolated from Humans in 1997–1998. *Virology* 254:115-123.
111. Baigent SJ, McCauley JW. 2001. Glycosylation of haemagglutinin and stalk-length of neuraminidase combine to regulate the growth of avian influenza viruses in tissue culture. *Virus Research* 79:177-185.
112. McAuley JL, Gilbertson BP, Trifkovic S, Brown LE, McKimm-Breschkin JL. 2019. Influenza Virus Neuraminidase Structure and Functions. *Front Microbiol* 10:39.
113. Durrant JD, Bush RM, Amaro RE. 2016. Microsecond Molecular Dynamics Simulations of Influenza Neuraminidase Suggest a Mechanism for the Increased Virulence of Stalk-Deletion Mutants. *The journal of physical chemistry B* 120:8590-8599.
114. Burmeister WP, Ruigrok RW, Cusack S. 1992. The 2.2 Å resolution crystal structure of influenza B neuraminidase and its complex with sialic acid. *The EMBO journal* 11:49-56.
115. Russell RJ, Haire LF, Stevens DJ, Collins PJ, Lin YP, Blackburn GM, Hay AJ, Gamblin SJ, Skehel JJ. 2006. The structure of H5N1 avian influenza neuraminidase suggests new opportunities for drug design. *Nature* 443:45-49.
116. Xu X, Zhu X, Dwek RA, Stevens J, Wilson IA. 2008. Structural Characterization of the 1918 Influenza Virus H1N1 Neuraminidase. *Journal of Virology* 82:10493.
117. Li Q, Qi J, Zhang W, Vavricka CJ, Shi Y, Wei J, Feng E, Shen J, Chen J, Liu D, He J, Yan J, Liu H, Jiang H, Teng M, Li X, Gao GF. 2010. The 2009 pandemic H1N1 neuraminidase N1 lacks the 150-cavity in its active site. *Nature Structural & Molecular Biology* 17:1266-1268.
118. Sun X, Li Q, Wu Y, Wang M, Liu Y, Qi J, Vavricka CJ, Gao GF. 2014. Structure of Influenza Virus N7: the Last Piece of the Neuraminidase “Jigsaw” Puzzle. *Journal of Virology* 88:9197.
119. Varghese JN, McKimm-Breschkin JL, Caldwell JB, Kortt AA, Colman PM. 1992. The structure of the complex between influenza virus neuraminidase and sialic acid, the viral receptor. *Proteins: Structure, Function, and Bioinformatics* 14:327-332.
120. Saito T, Taylor G, Webster RG. 1995. Steps in maturation of influenza A virus neuraminidase. *Journal of Virology* 69:5011.
121. Colman PM, Varghese JN, Laver WG. 1983. Structure of the catalytic and antigenic sites in influenza virus neuraminidase. *Nature* 303:41-44.
122. Amaro RE, Swift RV, Votapka L, Li WW, Walker RC, Bush RM. 2011. Mechanism of 150-cavity formation in influenza neuraminidase. *Nature Communications* 2:388.
123. Laver WG, Colman PM, Webster RG, Hinshaw VS, Air GM. 1984. Influenza virus neuraminidase with hemagglutinin activity. *Virology* 137:314-323.
124. Webster RG, Air GM, Metzger DW, Colman PM, Varghese JN, Baker AT, Laver WG. 1987. Antigenic structure and variation in an influenza virus N9 neuraminidase. *Journal of virology* 61:2910-2916.
125. Nuss JM, Air GM. 1991. Transfer of the hemagglutinin activity of influenza virus neuraminidase subtype N9 into an N2 neuraminidase background. *Virology* 183:496-504.
126. Varghese JN, Colman PM, van Donkelaar A, Blick TJ, Sahasrabudhe A, McKimm-Breschkin JL. 1997. Structural evidence for a second sialic acid binding site in avian influenza virus neuraminidases. *Proceedings of the National Academy of Sciences* 94:11808.
127. Uhlenendorff J, Matrosovich T, Klenk H-D, Matrosovich M. 2009. Functional significance of the hemadsorption activity of influenza virus neuraminidase and its alteration in pandemic viruses. *Archives of Virology* 154:945-957.
128. Lai JCC, Garcia J-M, Dyason JC, Böhm R, Madge PD, Rose FJ, Nicholls JM, Peiris JSM, Haselhorst T, von Itzstein M. 2012. A Secondary Sialic Acid Binding Site on Influenza Virus Neuraminidase: Fact or Fiction? *Angewandte Chemie International Edition* 51:2221-2224.
129. Dai M, McBride R, Dortmans JCFM, Peng W, Bakkers MJG, de Groot RJ, van Kuppeveld FJM, Paulson JC, de Vries E, de Haan CAM. 2017. Mutation of the Second Sialic Acid-Binding Site, Resulting in Reduced Neuraminidase Activity, Preceded the Emergence of H7N9 Influenza A Virus. *Journal of virology* 91:e00049-17.

130. Kobasa D, Rodgers ME, Wells K, Kawaoka Y. 1997. Neuraminidase hemadsorption activity, conserved in avian influenza A viruses, does not influence viral replication in ducks. *Journal of virology* 71:6706-6713.
131. Rudino-Pinera E, Tunnah P, Crennell SJ, Webster RG, Laver WG, Garman EF. The Crystal Structure of Type a Influenza Virus Neuraminidase of the N6 Subtype Reveals the Existence of Two Separate Neu5Ac Binding Sites. <http://www.rcsb.org/structure/1W1X>.
132. Hirst GK. 1941. The Agglutination of Red Cells by Allantoic Fluid of Chick Embryos Infected with Influenza virus. *Science* 94:22.
133. Gottschalk A. 1956. Neuraminic acid; the functional group of some biologically active mucoproteins. *The Yale journal of biology and medicine* 28:525-537.
134. Jianzhi G, Wenfang X, Jie Z. 2007. Structure and Functions of Influenza Virus Neuraminidase. *Current Medicinal Chemistry* 14:113-122.
135. Taylor NR, von Itzstein M. 1994. Molecular Modeling Studies on Ligand Binding to Sialidase from Influenza Virus and the Mechanism of Catalysis. *Journal of Medicinal Chemistry* 37:616-624.
136. Takahashi T, Suzuki Y, Nishinaka D, Kawase N, Kobayashi Y, Hidari KI, Miyamoto D, Guo CT, Shortridge KF, Suzuki T. 2001. Duck and human pandemic influenza A viruses retain sialidase activity under low pH conditions. *J Biochem* 130:279-83.
137. Suzuki T, Takahashi T, Saito T, Guo C-T, Hidari KI-PJ, Miyamoto D, Suzuki Y. 2004. Evolutional analysis of human influenza A virus N2 neuraminidase genes based on the transition of the low-pH stability of sialidase activity1. *FEBS Letters* 557:228-232.
138. Takahashi T, Suzuki T. 2015. Low-pH Stability of Influenza A Virus Sialidase Contributing to Virus Replication and Pandemic. *Biological and Pharmaceutical Bulletin* 38:817-826.
139. Suzuki T, Takahashi T, Guo C-T, Hidari KIPJ, Miyamoto D, Goto H, Kawaoka Y, Suzuki Y. 2005. Sialidase activity of influenza A virus in an endocytic pathway enhances viral replication. *Journal of virology* 79:11705-11715.
140. Smith BJ, Huyton T, Joosten RP, McKimm-Breschkin JL, Zhang J-G, Luo CS, Lou M-Z, Labrou NE, Garrett TPJ. 2006. Structure of a calcium-deficient form of influenza virus neuraminidase: implications for substrate binding. *Acta Crystallographica Section D* 62:947-952.
141. Burmeister WP, Cusack S, Ruigrok RWH. 1994. Calcium is needed for the thermostability of influenza B virus neuraminidase. *Journal of General Virology* 75:381-388.
142. Wang M, Qi J, Liu Y, Vavricka CJ, Wu Y, Li Q, Gao GF. 2011. Influenza A virus N5 neuraminidase has an extended 150-cavity. *Journal of virology* 85:8431-8435.
143. Wang H, Dou D, Östbye H, Revol R, Daniels R. 2019. Structural restrictions for influenza neuraminidase activity promote adaptation and diversification. *Nature Microbiology* 4:2565-2577.
144. Mochalova L, Kurova V, Shtyrya Y, Korchagina E, Gambaryan A, Belyanchikov I, Bovin N. 2007. Oligosaccharide specificity of influenza H1N1 virus neuraminidases. *Archives of Virology* 152:2047-2057.
145. Garcia J-M, Lai JCC, Haselhorst T, Choy KT, Yen H-L, Peiris JSM, von Itzstein M, Nicholls JM. 2014. Investigation of the binding and cleavage characteristics of N1 neuraminidases from avian, seasonal, and pandemic influenza viruses using saturation transfer difference nuclear magnetic resonance. *Influenza and Other Respiratory Viruses* 8:235-242.
146. Kobasa D, Kodihalli S, Luo M, Castrucci MR, Donatelli I, Suzuki Y, Suzuki T, Kawaoka Y. 1999. Amino acid residues contributing to the substrate specificity of the influenza A virus neuraminidase. *Journal of virology* 73:6743-6751.
147. Baum LG, Paulson JC. 1991. The N2 neuraminidase of human influenza virus has acquired a substrate specificity complementary to the hemagglutinin receptor specificity. *Virology* 180:10-15.
148. Gambaryan AS, Matrosovich MN. 2015. What adaptive changes in hemagglutinin and neuraminidase are necessary for emergence of pandemic influenza virus from its avian precursor? *Biochemistry (Mosc)* 80:872-80.

149. Varki NM, Varki A. 2007. Diversity in cell surface sialic acid presentations: implications for biology and disease. *Laboratory Investigation* 87:851-857.
150. Varki A, Schnaar R, Schauer R. 2017. Sialic Acids and Other Nonulosonic Acids. In: Varki A, Cummings RD, Esko JD, et al., editors. *Essentials of Glycobiology* [Internet]. 3rd edition. Cold Spring Harbor (NY): Cold Spring Harbor Laboratory Press; 2015-2017 Chapter 15.
151. Ng PSK, Böhm R, Hartley-Tassell LE, Steen JA, Wang H, Lukowski SW, Hawthorne PL, Trezise AEO, Coloe PJ, Grimmond SM, Haselhorst T, von Itzstein M, Paton AW, Paton JC, Jennings MP. 2014. Ferrets exclusively synthesize Neu5Ac and express naturally humanized influenza A virus receptors. *Nature communications* 5:5750-5750.
152. Schauer R, Srinivasan GV, Coddeville B, Zanetta J-P, Guérardel Y. 2009. Low incidence of N-glycolylneuraminic acid in birds and reptiles and its absence in the platypus. *Carbohydrate Research* 344:1494-1500.
153. Stanley P, Taniguchi N, Aebi M. 2017. N-Glycans. In: Varki A, Cummings RD, Esko JD, et al., editors. *Essentials of Glycobiology* [Internet]. 3rd edition. Cold Spring Harbor (NY): Cold Spring Harbor Laboratory Press; 2015-2017 Chapter 9.
154. Brockhausen I, Stanley P. 2017. O-GalNAc Glycans. In: Varki A, Cummings RD, Esko JD, et al., editors. *Essentials of Glycobiology* [Internet]. 3rd edition. Cold Spring Harbor (NY): Cold Spring Harbor Laboratory Press; 2015-2017 Chapter 10.
155. Ablan S, Rawat SS, Blumenthal R, Puri A. 2001. Entry of influenza virus into a glycosphingolipid-deficient mouse skin fibroblast cell line. *Archives of Virology* 146:2227-2238.
156. Yang H, Carney PJ, Chang JC, Guo Z, Villanueva JM, Stevens J. 2015. Structure and receptor binding preferences of recombinant human A(H3N2) virus hemagglutinins. *Virology* 477:18-31.
157. Lai SK, Wang Y-Y, Wirtz D, Hanes J. 2009. Micro- and macrorheology of mucus. *Advanced Drug Delivery Reviews* 61:86-100.
158. Lillehoj EP, Kato K, Lu W, Kim KC. 2013. Chapter Four - Cellular and Molecular Biology of Airway Mucins, p 139-202. *In* Jeon KW (ed), *International Review of Cell and Molecular Biology*, vol 303. Academic Press.
159. Kim N, Duncan GA, Hanes J, Suk JS. 2016. Barriers to inhaled gene therapy of obstructive lung diseases: A review. *Journal of Controlled Release* 240:465-488.
160. Yang X, Steukers L, Forier K, Xiong R, Braeckmans K, Van Reeth K, Nauwynck H. 2014. A beneficiary role for neuraminidase in influenza virus penetration through the respiratory mucus. *PLoS One* 9:e110026.
161. Cohen M, Zhang X-Q, Senaati HP, Chen H-W, Varki NM, Schooley RT, Gagneux P. 2013. Influenza A penetrates host mucus by cleaving sialic acids with neuraminidase. *Virology journal* 10:321-321.
162. Kesimer M, Scull M, Brighton B, DeMaria G, Burns K, O'Neal W, Pickles RJ, Sheehan JK. 2009. Characterization of exosome-like vesicles released from human tracheobronchial ciliated epithelium: a possible role in innate defense. *FASEB journal : official publication of the Federation of American Societies for Experimental Biology* 23:1858-1868.
163. Gaymard A, Le Briand N, Frobert E, Lina B, Escuret V. 2016. Functional balance between neuraminidase and haemagglutinin in influenza viruses. *Clinical Microbiology and Infection* 22:975-983.
164. Byrd-Leotis L, Cummings RD, Steinhauer DA. 2017. The Interplay between the Host Receptor and Influenza Virus Hemagglutinin and Neuraminidase. *International journal of molecular sciences* 18:1541.
165. Vahey MD, Fletcher DA. 2019. Influenza A virus surface proteins are organized to help penetrate host mucus. *eLife* 8:e43764.
166. Couceiro JNSS, Paulson JC, Baum LG. 1993. Influenza virus strains selectively recognize sialyloligosaccharides on human respiratory epithelium; the role of the host cell in selection of hemagglutinin receptor specificity. *Virus Research* 29:155-165.

167. Xu R, Zhu X, McBride R, Nycholat CM, Yu W, Paulson JC, Wilson IA. 2012. Functional Balance of the Hemagglutinin and Neuraminidase Activities Accompanies the Emergence of the 2009 H1N1 Influenza Pandemic. *Journal of Virology* 86:9221.
168. Yen H-L, Liang C-H, Wu C-Y, Forrest HL, Ferguson A, Choy K-T, Jones J, Wong DD-Y, Cheung PP-H, Hsu C-H, Li OT, Yuen KM, Chan RWY, Poon LLM, Chan MCW, Nicholls JM, Krauss S, Wong C-H, Guan Y, Webster RG, Webby RJ, Peiris M. 2011. Hemagglutinin–neuraminidase balance confers respiratory-droplet transmissibility of the pandemic H1N1 influenza virus in ferrets. *Proceedings of the National Academy of Sciences* 108:14264.
169. Banks J, Plowright L. 2003. Additional Glycosylation at the Receptor Binding Site of the Hemagglutinin (HA) for H5 and H7 Viruses May Be an Adaptation to Poultry Hosts, but Does It Influence Pathogenicity? *Avian Diseases* 47:942-950.
170. Matrosovich M, Zhou N, Kawaoka Y, Webster R. 1999. The Surface Glycoproteins of H5 Influenza Viruses Isolated from Humans, Chickens, and Wild Aquatic Birds Have Distinguishable Properties. *Journal of Virology* 73:1146.
171. Ives JAL, Carr JA, Mendel DB, Tai CY, Lambkin R, Kelly L, Oxford JS, Hayden FG, Roberts NA. 2002. The H274Y mutation in the influenza A/H1N1 neuraminidase active site following oseltamivir phosphate treatment leave virus severely compromised both in vitro and in vivo. *Antiviral Research* 55:307-317.
172. Herlocher ML, Carr J, Ives J, Elias S, Truscon R, Roberts N, Monto AS. 2002. Influenza virus carrying an R292K mutation in the neuraminidase gene is not transmitted in ferrets. *Antiviral Research* 54:99-111.
173. Carr J, Ives J, Kelly L, Lambkin R, Oxford J, Mendel D, Tai L, Roberts N. 2002. Influenza virus carrying neuraminidase with reduced sensitivity to oseltamivir carboxylate has altered properties in vitro and is compromised for infectivity and replicative ability in vivo. *Antiviral Res* 54:79-88.
174. Ginting TE, Shinya K, Kyan Y, Makino A, Matsumoto N, Kaneda S, Kawaoka Y. 2012. Amino Acid Changes in Hemagglutinin Contribute to the Replication of Oseltamivir-Resistant H1N1 Influenza Viruses. *Journal of Virology* 86:121.
175. Samson M, Abed Y, Desrochers F-M, Hamilton S, Luttick A, Tucker SP, Pryor MJ, Boivin G. 2014. Characterization of Drug-Resistant Influenza Virus A(H1N1) and A(H3N2) Variants Selected & In Vitro with Laninamivir. *Antimicrobial Agents and Chemotherapy* 58:5220.
176. Hensley SE, Das SR, Gibbs JS, Bailey AL, Schmidt LM, Bennink JR, Yewdell JW. 2011. Influenza A virus hemagglutinin antibody escape promotes neuraminidase antigenic variation and drug resistance. *PloS one* 6:e15190-e15190.
177. Bloom JD, Gong LI, Baltimore D. 2010. Permissive Secondary Mutations Enable the Evolution of Influenza Oseltamivir Resistance. *Science* 328:1272.
178. Stevens J, Blixt O, Paulson JC, Wilson IA. 2006. Glycan microarray technologies: tools to survey host specificity of influenza viruses. *Nature Reviews Microbiology* 4:857-864.
179. Liang C-H, Wu C-Y. 2009. Glycan array: a powerful tool for glycomics studies. *Expert Review of Proteomics* 6:631-645.
180. Potier M, Mameli L, Bélisle M, Dallaire L, Melançon SB. 1979. Fluorometric assay of neuraminidase with a sodium (4-methylumbelliferyl- $\alpha$ -d-N-acetylneuraminate) substrate. *Analytical Biochemistry* 94:287-296.
181. Buxton RC, Edwards B, Juo RR, Voyta JC, Tisdale M, Bethell RC. 2000. Development of a Sensitive Chemiluminescent Neuraminidase Assay for the Determination of Influenza Virus Susceptibility to Zanamivir. *Analytical Biochemistry* 280:291-300.
182. Lambré CR, Terzidis H, Greffard A, Webster RG. 1991. An enzyme-linked lectin assay for sialidase. *Clinica Chimica Acta* 198:183-193.
183. Gulati U, Wu W, Gulati S, Kumari K, Waner JL, Air GM. 2005. Mismatched hemagglutinin and neuraminidase specificities in recent human H3N2 influenza viruses. *Virology* 339:12-20.

184. Zhu X, McBride R, Nycholat CM, Yu W, Paulson JC, Wilson IA. 2012. Influenza virus neuraminidases with reduced enzymatic activity that avidly bind sialic Acid receptors. *Journal of virology* 86:13371-13383.
185. Guo H, Rabouw H, Slomp A, Dai M, van der Vegt F, van Lent JWM, McBride R, Paulson JC, de Groot RJ, van Kuppeveld FJM, de Vries E, de Haan CAM. 2018. Kinetic analysis of the influenza A virus HA/NA balance reveals contribution of NA to virus-receptor binding and NA-dependent rolling on receptor-containing surfaces. *PLOS Pathogens* 14:e1007233.
186. Lai JCC, Karunaratna HMTK, Wong HH, Peiris JSM, Nicholls JM. 2019. Neuraminidase activity and specificity of influenza A virus are influenced by haemagglutinin-receptor binding. *Emerging Microbes & Infections* 8:327-338.
187. Kosik I, Yewdell JW. 2017. Influenza A virus hemagglutinin specific antibodies interfere with virion neuraminidase activity via two distinct mechanisms. *Virology* 500:178-183.
188. Hirst GK. 1942. The quantitative determination of influenza virus and antibodies by means of red cell agglutination. *The Journal of experimental medicine* 75:49-64.
189. Casalegno J-S, Ferraris O, Escuret V, Bouscambert M, Bergeron C, Linès L, Excoffier T, Valette M, Frobert E, Pillet S, Pozzetto B, Lina B, Ottmann M. 2014. Functional balance between the hemagglutinin and neuraminidase of influenza A(H1N1)pdm09 HA D222 variants. *PLoS one* 9:e104009-e104009.
190. Sakai T, Nishimura SI, Naito T, Saito M. 2017. Influenza A virus hemagglutinin and neuraminidase act as novel motile machinery. *Scientific reports* 7:45043-45043.
191. Sakai T, Takagi H, Muraki Y, Saito M. 2018. Unique Directional Motility of Influenza C Virus Controlled by Its Filamentous Morphology and Short-Range Motions. *Journal of virology* 92:e01522-17.
192. Benton DJ, Martin SR, Wharton SA, McCauley JW. 2015. Biophysical measurement of the balance of influenza a hemagglutinin and neuraminidase activities. *The Journal of biological chemistry* 290:6516-6521.
193. Mechaly A, Cohen H, Cohen O, Mazor O. 2016. A bilayer interferometry-based assay for rapid and highly sensitive detection of biowarfare agents. *Analytical Biochemistry* 506:22-27.
194. Auer S, Koho T, Uusi-Kerttula H, Vesikari T, Blazevic V, Hytönen VP. 2015. Rapid and sensitive detection of norovirus antibodies in human serum with a bilayer interferometry biosensor. *Sensors and Actuators B: Chemical* 221:507-514.
195. Takemoto DK, Skehel JJ, Wiley DC. 1996. A Surface Plasmon Resonance Assay for the Binding of Influenza Virus Hemagglutinin to Its Sialic Acid Receptor. *Virology* 217:452-458.
196. Sauter NK, Bednarski MD, Wurzburg BA, Hanson JE, Whitesides GM, Skehel JJ, Wiley DC. 1989. Hemagglutinins from two influenza virus variants bind to sialic acid derivatives with millimolar dissociation constants: a 500-MHz proton nuclear magnetic resonance study. *Biochemistry* 28:8388-8396.
197. Wang CC, Chen JR, Tseng YC, Hsu CH, Hung YF, Chen SW, Chen CM, Khoo KH, Cheng TJ, Cheng YSE, Jan JT, Wu CY, Ma C, Wong CH. 2009. Glycans on influenza hemagglutinin affect receptor binding and immune response. *Proceedings of the National Academy of Sciences* 106:18137.
198. Gallagher JR, McCraw DM, Torian U, Gulati NM, Myers ML, Conlon MT, Harris AK. 2018. Characterization of Hemagglutinin Antigens on Influenza Virus and within Vaccines Using Electron Microscopy. *Vaccines (Basel)* 6.



## Chapter 2

### **Substrate binding by the second sialic acid-binding site of influenza A virus N1 neuraminidase contributes to enzymatic activity**

Wenjuan Du<sup>a</sup>, Meiling Dai<sup>a</sup>, Zeshi Li<sup>b</sup>, Geert-Jan Boons<sup>b</sup>, Ben Peeters<sup>c</sup>, Frank J. M. van Kuppeveld<sup>a</sup>, Erik de Vries<sup>a</sup>, Cornelis A. M. de Haan<sup>a</sup>

<sup>a</sup> Virology Division, Department of Infectious Diseases and Immunology, Faculty of Veterinary Medicine, Utrecht University, Utrecht, The Netherlands

<sup>b</sup> Department of Chemical Biology and Drug Discovery, Utrecht Institute for Pharmaceutical Sciences, Bijvoet Center for Biomolecular Research, Utrecht University, Utrecht, The Netherlands

<sup>c</sup> Department of Virology, Wageningen Bioveterinary Research, Lelystad, The Netherlands

## **Abstract**

The influenza A virus (IAV) neuraminidase (NA) protein plays an essential role in the release of virus particles from cells and decoy receptors. The NA enzymatic activity presumably needs to match the activity of the IAV hemagglutinin (HA) attachment protein and the host sialic acid (SIA) receptor repertoire. We analyzed the enzymatic activities of N1 NA proteins derived from avian (H5N1) and human (H1N1) IAVs and analyzed the role of the 2<sup>nd</sup> SIA-binding site, located adjacent to the conserved catalytic site, therein. SIA-contact residues in the 2<sup>nd</sup> SIA-binding site of NA are highly conserved in avian, but not in human IAVs. All N1 proteins preferred cleaving  $\alpha$ 2,3- over  $\alpha$ 2,6-linked SIAs, even when their corresponding HA protein displayed a strict preference for  $\alpha$ 2,6-linked SIAs, indicating that the specificity of the NA protein does not need to fully match that of the corresponding HA protein. NA activity was affected by substitutions in the 2<sup>nd</sup> SIA-binding site that are observed in avian and human IAVs, at least when multivalent rather than monovalent substrates were used. These mutations included both SIA-contact residues and residues that do not directly interact with SIA in all three loops of the 2<sup>nd</sup> SIA-binding site. Substrate binding via the 2<sup>nd</sup> SIA-binding site enhanced the catalytic activity of N1. Our results indicate an important role for the N1 2<sup>nd</sup> SIA-binding site in binding to and cleavage of multivalent substrates. Mutation of the 2<sup>nd</sup> SIA-binding site was also shown to affect virus replication in vitro.

**Significance**

Avian and human influenza A viruses (IAVs) preferentially bind  $\alpha$ 2,3- or  $\alpha$ 2,6-linked sialic acids (SIAs), respectively. A functional balance between the hemagglutinin (HA) attachment and neuraminidase (NA) proteins is thought to be important for host tropism. What this balance entails at the molecular level is, however, not well understood. We now show that N1 proteins of both avian and human viruses prefer cleaving avian- over human-type receptors, although human viruses were relatively better in cleavage of the human-type receptors. In addition, we show that substitutions at different positions in the 2<sup>nd</sup> SIA-binding site found in NA proteins of human IAVs have a profound effect on binding and cleavage of multivalent, but not monovalent, receptors and affect virus replication. Our results indicate that the HA-NA balance can be tuned via modification of substrate binding via this site and suggest an important role of the 2<sup>nd</sup> SIA-binding site in host tropism.

## Introduction

Influenza A virus (IAV) particles contain a hemagglutinin (HA) protein that binds sialic acid (SIA)-containing receptors and a neuraminidase (NA) protein that cleaves SIA from sialosides. The NA protein is essential for release of virus particles from infected cells and decoy receptors (e.g. in mucus) and for preventing virion aggregation. The NA protein is also an important target of the immune response and antiviral drugs (1-3). The IAV NA protein appears, however, relatively understudied compared to the HA protein.

The IAV NA protein is a tetrameric, type II transmembrane protein, of which 9 subtypes are known (N1-N9). Its globular head domain is linked to the transmembrane domain via a thin stalk. Tetramerization of NA is required for enzymatic activity (4). The head domain contains the active site, which is composed of several highly conserved catalytic residues that contact SIA and structural residues that keep the catalytic residues in place (5, 6). In addition, the NA proteins of some IAVs have been shown to bind sialosides via a 2<sup>nd</sup> SIA binding-site that consists of three loops and is located next to the catalytic site (5,7, 29). Binding of substrates via the 2<sup>nd</sup> SIA-binding site enhances the catalytic activity of NA against these substrates (8, 9), although this has so far only been studied for N2 and N9 proteins. In general, most residues that contact SIA in the 2<sup>nd</sup> SIA-binding site are highly conserved in avian IAVs, but much less so in human IAVs (8, 10).

A functional balance between the IAV HA and NA proteins is thought to be important for efficient replication and transmission (11-13), although it is not clear what this functional balance entails at the molecular level. The optimal balance between the HA and NA proteins is probably adapted to the receptor repertoire of a specific host (12) and needs tuning when IAVs encounter the SIA repertoire of a new host or when IAVs acquire altered HA receptor-binding properties. The HA proteins of avian and human viruses generally prefer binding to  $\alpha$ 2,3- and  $\alpha$ 2,6-linked sialosides, respectively. The few studies that addressed the substrate specificity of NA proteins of human and avian viruses generally indicate preferred cleavage by all NAs of  $\alpha$ 2,3-linked SIAs (14, 15, 16). In these studies, however, monovalent soluble synthetic substrates or resialylated red blood cells were used, which are not representative of the multivalent substrates found in mucus or on host cells.

The enzymatic activity of the NA protein may be modified via mutation of the catalytic site residues, although these residues are generally highly conserved (5, 6). In addition, residues have been identified that affect the enzymatic activity of NA via long range interactions (16, 18). The overall NA enzymatic activity can also be adapted via modification of NA expression levels or NA folding and oligomerization (16). Alternatively, the NA enzymatic activity may be decreased by shortening the stalk domain, thereby reducing the substrate accessibility of the NA proteins in the context of virus particles

(reviewed in 19). More recently, it was shown for N2 and N9 that the enzymatic activity for multivalent substrates may also be adapted by manipulating the binding of these substrates to NA via the 2<sup>nd</sup> SIA-binding site (8, 9, 20). N2 proteins of human pandemic viruses were shown to display decreased SIA binding and cleavage due to mutation of a SIA-contact residue in the 370-loop of the 2<sup>nd</sup> SIA-binding site (8). For the N9 protein, which preferentially binds  $\alpha$ 2,3-linked sialosides, it was shown that substitution of a non-SIA-contact residue in the 400-loop could also affect binding and cleavage of substrates (9). To what extent other substitutions in the 2<sup>nd</sup> SIA-binding site and the 2<sup>nd</sup> SIA-binding site in other NA subtypes affect/contribute to binding and cleavage of multivalent substrates is not known.

N1 proteins have also been shown to bind SIA, presumably via their 2<sup>nd</sup> SIA-binding site, using saturation-transfer difference (STD)-NMR (21). N1 proteins of two human viruses displayed much lower affinity than N1 of an avian virus. The functional consequences of these differences in SIA binding are, however, not known. Furthermore, it is not known which substitutions in the 2<sup>nd</sup> SIA-binding site are responsible for the observed differences. In the present study, we made a comparative analysis of the enzymatic activity of NA proteins derived from highly pathogenic avian IAV H5N1, new pandemic human IAV H1N1 (H1N1pdm09), and a laboratory-adapted human IAV H1N1 (WSN) by using a recombinant soluble expression approach in combination with different mono- and multivalent substrates. The avian and human N1 proteins were shown to differ in their activity and specificity, although all NA proteins preferred cleavage of  $\alpha$ 2,3-linked SIAs when the glycoprotein fetuin was used as substrate. The N1 proteins derived from human viruses were, however, relatively better in cleaving  $\alpha$ 2,6-linked sialosides. Mutations were identified in the 2<sup>nd</sup> SIA-binding site, involving both SIA-contact and non-SIA-contact residues in all three loops, that affected activity and specificity of the N1 proteins. By using recombinant viruses, the 2<sup>nd</sup> SIA-binding site in N1 was also shown to affect virus replication in vitro. Our results indicate that the enzymatic activity and/or specificity of IAV N1 proteins may be modified by mutation of residues at different positions in the 2<sup>nd</sup> SIA-binding site, and that binding of substrates via the 2<sup>nd</sup> SIA-binding site plays an important role in N1 activity and virus replication.

## Results

Previously, we expressed recombinant soluble tetrameric versions of the N1 proteins derived from different highly pathogenic H5N1 viruses (A/duck/Hunan/795/2002, A/Vietnam/1194/04, A/turkey/Turkey/1/2005 and A/Hubei/1/2010; referred to as HN, VN, TK and HB NA proteins) and analysed their enzymatic activities using the monovalent substrate MUNANA (17). In the current study, we analysed the enzymatic activity of these proteins by enzyme-linked lectin assays (ELLAs) (9) using the glycoproteins fetuin and transferrin. Multivalent sialylated glycoproteins better mimic the substrates that NA proteins encounter in vivo than the monovalent MUNANA. Furthermore, the contribution of SIA binding via the 2<sup>nd</sup> SIA-binding site to NA catalytic activity cannot be observed with MUNANA, but only with multivalent substrates (8, 9). Fetuin contains mono-, bi-, and tri-antennary glycans with  $\alpha$ 2,3- and  $\alpha$ 2,6-linked SIAs in 2:1 ratio (22), while transferrin contains two bi-antennary N-linked glycan chains with only  $\alpha$ 2,6-linked SIAs (23, 24). Cleavage of SIAs from fetuin and transferrin by serially diluted NA proteins was quantified by analysing the binding of lectins with different binding specificities. ECA specifically recognizes glycans containing terminal Gal $\beta$ 1-4GlcNAc, which generally correspond to desialylated N-linked sugars (25), while PNA binds to terminal Gal $\beta$ 1-3GalNAc corresponding with desialylated O-linked glycans (26). MALI and SNA specifically bind  $\alpha$ 2,3- or  $\alpha$ 2,6-linked SIAs, respectively (27, 28).

Analysis of the relative specific activities of the different proteins when using the MUNANA substrate indicated that the HN, TK and HB proteins cleave this substrate 2- to 3-fold more efficiently than the VN protein (Fig. 1A), in agreement with previous results (17). A remarkably different result was obtained when the relative specific activity was determined with fetuin using ECA staining (Fig. 1B). While the specific activities of the HN, VN and TK proteins reflected the specific activity as determined with MUNANA, the specific activity of the HB protein was much higher with this substrate. This increase was smaller with transferrin, which only contains  $\alpha$ 2,6-linked sialosides (Fig. 1C), while similarly increased specific activities for the HB protein were obtained when other lectins in combination with fetuin were used (Fig. 2). Graphing the specific activities of each NA protein determined for each glycoprotein-lectin combination normalized to its MUNANA specific activity showed that all proteins preferred cleaving  $\alpha$ 2,3- (determined with fetuin-MALI) over  $\alpha$ 2,6- (determined with fetuin-SNA) linked SIAs (Fig. 2). In agreement herewith, the specific activities were higher when determined with fetuin-ECA than with transferrin-ECA. The HB protein displayed the largest preference for the cleavage of  $\alpha$ 2,3- over  $\alpha$ 2,6-linked SIAs in agreement with the much higher increase in the specific activity of this protein when fetuin-ECA was used compared to transferrin-ECA (Fig. 1B and C and Fig. 2).

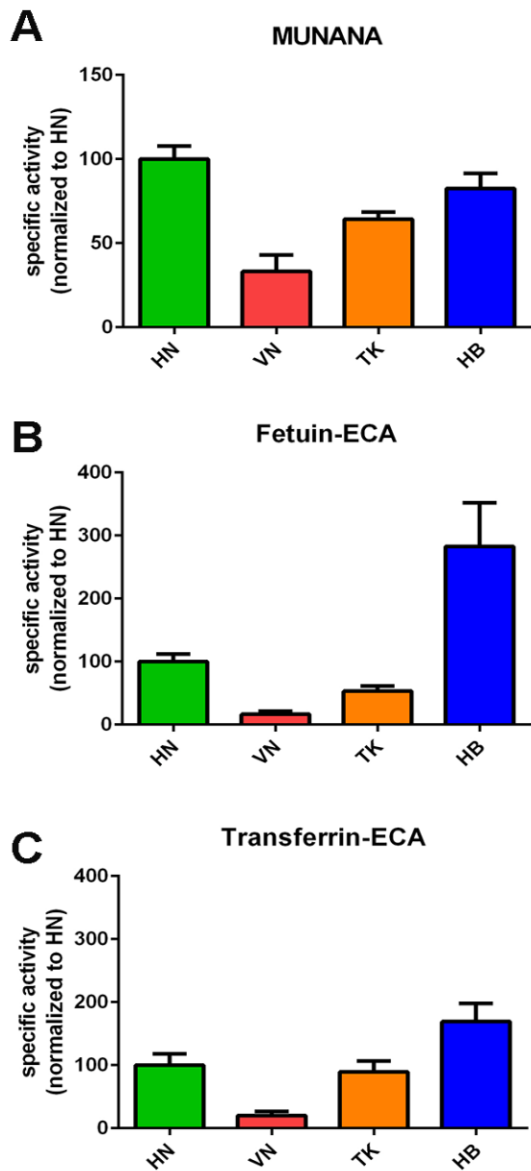


**Figure 1. Specific activity of H5N1 NA proteins using monovalent and multivalent substrates.**

(A) Specific activity of indicated H5N1 NA proteins using the substrate MUNANA is graphed normalized to the specific activity of NA HN. (B, C) Specific activity of indicated NA proteins was determined by ELLA using different glycoprotein-lectin combinations, Fetuin-ECA (B) and Transferrin-ECA (C), and graphed normalized to that of NA HN. Means of 3 independent experiments performed in triplicate are shown. Standard deviations are indicated.

Increased cleavage of sialosides present on fetuin, but not of MUNANA, by HB is indicative of increased binding of this NA protein to fetuin via its 2<sup>nd</sup> SIA-binding site. Sequence analysis of the H5N1 NA proteins showed that the HB protein differs from the others by mutation N369H in the 370 loop of the 2<sup>nd</sup> SIA binding site (Table 1 and Fig. 3). Although this substitution does not involve a SIA-contact residue according to available crystal structures (7, 29) (Fig. 4A and B), we analysed whether the observed increased cleavage of fetuin by the HB protein could be attributed to this mutation. To this end, we introduced the N369H mutation in the HN protein. As expected, this mutation did not appreciably affect the ability of the resulting protein (HN-N369H) to cleave MUNANA or transferrin (Fig. 5A and C). In contrast, this mutation resulted in a higher specific activity, which was similar to that of the HB protein, when fetuin was used as substrate (Fig. 5B).

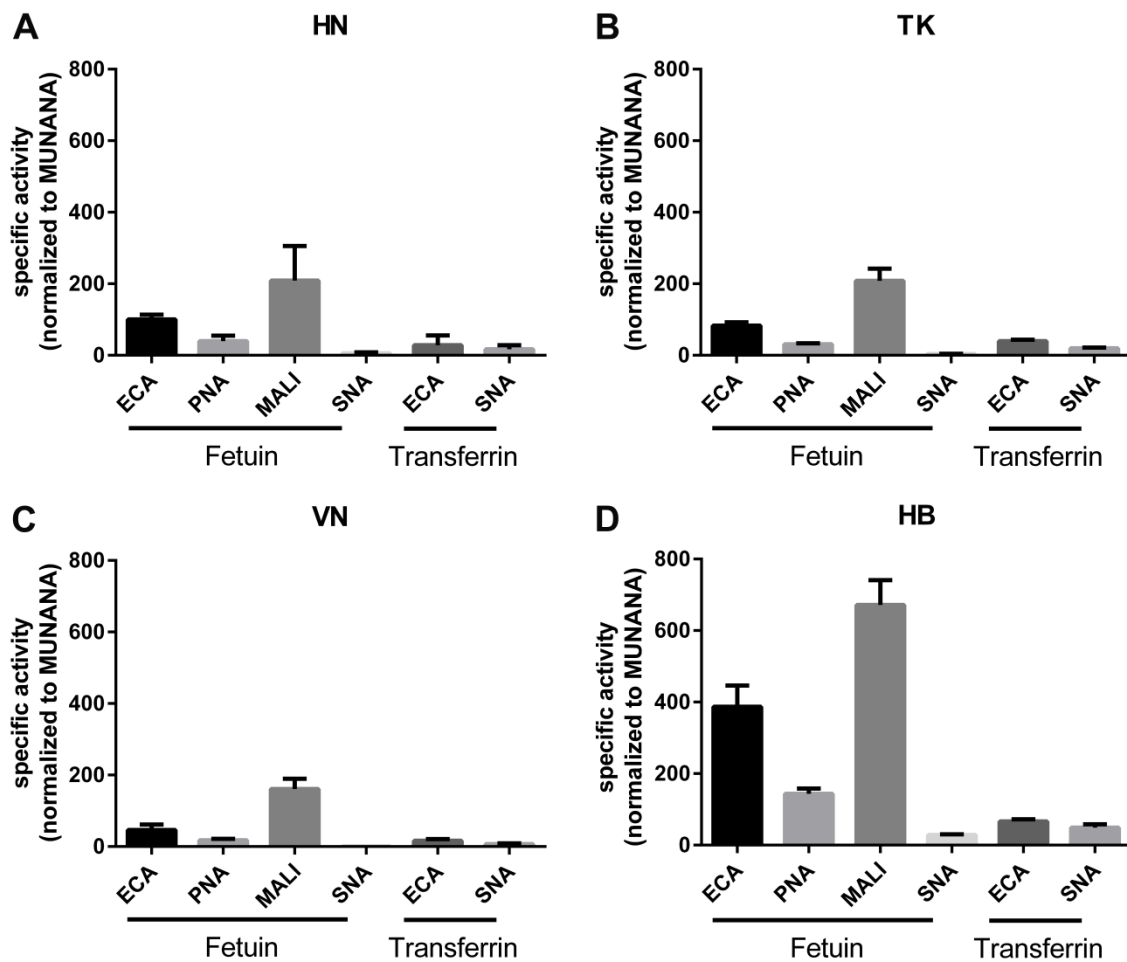


**Fig. 2. Specificity of H5N1 NA proteins.** The specific activities of the indicated H5N1 NA proteins were determined by ELLA using different glycoprotein-lectin combinations and graphed normalized to the specific activity determined with MUNANA. Means of 3 independent experiments performed in triplicate are shown. Standard deviations are indicated.

These results may be explained by the mutant HN and the HB proteins displaying increased binding to fetuin via their 2<sup>nd</sup> SIA-binding site. We were not able, however, to demonstrate binding of the N1 proteins to fetuin in a solid phase-binding assay or to chicken or human erythrocytes in a hemagglutination assay when the N1 proteins were complexed using antibodies similarly as described before (9). The N1 proteins were also negative in the hemagglutination assays when the antibody-NA complexes were linked to lumazine synthase nanoparticles (Fig. 6A). In this latter assay, which is more sensitive, the N9 protein of A/Anhui01/2013(H7N9) was shown to be hemagglutination positive, although it was previously found to be binding-negative (9). As an alternative assay, we expressed full



length, transmembrane domain-containing HB and HN NA proteins and generated membrane vesicles (30). Previously, we showed that these full length NA

**Table 1. Sequence alignment of 2<sup>nd</sup> SIA-binding site of N1 proteins used in this study**

N1 protein	370 loop <sup>a</sup>	400 loop	430 loop
Avian IAV			
HN/TK/VN	K <u>STNS</u> <u>SRSG</u>	A <u>ITD</u> <u>WS</u>	P <u>KE</u>
HB	K <u>STH</u> <u>SRSG</u>	A <u>ITD</u> <u>WS</u>	P <u>KE</u>
Human IAV			
WSN	K <u>SDSS</u> <u>SRH</u>	A <u>MTD</u> <u>RS</u>	P <u>EE</u>
CA/09	K <u>SISS</u> <u>SRN</u>	G <u>INE</u> <u>WS</u>	P <u>KE</u>
Mutant HN			
HN N369H	K <u>STH</u> <u>SRSG</u>	A <u>ITD</u> <u>WS</u>	P <u>KE</u>
HN TN-IS	K <u>SISS</u> <u>SRSG</u>	A <u>ITD</u> <u>WS</u>	P <u>KE</u>
HN TN-DS	K <u>SDSS</u> <u>SRSG</u>	A <u>ITD</u> <u>WS</u>	P <u>KE</u>
HN S372H	K <u>STNS</u> <u>RHG</u>	A <u>ITD</u> <u>WS</u>	P <u>KE</u>
HN S372N	K <u>STNS</u> <u>RNG</u>	A <u>ITD</u> <u>WS</u>	P <u>KE</u>
HN I400M	K <u>STNS</u> <u>SRSG</u>	A <u>MTD</u> <u>WS</u>	P <u>KE</u>
HN W403R	K <u>STNS</u> <u>SRSG</u>	A <u>ITD</u> <u>RS</u>	P <u>KE</u>
HN K432E	K <u>STNS</u> <u>SRSG</u>	A <u>ITD</u> <u>WS</u>	P <u>EE</u>
Other HN mutants	K <u>STNS</u> <u>SRSG</u>	A <u>ITD</u> <u>WS</u>	P <u>KE</u>

<sup>a</sup> Residues corresponding to the SIA contact-residues in the N9 protein (see Fig. 4; S367, S370, S372, I400, W403, K432) are underlined. Residues that differ between the HN and other N1 proteins in the 2<sup>nd</sup> SIA-binding site are coloured black. Mutations introduced in the HN protein are also coloured black.

proteins display similar expression levels and have the same specific activity for MUNANA (17). The membrane vesicles were analysed in a biolayer interferometry binding experiment using similar amounts of NA protein based on MUNANA activity (17) (Fig. 6B). Streptavidin sensors were coated with biotinylated synthetic glycans containing either  $\alpha$ 2,3- or  $\alpha$ 2,6-linked sialoglycans (3'SLNLNLN and 6'SLNLNLN, respectively). In the absence of the NA inhibitor oseltamivir carboxylate (OsC) no binding was observed. In the presence of OsC, which occupies the NA active site, HB but not HN-containing vesicles bound to sensors coated with 3'SLNLNLN, but not with 6'SLNLNLN. Also the HN-N369H protein-containing vesicles displayed binding specifically to 3'SLNLNLN, thereby confirming the importance of the 369 residue for binding via the 2<sup>nd</sup> SIA-binding site.

SIA-contact residues in the 2<sup>nd</sup> SIA-binding site are highly conserved in N2 proteins of avian IAVs, but much less so in human IAVs (8, 10). Also for N1, the conservation of the 2<sup>nd</sup> SIA-binding site appears lost in human IAVs (8, 10, 13), although a detailed analysis of the conservation of the 2<sup>nd</sup> SIA-binding site of avian and human viruses has not been performed. Therefore, we studied the conservation of the 3 loops of the 2<sup>nd</sup> SIA-binding site of N1 by generating sequence logos based on multiple sequence alignments using N1 sequences of avian and human viruses available via the Influenza Research Database (<https://www.fludb.org/>). While the SIA-contact residues are highly conserved in the N1 protein of avian viruses, it is clear that this conservation is lost for both the seasonal and the H1N1pdm09 viruses (Fig. 7). Both for the seasonal and the H1N1pdm09 viruses, the contact residue at position 372 is essentially invariably mutated. Interestingly, the residue at position 369 that is mutated in the HB compared to the HN protein is much less conserved compared to all other residues in the loops that constitute the 2<sup>nd</sup> SIA-binding site in N1 of avian viruses.

As a next step, we compared the enzymatic activity and specificity of the HN N1 protein with the N1 proteins of the H1N1pdm09 virus (referred to as CA/09) and the human (laboratory-adapted) H1N1 WSN virus (referred to as WSN) (Fig. 8A). The CA/09 and the WSN proteins displayed 2- to 3-fold lower specific activity than the HN protein when MUNANA was used. A similar (CA/09) or even larger (WSN) decrease in specific activity was observed with fetuin-ECA (Fig. 8B). The specific activities of CA/09 and WSN NA proteins were relatively higher with transferrin as substrate (Fig. 8C), with the CA/09 protein even displaying a similar specific activity as the HN protein. When the different specific activities are graphed relative to the MUNANA specific activity (Fig. 8D), it is clear that particularly the WSN protein displayed a decreased ability to cleave  $\alpha$ 2,3-linked SIAs (determined with fetuin-MALI). The CA/09 protein was relatively better in cleaving  $\alpha$ 2,6-linked SIAs than the HN protein, which was most apparent when transferrin was used as substrate.

Subsequently, we analysed to what extent the differences in the enzymatic activities between the different NA proteins could be attributed to changes in the 2<sup>nd</sup> SIA-binding site. In the 370 loop, HN NA differs from WSN NA at positions 368/369 (TN vs DS), while again other residues (IS) are found in the CA/09 protein at these positions (Table 1 and Fig. 3). In addition, S372, which unlike residues at position 368/369 is a SIA-contact residue (Fig. 4), is replaced with H in the WSN and with N in CA/09 protein. In the 400 and 430 loops, positions that are SIA-contact residues in N9 (Fig. 2) are substituted. In the 400 loop, residues I400 and W403 of HN are replaced in WSN NA with M and R, respectively. In the 430 loop, the K432E substitution is observed in WSN NA.

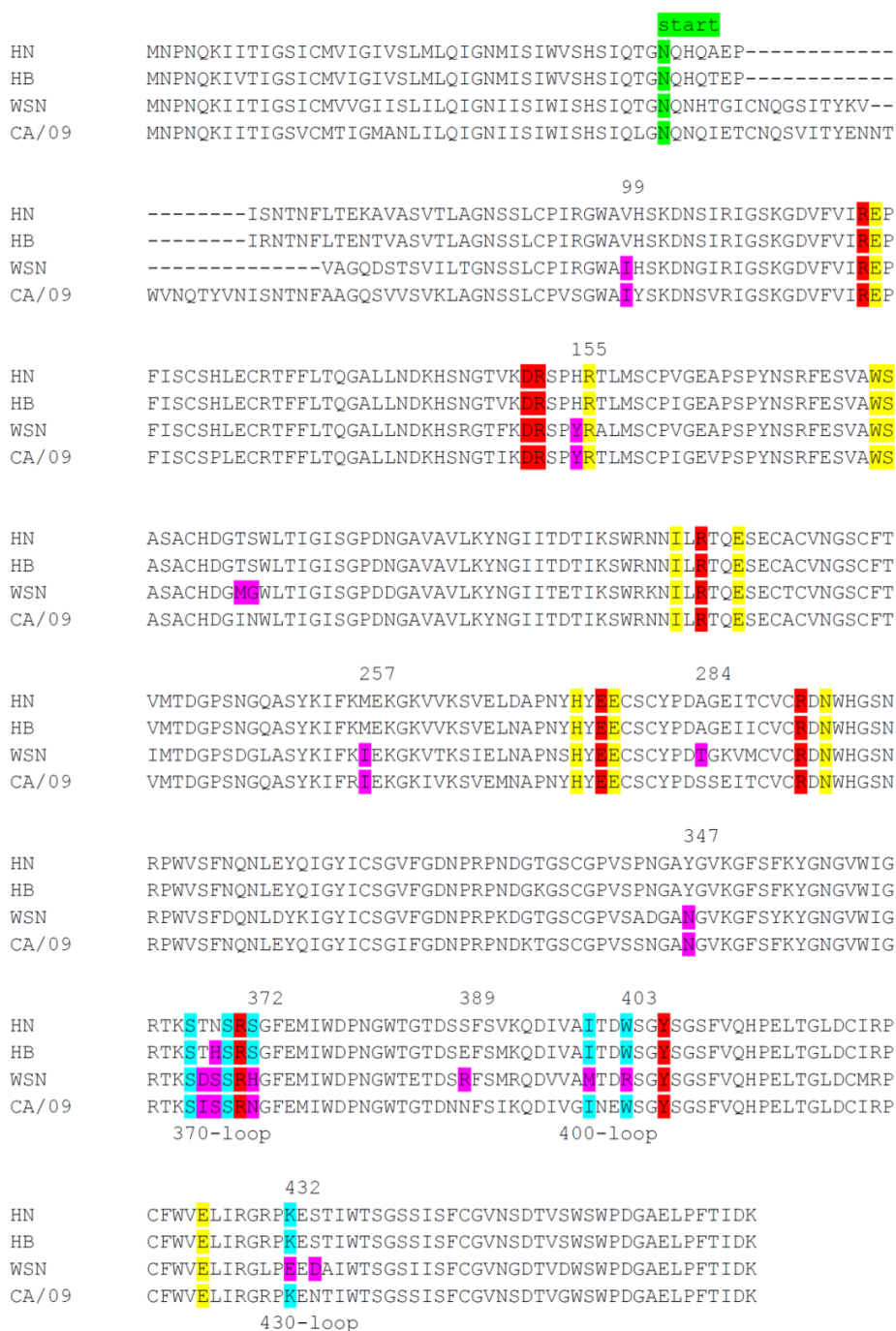


**Fig. 3. Alignment of N1 proteins.** Alignment of several N1 proteins analysed in this study is shown. Start of the N1 protein ectodomain expressed as a recombinant soluble fusion protein is indicated. Catalytic and framework residues in the active site are colored in red and yellow, respectively (5, 6). SIA-contact residues in the 2<sup>nd</sup> SIA-binding site, based on the N9 crystal structure (7) are coloured light blue. Residues introduced in HN N1 are coloured purple. N2 numbering is indicated.

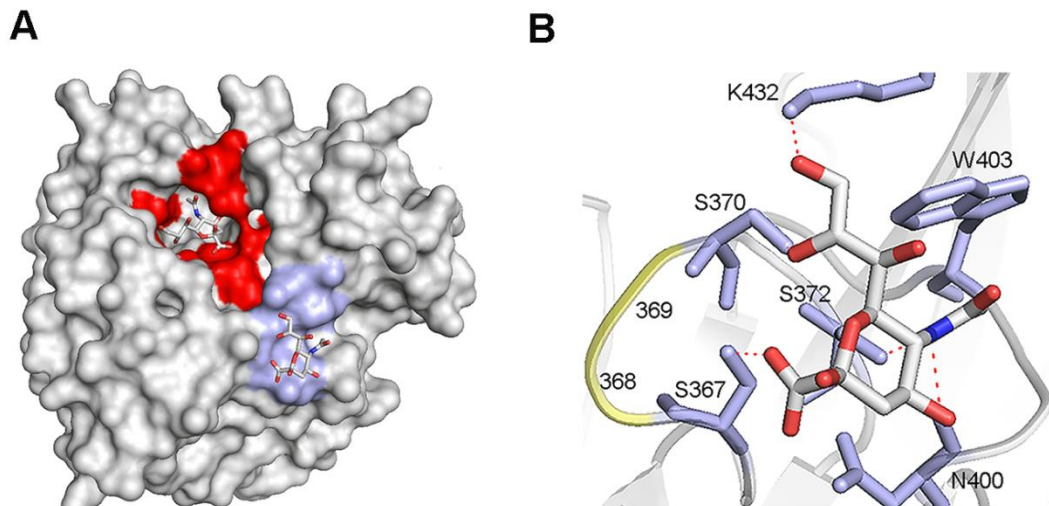


**Figure 4. Structure of the N9 2<sup>nd</sup> SIA-binding site.** (A-B) Crystal structure of N9 from A/tern/Australia/G70C/75 in complex with SIA Neu5Ac (PDB 1MWE)(7). (A) Surface representation. The NA active site and the 2<sup>nd</sup> SIA-binding site (SIA-contact residues) are coloured red and light blue, respectively. The Neu5Ac moieties in these sites are shown as sticks (oxygen in red; nitrogen in blue; carbon in gray). (B) Structure of the 2<sup>nd</sup> SIA-binding site. Neu5Ac is shown as sticks (oxygen in red; nitrogen in blue; carbon in gray). Residues in the 2<sup>nd</sup> SIA-binding site that directly contact Neu5Ac (S367, S370, S372, N400, W403 and K432) are shown in stick representation (light blue), amino acids at positions 368 and 369 that differ between HN and WSN, and CA/09, are shown in cartoon representation (yellow). Hydrogen bonds between Neu5Ac and residues in the 2<sup>nd</sup> SIA-binding site are shown as dashed red lines. Figures were made using PyMOL.

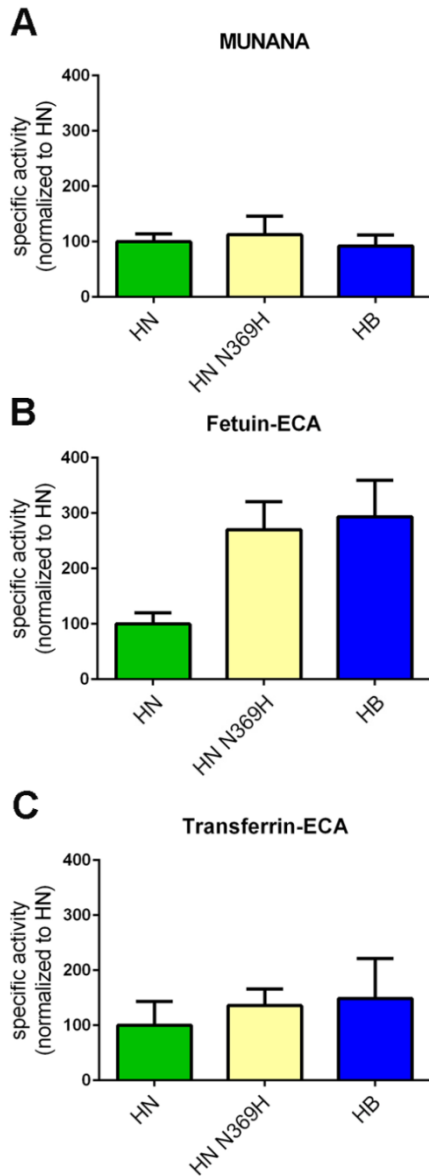


**Figure 5. Substitution N369H affects H5N1 NA enzymatic activity.** Specific activities of the indicated (mutant) H5N1 NA proteins determined by MUNANA assay (A) or by ELLA using fetuin (B) or transferrin (C) in combination with lectin ECA were graphed normalized to that of N1 HN. Means of two independent experiments performed in triplicate are shown. Standard deviations are indicated.

All the substitutions mentioned above were introduced in the background of the HN protein and the enzymatic activity of the resulting proteins was investigated using MUNANA, fetuin and transferrin as substrates. Mutation of the TN residues at position 368 and 369 in the 370-loop to IS or DS, had only limited effect on the cleavage of MUNANA (Fig. 9A). While the TN to IS substitutions had a small positive effect on the cleavage of both fetuin and transferrin, the TN to DS substitutions had a large negative effect on the cleavage of sialosides linked to fetuin. This negative effect was smaller when transferrin was used (Fig. 9B and C). As a result, the HN TN-DS protein was relatively better in cleaving  $\alpha$ 2,6-linked SIAs linked to transferrin (transferrin-ECA/SNA) than  $\alpha$ 2,3-linked SIAs linked to fetuin (fetuin-ECA/MALI) compared to the wild type HN and the HN TN-IS proteins (Fig. 10). These results indicate that, similar to the N369H mutation, substitutions of residues in the 370-loop of the 2<sup>nd</sup> SIA-

binding site not directly contacting SIA can affect cleavage of glycoprotein-linked sialosides. Most likely, this is not explained by these mutations affecting cleavage per se (as determined with MUNANA), but rather because they affect the interaction of the NA protein with multivalent substrates via the 2<sup>nd</sup> SIA-binding site. Mutation of the SIA-contact residue at position 372 into N or H (found in CA/09 and WSN N1 proteins, respectively) had no significant negative effects on the cleavage of MUNANA (Fig. 9A), while cleavage of both glycoproteins was consistently negatively affected (Fig. 9B and C), with the S372H mutation, found in WSN NA, having the largest negative effect.

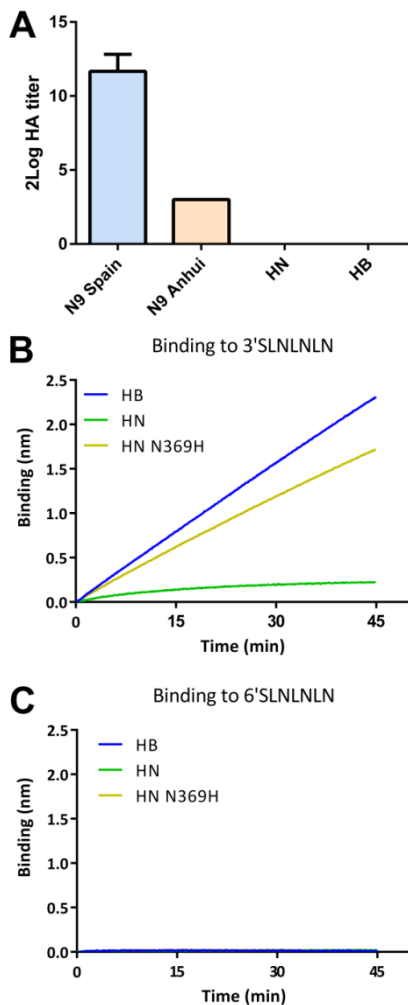


**Fig. 6. Substrate binding of NA proteins via the 2<sup>nd</sup> SIA-binding site.** A). HN and HB NA proteins, and N9 proteins with different binding properties (9) were complexed to lumazine synthase nanoparticles displaying domain B of protein A using anti-Strep tag monoclonal antibodies. Limiting dilutions of these complexes were incubated with red blood cells in the presence of OsC and hemagglutination titers were determined. Standard deviations are indicated. B). Membrane vesicles containing full length HN, HN N369H, or HB proteins were analyzed for their ability to bind 3'SLNLNLN or 6'SLNLNLN in the presence of OsC using biolayer interferometry. Representative experiments are shown.

Substitution of residues in the 400-loop either had a small negative effect on cleavage of all substrates including MUNANA (I400M) or specifically had a negative effect on the cleavage of sialosides linked to fetuin or transferrin (W403R) (Fig. 9A and B). While a N at position 400 was also shown to be a SIA-contact residue in the N9 protein (Fig. 4), this interaction may already be affected by the presence of an I in the HN protein, thereby explaining why the I400M mutation did not result in a specific negative affect on the cleavage of glycoprotein-linked glycans. The negative effect of the substitution at position

403 is in agreement with the W being a SIA-contact residue (Fig. 4). Interestingly, the negative effect of this latter substitution on the cleavage of transferrin-linked sialosides appeared larger than that of fetuin-linked sialosides (Fig. 9 and 10), suggesting that N1 proteins may also bind to some extent to  $\alpha$ 2,6-linked SIAs and that mutations in the 2<sup>nd</sup> SIA-binding site may differentially affect binding to  $\alpha$ 2,3- or  $\alpha$ 2,6-linked SIAs. The largest negative effect on the cleavage of fetuin-linked sialosides was observed when the SIA-contact residue in the 430-loop (i.e. K432) was substituted by E as observed in WSN NA (Fig. 9B). This substitution, which even resulted in increased cleavage of MUNANA (Fig. 9A), also decreased cleavage of transferrin-linked glycans (Fig. 9C), but to a smaller extent than the cleavage of fetuin-linked sialosides. In agreement herewith, the HN K432E NA protein displayed a much less pronounced preference for the cleavage of fetuin- over transferrin-linked sialosides (Fig. 10).

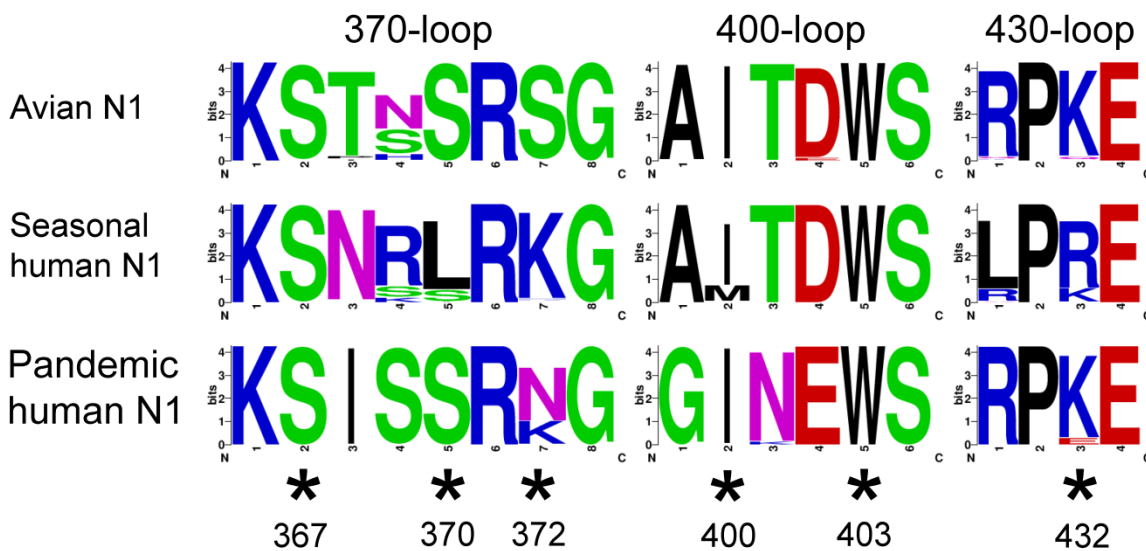


**Fig. 7. Sequence logos of the 2<sup>nd</sup> SIA-binding site of avian and human N1 proteins.** Sequence logos were generated for the three loops that constitute the 2<sup>nd</sup> SIA-binding site using the Weblogo website (<http://weblogo.berkeley.edu/>) (37) using all sequences available of avian N1 viruses, human N1 viruses prior to 2009 (Seasonal human N1) and human H1N1pdm09 viruses between 2009 and 2014 (Pandemic human N1) via the Influenza Research Database (<https://www.fludb.org/>). Asterisks indicate SIA-contact residues according to the N9 crystal structure (7).

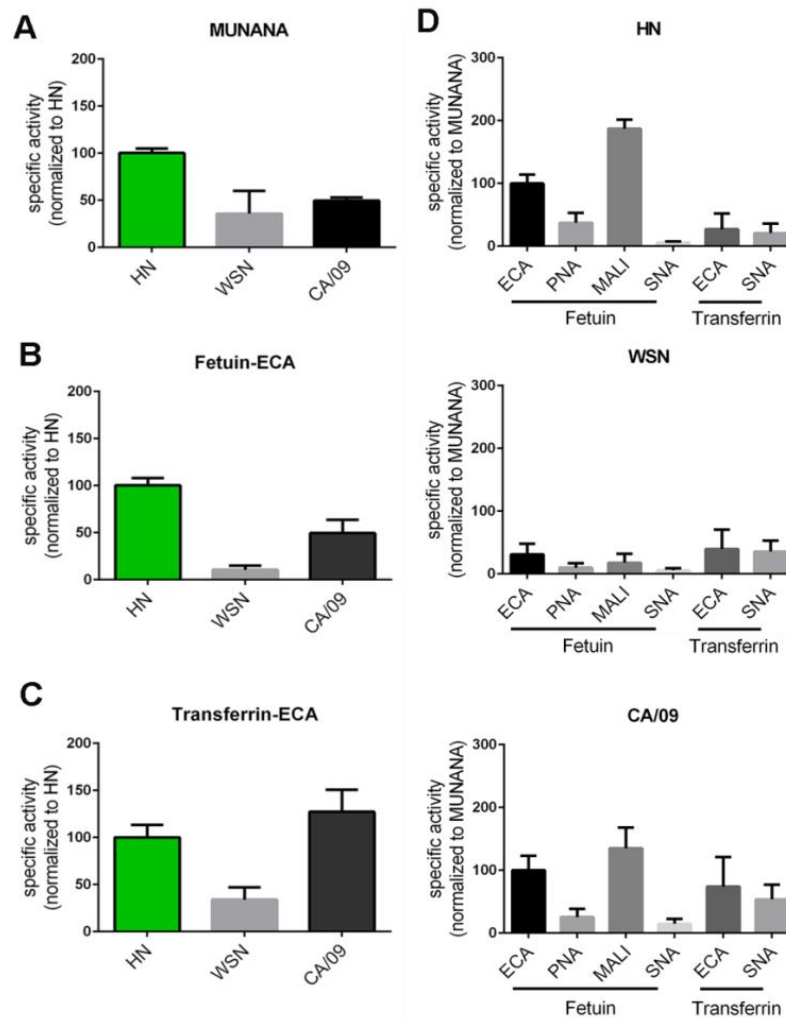


**Figure 8. Enzymatic activity of HN, WSN and CA/09 NA proteins using monovalent and multivalent substrates.** Specific activities of indicated N1 proteins determined by MUNANA assay (A) or by ELLA using fetuin (B) and transferrin (C) in combination with lectin ECA were graphed normalized to that of N1 HN. (D) Substrate specificities of the indicated N1 proteins were determined by ELLA using different glycoprotein-lectin combinations and graphed normalized to the specific activity determined with MUNANA. Means of 2-3 independent experiments performed in triplicate are shown for the MUNANA and ELLA assays. Standard deviations are indicated.

The CA/09 and the WSN proteins displayed much lower expression levels than the N1 proteins of the H5N1 viruses. For unknown reasons, these expression levels were reduced even more by the introduction of reciprocal mutations in the 2<sup>nd</sup> SIA-binding site of these proteins, which precluded further analysis in the solid phase cleavage assays. To determine the specificity of the observed effects of the substitutions in or close to the 2<sup>nd</sup> SIA-binding site, several other mutations found in WSN NA compared to the HN protein, at positions that are also substituted in the CA/09 protein (Fig. 3), were introduced in the HN protein and the specific activities of the resulting proteins were determined using



MUNANA as well as fetuin and transferrin. With the exception of the H155Y and the S434D mutations, these single and double substitutions (V99I, T5186/187MG, M257I, A284T, Y347N, S389R; N2 numbering) did not appreciably affect the specific activities of the mutant HN proteins regardless of the substrates used (Fig. 11). The H155Y substitution, located next to a framework residue (Fig. 3), resulted in reduced specific activity for all three substrates (Fig. 11A-C). The S434D mutation, which is located two residues downstream of the K432 residue (Fig. 3), reduced cleavage of sialosides linked to fetuin and transferrin (Fig. 11B and C), while the specific activity against MUNANA was not significantly affected (Fig. 11A). The S434D mutation may very well affect the conformation of the 430 loop and therefore substrate binding and cleavage.

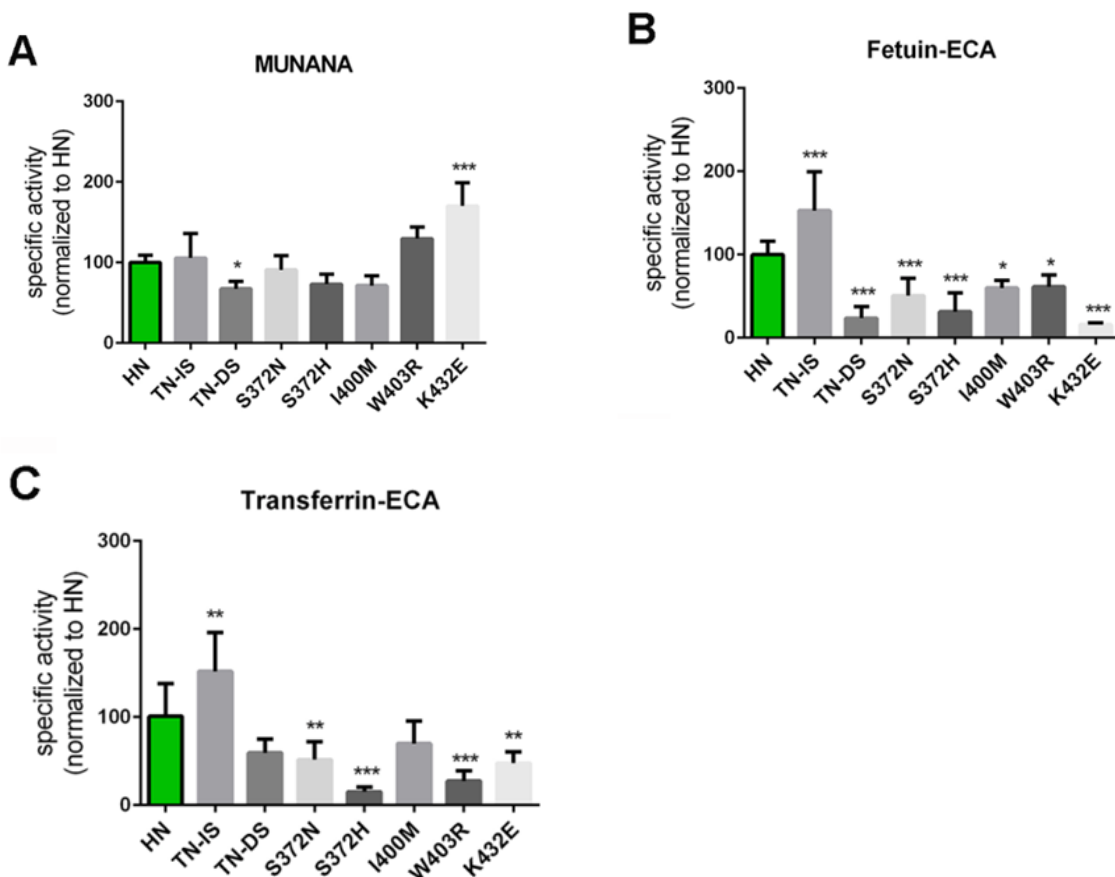


**Figure 9. Effect of substitutions in the 2<sup>nd</sup> SIA-binding site on NA enzymatic activity.** Specific activities of wild type and mutant HN determined by MUNANA assay (A) or by ELLA using fetuin (B) and transferrin (C) in combination with lectin ECA were graphed normalized to that of wild type HN. Means of 2-3 independent experiments performed in triplicate are shown. Standard deviations are indicated. The level of significance was expressed as \* $P < 0.05$ , \*\*  $P < 0.01$ , \*\*\*  $P < 0.001$ .

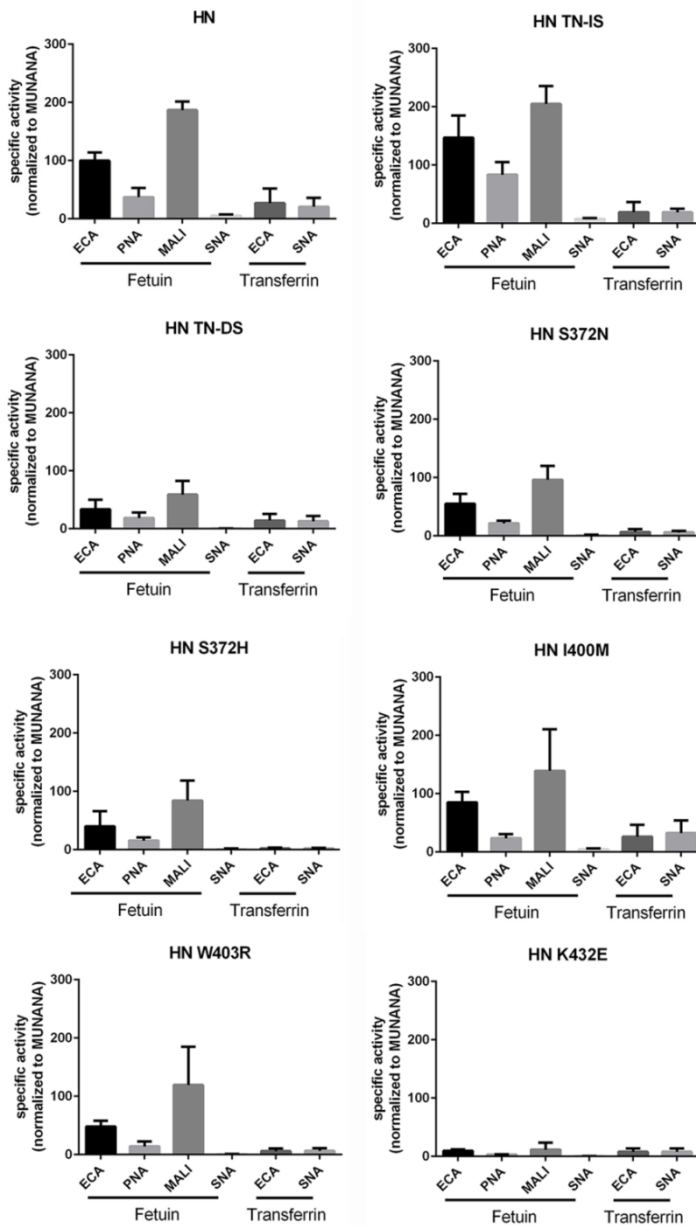


**Figure 10. Substrate specificity of mutant HN NA proteins.** Substrate specificities of indicated mutant HN proteins (same as shown in Fig. 5) were determined by ELLA using different glycoprotein-lectin combinations and graphed normalized to the specific activity determined with MUNANA. Means of 2-3 independent experiments performed in triplicate are shown. Standard deviations are indicated

In order to analyse the importance of the 2<sup>nd</sup> SIA-binding site for replication in vitro, recombinant H5N1 viruses were generated in the background of PR8 (6+2) with and without a functional 2<sup>nd</sup> SIA-binding site. These viruses carried the HN HA and NA genes. Plasmids used to generate viruses with the wild type and mutant N1 genes contained the AAA (K432) and GAG (E432) codon respectively. The K432E substitution had a large negative effect on the cleavage of fetuin- and transferrin-linked sialosides, but not MUNANA (Fig. 9). The wild type H5N1 virus was readily generated and its identity was confirmed by sequence analysis of the HA and NA genes. For the mutant H5N1 virus, however, already after one passage a large proportion contained the AAG codon encoding K432 as determined by sequence analysis of cloned PCR products. While the rapid reversion of the H5N1 mutant virus precluded detailed

analysis of the in vitro growth kinetics, it indicates that the presence of a functional 2<sup>nd</sup> SIA-binding site in N1 is beneficial for in vitro growth. We also generated recombinant PR8 viruses (7+1) carrying the wild type (K432) and mutant (E432) HN NA genes combined with the PR8 HA gene. The identity of these viruses was confirmed by sequence analysis. The virus carrying the wild type HN protein grew to significantly higher titers than the one with the mutant HN protein (Fig. 12), indicating that also when combined with PR8 HA, the 2<sup>nd</sup> SIA-binding site in N1 affects growth in vitro.

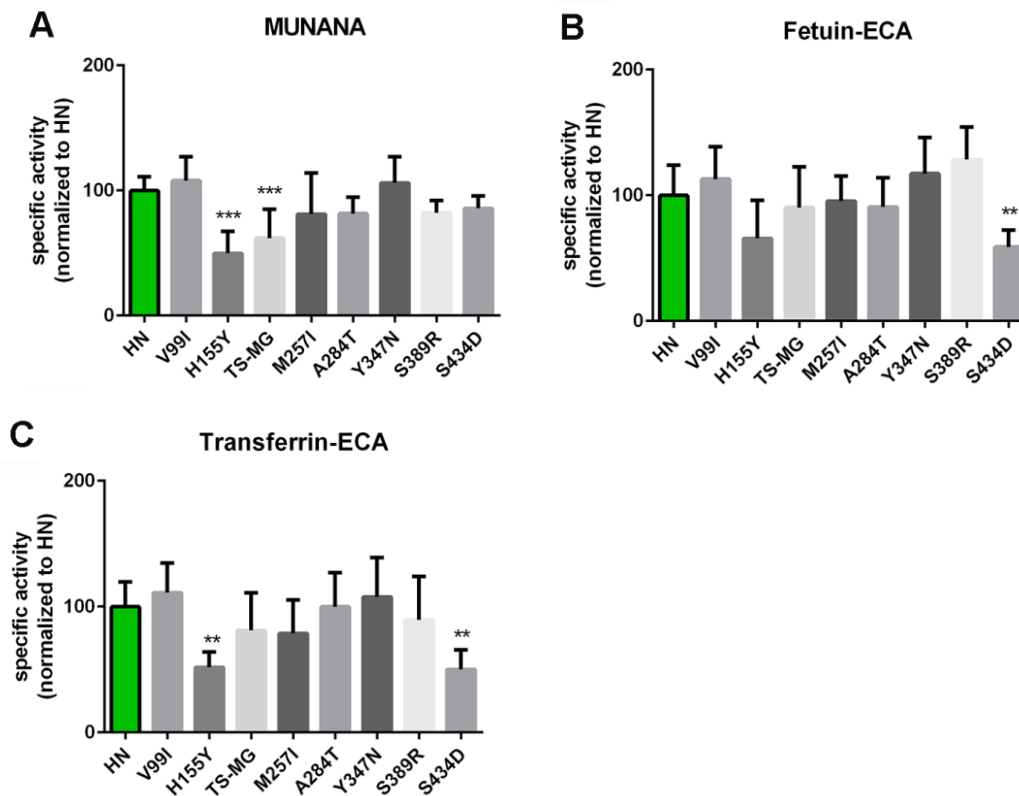


**Figure 11. Effect of substitutions outside the 2<sup>nd</sup> SIA-binding site on NA enzymatic activity.** Specific activities of wild type and mutant HN determined by MUNANA assay (A) or by ELLA using fetuin (B) or transferrin (C) in combination with lectin ECA were graphed normalized to that of wild type HN. Means of at least two independent experiments performed in triplicate are shown. Standard deviations are indicated. The level of significance was expressed as \* $P < 0.05$ , \*\*  $P < 0.01$ , \*\*\*  $P < 0.001$ .

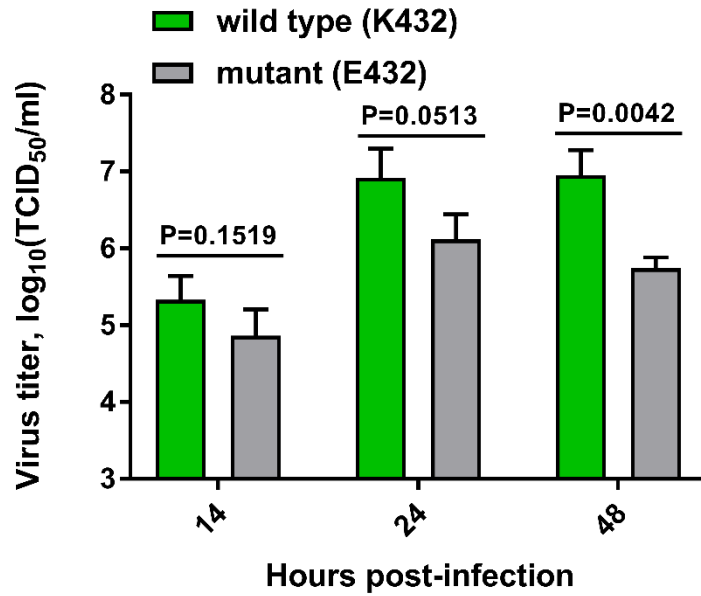


**Fig. 12. Replication of viruses with and without a 2<sup>nd</sup> SIA-binding site.** MDCK-II cells were infected with PR8 (7+1) viruses carrying wild type (K432) or mutant (E432) HN NA proteins at MOI 0.001. Virus in the supernatant at the indicated time points post-infection was titrated and expressed as log<sub>10</sub> (TCID<sub>50</sub>/ml). Means of three independent experiments are graphed. Standard deviations are indicated. Significant differences were analysed using the Student t test and the P values are shown.

## Discussion

In general, avian and human IAVs, including the H5N1 and H1N1 viruses analysed in this study (31-33), prefer binding to  $\alpha$ 2,3- or  $\alpha$ 2,6-linked sialosides, respectively. Nevertheless, all corresponding NA proteins preferentially cleaved  $\alpha$ 2,3-linked SIAs when fetuin, containing both types of sialosides, was used as substrate. The human H1N1 viruses were relatively better, however in cleaving  $\alpha$ 2,6-linked SIAs than the avian H5N1 viruses, which was also apparent when transferrin, which only contains  $\alpha$ 2,6-linked SIAs was used. Assuming that IAVs evolve an optimal HA-NA balance for their replication, these results indicate such a balance does not require the NA proteins to fully mimic the specificity of the corresponding HA protein. Our results furthermore indicate that the enzymatic activity of IAV N1 is considerably affected by the 2<sup>nd</sup> SIA-binding site. Most substitutions in this site had only a very limited effect on NA activity per se as measured with the monovalent MUNANA substrate. However, the effects were much larger, when the N1 proteins were analysed with solid phase-cleavage assays using multivalent glycoproteins, which better mimic the substrates found in mucus or on the cell surface. Our results indicate that binding of N1 to glycoprotein substrates is an important determinant of NA enzymatic activity and as this feature is strictly conserved in avian, but not in human viruses and was shown to affect virus replication in vitro, the 2<sup>nd</sup> SIA-binding site is likely to play an important role in host tropism.

Different mutations in the 2<sup>nd</sup> SIA-binding site were shown to have different effects on NA cleavage activity and specificity. While some mutations particularly affected cleavage of fetuin-linked glycans (N369H and TN368/369DS in the 370 loop, and K432E in the 430 loop), other mutations appeared to similarly affect cleavage of fetuin- and transferrin-linked sialosides (S372N/H and S434D) or even to have a larger effect on the cleavage of sialosides linked to transferrin (W403R). Furthermore, NA activity could not only be modified by mutation of SIA-contact residues in the 370 (8) (this study), 400 (8) (this study) and 430 loops (this study), but also by substitution of non-SIA-contact residues in the 370 loop (this study), the 400 loop (9) and the 430 loop (this study). Surprisingly, substitution of non-SIA-contact residues in the 370 loop (position 368/369) even resulted in larger effects than mutation of a contact residue (position 372) in this loop. Possibly, these non-SIA-contact residues interact with the penultimate galactose in the glycan chain. The most dramatic effects, however, were observed after substitution of the K432 residue in the 430 loop. Strikingly, while the residue at position 432 appears to be very important for binding and enzymatic activity of N1, for other NA subtypes this residue is less conserved than the other SIA-contact residues in the 2<sup>nd</sup> SIA-binding site of the NA proteins of avian IAVs. This may be related to the apparent lack of hydrogen bond interaction between the residue at position 432 and SIA in N2, N5 and N6 (29). Collectively, these results demonstrate the

large arsenal available to IAVs to modulate the activity of their NA proteins via the 2<sup>nd</sup> SIA-binding site, which is a thus far underappreciated feature.

Binding via the 2<sup>nd</sup> SIA-binding site enhances the catalytic activity of N1. The higher specific activity of the HB protein for fetuin, compared to that of the HN protein, can be attributed to a single mutation in the 2<sup>nd</sup> SIA-binding site (N369H), which specifically enhances binding to  $\alpha$ 2,3-linked sialosides (Fig. 6). In agreement herewith, this mutation has only a marginal effect on the cleavage of sialosides linked to transferrin, which only contains  $\alpha$ 2,6-linked SIAs (Fig. 5). Other mutations in the 2<sup>nd</sup> SIA-binding site, however, were shown to significantly affect cleavage of sialosides linked to transferrin (e.g. S372H or W403R; Fig. 8), suggesting that the HN N1 protein is also able to bind to some extent to  $\alpha$ 2,6-linked sialosides. The low receptor-binding avidity of the N1 proteins via their 2<sup>nd</sup> SIA-binding site precluded, however, detailed analysis of the N1 receptor-binding preference. Previously, we showed that N9 proteins only display appreciable binding to  $\alpha$ 2,3-linked sialosides via their 2<sup>nd</sup> SIA-binding site using glycan array analysis (9). In contrast, a N2 protein with a functional 2<sup>nd</sup> SIA-binding site was shown to hemadsorb erythrocytes containing either type of sialoside (8). To determine whether the receptor specificity of the 2<sup>nd</sup> SIA-binding site of different NA subtypes differs, a head-to-head comparison and more sensitive binding assays are needed. It is clear, however, that NA proteins of different subtypes may differ remarkably in their receptor binding avidity as demonstrated by the differences observed in the hemagglutination assay for the N9 and N1 proteins (Fig. 6B). Whether N1 proteins generally display a lower avidity than N9 proteins remains to be determined.

The H1N1pdm09 and the WSN viruses both contain several mutations in the 2<sup>nd</sup> SIA-binding site that negatively affect cleavage of specifically multivalent substrates. Substitutions in the 2<sup>nd</sup> SIA-binding site, which are observed in all pandemic human viruses (8, 10), may be selected as they tune the balance between the (novel) receptor repertoire of humans, the (altered) receptor binding-properties of HA and the enzymatic activity of NA. Alternatively, these mutations may be selected as a result of immune pressure on the surface-exposed 2<sup>nd</sup> SIA-binding site. The selective advantage of being able to bind to avian-type receptors via the 2<sup>nd</sup> SIA-binding site may be lost for human viruses carrying HA proteins that only bind to human-type receptors. The high conservation of the SIA-contact residues in the 2<sup>nd</sup> SIA-binding site of NA proteins of avian viruses suggests an important role for this binding site for virus replication and/or transmission of viruses carrying HA proteins preferring binding to avian-type receptors. Indeed, recombinant H5N1 virus carrying a mutated 2<sup>nd</sup> SIA-binding site, as a result of substitution K432E, rapidly reverted to a functional 2<sup>nd</sup> SIA-binding site through back mutation of the residue at position 432. The rapid reversion of this virus precluded detailed growth analysis, but also when combined with PR8 HA, which displays dual specificity for both human and avian receptors (38, 39), mutation of the 2<sup>nd</sup> SIA-binding site significantly affected in vitro growth. The importance of the

2<sup>nd</sup> SIA-binding site for replication and transmission in vivo remains to be established. Mutation of the 2<sup>nd</sup> SIA-binding site in a N2 protein, which reduced NA hemadsorption activity, negatively affected replication of a recombinant virus in chicken embryo fibroblasts, but strikingly not in ducks compared to the control virus (34). Of note, in these recombinant viruses, the NA proteins were combined with non-cognate HA proteins. Clearly more research on this topic is needed to irrefutably demonstrate the importance of the 2<sup>nd</sup> SIA-binding site for virus replication and transmission in vivo.

## Materials and Methods

**Protein expression and purification.** Expression plasmids encoding the NA ectodomain (head plus stalk domain) of A/duck/Hunan/795/2002(H5N1) (GenBank accession no. BAM85820.1; referred to as N1 HN), A/Vietnam/1194/04(H5N1) (GenBank accession no. AAT73327; referred to as N1 VN), A/turkey/Turkey/1/2005(H5N1) (GenBank accession no. ABQ58915.1; referred to as N1 TK), A/Hubei/1/2010(H5N1) (GenBank accession no. AEO89183.1; referred to as N1 HB), A/Anhui/1/2013(H7N9) (GISAID isolate EPI439507, referred to as N9 Anhui) and of A/Anas crecca/Spain/1460/2008(H7N9) (GenBank accession no. HQ244409.1, referred to as N9 Spain) fused to a *Staphylothermus marinus* tetrabrachion tetramerization domain and a double Strep-tag have been described previously (9, 17). Similar expression plasmids were constructed for the N1 protein of A/WSN/1933(H1N1) (Genbank accession no. AAA91328.1, referred to as N1 WSN) and A/California/04/2009(H1N1) (GenBank accession no. ACP41107.1, referred to as N1 CA/09). Mutations of interest were introduced into the corresponding NA genes by using the Q5 Site-Directed Mutagenesis Kit (New England Biolabs) and confirmed by sequencing. NA proteins were expressed by transfection of HEK293T cells (ATCC) with the NA gene-containing plasmids and the proteins were purified from the cell culture supernatants, similarly as described previously (35). Quantification of the purified proteins was performed by comparative coomassie gel staining using standard BSA samples (Sigma-Aldrich) with known concentrations as a reference.

**Enzyme activity assays.** The activity of N1 proteins toward the synthetic monovalent substrate MUNANA (Sigma-Aldrich) was determined by using a fluorometric assay similarly to what was described previously (17). The activities of the NA proteins toward multivalent glycoprotein substrates fetuin and transferrin were analyzed by ELLA similarly as described previously (9). While NA activity results in increased binding of the ECA and PNA lectins, which bind to desialylated glycans, decreased binding of MAL I and SNA is observed after NA cleavage as these latter two lectins bind to sialylated glycans. Lectin binding and MUNANA cleavage was measured after incubation of the substrates with limiting dilutions of NA. The amount of NA protein corresponding with half maximum lectin binding or MUNANA cleavage was determined from the resulting curves by fitting the data by nonlinear regression analysis using Prism 6.05 software (GraphPad) as described previously (9, 17). The reciprocal of this amount is a measure for the relative specific activity (activity per amount of protein).

**Hemagglutination assay.** The SIA-binding ability of NA proteins was analyzed using hemagglutination assays. Purified NA protein (4  $\mu$ g) was precomplexed with anti-Strep tag mouse antibody (IBA; 2  $\mu$ g) and with lumazine synthase nanoparticles genetically fused to domain B of protein A (0.25  $\mu$ g; (36) on ice for half an hour prior to incubation of limiting dilutions of these complexes with 0.5% human



erythrocytes for 2 hours at 4°C in the presence of 5 µM Zanamivir (GlaxoSmithKline). The hemagglutination assays were performed twice in duplicate. The mean values of these experiments are graphed.

**Biolayer interferometry.** HEK293T cells were transfected with expression plasmids encoding full length N1 HN and HB proteins (17) as described above. 72 hr post transfection, cells were vesiculated similarly as described previously (30), and vesicle preparations were purified using Capto Core 700 beads (GE Healthcare Life Sciences) according to the manufacturer's instructions. NA activity in the purified vesicle preparations was determined using the MUNANA assay described above. Similar amounts of NA activity, and thus NA protein (17), were applied in the Biolayer interferometry assays using the OctetRED384 (Fortebio) with streptavidin biosensors loaded to saturation with biotinylated 3'SLNLNLN or 6'SLNLNLN. Association of the NA containing vesicles was analyzed for 45 min in the absence or presence of 10µM OsC (Roche).

**Recombinant viruses.** Recombinant IAV containing the HN NA gene [from A/duck/Hunan/795/2002(H5N1)] combined with either its cognate HA gene (Accession number CY028963; 6+2 virus) or with the HA gene of strain A/Puerto Rico/8/34 H1N1 (PR8; 7+1 virus) in the genetic background of PR8 were generated by means of reverse genetics, using PR8 plasmids provided by drs Hoffmann and Webster (St. Jude Children's Research Hospital, Memphis) as described (40, 41). Ready-to-use plasmids consisting of synthetic H5 or N1 genes in vector pHW2000 were obtained from GenScript. The H5 and N1 genes were flanked by the 3' and 5' untranslated regions of the corresponding segments from PR8. The AAA codon encoding K432 in wild type HN N1, was replaced by the GAG codon encoding E432 in the mutant HN N1. The nucleotide sequence encoding the wild-type multi-basic amino-acid sequence was modified to encode a low-pathogenic cleavage site as described previously (41). Viruses were grown in MDCK-II cells.

**Statistical analysis.** The mean values of at least 2 experiments performed in duplicate/triplicate with independently generated protein preparations are graphed. All statistical analyses were performed by one-way analysis of variance (ANOVA) using Tukey's multiple comparisons test (Graph Pad Prism 6.05). The level of significance was expressed as \*P<0.05, \*\* P<0.01, \*\*\* P<0.001.

### **Acknowledgements**

M.D. and W.D. were supported by grants from the Chinese Scholarship Council. C.A.M.d.H. was supported by the Dutch Ministry of Economic Affairs, Agriculture, and Innovation, within the Castellum Project "Zoonotic Avian Influenza". The funders had no role in study design, data collection and analysis, decision to publish, or preparation of the manuscript. The authors thank Roche for kindly providing OsC and Olav de Leeuw for technical assistance.

## References

1. Yen, HL, Herlocher, LM, Hoffmann, E, Matrosovich, MN, Monto, AS, Webster, RG, Govorkova, EA. 2005. Neuraminidase inhibitor-resistant influenza viruses may differ substantially in fitness and transmissibility. *Antimicrob. Agents Chemother.* 49:4075-4084. doi: 49/10/4075.
2. Wohlbold, TJ, Nachbagauer, R, Xu, H, Tan, GS, Hirsh, A, Brokstad, KA, Cox, RJ, Palese, P, Krammer, F. 2015. Vaccination with adjuvanted recombinant neuraminidase induces broad heterologous, but not heterosubtypic, cross-protection against influenza virus infection in mice. *MBio.* 6:e02556-14. doi: 10.1128/mBio.02556-14.
3. Jiang, L, Fantoni, G, Couzens, L, Gao, J, Plant, E, Ye, Z, Eichelberger, MC, Wan, H. 2015. Comparative Efficacy of Monoclonal Antibodies That Bind to Different Epitopes of the 2009 Pandemic H1N1 Influenza Virus Neuraminidase. *J. Virol.* 90:117-128. doi: 10.1128/JVI.01756-15].
4. Saito, T, Taylor, G, Webster, RG. 1995. Steps in maturation of influenza A virus neuraminidase. *J. Virol.* 69:5011-5017.
5. Air, GM. 2012. Influenza neuraminidase. *Influenza and Other Respiratory Viruses.* 6:245-256.
6. Burmeister, WP, Ruigrok, RW, Cusack, S. 1992. The 2.2 Å resolution crystal structure of influenza B neuraminidase and its complex with sialic acid. *EMBO J.* 11:49-56.
7. Varghese, JN, Colman, PM, van Donkelaar, A, Blick, TJ, Sahasrabudhe, A, McKimm-Breschkin, JL. 1997. Structural evidence for a second sialic acid binding site in avian influenza virus neuraminidases. *Proc. Natl. Acad. Sci. U. S. A.* 94:11808-11812.
8. Uhlenhorff, J, Matrosovich, T, Klenk, H, Matrosovich, M. 2009. Functional significance of the hemadsorption activity of influenza virus neuraminidase and its alteration in pandemic viruses. *Arch. Virol.* 154:945-957.
9. Dai, M, McBride, R, Dortmans, JC, Peng, W, Bakkers, MJ, de Groot, RJ, van Kuppeveld, FJ, Paulson, JC, de Vries, E, de Haan, CA. 2017. Mutation of the 2<sup>nd</sup> Sialic Acid-Binding Site Resulting in Reduced Neuraminidase Activity Preceded Emergence of H7N9 Influenza A Virus. *J. Virol.* .;90:9457-70. doi: 10.1128/JVI.01346-16.
10. Kobasa, D, Rodgers, ME, Wells, K, Kawaoka, Y. 1997. Neuraminidase hemadsorption activity, conserved in avian influenza A viruses, does not influence viral replication in ducks. *J. Virol.* 71:6706-6713.
11. Yen, HL, Liang, CH, Wu, CY, Forrest, HL, Ferguson, A, Choy, KT, Jones, J, Wong, DD, Cheung, PP, Hsu, CH, Li, OT, Yuen, KM, Chan, RW, Poon, LL, Chan, MC, Nicholls, JM, Krauss, S, Wong, CH, Guan, Y, Webster, RG, Webby, RJ, Peiris, M. 2011. Hemagglutinin-neuraminidase balance confers respiratory-droplet transmissibility of the pandemic H1N1 influenza virus in ferrets. *Proc. Natl. Acad. Sci. U. S. A.* 108:14264-14269. doi: 10.1073/pnas.1111000108.
12. Xu, R, Zhu, X, McBride, R, Nycholat, CM, Yu, W, Paulson, JC, Wilson, IA. 2012. Functional balance of the hemagglutinin and neuraminidase activities accompanies the emergence of the 2009 H1N1 influenza pandemic. *J. Virol.* 86:9221-9232. doi: 10.1128/JVI.00697-12.
13. Gambaryan, A, Matrosovich, M. 2015. What adaptive changes in hemagglutinin and neuraminidase are necessary for emergence of pandemic influenza virus from its avian precursor? *Biochemistry (Moscow).* 80:872-880.
14. Franca de Barros, J,Jr, Sales Alviano, D, da Silva, MH, Dutra Wigg, M, Sales Alviano, C, Schauer, R, dos Santos Silva Couceiro, JN. 2003. Characterization of sialidase from an influenza A (H3N2) virus strain: kinetic parameters and substrate specificity. *Intervirology.* 46:199-206. doi: 72428.
15. Baum, LG, Paulson, JC. 1991. The N2 neuraminidase of human influenza virus has acquired a substrate specificity complementary to the hemagglutinin receptor specificity. *Virology.* 180:10-15.
16. Gerlach, T, Kühling, L, Uhlenhorff, J, Laukemper, V, Matrosovich, T, Czudai-Matwich, V, Schwalm, F, Klenk, HD, Matrosovich, M. 2012. Characterization of the neuraminidase of the H1N1/09 pandemic influenza virus. *Vaccine.* 30:7348-52.
17. Dai, M, Guo, H, Dortmans, J, Dekkers, J, Nordholm, J, Daniels, R, van Kuppeveld, FJ, de Vries, E, de Haan, CA. 2016. Identification of residues that affect oligomerization and/or enzymatic activity of influenza virus H5N1 neuraminidase proteins. *J. Virol.* . doi: JVI.01346-16.

18. Kobasa, D, Kodihalli, S, Luo, M, Castrucci, MR, Donatelli, I, Suzuki, Y, Suzuki, T, Kawaoka, Y. 1999. Amino acid residues contributing to the substrate specificity of the influenza A virus neuraminidase. *J. Virol.* 73:6743-6751.
19. Wagner, R, Matrosovich, M, Klenk, H. 2002. Functional balance between haemagglutinin and neuraminidase in influenza virus infections. *Rev. Med. Virol.* 12:159-166.
20. Benton, DJ, Wharton, SA, Martin, SR, McCauley, JW. 2017. Role of Neuraminidase in Influenza A(H7N9) Virus Receptor Binding. *J. Virol.* 91:10.1128/JVI.02293-16. Print 2017 Jun 1. doi: e02293-16.
21. Lai, JC, Garcia, J, Dyason, JC, Böhm, R, Madge, PD, Rose, FJ, Nicholls, JM, Peiris, J, Haselhorst, T, Von Itzstein, M. 2012. A secondary sialic acid binding site on influenza virus neuraminidase: fact or fiction? *Angewandte Chemie International Edition.* 51:2221-2224.
22. Baenziger, JU, Fiete, D. 1979. Structure of the complex oligosaccharides of fetuin. *J. Biol. Chem.* 254:789-795.
23. Montreuil, J. 1975. Complete structure of two carbohydrate units of human serotransferrin. *Studies on glycoconjugates XIV. FEBS Lett.* 50:296-304.
24. von Bonsdorff, L, Tölö, H, Lindeberg, E, Nyman, T, Harju, A, Parkkinen, J. 2001. Development of a pharmaceutical apotransferrin product for iron binding therapy. *Biologicals.* 29:27-37.
25. Wu, AM, Wu, JH, Tsai, M, Yang, Z, Sharon, N, Herp, A. 2007. Differential affinities of Erythrina cristagalli lectin (ECL) toward monosaccharides and polyvalent mammalian structural units. *Glycoconj. J.* 24:591-604.
26. Sharma, V, Srinivas, VR, Adhikari, P, Vijayan, M, Surolia, A. 1998. Molecular basis of recognition by Gal/GalNAc specific legume lectins: influence of Glu 129 on the specificity of peanut agglutinin (PNA) towards C2-substituents of galactose. *Glycobiology.* 8:1007-1012. doi: cwb103.
27. Geisler, C, Jarvis, DL. 2011. Effective glycoanalysis with Maackia amurensis lectins requires a clear understanding of their binding specificities. *Glycobiology.* 21:988-993.
28. Shibuya, N, Goldstein, IJ, Broekaert, WF, Nsimba-Lubaki, M, Peeters, B, Peumans, WJ. 1987. The elderberry (*Sambucus nigra* L.) bark lectin recognizes the Neu5Ac(alpha 2-6)Gal/GalNAc sequence. *J. Biol. Chem.* 262:1596-1601.
29. Sun, X, Li, Q, Wu, Y, Wang, M, Liu, Y, Qi, J, Vavricka, CJ, Gao, GF. 2014. Structure of influenza virus N7: the last piece of the neuraminidase "jigsaw" puzzle. *J. Virol.* 88:9197-9207. doi: 10.1128/JVI.00805-14.
30. Del Piccolo, N, Placone, J, He, L, Agudelo, SC, Hristova, K. 2012. Production of plasma membrane vesicles with chloride salts and their utility as a cell membrane mimetic for biophysical characterization of membrane protein interactions. *Anal. Chem.* 84:8650-8655. doi: 10.1021/ac301776j.
31. de Vries, RP, de Vries, E, Moore, KS, Rigter, A, Rottier, PJ, de Haan, CA. 2011. Only two residues are responsible for the dramatic difference in receptor binding between swine and new pandemic H1 hemagglutinin. *J. Biol. Chem.* 286:5868-5875. doi: 10.1074/jbc.M110.193557.
32. Wickramasinghe, IN, de Vries, RP, Grone, A, de Haan, CA, Verheije, MH. 2011. Binding of avian coronavirus spike proteins to host factors reflects virus tropism and pathogenicity. *J. Virol.* 85:8903-8912. doi: 10.1128/JVI.05112-11.
33. Leung, HS, Li, OT, Chan, RW, Chan, MC, Nicholls, JM, Poon, LL. 2012. Entry of influenza A Virus with an alpha2,6-linked sialic acid binding preference requires host fibronectin. *J. Virol.* 86:10704-10713. doi: 10.1128/JVI.01166-12.
34. Kobasa, D, Rodgers, ME, Wells, K, Kawaoka, Y. 1997. Neuraminidase hemadsorption activity, conserved in avian influenza A viruses, does not influence viral replication in ducks. *J. Virol.* 71:6706-6713.
35. Bosch, BJ, Bodewes, R, de Vries, RP, Kreijtz, JH, Bartelink, W, van Amerongen, G, Rimmelzwaan, GF, de Haan, CA, Osterhaus, AD, Rottier, PJ. 2010. Recombinant soluble, multimeric HA and NA exhibit distinctive types of protection against pandemic swine-origin 2009 A(H1N1) influenza virus infection in ferrets. *J. Virol.* 84:10366-10374. doi: 10.1128/JVI.01035-10.
36. Li, W, Hulswit, RJG, Widjaja, I, Raj, VS, McBride, R, Peng, W, Widagdo, W, Tortorici, MA, van Dieren, B, Lang, Y, van Lent, JWM, Paulson, JC, de Haan, CAM, de Groot, RJ, van Kuppeveld, FJM, Haagsma, BL, Bosch, BJ. 2017. Identification of sialic acid-binding function for the Middle East respiratory

- syndrome coronavirus spike glycoprotein. *Proc. Natl. Acad. Sci. U. S. A.* . 114:E8508-E8517. doi: 201712592.
37. Crooks, GE, Hon, G, Chandonia, JM, Brenner, SE. 2004. WebLogo: A sequence logo generator, *Genome Research*. 14:1188-1190
38. Gamblin, SJ, Haire, LF, Russell, RJ, Stevens, DJ, Xiao, B, Ha, Y, Vasisht, N, Steinhauer, DA, Daniels, RS, Elliot, A, Wiley, DC, Skehel, JJ. 2004The structure and receptor binding properties of the 1918 influenza hemagglutinin. *Science*. 303:1838-42.
39. Rogers, GN, D'Souza, BL. 1989. Receptor binding properties of human and animal H1 influenza virus isolates. *Virology*. 173:317-22.
40. Hoffmann, E, Krauss, S, Perez, D, Webby, R, Webster, RG. Eight-plasmid system for rapid generation of influenza virus vaccines. 2002. *Vaccine*. 20:3165-70.
41. Peeters, B, Reemers, S, Dortmans, J, de Vries, E, de Jong, M, van de Zande, S, Rottier, PJM, de Haan, CAM. 2017. Genetic versus antigenic differences among highly pathogenic H5N1 avian influenza A viruses: Consequences for vaccine strain selection. *Virology*. 503:83-93.



## Chapter 3

# The 2<sup>nd</sup> sialic acid-binding site of influenza A virus neuraminidase is an important determinant of the hemagglutinin neuraminidase-receptor balance

Wenjuan Du<sup>1</sup>, Hongbo Guo<sup>1</sup>, Vera S. Nijman<sup>1</sup>, Jennifer Doedt<sup>2</sup>, Erhard van der Vries<sup>1</sup>, Joline van der Lee<sup>1</sup>, Zeshi Li<sup>3</sup>, Geert-Jan Boons<sup>3</sup>, Frank J. M. van Kuppeveld<sup>1</sup>, Erik de Vries<sup>1</sup>, Mikhail Matrosovich<sup>2</sup>, Cornelis A. M. de Haan<sup>1</sup>

1 Virology Division, Faculty of Veterinary Medicine, Utrecht University, Utrecht, The Netherlands

2 Institute of Virology, Philipps University, Marburg, Germany

3 Department of Chemical Biology and Drug Discovery, Utrecht University, Utrecht, the Netherlands

## **Abstract**

Influenza A virus (IAV) neuraminidase (NA) receptor-destroying activity and hemagglutinin (HA) receptor-binding affinity need to be balanced with the host receptor repertoire for optimal viral fitness. NAs of avian, but not human viruses, contain a functional 2<sup>nd</sup> sialic acid (SIA)-binding site (2SBS) adjacent to the catalytic site, which contributes to sialidase activity against multivalent substrates. The receptor-binding specificity and potentially crucial contribution of the 2SBS to the HA-NA balance of virus particles is, however, poorly characterized. Here, we elucidated the receptor-binding specificity of the 2SBS of N2 NA and established an important role for this site in the virion HA-NA-receptor balance. NAs of H2N2/1957 pandemic virus with or without a functional 2SBS and viruses containing this NA were analysed. Avian-like N2, with a restored 2SBS due to an amino acid substitution at position 367, was more active than human N2 on multivalent substrates containing  $\alpha$ 2,3-linked SIAs, corresponding with the pronounced binding-specificity of avian-like N2 for these receptors. When introduced into human viruses, avian-like N2 gave rise to altered plaque morphology and decreased replication compared to human N2. An opposite replication phenotype was observed when N2 was combined with avian-like HA. Specific bio-layer interferometry assays revealed a clear effect of the 2SBS on the dynamic interaction of virus particles with receptors. The absence or presence of a functional 2SBS affected virion-receptor binding and receptor cleavage required for particle movement on a receptor-coated surface and subsequent NA-dependent self-elution. The contribution of the 2SBS to virus-receptor interactions depended on the receptor-binding properties of HA and the identity of the receptors used. We conclude that the 2SBS is an important and underappreciated determinant of the HA-NA-receptor balance. The rapid loss of a functional 2SBS in pandemic viruses may have served to balance the novel host receptor-repertoire and altered receptor-binding properties of the corresponding HA protein.



## Author Summary

Influenza A viruses infect birds and mammals. They contain receptor-binding (HA) and receptor-destroying (NA) proteins, which are crucial determinants of host tropism and pathogenesis. It is generally accepted that the functional properties of HA and NA need to be well balanced to enable virion penetration of the receptor-rich mucus layer, binding to host cells, and release of newly assembled particles. This HA-NA-receptor balance is, however, poorly characterized resulting in part from a lack of suitable assays to measure this balance. In addition, NA is much less studied than HA. NA contains, besides its receptor-cleavage site, a 2<sup>nd</sup> receptor-binding site, which is functional in avian, but not in human viruses. We now show that this 2<sup>nd</sup> receptor-binding site prefers binding to avian-type receptors and promotes cleavage of substrates carrying this receptor. Furthermore, by using novel assays, we established an important role for this site in the HA-NA-receptor balance of virus particles as it contributes to receptor binding and cleavage by virions, the latter of which is required for virion movement and self-elution from receptors. The results may provide an explanation for the rapid loss of a functional 2<sup>nd</sup> receptor-binding site in human pandemic viruses.

## Introduction

Influenza A virus (IAV) particles contain hemagglutinin (HA) and neuraminidase (NA) glycoproteins. HA functions as a sialic acid (SIA)-binding and fusion protein. NA has receptor-destroying activity by cleaving SIAs from sialoglycans. The HA and NA protein functionalities are critical for host tropism and need to be well balanced in relation to the host receptor repertoire for optimal in vivo viral fitness [1-3]. However, there is no standard assay and unit for measuring a functional balance and the precise mode by which HA- and NA-receptor interactions contribute to the balance at the molecular level remains mostly unexplored. An optimal HA-NA balance is hypothesized to allow virions to penetrate the heavily sialylated mucus layer, to attach to host cells prior to virus entry, and to be released from cells after assembly [4-7].

Aquatic birds constitute the natural reservoir of IAVs. Occasionally IAVs from birds cross the host species barrier and manage to adapt to non-avian species, including humans. The human receptor repertoire differs from avians and requires adaptations in the SIA-interacting HA and NA proteins for optimal interaction. The HA protein of avian IAVs prefers binding to terminally located SIAs linked to the penultimate galactose via an  $\alpha$ 2,3-linkage. Human IAVs preferentially bind to  $\alpha$ 2,6-linked sialosides [8-11]. Internal sugars and their linkages as well as glycan branching have been shown to determine fine specificity of HA-receptor binding [12-17]. Changes in the receptor-binding properties of the HA proteins are achieved by mutations in the receptor binding site, which have been well documented for several HA subtypes [1, 10, 11, 18]. Much less is known about the adaptations in NA required to match the corresponding HA proteins.

NA is a type II transmembrane protein that forms mushroom-shaped homotetramers. Tetramerization is essential for its enzymatic activity [19, 20]. The enzyme active site is located in the globular head domain that is linked to the endodomain via a thin stalk. The active site is made up by catalytic residues that directly contact SIA and by framework residues that keep the active site in place [21, 22]. The catalytic and the framework residues are extremely conserved between avian and human IAVs [23]. Nevertheless, although both avian and human NA proteins preferentially cleave  $\alpha$ 2,3-linked SIAs, human viruses appear relatively better at cleaving  $\alpha$ 2,6-linked SIAs [24-27].

Adjacent to the catalytic site, NA contains a 2<sup>nd</sup> SIA-binding site (2SBS; also referred to as hemadsorption site) (Fig S1)[28-31]. The 2SBS is made up by three loops, which contain residues that interact with SIA. Mutations in these loops in N1, N2 and N9 affected NA binding of erythrocytes [28, 32-35] or sialosides [26, 33] and enzymatic cleavage of multivalent substrates [28, 33] but not of monovalent substrates [26, 28, 33]. A detailed analysis of the receptor binding properties of the 2SBS of most NAs is lacking. N1 and N2 proteins bind to  $\alpha$ 2,3- as well as  $\alpha$ 2,6-linked SIAs based on binding

of resialylated erythrocytes [28, 35] whereas N1 and N9 proteins mainly bind, via their 2SBS, to  $\alpha$ 2,3-linked sialosides present on glycan arrays [33] or in biolayer interferometry assays [26]. Interestingly, the high conservation of SIA-contact residues in the 2SBS of avian IAV is lost in N1 and N2 of human IAVs [1, 26, 28, 30] that, supposedly, all lack a functional 2SBS. For N2 of avian viruses, the conservation of the 2SBS is only lost in viruses of the H9N2 subtype, which mainly infect *Galliformes* species, in contrast to other N2-containing viruses, which mainly infect *Non-Galliformes* species. [36](Fig. S2). Conservation of the SIA-contact residues in the 2SBS of N2 is also lost in canine and not restored in swine viruses, the latter of which are generally derived from human viruses (Fig. S2). It is tempting to hypothesize that the loss of a functional 2SBS in pandemic viruses is part of a required adaptation of the HA-NA balance in order to deal with the altered receptor repertoire in the novel human host [1, 28]. At first, to test this hypothesis, a detailed analysis of the contribution of (mutations in) the 2SBS to receptor binding and cleavage in the context of IAV particles is necessary as the interplay with HA proteins binding to either avian- or human-type receptors needs to be taken into account.

We define the HA-NA balance as the balance between the activities of HA and NA in virus particles in relation to their functional receptors on cells and decoy receptors present e.g. in mucus. We have recently established novel kinetic assays based on biolayer interferometry (BLI) with which, in the context of virus particles, HA binding, NA cleavage and their balance can be monitored in real time using synthetic glycans and sialylated glycoproteins [37]. Multivalent IAV-receptor binding is established by multiple low affinity interactions of several HA trimers and sialosides [38, 39]. This enables a dynamic binding mode in which individual interactions are rapidly formed and broken without causing dissociation of the virus but providing access of NA to temporarily free SIAs. Cleavage by NA results in reduced SIA-receptor density, in virus movement and ultimately in virion dissociation [37]. How fast this occurs depends on the HA-NA-receptor balance governing the dynamics of virus-glycan interactions.

In the present study, we applied these novel BLI assays to study the HA-NA-receptor balance of viruses that have a single amino acid substitution in the 2SBS. We first performed a detailed analysis of the functional importance of the 2SBS in N2 for substrate binding and cleavage by comparing NA of the pandemic H2N2 virus from 1957, containing a mutated 2<sup>nd</sup> SIA-binding site, with an avian-like NA, in which the 2<sup>nd</sup> SIA binding site was restored. Preferred binding to  $\alpha$ 2,3-linked sialosides was shown to result in enhanced cleavage of substrates containing these glycans. Analysis of the HA-NA-receptor balance of viruses containing these N2 proteins in combination with H3 proteins that prefer binding to avian or human-type receptors clearly demonstrated a role for the 2SBS in the complex and dynamic interplay between HA, NA and receptor, which has been largely overlooked until now.

The functional importance of the 2SBS for the HA-NA-receptor balance may explain the conservation and loss of this site in avian and human IAVs, respectively.

## Results

### The 2SBS in N2 is an important determinant of NA catalytic activity.

We first analysed the receptor binding and cleavage activity of N2 NA with and without a functional 2SBS using purified recombinant soluble NA expressed in HEK293T cells [20]. In NA of A/Singapore/1/1957 (H2N2) pandemic virus (referred to as human N2 [hN2]) one of the SIA-contact residues in the 2SBS is mutated compared to the avian consensus sequence (S367N, Fig. S3). Introduction of the reciprocal mutation (N367S) in this NA restored the 2SBS (referred to as avian-like N2 [aN2]) [28]. hN2 and aN2 displayed similar specific activities when using the monovalent MUNANA [2'-(4-Methylumbelliferyl)- $\alpha$ -D-N-acetylneuraminic acid] substrate (Fig. 1A, Fig. S4A and B), indicating that mutation of the 2SBS did not affect the catalytic activity of the N2 proteins *per se*. Similar results were obtained previously using membrane-associated proteins [28], indicating that the activity of the recombinant soluble proteins accurately reflects the activity of their membrane-bound counterparts as concluded earlier for N1 [20]. Cleavage of SIAs from fetuin and transferrin sialoglycoproteins was quantified by enzyme-linked lectin assay (ELLA), by analysing the increase or decrease in binding of lectins depending on their binding specificities (Fig. S4). ECA (*Erythrina Cristagalli* lectin) specifically binds glycans containing terminal Gal $\alpha$ 1,4GlcNAc corresponding to non-sialylated N-linked sugars [40], while PNA (peanut agglutinin) binds to terminal Gal 1,3GalNAc, which generally corresponds to non-sialylated O-linked sugars [41]. NA activity thus results in increased binding of these lectins. MAL I (*Maackia Amurensis* Lectin I) and SNA (*Sambucus Nigra* Lectin) specifically bind  $\alpha$ 2,3- or  $\alpha$ 2,6-linked SIAs, respectively [42, 43]. Binding of SNA and MAL I is decreased by NA activity. For all lectins analysed, aN2 was more active than hN2 using fetuin, containing  $\alpha$ 2,3- and  $\alpha$ 2,6-linked SIAs (Fig. 1A) [44]. In contrast, no statistically significant difference was observed using transferrin that only contains  $\alpha$ 2,6-linked sialoglycans (Fig. 1A) [45, 46]. Plotting the specific activities of the NA proteins relative to their specific activities as determined by the fetuin-ECA combination resulted in similar activity profiles (Fig. 1B), which mimic those determined previously for N1 and N9 [26, 33]. Both hN2 and aN2 preferred cleavage of  $\alpha$ 2,3- (determined with fetuin-MAL I) over  $\alpha$ 2,6- (determined with fetuin-SNA) linked SIAs (Fig. 1B). In agreement herewith, the specific activities were higher when determined with the fetuin-ECA than with the transferrin-ECA combination as fetuin, but not transferrin, contains  $\alpha$ 2,3-linked SIAs (Fig.1B).

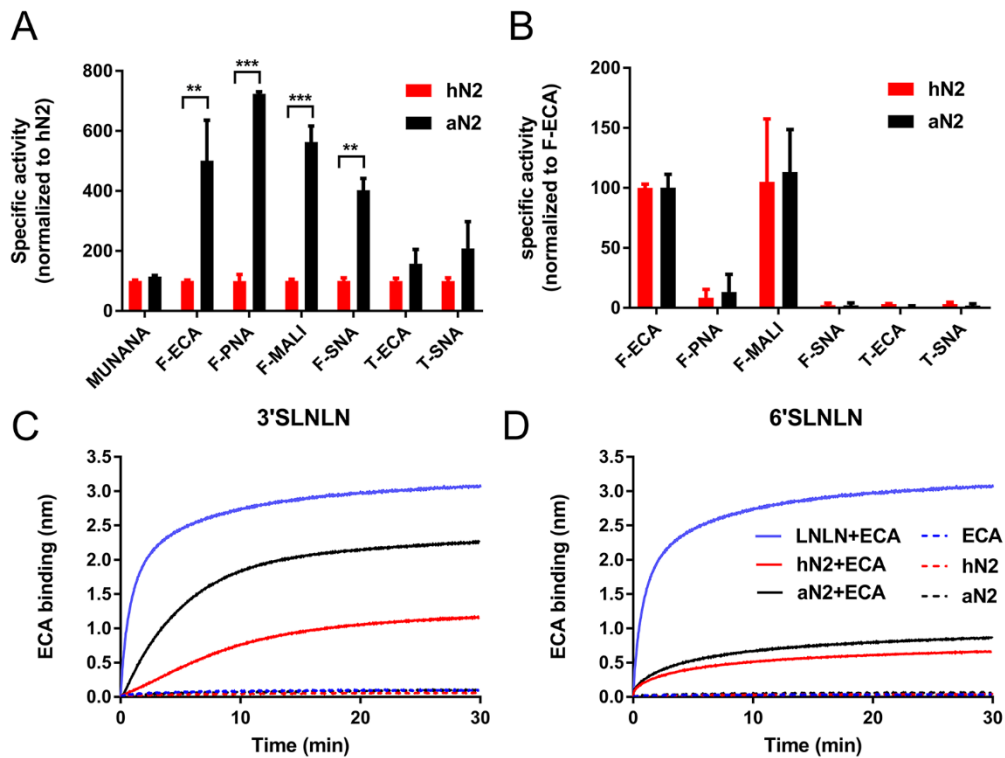


**Fig. 1. Enzymatic activity of N2 proteins assayed using different substrates.** (A) Specific activity of hN2 and aN2 was determined by MUNANA assay and ELLA using different glycoprotein-lectin combinations (Fetuin-ECA, Fetuin-PNA, Fetuin-MAL I, Fetuin-SNA, Transferrin-ECA and Transferrin-SNA) and normalized to the specific activity of hN2 for MUNANA and each glycoprotein-lectin combination. (B) Specific activity of hN2 and aN2 is graphed normalized to the specific activity as determined for each protein by the Fetuin-ECA combination. Mean values and standard deviations from two independent experiments performed in triplicate are shown. Stars depict P values calculated using an unpaired two-tailed Student t test (\*\*,  $P < 0.01$ ; \*\*\*,  $P < 0.001$ ). (C and D) BLI kinetic assay of NA enzymatic activity. Streptavidin biosensors were coated with biotinylated synthetic glycans (3'SLNLN, 6'SLNLN or LNLN). Subsequently, the sensors were incubated in buffer containing 4  $\mu$ g aN2 or hN2 in the absence or presence of 8  $\mu$ g ECA or ECA alone. ECA binding to sensors coated with 3'SLNLN or 6'SLNLN is a measure for SIA cleavage from these receptors by NA. Experiments were independently performed three times. Representative experiments are shown.

These results show that an avian-like 2SBS in N2 contributes to cleavage of the sialoglycoprotein fetuin containing  $\alpha$ 2,3- and  $\alpha$ 2,6-linked SIAs. We next used BLI to study the kinetics of NA activity on a multivalent surface coated with either an avian receptor (3'SLNLN: NeuA $\alpha$ 2-3Gal $\beta$ 1-4GlcNAc $\beta$ 1-3Gal $\beta$ 1-4GlcNAc) or a human receptor (6'SLNLN: NeuA $\alpha$ 2-6Gal $\beta$ 1-4GlcNAc $\beta$ 1-3Gal $\beta$ 1-4GlcNAc). NA activity can be directly monitored in real-time by the specific binding of the lectin ECA to terminal

Gal $\beta$ 1-4GlcNAc glycotopes that become available upon removal of SIA by NA (Fig. 1C and D, red and black lines). Note that cleavage of the small SIA moiety is not detected directly by BLI (Fig. 1C and D, dashed red and black lines). Binding of ECA to a sensor coated with LNLN (Gal $\beta$ 1-4GlcNAc $\beta$ 1-3Gal $\beta$ 1-4GlcNAc, Fig. 1C and D blue lines) rapidly reaches the maximum ECA binding signal (representing 100% de-sialylation) assuring that ECA binding during the relatively slow accumulation of de-sialylated glycans by NA activity (red and black lines) reflects the cleavage kinetics of the N2 proteins. Both hN2 and aN2 more efficiently cleaved 3'SLNLN over 6'SLNLN. Especially the aN2 protein displayed much more efficient cleavage of 3'SLNLN. We conclude that restoration of the 2SBS in hN2 to the avian consensus sequence results in enhanced cleavage of substrates containing  $\alpha$ 2,3-linked SIAs.

### **N2 proteins prefer binding to $\alpha$ 2,3- over $\alpha$ 2,6-linked SIAs via their 2SBS**

The increased cleavage by aN2 of substrates containing  $\alpha$ 2,3-linked SIAs is expected to result from specifically increased binding to  $\alpha$ 2,3-linked SIAs due to the presence of an avian 2SBS, although N2 proteins were reported to bind both  $\alpha$ 2,3- and  $\alpha$ 2,6-linked SIAs by using resialylated erythrocytes [28]. We observed hemagglutination for recombinant soluble aN2 but not for hN2 (Fig. S5A). However, no specific binding to synthetic  $\alpha$ 2,3- and  $\alpha$ 2,6-linked sialoglycans by BLI could be observed for the recombinant soluble N2 proteins, which could be due to low affinity of the 2SBS. By embedding the N2 proteins in membrane vesicles highly multivalent receptor interactions may increase receptor-binding avidity. To this end, full length N2 proteins were expressed in 293T cells. N2 virus-like particles (VLPs) [47] were directly harvested from the culture supernatant, while cells were treated with hypotonic and hypertonic buffers, resulting in the release of N2 protein-containing vesicles [48]. Preparations containing similar amounts of N2, based on MUNANA activity (Fig. 1A) were used to determine the receptor specificity of the 2SBS by BLI [26]. Negligible binding was obtained for hN2 VLPs (Fig. 2A and B) or vesicles (Fig. S5D and E) to  $\alpha$ 2,3- or  $\alpha$ 2,6-linked SIAs, regardless of the presence of the NA inhibitor oseltamivir carboxylate (OC), which binds the NA catalytic site. In contrast, highly 3'SLNLN-specific, binding was observed for aN2 VLPs and vesicles (Fig. 2A and B; Fig. S5D and E) in the presence of OC leading to the conclusion that aN2 has much higher lectin activity than hN2 due to the presence of a functional 2SBS. The observed  $\alpha$ 2,3-linked SIA specificity is in agreement with the particularly enhanced cleavage of substrates containing  $\alpha$ 2,3-linked SIAs (Fig. 1). No binding of aN2 VLPs to 3'SLNLN was observed in the absence of OC, which is likely explained by immediate self-elution of VLPs carrying active NA proteins.

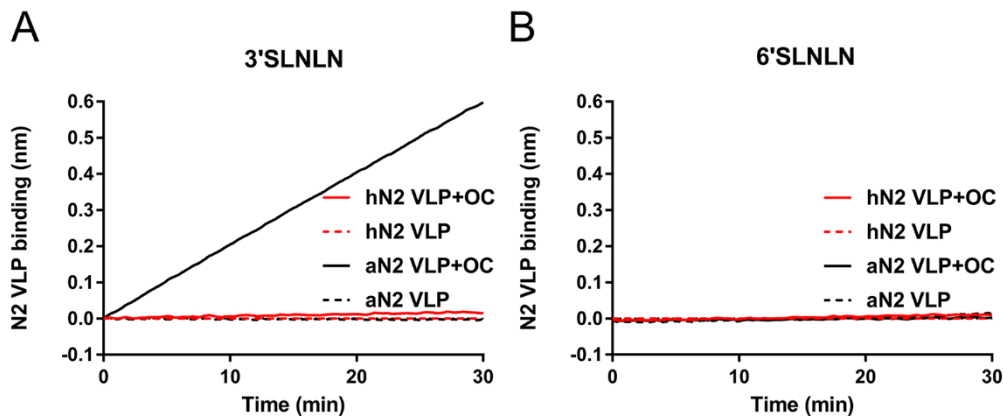


**Fig. 2. Substrate binding of N2 VLPs via the 2SBS.** VLPs containing full length hN2 and aN2 were analysed for their ability to bind 3'SLNLN (A) or 6'SLNLN (B) in the absence or presence of OC using BLI as described in the legend to Fig. 1. Similar amounts of N2 were applied based on the MUNANA assay as hN2 and aN2 proteins have identical enzymatic activities with respect to this substrate (Fig. 1). Experiments were independently performed twice. Representative experiments are shown.

### Restoration of the N2 2SBS affects virus replication

To examine the contribution of the 2SBS to the HA-NA balance of virus particles we examined the replication phenotype of recombinant viruses containing either aN2 or the hN2 in the background of the 1968 pandemic virus A/Hong Kong/1/68 (H3N2) (referred to as hH3aN2 and hH3hN2) [28]. The hH3hN2 virus, lacking a functional 2SBS, produced large and clear plaques on Vero cells (Fig. 3A, and B, Fig. S6A and B) as compared to the smaller, fuzzy plaques of the hH3aN2 virus with a functional 2SBS. Staining of plaques at 48 h post infection indicated that all cells within the plaques of hH3hN2 virus were infected, whereas many non-infected cells could be observed in the hH3aN2 plaques. This could be due to the more active aN2, which may destroy receptors on cells before the virus can enter into the cells. hH3aN2 reached lower titres than the hH3hN2 virus at 24 and 48 h post infection when Vero cells were used (Fig. 3C), while no significant differences were observed for replication in MDCK cells (Fig. 3D). Differences in cell surface sialosides and their distribution may explain differences between replication in Vero and MDCK cells. Although the sialylation patterns of MDCK and Vero cells are poorly characterized, both cell lines can be infected with human and avian IAVs and express  $\alpha$ 2,3- and  $\alpha$ 2,6-linked SIAs [49-51]. From these results we conclude that the absence or presence of a functional 2SBS in N2 may affect virus replication kinetics in a cell type-dependent manner.

### A functional 2SBS contributes to receptor binding of virus particles

Using a recently established BLI-based kinetic binding assay [37] an enhanced initial binding rate to 3'SLNLN but not 6'SLNLN (Fig. 4A-B), was observed for hH3aN2 virus containing a functional 2SBS in



comparison to hH3hN2. As a result the hH3aN2 virus displayed a higher initial binding-rate ratio 3'SLNLN/6'SLNLN than hH3hN2 (Fig. 4C, red and black bars). Next, two recombinant soluble glycoproteins containing mainly N-linked glycans (lysosomal-associated membrane glycoprotein 1 [LAMP1], ca. 18 N- and 6 O-linked glycans [52, 53]), or O-linked glycans (glycophorin A, ca. 16 O- and a single N-linked glycan [54, 55]) were used in BLI as recently described for recombinant fetuin [37]. LAMP1 and glycophorin A mimic the presumed functional and decoy receptors found on cells (LAMP1) and on mucins (glycophorin A) that are rich in N- or O-glycans, respectively. Analysis of the glycans on these glycoproteins by lectin binding using BLI confirmed the presence of sialylated N-linked glycans (both  $\alpha$ 2,3- and  $\alpha$ 2,6-linked) on both proteins, while only glycophorin A was shown to contain sialylated O-glycans (Fig. S7). Again, a functional 2SBS (present in aN2) contributed to virus binding (Fig. 4D and E). This contribution was larger for binding to glycophorin A than to LAMP1 as judged from the initial binding rates (Fig. 4F).

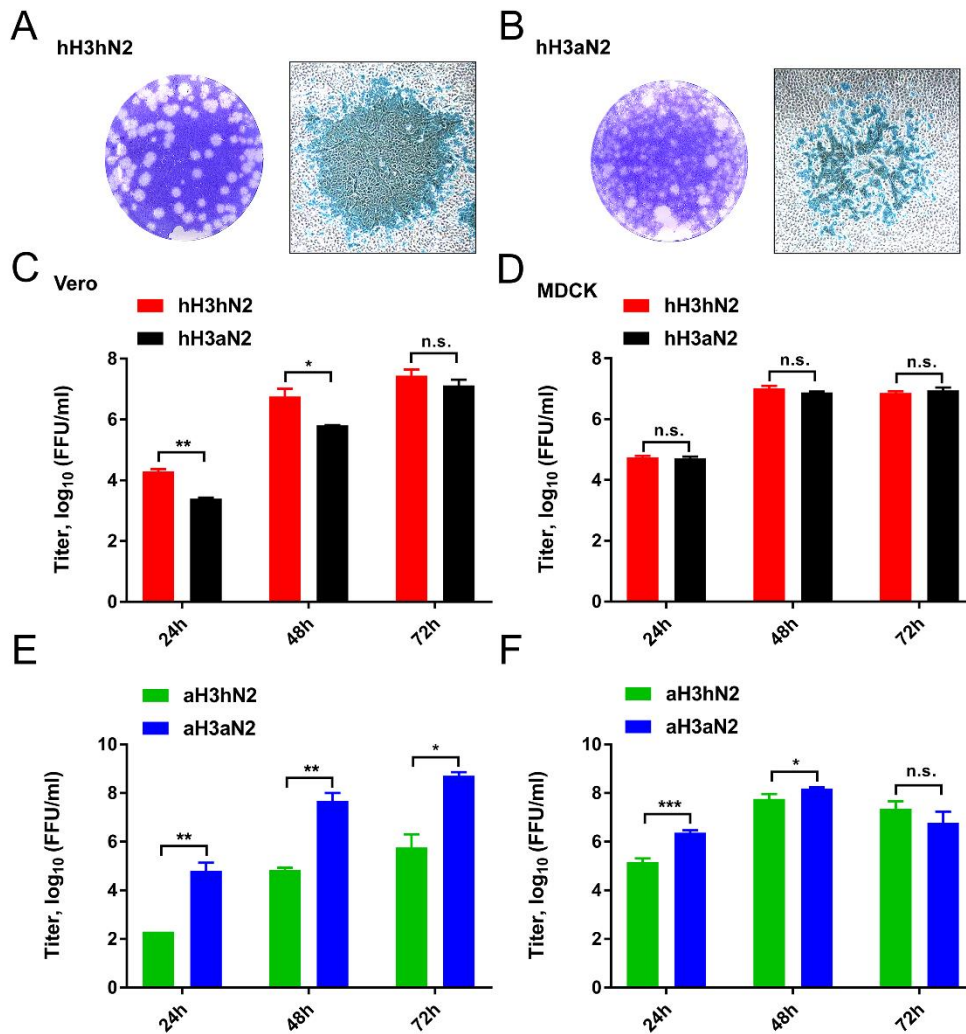


**Fig. 3. Plaque morphology and replication kinetics of recombinant viruses** Plaque assays were performed for hH3hN2 (A) and hH3aN2 (B) viruses using Vero cells followed by crystal violet dye

staining (left panels) or by immunostaining of infected cells (right panels). Vero (C and E) or MDCK (D and F) cells were infected with hH3hN2 or hH3aN2 (C and D), or with aH3hN2 or aH3aN2 (E and F). Virus in the cell culture supernatants at the indicated times post infection was titrated, and the titres were expressed as  $\log_{10}$  (FFU/ml). Standard deviations are indicated. Significant differences were analysed using an unpaired two-tailed Student *t* test (\*,  $P < 0.05$ ; \*\*,  $P < 0.01$ ; \*\*\*,  $P < 0.001$ ; n.s., not significant).

The HA of the 1968 pandemic H3N2 virus (referred to as hH3) prefers binding to terminal  $\alpha 2,6$ -linked SIAs [56, 57]. The results above implicate that, besides adaptations in HA, also adaptations in the 2SBS may contribute to a specificity-switch when an avian IAV adapts to humans. We therefore studied the effect of the 2SBS in NA when combined with an avian-type HA preferring binding to  $\alpha 2,3$ -linked SIAs. We generated the corresponding recombinant A/Hong Kong/1/68 (H3N2) viruses containing 7 amino acid substitutions in the HA (see Fig. S8A). These substitutions reverted the HA back to the avian consensus sequence (referred to as avian-like aH3), including the crucial substitutions Q226L and G228S, which enable HA preferential binding to avian-type receptors [56, 57]. The resulting viruses are referred to as aH3hN2 and aH3aN2, depending on the absence and presence of the functional 2SBS, respectively. We confirmed the receptor-binding specificities of soluble hH3 and aH3 proteins by solid phase fetuin- and transferrin-binding assays and BLI (Fig. S8B and C). As expected, aH3 displayed higher binding levels to fetuin, containing  $\alpha 2,3$ - and  $\alpha 2,6$ -linked SIAs, than hH3, while hH3 bound better than aH3 to transferrin, which only contains  $\alpha 2,6$ -linked sialoglycans. BLI analysis using H3-containing vesicles obtained from cells expressing full-length versions of hH3 or aH3 confirmed the different receptor-binding properties of these H3 proteins to 3'SLNLN and 6'SLNLN (Fig. S8D and E). In contrast to viruses containing hH3, the presence of a functional 2SBS in aN2 enhanced replication of viruses with aH3 both on Vero (Fig. 3E) and MDCK (Fig. 3F) cells. Differences in virus replication were smaller for MDCK than for Vero cells. We next analysed receptor-binding properties of aH3hN2 and aH3aN2 viruses using BLI. As observed before for the hH3-containing viruses (Fig. 4C; red and black bars), a functional 2SBS enhanced binding to 3'SLNLN but not 6'SLNLN when N2 was combined with aH3 (Fig. 4C). However, viruses containing aH3 displayed similar binding kinetics in the presence of OC regardless of the presence of a functional 2SBS for both LAMP1 and glycophorin A (Fig. 4G, H and I). From these results we conclude that a functional 2SBS site in NA contributes to virion-receptor binding in a HA- and receptor-dependent

manner.

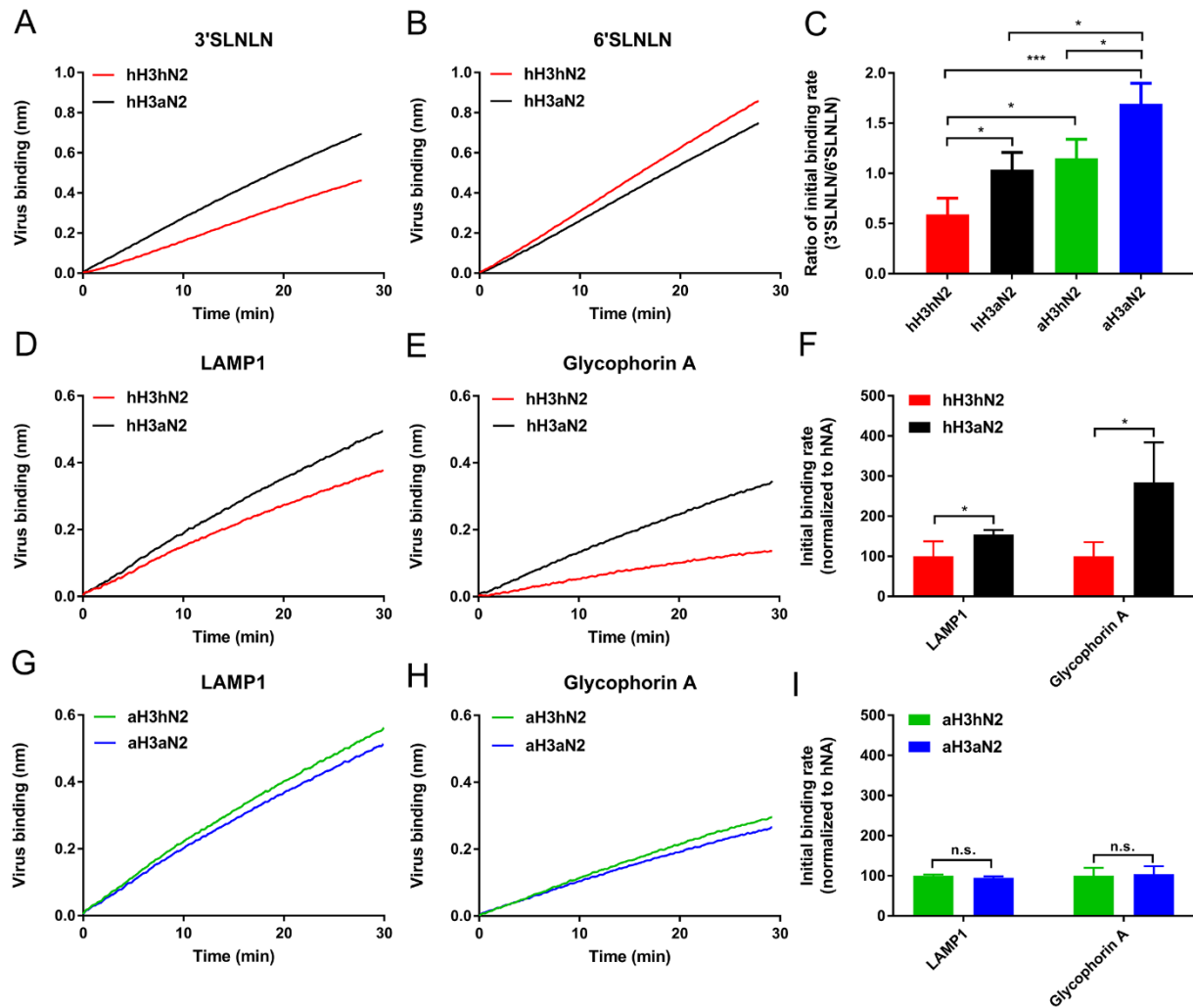


**Fig. 4. Binding of H3N2 viruses to LAMP1 and glycoporphin A.** Identical number of hH3hN2 and hH3aN2 virus particles (determined using Nanoparticle Tracking Analysis; Nanosight NS300; Fig. S10) were analysed for their ability to bind 3'SLNLN (A), 6'SLNLN (B), LAMP1 (D) and glycoporphin A (E) in the presence of OC using BLI. (C) Initial binding rates ( $v_{obs}=dB/dT$ ) were determined as described previously [37] and ratios (3'SLNLN/6'SLNLN) were determined and graphed normalized to hH3aN2. Identical number of aH3hN2 and aH3aN2 virus particles were analysed for their ability to bind LAMP1 (G) and glycoporphin A (H) in the presence of OC using BLI. Initial binding rates of the different virus-receptor combinations were determined and normalized to either hH3hN2 or aH3hN2 (F and I). Experiments were performed three times and representative experiments are shown (A, B, D, E, G, H). Mean values of these three independent experiments are shown (C, F, I). Standard deviations are indicated. Stars depict P values calculated using one-way ANOVA (C) or an unpaired two-tailed Student t test (F, I) (\*,  $P<0.05$ ; \*\*\*,  $P<0.001$ ).

**Substrate binding by NA and HA both affect enzymatic cleavage by NA in virus particles**

The NA enzymatic activity of the different recombinant viruses with and without a functional 2SBS was analysed using the monovalent soluble substrate MUNANA, by ELLA and by BLI. The different viruses displayed a similar NA activity per particle using the monovalent soluble substrate MUNANA (Fig. 5A). As also the NA proteins do not differ in their MUNANA activity regardless of the presence or absence of a functional 2SBS (Fig. 1A), we conclude that similar amounts of NA are incorporated into virions of the four viruses. The viruses differed, however, in their specific activities when the multivalent glycoprotein fetuin was used as substrate in an ELLA (Fig. 5B). hH3hN2 virus was less active compared to viruses containing aH2 and/or aH3, indicating a contribution of receptor binding via HA and the 2SBS to NA enzymatic activity in the context of virus particles. In agreement with the results obtained with the recombinant proteins (Fig. 1B), cleavage of  $\alpha$ 2,6-linked SIA found on transferrin was less efficient and did not appear to differ significantly between the different viruses (Fig. S9).

The ELLAs (Fig. 5B and Fig. S9) indicate that both receptor binding via HA and the 2SBS of NA contribute to the sialidase specific activity of virus particles. These endpoint assays do not, however, elucidate the HA-NA balance of these viruses, for which kinetic BLI assays are required [37]. Preliminary experiments showed inefficient cleavage of the synthetic glycans by the recombinant viruses. Kinetic assays to determine the HA-NA balance of these viruses were therefore performed with the glycoprotein receptors (LAMP1 or glycoporphin A). In the absence of OC, that is, with active NA proteins, no appreciable binding of hH3-containing viruses could be detected indicating efficient receptor cleavage by NA (Fig. 5C and D). Limited binding could be detected, however, for the aH3-containing viruses in the absence of OC. The binding curve of the virus with a functional 2SBS (aH3aH2) bended earlier and had a smaller area under the curve than that of the virus without a functional 2SBS (aH3hN2) for both LAMP1 and glycoporphin A. This bending of the curves is explained by ongoing cleavage of SIAs by viruses attached to the sensor-attached glycoproteins, resulting in release of bound virus particles [37]. The earlier bending and smaller area under the curve observed for the aH3aH2 virus is indicative of more efficient cleavage of the sensor-attached receptors by this virus than by aH3hN2, lacking a functional 2SBS.

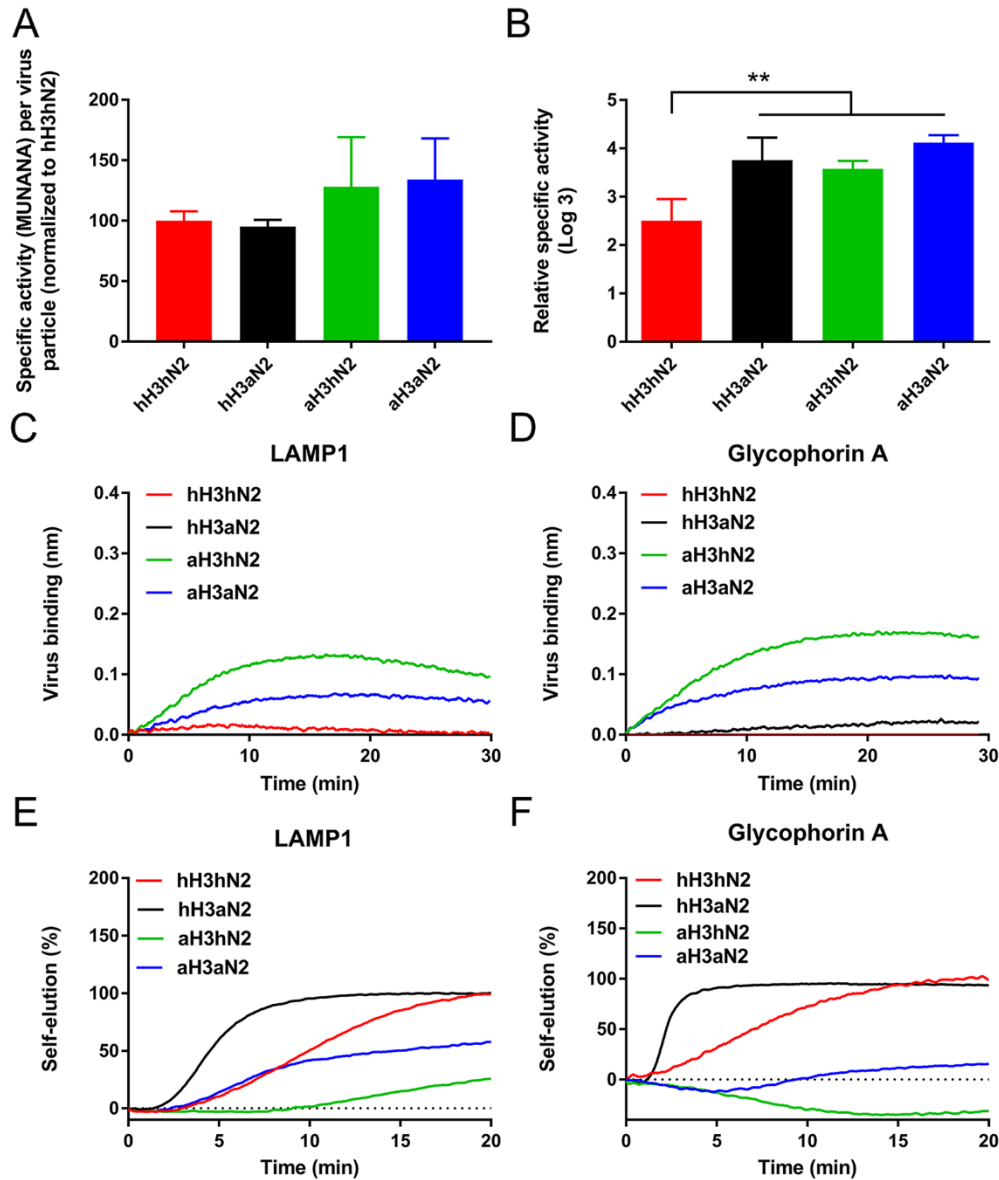


**Fig. 5. NA enzymatic activity in virus particles.** (A) Numbers of particles in virus preparations were determined using Nanoparticle Tracking Analysis (Nanosight NS300); the NA activity in these preparations was analysed by MUNANA assay. Relative NA activity per virion is graphed ( $N=3$ ). (B) Virus preparations were normalized based on their MUNANA activity. Fetuin-coated plates were incubated with serial dilutions of viruses in the absence of OC. Cleavage of SIAs from glycoproteins was monitored using ECA, which binds desialylated glycans. Dilutions corresponding to half-maximum lectin binding were determined by non-linear regression analysis and used to calculate the specific activity of the different viruses. See Fig. S9 for curves. Mean values of two independent experiments performed in duplicate are shown. Standard deviations are indicated. Stars depict  $P$  values calculated using one-way ANOVA (\*\*,  $P<0.01$ ). (C and D) Identical number of hH3hN2 and hH3aN2, and aH3hN2 and aH3aN2 virus particles were analysed for their ability to bind LAMP1 (C) or glycophorin A (D) in

*the absence of OC using BLI. (E and F) After binding of virus preparations with identical particle numbers to LAMP1 (E) or glycoporphin A (F) in the presence of OC (similarly as shown in Fig. 4), OC was removed by three repeated washes and virion self-elution in the absence of OC was monitored. Dissociation of virus particles was normalized to the virus association levels in the presence of OC. Experiments were performed three times. Representative experiments are shown.*

The effect of receptor binding via NA and HA on NA activity of virions was analysed further by NA-dependent virion self-elution from a receptor-coated BLI sensor after prior binding of the virions in the presence of OC. Self-elution of IAV particles requires NA activity and self-elution is not observed when NA activity is blocked by OC [37]. After binding of the four recombinant viruses to LAMP1 and glycoporphin A in the presence of OC, OC was removed by repeated short washes in Dulbecco's phosphate buffered saline (PBS) with Calcium and Magnesium and virus self-elution was monitored. Clearly, viruses with aN2 proteins eluted faster from the sensors than the viruses with hN2 (compare hN3aN2 with hN3hN2 and aH3aN2 with aH3hN2; Fig. 5 E and F), for both glycoprotein receptors. Of note, NA-dependent self-elution of virus particles is often preceded by an apparent increase in virus binding [37] represented here as negative self-elution, particularly in the case of aH3aN2 and aH3hN2 (Fig. 5F). The larger negative area of self-elution for aH3hN2 reflects the reduced NA activity of this virus compared to aH3aN2. Also the identity of HA affected the virus self-elution rate. Viruses with hH3 eluted faster than corresponding viruses with aH3 (e.g. compare hH3aN2 with aH3aN2). For hH3aN2, self-elution was faster from glycoporphin A than from LAMP1. For aH3-containing viruses, the opposite was observed. Differences in virion self-elution observed for different HA-receptor combinations could be due the different receptor repertoires present on the two proteins (Fig. S7). The results indicate that receptor binding via the 2SBS of NA contributes to enzymatic cleavage by NA in virions and to virion self-elution from a receptor-coated surface. Virion self-elution was also shown to depend on the identity of the HA and the glycoprotein receptor used.

### **The 2SBS in 1968 pandemic H3N2**

The S367N mutation in the 2SBS of N2 was rapidly obtained after emergence of the H2N2 pandemic virus in 1957 and was observed in human H2N2 viruses until 1958. Most viruses isolated thereafter did not contain the S367N mutations but rather contained the S370L mutation, which also results in loss of a SIA-contact residue in the 370 loop (Fig. S3) and hemadsorption activity [28]. Both single mutations had a similar negative effect on catalytic activity of the 1957 NA [28]. These results indicate that there was not a strong selection against S367 per se, but rather against a functional 2SBS, which is achieved by either mutation. However, several additional mutations accumulated in time in the three loops of the 2SBS. N2 from the A/Hong Kong/68 (H3N2) (referred to as HK N2) contains five mutations (S370L, N400S, N401D, W403R, P432K) in the 2SBS compared to the avian

consensus sequence (Fig. 6A). To analyse the contribution of the 2SBS to the enzymatic activity of these different N2 proteins, a comparative analysis of recombinant proteins and viruses using monovalent and multivalent substrates was performed. The HK N2 protein was 4-5 fold less active

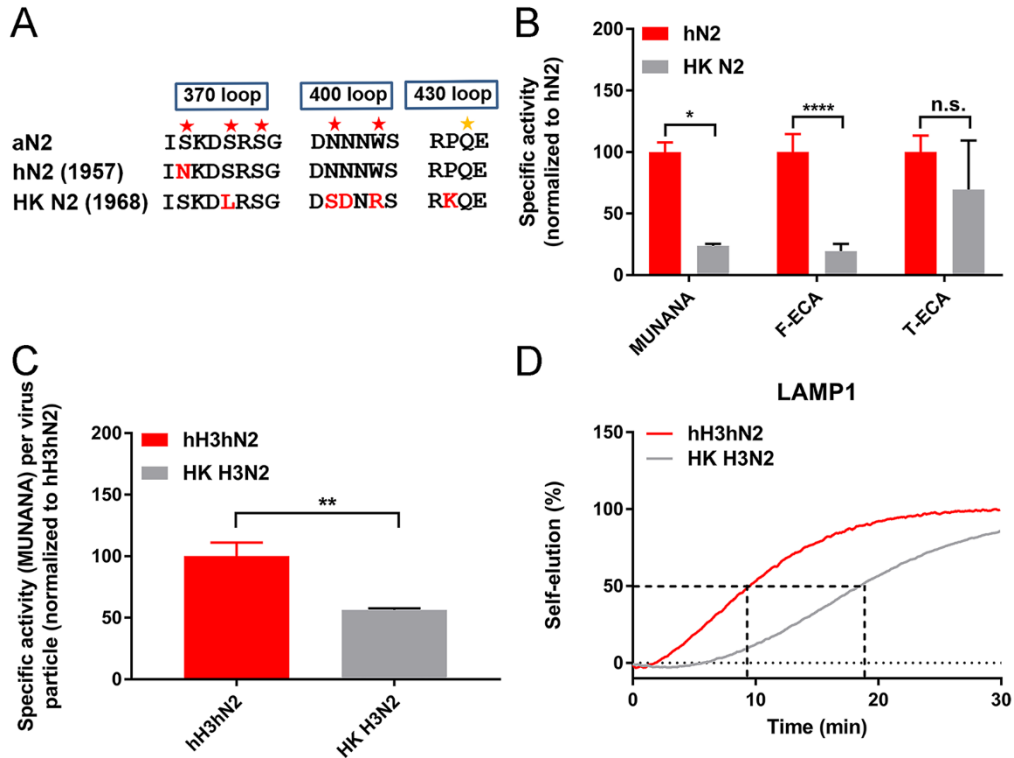


**Fig. 6. Enzymatic activity of HK N2 protein.** (A) Sequences of the three loops that make up the 2SBS of aN2, hN2 and HK N2 are shown. Red asterisks indicate SIA-contact residues in N2. The orange asterisk indicates an additional SIA-contact residue in the 430 loop of N9. Residues that differ from the aN2 sequence, which corresponds to the avian N2 consensus sequence, are shown in red. (B) Specific activity of hN2 and HK N2 recombinant soluble proteins as determined using the MUNANA assay or ELLA using the Fetuin-ECA (F-ECA) combination are graphed relative to hN2. (C) Relative NA activity (determined by MUNANA assay) per virus particle is graphed for hH3hN2 and HK H3N2 viruses. (B and C) Mean values of three independent experiments are shown. Standard deviations are indicated. Stars depict P values calculated using an unpaired two-tailed Student t test (\*,  $P < 0.05$ ; \*\*,  $P < 0.01$ ; \*\*\*\*,  $P < 0.0001$ ). (D) BLI analysis of virion self-elution from LAMP1-coated sensors was analysed for hH3hN2 and HK H3N2 virus particles. Prior to self-elution in the absence of OC, viruses were bound to similar levels to LAMP1 in the presence of OC. The experiment was performed three times, a representative experiment is shown.

than hN2 both on the monovalent substrate MUNANA and the multivalent substrate fetuin. Cleavage of sialoglycans attached to transferrin was not significantly affected (Fig. 6B). We also compared the NA activity of recombinant H3N2 viruses only differing in their NA segment. HK H3N2 virus, containing the 1968 HK N2 protein, displayed 2-fold lower NA activity per virus particle than the hH3hN2 virus, containing the 1957 N2 protein, as determined by MUNANA cleavage (Fig. 6C). Similarly, the time required for 50% self-elution of virions from the multivalent receptor LAMP1, was 2-fold longer for HK H3N2 than for hH3hN2 (Fig. 6D). Thus, hN2 from 1957 and 1968 HK N2 differ to a similar extent in their catalytic activity both when monovalent or multivalent substrates are used. As receptor-binding via the 2SBS only increases NA activity for multivalent, but not monovalent substrates, we conclude that these differences do not result from differences in receptor-binding by their (non-functional) 2SBS. Moreover, the difference observed when comparing the two recombinant proteins is similar to the difference in activity of the two NAs in the virus context.



## Discussion

Since the discovery of hemadsorption activity in NA 1984 [58] and the structural evidence of the 2SBS in N9 1997 [29], only few studies have addressed 2SBS-mediated receptor binding and the functional consequences thereof for NA activity [26, 28, 33, 34, 59]. We now show that the 2SBS is an important factor in the complex interplay between HA, NA and receptors, referred to as the HA-NA-receptor balance. A functional 2SBS in N2 was shown to prefer binding to  $\alpha$ 2,3-linked sialosides similarly to N1 [26] and N9 [33]. In agreement herewith, it enhances catalytic activity against substrates carrying  $\alpha$ 2,3-linked SIAs. The contribution of the 2SBS to the HA-NA-receptor balance of virus particles was shown to be receptor- and HA protein-dependent as demonstrated by kinetic analysis of receptor-binding and -cleavage of virions using BLI. The 2SBS was shown to contribute to receptor binding also when NA was combined with a receptor-binding HA in IAV virions, as well as to cleavage of receptors by virions and to virion self-elution from a receptor-coated surface. The absence or presence of a functional 2SBS also affected virus replication in a cell type- and HA-dependent manner. Our results indicate that mutation of the 2SBS as observed in early human pandemic viruses negatively affects the catalytic activity of NA and may serve to restore the HA-NA-receptor balance of viruses carrying HA proteins with altered receptor-binding properties in relation to a novel host sialome. Conservation of the 2SBS in most avian strains, with the notable exception of H9N2 viruses, is lost in human [26, 29, 30, 34], swine and canine variants (Fig. S2). Strong conservation usually reflects a critical function. It would be very interesting to investigate in depth whether a critical function for the 2SBS in avian strains, for instance related to the HA-NA-receptor balance, is not required for efficient replication and transmission of human, canine and swine strains.

N2 prefers binding of  $\alpha$ 2,3- over  $\alpha$ 2,6-linked SIAs via its 2SBS. The specificity of the N2 2SBS correlates with the enhanced cleavage of substrates carrying  $\alpha$ 2,3-linked SIAs compared to substrates carrying only  $\alpha$ 2,6-linked sialosides. Of note, enhanced activity was also observed for  $\alpha$ 2,6-linked SIAs at least when these sialosides were linked to substrates additionally carrying  $\alpha$ 2,3-linked SIAs (Fig. 1A; fetuin-SNA combination). These results indicate that the 2SBS enhances catalytic activity by bringing sialosides on multivalent substrates close to the catalytic site and that, depending on the substrate used, the enhanced cleavage of SIAs not necessarily matches the specificity of the 2SBS. Preferred binding of avian-type receptors via its 2SBS was previously also observed for N9 [33] and N1 [26], suggesting that this is a conserved feature for NAs of different subtypes. We cannot exclude, however, that the 2SBS of different NA subtypes may differ in their receptor-binding fine specificity, as structural differences were observed in the interactions between ligands and the 2SBS for different NA subtypes [30]. In N9, the conserved K432 residue in the 2SBS forms a hydrogen bond with SIA [29] and mutation K432E in N1 has a large negative effect on the cleavage of multivalent

substrates [26]. In contrast, several other avian NA subtypes, including N2, contain a Q or E residue at this position, which does not form a hydrogen bond with SIA in the few available crystal structures [30]. Previously, it was shown that N1 and N2 NAs bound with similar efficiency to both avian and human type receptors SIAs [28, 35]. This discrepancy is probably explained by the different methods used to analyse the receptor specificity of the 2SBS. In the previous reports, a red blood cell binding assay was employed, in which desialylation of erythrocytes was followed by resialylation using  $\alpha$ 2,3- or  $\alpha$ 2,6-sialyltransferases. Binding to resialylated erythrocytes might be affected by prior incomplete desialylation. Alternatively, a higher receptor density on erythrocytes compared to the BLI sensor surface might allow for binding of  $\alpha$ 2,6-linked SIAs. The ability of the 2SBS to bind human-type receptors to some extent is also suggested by the modestly increased or decreased cleavage of SIAs from substrates only containing  $\alpha$ 2,6-linked SIAs upon the introduction of mutations in the 2SBS (this study and [26, 28]).

The 2SBS contributed to receptor-binding also when NA was combined with a receptor-binding HA in IAV virions. In combination with HA preferring binding to  $\alpha$ 2,6-linked SIAs (hH3), the 2SBS enhanced binding for all receptors analysed, except 6'SLNLN, to which the recombinant aN2 protein did not bind. Binding to glycoporphin A, carrying many O-linked sugars also found on mucins, was more enhanced by the 2SBS than binding to LAMP1, which carries mostly sialylated N-glycans. The functional significance of this difference remains to be determined. When combined with HA that prefers binding to  $\alpha$ 2,3-sialosides (aH3), the enhancing effect of the 2SBS was not observed for the glycoprotein receptors analysed. Thus, the contribution of NA to virion-receptor binding depends on the specificity/affinity of the corresponding HA and the receptors present. Previously it was shown that the active site of NA contributes to virion-receptor binding in case of a low-activity catalytic site [37], a characteristic which is also appears to be displayed by recent H3N2 viruses [60, 61]. As we now show that a functional 2SBS in NA can also contribute to virion-receptor binding, two mechanisms exist by which NA can assist in binding of virions to host cells.

A complex interplay between HA, NA and receptor determines the attachment of virus particles to and release from a receptor-containing surface. This HA-NA-receptor balance can be experimentally determined using kinetic BLI assays by analysis of virus binding in the absence or presence of NA inhibitors and self-elution from different receptors (this paper and [37]). The HA-NA-receptor balance determines the residence time of a virus on a sialylated surface and the speed by which it moves over this surface. We assume that an optimal balance is important for virions to efficiently pass the heavily sialylated mucus layer, while still allowing virion attachment to host cells resulting in endocytic uptake. The complexity of the HA-NA-receptor balance is exemplified by the contribution of NA to receptor binding [37] and of HA to the apparent catalytic activity of NA (this paper)[37, 62].

We now show that the HA-NA-receptor balance as reflected for example in virion self-elution (Fig 5) is affected by a functional 2SBS, depending on the particular HA with which NA is combined and the receptors used. Changes in the 2SBS of NA should thus be considered in the context of mutations affecting the receptor-binding site of HA and the catalytic site of NA.

The 2SBS of N2 appears to accumulate more mutations than other surface exposed parts of the NA protein (Fig. S3). While the 1957 N2 protein has a single substitution in the 2SBS, the 1968 N2 protein contains five mutations in this site. The accumulation of several mutations in the 2SBS was found to have no further negative effects on the enzyme-enhancing function of 2SBS as compared to a single mutation of a SIA contact residues in the 2SBS of an early pandemic virus from 1957. Although we cannot exclude that the accumulation of mutations in the 2SBS of N2 indicates ongoing adaptation of NA to the human host or serves to restore subtle deviations in the HA-NA-receptor balance resulting from other mutations in HA and/or NA, it seems more likely that it rather results from continuous immune pressure on this site [22, 63] in combination with loss of functional importance of the 2SBS in human viruses.

An important role for the NA 2SBS in IAV replication *in vivo* is suggested by the conservation of this site among NA subtypes of most avian viruses, the rapid loss of this site in human pandemic viruses ([1, 26, 28, 30, 36] and Fig. S2), the important role of this site in HA-NA-receptor balance (this study) and observations that this site affects virus replication *in vitro* ([26, 34, 59] and this study). Of note, we now show that the presence or absence of a functional 2SBS affected virus replication depending on the receptor-binding properties of HA, with which NA was combined. Replication of viruses with a human or avian-like HA is enhanced by the absence or presence of a functional 2SBS, respectively, although some cell-dependent differences were observed. The absence or presence of a functional 2SBS was reported not to affect influenza viral replication in ducks [34]. However, in this latter study recombinant viruses were used containing HA from a H2N9 and NA from a H3N2 virus. This may have resulted in a mismatched HA-NA combination in which the presence of the 2SBS might be of minor influence on replication. Alternatively, the 2SBS may be important for virus transmission rather than for replication in ducks *per se*. Clearly, additional experiments are needed to demonstrate the importance of the 2SBS for IAV replication and transmission *in vivo*. Interestingly, both for H9N2 and H7N9 viruses, the well-known Q226L mutation in the receptor-binding site of HA, resulting in a shift from avian to human receptor specificity, is associated with mutations in the 2SBS that negatively affect receptor binding [33, 36]. These avian viruses thus display a striking parallel with the changes observed in the receptor-binding sites of HA and NA of avian-origin pandemic viruses. We propose that mutations in the 2SBS of avian viruses may be indicative of an as of yet underappreciated, increased potential of avian viruses to cross the host species barrier. Of note, also upon introduction

of coronavirus OC43 into humans, the lectin function of the receptor-destroying hemagglutinin-esterase protein was lost through progressive accumulation of mutations resulting in reduced cleavage of multivalent substrates [64]. Thus, both coronaviruses and IAVs appear to adapt to the sialoglycome of the human respiratory tract by tuning the virion receptor-binding and cleavage functions, the latter among others by mutation of the lectin domain of the receptor-destroying NA.

## Materials and Methods

**Expression of recombinant proteins.** Human-codon optimized cDNAs (Genescript) encoding the N2 ectodomain of A/Singapore/1/57(H2N2) (GenBank accession no. AY209895.1; referred to as human N2 [hN2]) and a variant thereof containing the N367S mutation (referred to as avian-like N2 [aN2]) were cloned into a pFRT expression plasmid (Thermo Fisher Scientific) in frame with sequences encoding a signal sequence derived from *Gaussia luciferase*, a Strep tag and a Tetrabrachion tetramerization domain, similarly as described previously [20]. The corresponding full length NA-coding plasmids were generated by replacement of the non-NA coding sequences by sequences encoding the NA transmembrane domain and cytoplasmic tail of N2 of A/Singapore/1/57(H2N2). Human-codon optimized cDNAs encoding FL H3 or the H3 ectodomain of A/Hong Kong/1/68 (H3N2) (GenBank accession no. CY033001; referred to as human H3 [hH3]) or of an variant thereof containing 7 amino acid substitutions, which revert the HA back to the avian consensus sequence [56] (referred to as avian-like H3 [aH3]) were cloned in pCD5 expression vectors similarly as described previously [65]. Codon optimized glycoproteins LAMP1 and glycophorin A ectodomain-encoding cDNAs (Genescript) were genetically fused to Fc-tag, for Protein-A based purification, and a Bap tag [66], for binding to octet sensors, and cloned in a pCAGGs vector, similarly as described previously for fetuin [37]. NA and glycoprotein expression plasmids were transfected into HEK293T (ATCC) cells using polyethylenimine (PolyScience) [20]. An expression vector encoding BirA ligase was cotransfected with the LAMP1- and glycophorin A-coding vectors [37]. Five days post transfection, cell culture media containing soluble NA proteins and glycoproteins were harvested and purified using Strep tactin or protein A containing beads [20, 37]. Purified NA proteins were quantified by quantitative densitometry of GelCode Blue (Thermo Fisher Scientific)-stained protein gels additionally containing bovine serum albumin (BSA) standards. The signals were imaged and analysed with an Odyssey imaging system (LI-COR). HEK293T cells were transfected with full-length NA constructs to obtain membrane vesicles. To this end, cells were vesiculated as described previously [26, 48]. VLPS and membrane vesicle preparations were purified using Capto Core 700 beads (GE Healthcare Life Sciences) according to the manufacturer's instructions and as detailed previously [67] to remove proteins smaller than 700 kDa. The amount of NA protein in the VLPs and vesicle preparations was determined using the MUNANA assay described below.

**Viruses.** Generation of recombinant virus HK H3N2, which harbours all genes from the pandemic virus A/Hong Kong/1/68 (H3N2) has been described before [57]. Also the generation of hH3hN2 and hH3aN2 viruses, which carry the N2 gene of the pandemic A/Singapore/1/1957 (H2N2) in the background of A/Hong Kong/1/68 (H3N2) has been described before [28]. The hH3aN2 virus contains substitution N367S in the N2 protein. aH3hN2 and aH3aN2 viruses were generated as described

previously [56] in the background of A/Hong Kong/1/68 (H3N2). These latter viruses carry the H3 protein of A/Hong Kong/1/68 (H3N2) containing 7 amino acid substitutions in HA which revert the HA back to the avian consensus sequence [56] combined with the N2 protein of A/Singapore/1/1957 (H2N2) with (aH3aN2) or without (aH3hN2) the N367S substitution. Virus stocks were grown in MDCK-II cells (ECACC). Viruses were inactivated by UV radiation using UV Stratalinker 1800 (Stratagene) on 50,000  $\mu$ Joules prior to their use in the binding and cleavage assays. UV inactivation did not affect the enzymatic activity of NA as determined with the MUNANA assay.

**NA cleavage assays.** The NA enzymatic activity was determined by using a fluorometric assay [68] in combination with 2'-(4-Methylumbelliferyl)- $\alpha$ -D-N-acetylneuraminic acid (MUNANA; Sigma-Aldrich) as described previously [20]. Enzymatic activity of the NA proteins towards multivalent glycoprotein substrates was analysed using a previously described enzyme-linked lectin assay (ELLA) [33]. In brief, fetuin- or transferrin-coated plates were incubated with serial dilutions of recombinant soluble NA proteins. After overnight incubation at 37°C, plates were washed and incubated with either biotinylated *Erythrina Cristagalli* Lectin (ECA, 1.25  $\mu$ g/ml; Vector Laboratories), biotinylated peanut agglutinin (PNA, 2.5  $\mu$ g/ml; Galab Technologied), biotinylated *Sambucus Nigra* Lectin (SNA, 1.25  $\mu$ g/ml; Vector Laboratories) or biotinylated *Maackia Amurensis* Lectin I (MAL I, 2.5  $\mu$ g/ml; Vector Laboratories). Cleavage of SIAs from fetuin and transferrin was quantified by analysing the increase (PNA and ECA) or decrease (MAL I and SNA) in binding of different lectins depending on their binding specificities (Fig. S4). The binding of ECA, PNA, SNA and MAL I was detected using horseradish peroxidase (HRP)-conjugated streptavidin (Thermo Fisher Scientific) and tetramethylbenzidine substrate (TMB, bioFX) in an ELISA reader EL-808 (BioTEK) by measuring the optical density (OD) at 450 nm. The data were fitted by non-linear regression using the Prism 6.05 software (GraphPad). The resulting curves were used to determine the amount of NA protein corresponding to half maximum MUNANA cleavage or lectin binding. The inverse of this amount is a measure of specific activity (activity per amount of protein) and was graphed relative to other NA proteins or substrate-lectin combinations.

**Plaque assay.** Plaque assays were performed in Vero cells (ATCC) as described previously [69]. One hour after infecting the cell monolayers with 30–50 plaque forming units of the virus in 1 ml of maintenance medium, the virus inoculum was removed and cells were covered the Avicel RC-581 overlay medium and cultures were incubated at 37°C in 5% CO<sub>2</sub> atmosphere. After three days of incubation, the overlay was removed by suction and the cells were stained with 1% crystal violet solution in 20% methanol in water. For immunostaining, cells were fixed with 4% paraformaldehyde solution for 30 min at 4°C, washed with PBS and permeabilized by incubation for 10–20 min with buffer containing 0.5% Triton-X-100 and 20 mM glycine in PBS. Cell layers were incubated with

monoclonal antibodies specific for the influenza A virus nucleoprotein (kindly provided by Dr. Alexander Klimov at Centers for Disease Control, USA) for 1 hour followed by another 1 hour incubation with peroxidase-labeled anti-mouse antibodies (DAKO, Denmark) and 30 min incubation with precipitate-forming peroxidase substrates True Blue. Stained plates were washed with water to stop the reaction, scanned on a flatbed scanner and the data were acquired by Adobe Photoshop 7.0 software.

**Virus replication in Vero or MDCK cells.** To characterize replication kinetics of different recombinant viruses, two replicate cultures of Vero or MDCK cells in 12-well plates were infected with each virus at MOI 0.001 (Vero cells) or 0.0001 (MDCK cells). Inocula were removed 1 hpi, fresh medium was added, and cultures were incubated at 37°C. Samples of culture supernatant were taken 24, 48 and 72 hpi and stored frozen. They were titrated together using focus formation assay in MDCK cells as described previously [57]. Numbers of infected cells per well were counted for the virus dilution that produced from 30 to 300 infected cells per well and recalculated into numbers of focus forming units (FFU) per ml of the original undiluted virus suspensions.

**Biolayer interferometry (BLI) binding and cleavage assays.** For the full length protein-containing vesicles and VLPs, similar amounts of NA activity, and thus NA protein, were applied in the BLI assays using the Octet RED348 (Fortebio). Inactivated virus preparations were analysed using Nanoparticle Tracking Analysis (Nanosight NS300, Malvern) as detailed below in order to use similar number of virus particles in the BLI assays. BLI assays were performed as described previously [37]. All experiments were carried out in Dulbecco's PBS with Calcium and Magnesium (Lonza) at 30 °C and with sensors shaking at 1000 rpm. Streptavidin biosensors were loaded to saturation with biotinylated synthetic glycans 2,3-sialyl-N-acetylactosamine-N-acetylactosamine (3'SLNLN), 2,6-sialyl-N-acetylactosamine-N-acetylactosamine (6'SLNLN), N-acetylactosamine-N-acetylactosamine (LNLN), LAMP1 or glycophorin A glycoproteins. Synthetic glycans were synthesized at the Department of Chemical Biology and Drug Discovery, Utrecht University, Utrecht, the Netherlands. For the NA kinetic cleavage assay, the sensors loaded with synthetic glycans were incubated in 100 µl buffer containing 4 µg recombinant soluble aN2 or hN2 in the absence or presence of 8 µg ECA. As controls, sensors were also incubated with ECA in the absence of N2. Association of the N2 VLPs, vesicles and virus particles was analysed for 30 minutes in the absence or presence of 10 µM OC (Roche). For viruses, the virus association phase in the presence of OC was followed by three 5 s washes and a dissociation phase in the absence of OC. Initial binding rates were determined similarly as previously described [37]. For lectin binding, the sensors loaded with recombinant glycoproteins were incubated with the different lectins (8 µg/100 µl) for 15 minutes.

**Nanoparticle tracking analysis (NTA).** NTA measurements were performed using a NanoSight NS300 instrument (Malvern) following the manufacturer's instructions. The UV-inactivated virus preparations were diluted with PBS to reach a particle concentration suitable for analysis with NTA. All measurements were performed at 19°C. Per analysis, the NanoSight NS300 recorded five 60 second sample videos, which were then analysed with the Nanoparticle Tracking analysis 3.0 software, resulting in quantitative information on particle number and particles sizes (Fig. S10). Each virus preparation was analysed twice and mean values were used. NTA measurements were validated by analysis of virus stocks quantified earlier by silver staining of viral proteins after electrophoresis on polyacrylamide gels [37]. Results obtained via both methods correlated well (less than 25% deviation).

### **Acknowledgements**

We thank Robert Webster (St. Jude Children's Research Hospital, Memphis, TN, USA) for pHW2000 reverse genetics plasmid. We thank Hanno Muller for technical assistance in part of the study.



## References

1. Gambaryan AS, Matrosovich MN. What adaptive changes in hemagglutinin and neuraminidase are necessary for emergence of pandemic influenza virus from its avian precursor? *Biochemistry (Mosc)*. 2015;80(7):872-80. doi: 10.1134/S000629791507007X. PubMed PMID: 26542001.
2. Byrd-Leotis L, Cummings RD, Steinhauer DA. The Interplay between the Host Receptor and Influenza Virus Hemagglutinin and Neuraminidase. *Int J Mol Sci*. 2017;18(7). doi: 10.3390/ijms18071541. PubMed PMID: 28714909; PubMed Central PMCID: PMC5536029.
3. Gaymard A, Le Briand N, Frobert E, Lina B, Escuret V. Functional balance between neuraminidase and haemagglutinin in influenza viruses. *Clin Microbiol Infect*. 2016;22(12):975-83. Epub 07/15. doi: 10.1016/j.cmi.2016.07.007. PubMed PMID: 27424943.
4. Yen HL, Liang CH, Wu CY, Forrest HL, Ferguson A, Choy KT, et al. Hemagglutinin-neuraminidase balance confers respiratory-droplet transmissibility of the pandemic H1N1 influenza virus in ferrets. *Proc Natl Acad Sci U S A*. 2011;108(34):14264-9. Epub 08/08. doi: 10.1073/pnas.1111000108. PubMed PMID: 21825167.
5. Xu R, Zhu X, McBride R, Nycholat CM, Yu W, Paulson JC, et al. Functional balance of the hemagglutinin and neuraminidase activities accompanies the emergence of the 2009 H1N1 influenza pandemic. *J Virol*. 2012;86(17):9221-32. Epub 06/20. doi: 10.1128/JVI.00697-12. PubMed PMID: 22718832.
6. Baigent SJ, McCauley JW. Influenza type A in humans, mammals and birds: determinants of virus virulence, host-range and interspecies transmission. *Bioessays*. 2003;25(7):657-71. doi: 10.1002/bies.10303. PubMed PMID: 12815721.
7. Cohen M, Zhang X-Q, Senaati HP, Chen H-W, Varki NM, Schooley RT, et al. Influenza A penetrates host mucus by cleaving sialic acids with neuraminidase. *Virology Journal*. 2013;10(1):321. doi: 10.1186/1743-422X-10-321. PubMed PMID: 24261589; PubMed Central PMCID: PMC3842836
8. Ito T, Kawaoka Y. Host-range barrier of influenza A viruses. *Vet Microbiol*. 2000;74(1-2):71-5. PubMed PMID: 10799779.
9. Russell RJ, Stevens DJ, Haire LF, Gamblin SJ, Skehel JJ. Avian and human receptor binding by hemagglutinins of influenza A viruses. *Glycoconj J*. 2006;23(1-2):85-92. doi: 10.1007/s10719-006-5440-1. PubMed PMID: 16575525.
10. Connor RJ, Kawaoka Y, Webster RG, Paulson JC. Receptor specificity in human, avian, and equine H2 and H3 influenza virus isolates. *Virology*. 1994;205(1):17-23. doi: 10.1006/viro.1994.1615. PubMed PMID: 7975212.
11. Matrosovich M, Tuzikov A, Bovin N, Gambaryan A, Klimov A, Castrucci MR, et al. Early alterations of the receptor-binding properties of H1, H2, and H3 avian influenza virus hemagglutinins after their introduction into mammals. *J Virol*. 2000;74(18):8502-12. PubMed PMID: 10954551.
12. Stevens J, Blixt O, Glaser L, Taubenberger JK, Palese P, Paulson JC, et al. Glycan microarray analysis of the hemagglutinins from modern and pandemic influenza viruses reveals different receptor specificities. *J Mol Biol*. 2006;355(5):1143-55. Epub 2005/11/18. doi: 10.1016/j.jmb.2005.11.002. PubMed PMID: 16343533.
13. Wasik BR, Barnard KN, Parrish CR. Effects of Sialic Acid Modifications on Virus Binding and Infection. *Trends Microbiol*. 2016;24(12):991-1001. Epub 08/01. doi: 10.1016/j.tim.2016.07.005. PubMed PMID: 27491885.
14. Peng W, de Vries RP, Grant OC, Thompson AJ, McBride R, Tsogtbaatar B, et al. Recent H3N2 Viruses Have Evolved Specificity for Extended, Branched Human-type Receptors, Conferring Potential for Increased Avidity. *Cell host & microbe*. 2017;21(1):23-34. Epub 2016/12/27. doi: 10.1016/j.chom.2016.11.004. PubMed PMID: 28017661; PubMed Central PMCID: PMC5233592.
15. de Vries RP, de Vries E, Moore KS, Rigter A, Rottier PJ, de Haan CA. Only two residues are responsible for the dramatic difference in receptor binding between swine and new pandemic H1

- hemagglutinin. *J Biol Chem.* 2011;286(7):5868-75. Epub 2010/12/20. doi: 10.1074/jbc.M110.193557. PubMed PMID: 21173148; PubMed Central PMCID: PMCPMC3037699.
16. Guo H, de Vries E, McBride R, Dekkers J, Peng W, Bouwman KM, et al. Highly pathogenic influenza A(H5Nx) viruses with altered H5 receptor-binding specificity. *Emerg Infect Dis.* 2017;23(2):220-31. Epub 2016/11/22. doi: 10.3201/eid2302.161072. PubMed PMID: 27869615; PubMed Central PMCID: PMCPMC5324792.
  17. Gambaryan A, Yamnikova S, Lvov D, Tuzikov A, Chinarev A, Pazynina G, et al. Receptor specificity of influenza viruses from birds and mammals: new data on involvement of the inner fragments of the carbohydrate chain. *Virology.* 2005;334(2):276-83. doi: 10.1016/j.virol.2005.02.003. PubMed PMID: 15780877.
  18. Tumpey TM, Maines TR, Van Hoeven N, Glaser L, Solórzano A, Pappas C, et al. A two-amino acid change in the hemagglutinin of the 1918 influenza virus abolishes transmission. *Science.* 2007;315(5812):655-9. doi: 10.1126/science.1136212. PubMed PMID: 17272724.
  19. Saito T, Taylor G, Webster RG. Steps in maturation of influenza A virus neuraminidase. *J Virol.* 1995;69(8):5011-7. PubMed PMID: 7541844.
  20. Dai M, Guo H, Dortmans JC, Dekkers J, Nordholm J, Daniels R, et al. Identification of Residues That Affect Oligomerization and/or Enzymatic Activity of Influenza Virus H5N1 Neuraminidase Proteins. *J Virol.* 2016;90(20):9457-70. Epub 09/29. doi: 10.1128/JVI.01346-16. PubMed PMID: 27512075.
  21. Shtyrya YA, Mochalova LV, Bovin NV. Influenza virus neuraminidase: structure and function. *Acta Naturae.* 2009;1(2):26-32. PubMed PMID: 22649600.
  22. Air GM. Influenza neuraminidase. *Influenza Other Respir Viruses.* 2011;6(4):245-56. Epub 11/16. doi: 10.1111/j.1750-2659.2011.00304.x. PubMed PMID: 22085243.
  23. Russell RJ, Haire LF, Stevens DJ, Collins PJ, Lin YP, Blackburn GM, et al. The structure of H5N1 avian influenza neuraminidase suggests new opportunities for drug design. *Nature.* 2006;443(7107):45-9. Epub 08/16. doi: 10.1038/nature05114. PubMed PMID: 16915235.
  24. Baum LG, Paulson JC. The N2 neuraminidase of human influenza virus has acquired a substrate specificity complementary to the hemagglutinin receptor specificity. *Virology.* 1991;180(1):10-5. PubMed PMID: 1984642.
  25. Li Y, Cao H, Dao N, Luo Z, Yu H, Chen Y, et al. High-throughput neuraminidase substrate specificity study of human and avian influenza A viruses. *Virology.* 2011;415(1):12-9. Epub 04/17. doi: 10.1016/j.virol.2011.03.024. PubMed PMID: 21501853.
  26. Du W, Dai M, Li Z, Boons GJ, Peeters B, van Kuppeveld FJM, et al. Substrate Binding by the Second Sialic Acid-Binding Site of Influenza A Virus N1 Neuraminidase Contributes to Enzymatic Activity. *J Virol.* 2018;92(20):e01243-18. doi: 10.1128/JVI.01243-18. PubMed PMID: 30089692 PubMed Central PMCID: PMCPMC6158415.
  27. Kobasa D, Kodihalli S, Luo M, Castrucci MR, Donatelli I, Suzuki Y, et al. Amino acid residues contributing to the substrate specificity of the influenza A virus neuraminidase. *J Virol.* 1999;73(8):6743-51. PubMed PMID: 10400772.
  28. Uhlenendorff J, Matrosovich T, Klenk HD, Matrosovich M. Functional significance of the hemadsorption activity of influenza virus neuraminidase and its alteration in pandemic viruses. *Arch Virol.* 2009;154(6):945-57. Epub 05/21. doi: 10.1007/s00705-009-0393-x. PubMed PMID: 19458903.
  29. Varghese JN, Colman PM, van Donkelaar A, Blick TJ, Sahasrabudhe A, McKimm-Breschkin JL. Structural evidence for a second sialic acid binding site in avian influenza virus neuraminidases. *Proc Natl Acad Sci U S A.* 1997;94(22):11808-12. PubMed PMID: 9342319.
  30. Sun X, Li Q, Wu Y, Wang M, Liu Y, Qi J, et al. Structure of influenza virus N7: the last piece of the neuraminidase "jigsaw" puzzle. *J Virol.* 2014;88(16):9197-207. Epub 06/04. doi: 10.1128/JVI.00805-14. PubMed PMID: 24899180.
  31. Lai JC, Garcia JM, Dyason JC, Bohm R, Madge PD, Rose FJ, et al. A secondary sialic acid binding site on influenza virus neuraminidase: fact or fiction? *Angew Chem Int Ed Engl.* 2012;51(9):2221-4. Epub 06/26. doi: 10.1002/anie.201108245. PubMed PMID: 22281708.

32. Nuss JM, Air GM. Transfer of the hemagglutinin activity of influenza virus neuraminidase subtype N9 into an N2 neuraminidase background. *Virology*. 1991;183(2):496-504. PubMed PMID: 1853557.
33. Dai M, McBride R, Dortmans JC, Peng W, Bakkers MJ, de Groot RJ, et al. Mutation of the Second Sialic Acid-Binding Site, Resulting in Reduced Neuraminidase Activity, Preceded the Emergence of H7N9 Influenza A Virus. *J Virol*. 2017;91(9). Epub 04/13. doi: 10.1128/JVI.00049-17. PubMed PMID: 28202753.
34. Kobasa D, Rodgers ME, Wells K, Kawaoka Y. Neuraminidase hemadsorption activity, conserved in avian influenza A viruses, does not influence viral replication in ducks. *J Virol*. 1997;71(9):6706-13. PubMed PMID: 9261394.
35. Hausmann J, Kretzschmar E, Garten W, Klenk HD. N1 neuraminidase of influenza virus A/FPV/Rostock/34 has haemadsorbing activity. *J Gen Virol*. 1995;76(Pt 7):1719-28. doi: 10.1099/0022-1317-76-7-1719. PubMed PMID: 9049377.
36. Matrosovich MN, Krauss S, Webster RG. H9N2 influenza A viruses from poultry in Asia have human virus-like receptor specificity. *Virology*. 2001;281(2):156-62. Epub 2001/03/30. doi: 10.1006/viro.2000.0799. PubMed PMID: 11277689.
37. Guo H, Rabouw H, Slomp A, Dai M, van der Vegt F, van Lent JWM, et al. Kinetic analysis of the influenza A virus HA/NA balance reveals contribution of NA to virus-receptor binding and NA-dependent rolling on receptor-containing surfaces. *PLoS Pathog*. 2018;14(8):e1007233. doi: 10.1371/journal.ppat.1007233. PubMed PMID: 30102740; PubMed Central PMCID: PMC6107293.
38. Sauter NK, Bednarski MD, Wurzburg BA, Hanson JE, Whitesides GM, Skehel JJ, et al. Hemagglutinins from two influenza virus variants bind to sialic acid derivatives with millimolar dissociation constants: a 500-MHz proton nuclear magnetic resonance study. *Biochemistry*. 1989;28(21):8388-96. doi: 10.1021/bi00447a018. PubMed PMID: 2605190.
39. Takemoto DK, Skehel JJ, Wiley DC. A surface plasmon resonance assay for the binding of influenza virus hemagglutinin to its sialic acid receptor. *Virology*. 1996;217(2):452-8. PubMed PMID: 8610436.
40. Wu AM, Wu JH, Tsai MS, Yang Z, Sharon N, Herp A. Differential affinities of Erythrina cristagalli lectin (ECL) toward monosaccharides and polyvalent mammalian structural units. *Glycoconj J*. 2007;24(9):591-604. Epub 09/06. doi: 10.1007/s10719-007-9063-y. PubMed PMID: 17805962.
41. Sharma V, Srinivas VR, Adhikari P, Vijayan M, Surolia A. Molecular basis of recognition by Gal/GalNAc specific legume lectins: influence of Glu 129 on the specificity of peanut agglutinin (PNA) towards C2-substituents of galactose. *Glycobiology*. 1998;8(10):1007-12. PubMed PMID: 9719681.
42. Geisler C, Jarvis DL. Effective glycoanalysis with Maackia amurensis lectins requires a clear understanding of their binding specificities. *Glycobiology*. 2011;21(8):988-93. PubMed PMID: 21863598.
43. Shibuya N, Goldstein IJ, Broekaert WF, Nsimba-Lubaki M, Peeters B, Peumans WJ. The elderberry (*Sambucus nigra* L.) bark lectin recognizes the Neu5Ac(alpha 2-6)Gal/GalNAc sequence. *J Biol Chem*. 1987;262(4):1596-601. PubMed PMID: 3805045.
44. Baenziger JU, Fiete D. Structure of the complex oligosaccharides of fetuin. *J Biol Chem*. 1979;254(3):789-95. PubMed PMID: 83994.
45. Spik G, Bayard B, Fournet B, Strecker G, Bouquelet S, Montreuil J. Studies on glycoconjugates. LXIV. Complete structure of two carbohydrate units of human serotransferrin. *FEBS Lett*. 1975;50(3):296-9. PubMed PMID: 1116600.
46. von Bonsdorff L, Tölö H, Lindeberg E, Nyman T, Harju A, Parkkinen J. Development of a pharmaceutical apotransferrin product for iron binding therapy. *Biologicals*. 2001;29(1):27-37. doi: 10.1006/biol.2001.0273. PubMed PMID: 11482890.
47. Lai JC, Chan WW, Kien F, Nicholls JM, Peiris JS, Garcia JM. Formation of virus-like particles from human cell lines exclusively expressing influenza neuraminidase. *J Gen Virol*. 2010;91(Pt 9):2322-30. Epub 05/26. doi: 10.1099/vir.0.019935-0. PubMed PMID: 20505010.

48. Del Piccolo N, Placone J, He L, Agudelo SC, Hristova K. Production of plasma membrane vesicles with chloride salts and their utility as a cell membrane mimetic for biophysical characterization of membrane protein interactions. *Anal Chem.* 2012;84(20):8650-5. Epub 10/03. doi: 10.1021/ac301776j. PubMed PMID: 22985263.
49. Hatakeyama S, Sakai-Tagawa Y, Kiso M, Goto H, Kawakami C, Mitamura K, et al. Enhanced expression of an alpha2,6-linked sialic acid on MDCK cells improves isolation of human influenza viruses and evaluation of their sensitivity to a neuraminidase inhibitor. *J Clin Microbiol.* 2005;43(8):4139-46. doi: 10.1128/JCM.43.8.4139-4146.2005. PubMed PMID: 16081961; PubMed Central PMCID: PMC1233980.
50. Govorkova EA, Murti G, Meignier B, de Taisne C, Webster RG. African green monkey kidney (Vero) cells provide an alternative host cell system for influenza A and B viruses. *J Virol.* 1996;70(8):5519-24. PubMed PMID: 8764064; PubMed Central PMCID: PMC190510.
51. Rapoport EM, Mochalova LV, Gabius H-J, Romanova J, Bovin NV. *Patterning of Lectins of Vero and MDCK Cells and Influenza Viruses: The Search for Additional Virus/Cell Interactions*: CRC; 2005. 87-108 p.
52. Carlsson SR, Lycksell PO, Fukuda M. Assignment of O-glycan attachment sites to the hinge-like regions of human lysosomal membrane glycoproteins lamp-1 and lamp-2. *Arch Biochem Biophys.* 1993;304(1):65-73. doi: 10.1006/abbi.1993.1322. PubMed PMID: 8323299.
53. Carlsson SR, Roth J, Piller F, Fukuda M. Isolation and characterization of human lysosomal membrane glycoproteins, h-lamp-1 and h-lamp-2. Major sialoglycoproteins carrying polylectosaminoglycan. *J Biol Chem.* 1988;263(35):18911-9. PubMed PMID: 3143719.
54. Yoshima H, Furthmayr H, Kobata A. Structures of the asparagine-linked sugar chains of glycophorin A. *J Biol Chem.* 1980;255(20):9713-8. PubMed PMID: 7430095.
55. Zdebska E, Koscielak J. A single-sample method for determination of carbohydrate and protein contents glycoprotein bands separated by sodium dodecyl sulfate- polyacrylamide gel electrophoresis. *Anal Biochem.* 1999;275(2):171-9. PubMed PMID: 10552901.
56. Van Poucke S, Doedt J, Baumann J, Qiu Y, Matrosovich T, Klenk HD, et al. Role of Substitutions in the Hemagglutinin in the Emergence of the 1968 Pandemic Influenza Virus. *J Virol.* 2015;89(23):12211-6. Epub 09/16. doi: 10.1128/JVI.01292-15. PubMed PMID: 26378170.
57. Matrosovich M, Matrosovich T, Uhlenhorff J, Garten W, Klenk HD. Avian-virus-like receptor specificity of the hemagglutinin impedes influenza virus replication in cultures of human airway epithelium. *Virology.* 2007;361(2):384-90. Epub 01/17. PubMed PMID: 17207830.
58. Laver WG, Colman PM, Webster RG, Hinshaw VS, Air GM. Influenza virus neuraminidase with hemagglutinin activity. *Virology.* 1984;137(2):314-23. PubMed PMID: 6485252.
59. Benton DJ, Wharton SA, Martin SR, McCauley JW. Role of Neuraminidase in Influenza A(H7N9) Virus Receptor Binding. *J Virol.* 2017;91(11). Epub 05/12. doi: 10.1128/JVI.02293-16. PubMed PMID: 28356530.
60. Lin YP, Gregory V, Collins P, Kloess J, Wharton S, Cattle N, et al. Neuraminidase receptor binding variants of human influenza A(H3N2) viruses resulting from substitution of aspartic acid 151 in the catalytic site: a role in virus attachment? *J Virol.* 2010;84(13):6769-81. Epub 04/21. doi: 10.1128/JVI.00458-10. PubMed PMID: 20410266
61. Mogling R, Richard MJ, Vliet SV, Beek RV, Schrauwen EJA, Spronken MI, et al. Neuraminidase-mediated haemagglutination of recent human influenza A(H3N2) viruses is determined by arginine 150 flanking the neuraminidase catalytic site. *J Gen Virol.* 2017;98(6):1274-81. doi: 10.1099/jgv.0.000809. PubMed PMID: 28612701; PubMed Central PMCID: PMC5962893.
62. Lai JCC, Karunarathna H, Wong HH, Peiris JSM, Nicholls JM. Neuraminidase activity and specificity of influenza A virus are influenced by haemagglutinin-receptor binding. *Emerg Microbes Infect.* 2019;8(1):327-38. doi: 10.1080/22221751.2019.1581034. PubMed PMID: 30866786
63. Webster RG, Air GM, Metzger DW, Colman PM, Varghese JN, Baker AT, et al. Antigenic structure and variation in an influenza virus N9 neuraminidase. *J Virol.* 1987;61(9):2910-6. Epub 09/01. PubMed PMID: 3612957.

64. Bakkers MJ, Lang Y, Feitsma LJ, Hulswit RJ, de Poot SA, van Vliet AL, et al. Betacoronavirus Adaptation to Humans Involved Progressive Loss of Hemagglutinin-Esterase Lectin Activity. *Cell Host Microbe*. 2017;21(3):356-66. doi: 10.1016/j.chom.2017.02.008. PubMed PMID: 28279346.
65. Cornelissen LA, de Vries RP, de Boer-Luijtz EA, Rigter A, Rottier PJ, de Haan CA. A single immunization with soluble recombinant trimeric hemagglutinin protects chickens against highly pathogenic avian influenza virus H5N1. *PLoS One*. 2010;5(5):e10645. doi: 10.1371/journal.pone.0010645. PubMed PMID: 20498717; PubMed Central PMCID: PMC2871037
66. Predonzani A, Arnoldi F, Lopez-Requena A, Burrone OR. In vivo site-specific biotinylation of proteins within the secretory pathway using a single vector system. *BMC Biotechnol*. 2008;8:41. doi: 10.1186/1472-6750-8-41. PubMed PMID: 18423015; PubMed Central PMCID: PMC2373293.
67. James KT, Cooney B, Agopsowicz K, Trevors MA, Mohamed A, Stoltz D, et al. Novel High-throughput Approach for Purification of Infectious Virions. *Sci Rep*. 2016;6:36826. Epub 11/09. doi: 10.1038/srep36826. PubMed PMID: 27827454.
68. Potier M, Mameli L, Bélisle M, Dallaire L, Melançon SB. Fluorometric assay of neuraminidase with a sodium (4-methylumbelliferyl-alpha-D-N-acetylneuraminic) substrate. *Anal Biochem*. 1979;94(2):287-96. PubMed PMID: 464297.
69. Matrosovich M, Matrosovich T, Garten W, Klenk HD. New low-viscosity overlay medium for viral plaque assays. *Virology*. 2006;346:63. Epub 08/31. doi: 10.1016/j.virol.2006.08.013. PubMed PMID: 16945126.
70. Vavricka CJ, Liu Y, Kiyota H, Sriwilaijaroen N, Qi J, Tanaka K, Wu Y, Li Q, Li Y, Yan J, Suzuki Y, Gao GF. Influenza neuraminidase operates via a nucleophilic mechanism and can be targeted by covalent inhibitors. *Nat Commun*. 2013;4:1491. doi: 10.1038/ncomms2487. PubMed PMID: 23422659.
71. Xu J, Davis CT, Christman MC, Rivaller P, Zhong H, Donis RO, et al. Evolutionary history and phylogenetics of influenza A and B neuraminidase (NA) genes inferred from large-scale sequence analyses. *PLoS One*. 2012;7(7):e38665. doi: 10.1371/journal.pone.0038665. PubMed PMID: 22808012 PubMed Central PMCID: PMC3394769

### Supplementary figures

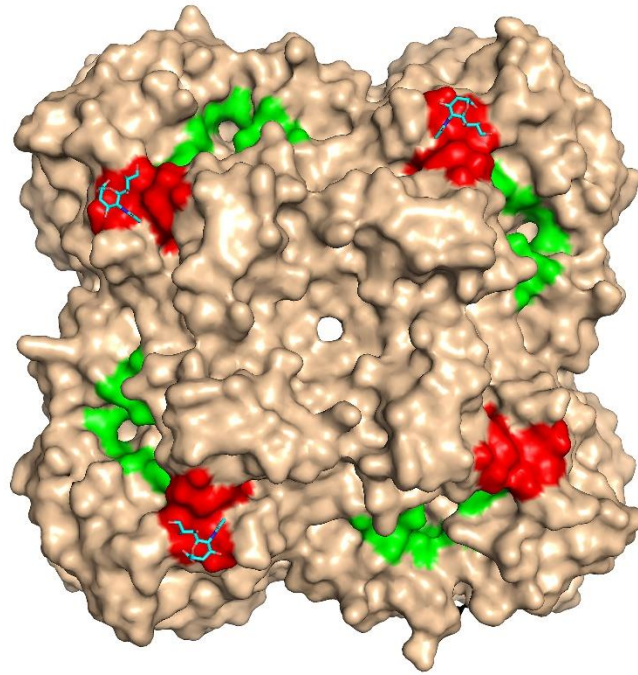


**Fig. S1. N2 Crystal structure.** (A) Surface representation of the crystal structure of the N2 from pandemic A/R1/5 +/1957 (H2N2) in complex with Neu5Ac (PDB ID:4H53; [70]) was depicted using Pymol software. Top view is shown. The SIA-contact residues in the NA active site and the 2SBS are coloured green and red, respectively. The Neu5Ac moieties in the 2SBS sites are shown in a stick representation.

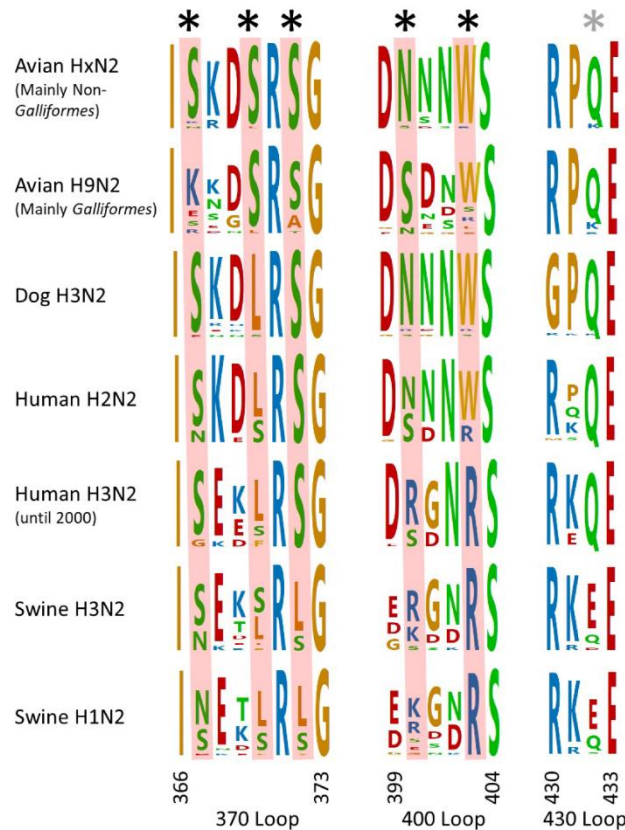


**Fig. S2. Sequence logos of the 2SBS of N2 proteins of viruses infecting different species.** Sequence logos were generated for the three loops (370, 400 and 430 loop) that constitute the 2SBS using DNASTAR Lasergene 14 software (MegAlign Pro 14). The overall height of the stack indicates the sequence conservation at that position, while the height of symbols within the stack indicates the relative frequency of each amino acid at that position. All sequences available for avian viruses containing N2 excluding H9N2 (indicated by Avian HxN2), avian H9N2, dog H3N2, human H2N2, human H3N2 until 2000, swine H3N2 and swine H1N2 from the Influenza Research Database (<https://www.fludb.org/>) were used. SIA-contact residues were highly conserved in Avian HxN2, but not in H9N2 viruses. Avian H9N2 viruses were mainly (>80%) found in Galliformes species (chicken, turkey and quail), while avian HxN2 viruses were isolated mainly from non-Galliformes species (>75%). Dog H3N2 viruses generally contain a S370L mutation in the 370 loop, which is known to affect functionality of the 2SBS [28], while in addition the identity of the 430 residue deviates from those found in avian viruses. Please note that the phylogenetic analysis shown in Fig. S3 indicates that human H2N2 viruses either have a mutated SIA-contact residue at position 367 or at position 370, both of which are known to disrupt the 2SBS [28]. Swine viruses containing N2, which are generally derived from human viruses [71], also contain a mutated 2SBS. SIA-contacting residues were labelled with asterisks in the sequence logo of the avian HxN2 viruses. The grey asterisk indicates an

additional SIA-contact residue in the 430 loop of N9. Numbering of the start and end residues of the three loops is indicated.

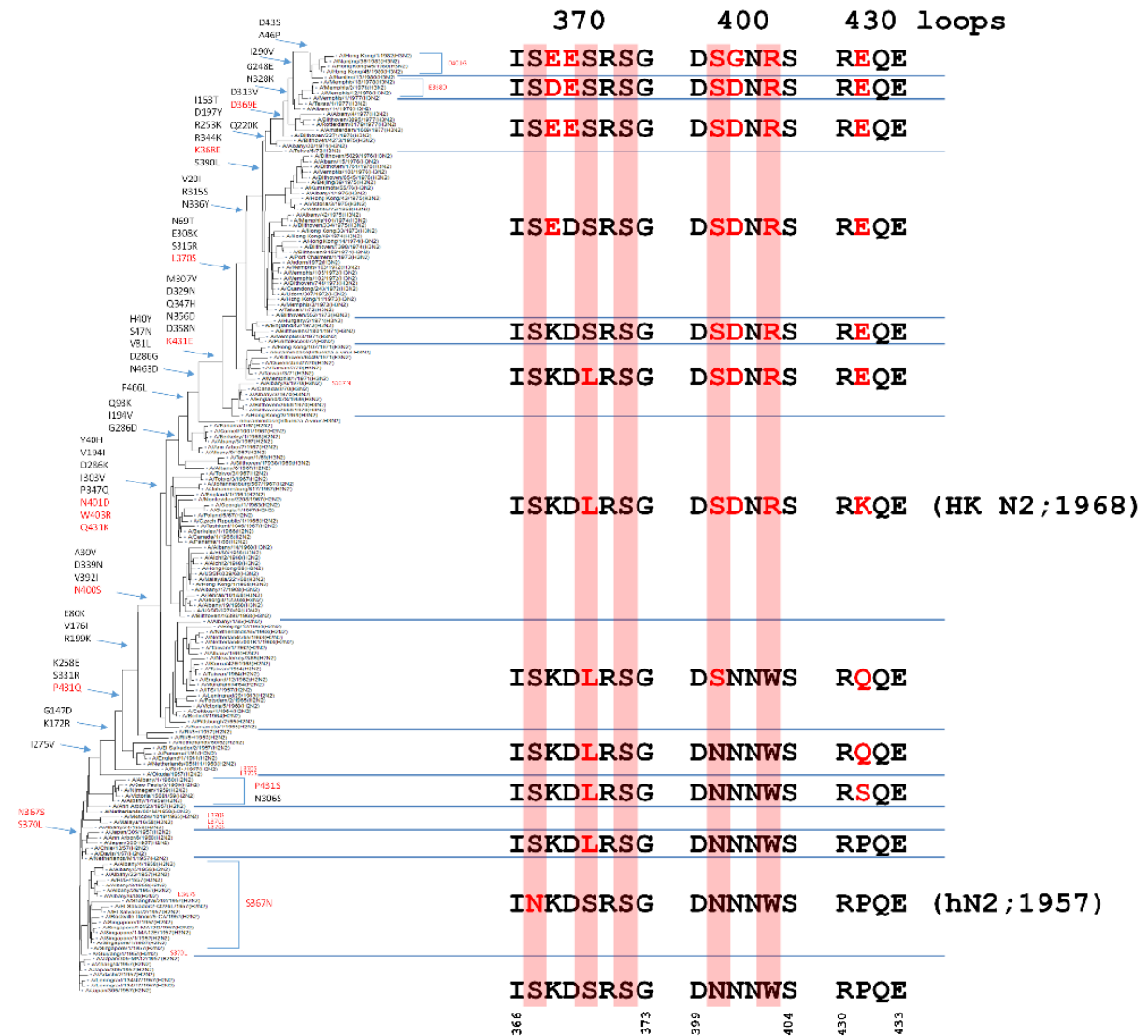


**Fig. S3. Phylogenetic analysis of N2 of human H2N2 and H3N2 viruses from 1957 until 1980.** All full-length and unique N2 protein sequences of human H2N2 and H3N2 viruses between 1957-1980 were downloaded from the GenBank and GISAID databases. N2 protein trees were constructed by using the PHYLIP neighbor-joining algorithm with the mPAM distance matrix. This tree was used as a guide tree to select N2 sequences representing all main branches of the tree. The selected N2 proteins were used to construct a summary tree with topology similar to that of the guide tree. Mutations that became fixed along the trunk of the tree are indicated as well as 2SBS residues that differ between different branches. On the right site the residues of the 370, 400 and 430 loops that make up the 2SBS are shown. SIA-contact residues in the N2 protein are indicated by the red shading. Mutations in N2 relative to the avian consensus sequence are shown in red.



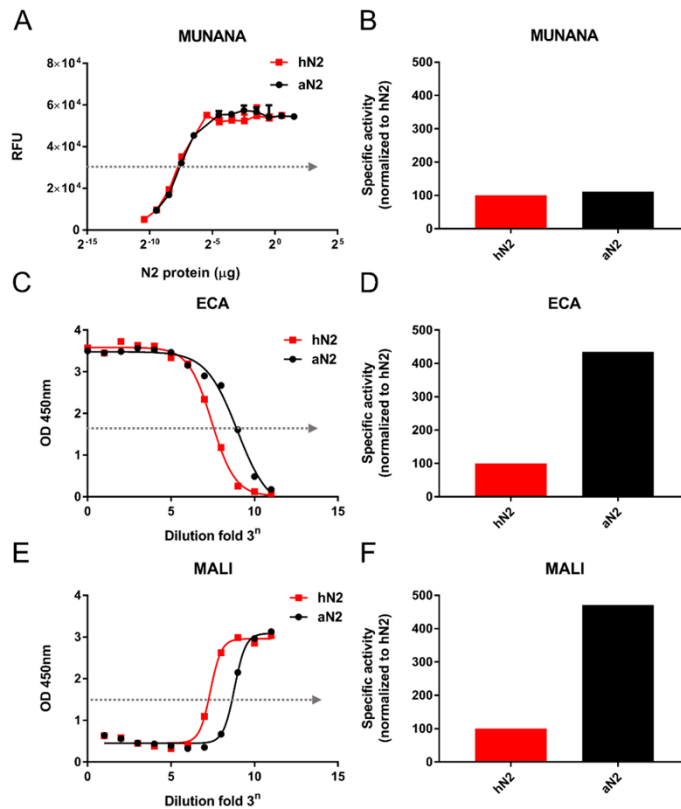


**Fig. S4. Enzymatic activity of N2 proteins using monovalent and multivalent substrates.** (A) The enzymatic activity of hN2 and aN2 proteins for a monovalent substrate was determined using the MUNANA fluorometric assay. To this end, limiting dilutions of the different N2 proteins were subjected to the assay and the fluorescence generated upon cleavage of MUNANA was measured using a plate reader (in relative fluorescent units [RFU]). The data were fitted by non-linear regression using the Prism 6.05 software (GraphPad). The resulting curves were used to determine the amount of NA protein corresponding to half maximum MUNANA cleavage (indicated by the arrow). The inverse of this amount is a measure of specific activity (activity per amount of protein) and was graphed relative to hN2 in (B). ELLAs were used to determine the relative specific activities of the N2 proteins for multivalent substrates (C-F). The OD 450nm values correspond to lectin binding upon incubation of the glycoprotein with different dilutions of the NA preparations. In the examples shown, removal of SIAs from fetuin was probed using the lectins ECA (C) and MAL I (E). Increasing dilutions of the NA preparations resulted in reduced cleavage of SIAs as indicated by the reduced binding of ECA, which (just as PNA) binds to desialylated glycans. The opposite was observed for MAL I (and SNA) which binds to sialylated glycans. The data were fitted by non-linear regression using the Prism 6.05 software (GraphPad). The resulting curves were used to determine the dilution (or amount) of NA protein corresponding to half maximum lectin binding (indicated by the arrow). This value was used

to determine the relative specific activity (activity per amount of protein) for a specific glycoprotein-lectin combination (D and F).

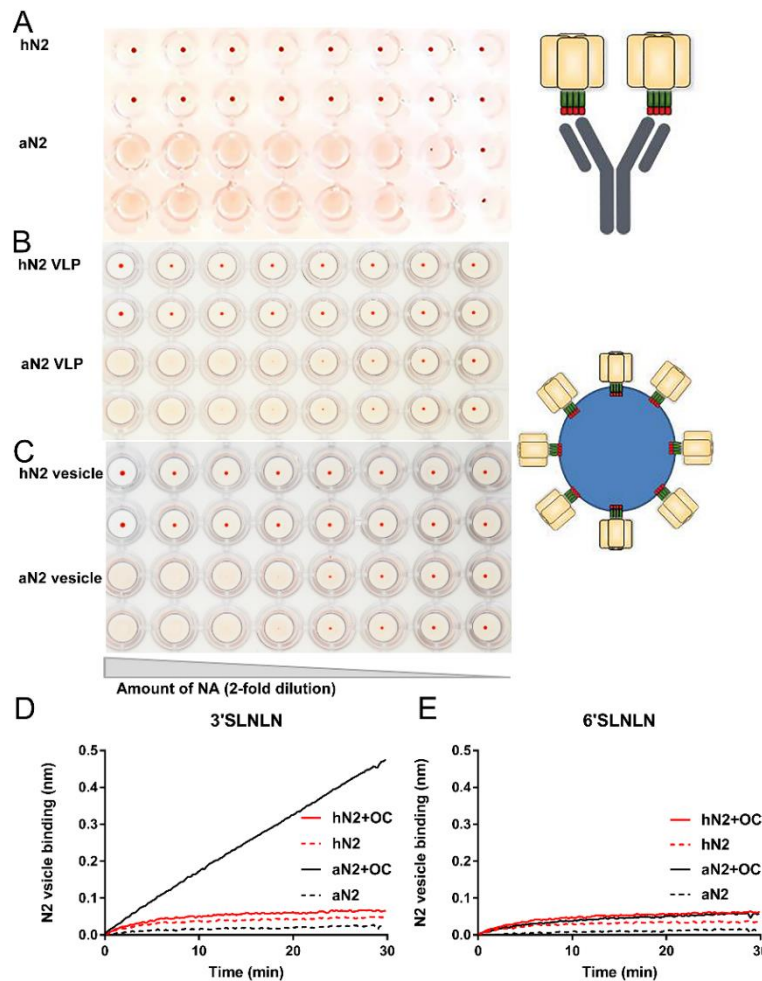


**Fig. S5. Hemagglutination assays.** (A) Identical amounts of recombinant soluble hN2 and aN2 protein were pre-complexed with a strepMabClassic-HRP and rabbit- $\alpha$ -mouse-HRP prior to their incubation with erythrocytes. Serial twofold dilutions of the antibody-N2 complexes were incubated with equal volumes of 0.5% human erythrocytes at 4°C for 2 h in the presence of OC. Red dots at the bottom of the wells indicate absence of hemagglutination. (B-C) Hemagglutination using membrane vesicles (B) or VLPs (C) containing identical amounts of N2 protein. Membrane vesicles containing full length hN2 and aN2 were analysed for their ability to bind 3'SLNLN (D) or 6'SLNLN (E) in the absence or presence of OC using BLI similarly as described in the legend to Fig. 2. Representative experiments (out of three performed) are shown.

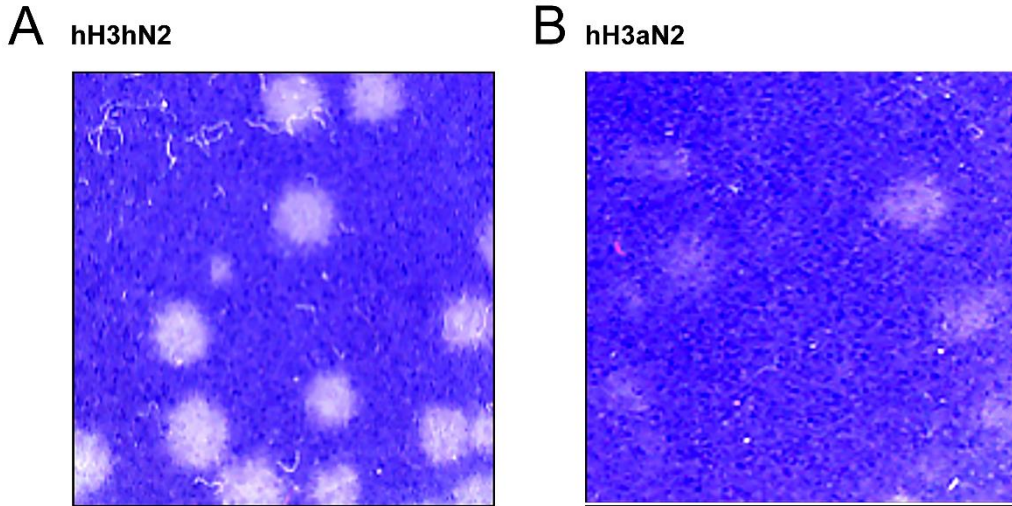


**Fig. S6. Plaque morphology of recombinant viruses.** Plaque assays were performed for hH3hN2 (A) and hH3aN2 (B) viruses using Vero cells followed by crystal violet dye staining.

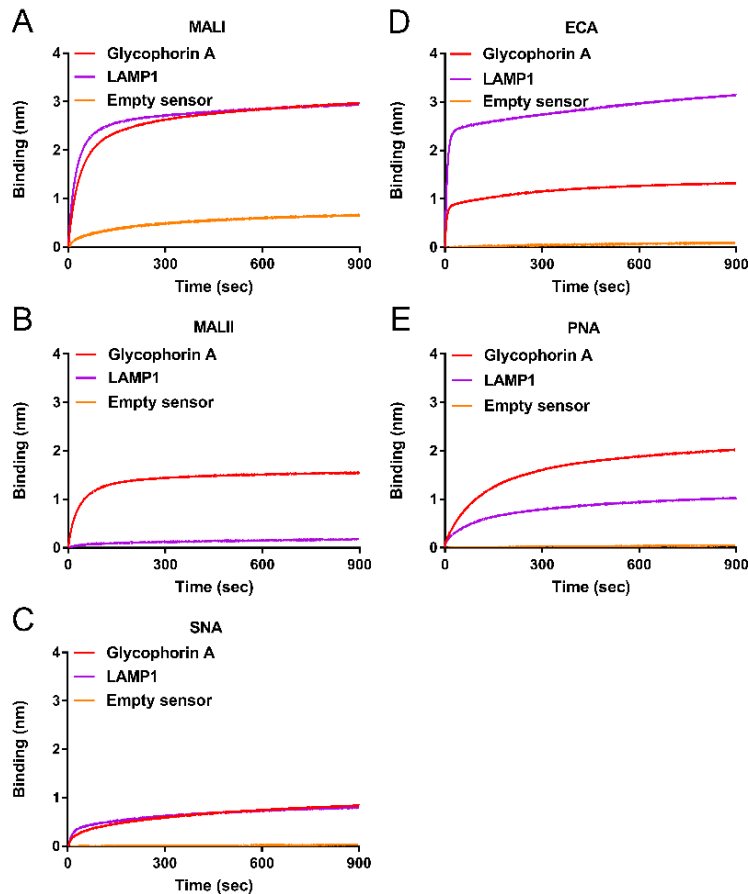


**Fig. S7. Analysis of glycans attached to glycoprotein A and LAMP1 using lectin binding.** Glycophorin A and Lamp1 were analysed for their attached glycans by BLI analysis of lectin binding to sensors coated with these glycoproteins. As a negative control, empty sensors were used. (A) Binding of MAL I, which is specific for SIA $\alpha$ 2,3Gal $\alpha$ 1,4GlcNAc oligosaccharide abundantly present on N-linked glycans.

(B) Binding of MAL II, which is specific for SIA $\alpha$ 2,3Gal 1,3GalNAc oligosaccharides abundantly present on O-linked glycans. (C) Binding of SNA, which is specific for SIA $\alpha$ 2,6Gal 1,4GlcNAc oligosaccharide abundantly present on N-linked glycans. (D) Binding of ECA, which is specific for terminal Gal 1,4GlcNAc glycans corresponding to non-sialylated N-linked sugars. (E) Binding of PNA, which is specific for terminal Gal 1,3GalNAc glycans corresponding to non-sialylated O-linked sugars.

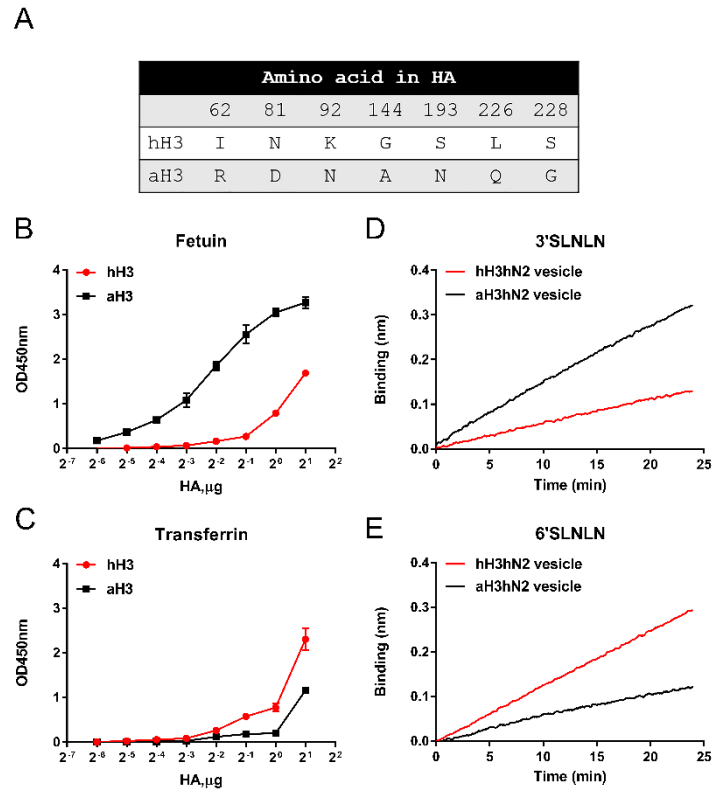


**Fig. S8. Substrate binding of soluble HA proteins and HA-containing vesicles.** Amino acid differences between hH3 and aH3 are indicated (A). Limiting dilutions of soluble H3 proteins complexed with a strepMabClassic-HRP and rabbit- $\alpha$ -mouse-HRP were used in the fetuin-(B) or transferrin-(C) binding assay. Optical density at 450 nm (OD450) corresponds to binding of HA to glycoproteins. Membrane vesicles obtained after co-expression of full length hH3 and hN2 or aH3 and hN2 were analysed for their ability to bind 3'SLNLN (D) or 6'SLNLN (E) in the presence of OC using BLI similarly as described in the legend to Fig. 2. Representative experiments are shown.

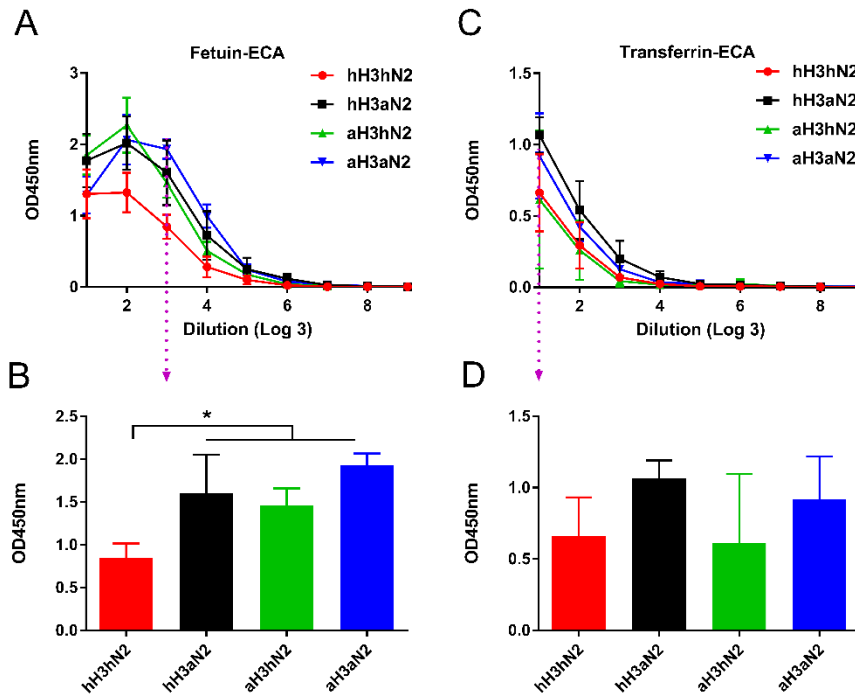


**Fig. S9. NA activity of recombinant viruses and soluble N2 proteins as determined by ELLA.** Virus preparations were normalized based on their MUNANA activity. Fetuin- (A) or transferrin- (C) coated plates were incubated with serial 3-fold dilutions of viruses (in the absence of OC). Cleavage of SIAs from glycoproteins was monitored using ECA, which binds desialylated glycans. OD450 values reflect lectin binding. Values obtained in the presence of OC (which blocks the NA protein) were considered as background values and subtracted from the values obtained in the absence of OC. OD450 values observed at a single dilution indicated by the vertical arrow in (A) and (C) are shown in (B) and (D). The ELLAs were performed twice in duplicate. The mean values of these experiments are shown. Stars depict P values calculated using one-way ANOVA (\*,  $P < 0.05$ ).

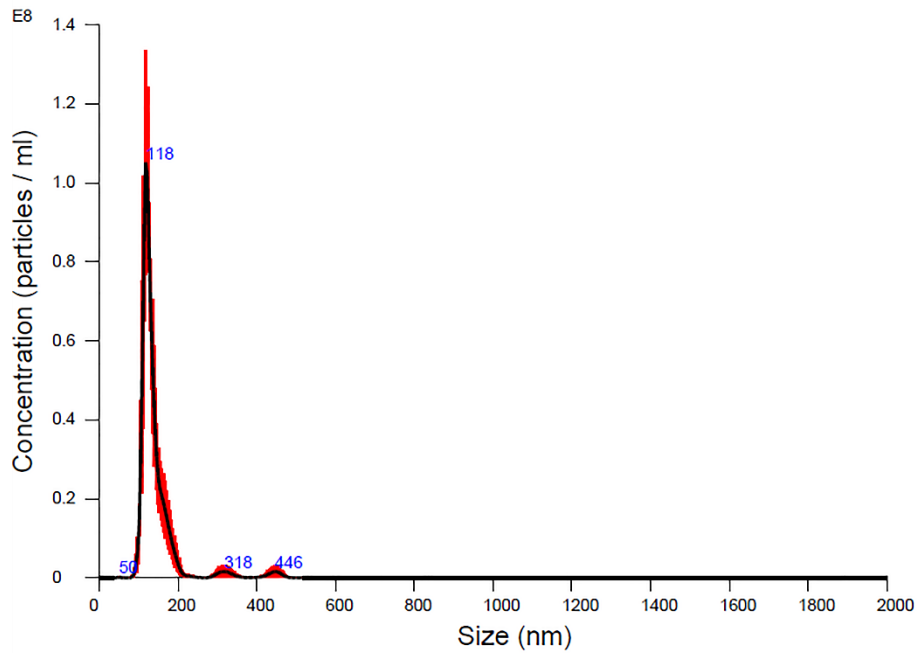


**Fig. S10 Example of a Nanoparticle tracking analysis (NTA) experiment.** Example of a NTA experiment performed using a NanoSight NS300 instrument with a hH3aN2 virus stock is shown. The black line indicates the mean of 5 measurements, while the red bars indicate the standard deviations. Mean diameters of the particles (in nm) of the different peaks are indicated. The main peak contains particles with an average diameter of 118 nm. The different virus preparations analysed in this study displayed similar particle-size distributions.

## Chapter 4

# Mutation of the second sialic acid-binding site of influenza A virus neuraminidase drives compensatory mutations in hemagglutinin

Wenjuan Du<sup>1</sup>, Margreet A. Wolfert<sup>2,3</sup>, Ben Peeters<sup>4</sup>, Frank J.M. van Kuppeveld<sup>1</sup>, Geert-Jan Boons<sup>2,3</sup>, Erik de Vries<sup>1</sup>, Cornelis A.M. de Haan\*<sup>1</sup>

1 Virology Division, Faculty of Veterinary Medicine, Utrecht University, Utrecht, The Netherlands.

2 Department of Chemical Biology and Drug Discovery, Utrecht Institute for Pharmaceutical Sciences, and Bijvoet Center for Biomolecular Research, Utrecht University, Utrecht, the Netherlands.

3 Complex Carbohydrate Research Center, University of Georgia, Athens, United States of America.

4 Wageningen Bioveterinary Research, Department of Virology, Lelystad, the Netherlands.

## **Abstract**

Influenza A viruses (IAVs) cause seasonal epidemics and occasional pandemics. Most pandemics occurred upon adaptation of avian IAVs to humans. This adaptation includes a hallmark receptor-binding specificity switch of hemagglutinin (HA) from avian-type  $\alpha$ 2,3- to human-type  $\alpha$ 2,6-linked sialic acids. Complementary changes of the receptor-destroying neuraminidase (NA) are considered to restore the precarious, but poorly described, HA-NA-receptor balance required for virus fitness. In comparison to the detailed functional description of adaptive mutations in HA, little is known about the functional consequences of mutations in NA in relation to their effect on the HA-NA balance and host tropism. An understudied feature of NA is the presence of a second sialic acid-binding site (2SBS) in avian IAVs and absence of 2SBS in human IAVs, which affects NA catalytic activity. Here we demonstrate that mutation of the 2SBS of avian IAV H5N1 disturbs the HA-NA balance. Passaging of a 2SBS-negative H5N1 virus on MDCK cells selected for progeny with a restored HA-NA balance. These viruses obtained mutations in NA that restored a functional 2SBS and/or in HA that reduced binding of avian-type receptors. Importantly, a particular HA mutation also resulted in increased binding of human-type receptors. Phylogenetic analyses of avian IAVs show that also in the field, mutations in the 2SBS precede mutations in HA that reduce binding of avian-type receptors and increase binding of human-type receptors. Thus, 2SBS mutations in NA can drive acquisition of mutations in HA that not only restore the HA-NA balance, but may also confer increased zoonotic potential.



### **Author summary**

Influenza pandemics can have devastating effects as was dramatically demonstrated by the so-called Spanish flu in 1918. Such pandemics are caused by animal influenza A viruses (IAVs) that are sufficiently adapted to humans. This adaptation includes among others a change in the receptor-binding properties of the viral hemagglutinin (HA). Some avian IAVs have already acquired the ability to bind to human-type receptors via their HA. We provide novel insights into the evolution of such viruses and elucidate a crucial role for NA herein. This study is expected to contribute to the timely recognition of animal viruses with increased zoonotic potential.

## Introduction

Influenza A viruses (IAVs) cause seasonal epidemics as well as occasional pandemics. The latter occur when animal viruses cross the host species barrier and adapt to humans. IAV particles contain hemagglutinin (HA) and neuraminidase (NA) glycoproteins with receptor-binding and -cleavage activities, respectively. HA binds to glycans terminating in N-acetylneuraminic acid (Neu5Ac; generally known as sialic acid [SIA]) and is a major host tropism determinant. Human viruses prefer binding to  $\alpha$ 2,6-linked SIA ( $\alpha$ 2,6 SIA; human-type receptor) expressed on human upper airway epithelia whereas most avian viruses prefer binding to  $\alpha$ 2,3-linked SIA ( $\alpha$ 2,3 SIA; avian-type receptor) present on bird intestinal epithelia [1]. Some avian viruses, such as recent H7N9 and H9N2 viruses, however also can bind to  $\alpha$ 2,6 SIA [2, 3] and are therefore regarded as viruses with increased zoonotic potential. What drives the selection of mutations in HA resulting in the binding of human-type receptors in these avian viruses is, however, not understood.

As yet, little is known about the importance of the NA in host tropism changes. Although the NAs of human IAVs are relatively better at cleaving  $\alpha$ 2,6 SIA they still, like avian IAVs, display a higher cleavage rate cleavage of  $\alpha$ 2,3 SIAs [4-8]. It has been suggested that not HA binding per se, but rather the binding properties of HA in relation to the activity of NA are important for optimal virus replication, fitness and host tropism [9-12]. HA and NA likely require a functional balance that matches the host sialome in order to escape from (mucus) decoy receptors, to enable cell attachment and endocytic uptake, and to allow release of newly assembled virus particles at the end of the infection cycle [12]. Importantly, high variability in the receptor-binding properties of HA (avidity and receptor fine-specificity) for avian as well as human IAVs has been observed [13-15], which may need to be accompanied by compensatory mutations in NA to maintain a functional balance.

The NA protein is a type II transmembrane protein assembling into a mushroom-shaped homotetramer. Each globular head domain contains a catalytic site, which is highly conserved between IAVs of different subtypes [6, 7]. A grossly neglected feature of NA is a second sialic acid-binding site (2SBS; also referred to as hemadsorption site) [16-19] adjacent to the catalytic site. The 2SBS consists of three loops (370, 400 and 430 loop) that contain residues interacting with SIA [17, 18]. A functional 2SBS enhances NA activity on multivalent, but not monovalent, substrates, probably by bringing substrates closer to the active site [4, 5, 16]. The presence or absence of a functional 2SBS was shown to affect virus replication in vitro [4, 5, 20-22], presumably by affecting the often mentioned, but poorly characterized HA-NA balance [20]. Of note, the 2SBS is conserved in most

avian viruses but is invariably lost in human viruses as well as in viruses from some other hosts [5, 16, 18, 20, 23]. This suggests an important, although so far unproven, role for the 2SBS in host tropism.

Recently, kinetic assays based on bio-layer interferometry (BLI) were introduced to study the balance between HA and NA in the context of virus particles. These assays allow monitoring of HA binding and NA cleavage in real time using synthetic glycans or sialylated glycoproteins [20, 24]. IAV particles are practically irreversibly attached to a receptor-coated surface, in the absence of NA activity, due to multivalent HA-receptor binding. The combined activity of HA and NA, however, results in virion movement on a receptor-coated surface until the receptor density is sufficiently decreased by receptor-destroying NA to allow virion release. The speed of this self-elution from a receptor-coated surface is determined by the avidity of HA and the activity of NA for a specific receptor, and thus reflects the HA-NA-receptor balance. By using BLI, N2-containing human viruses with a functional 2SBS elute faster from a receptor-coated surface than those without, indicating that the HA-NA balance can be affected by the receptor-binding properties of the 2SBS of NA in addition to those of HA [20, 24].

In the present study we show that mutation of the 2SBS in NA disturbs the HA-NA balance of avian H5N1 virus. Importantly, we establish the existence of a functional HA-NA crosstalk by showing that a mutated, non-functional 2SBS drives the selection of mutations in HA that modify its receptor-binding properties, thereby restoring the HA-NA balance. As a corollary, an acquired mutation also resulted in concomitant enhanced binding to human-type receptors. These findings are corroborated by phylogenetic analyses of H9N2 viruses. Also for H9N2 viruses mutations in the 2SBS are selected prior to the acquisition of mutations in the receptor-binding site (RBS) of HA that decrease binding to avian-type receptors and increase binding to human-type receptors. Collectively, these results emphasize the importance of the 2SBS for the HA-NA balance of avian viruses and provide an explanation for the evolution of avian viruses that bind to human-type receptors.

## Results

### **Mutation of the 2SBS affects the HA-NA balance of H5N1 virus and selects for mutations in HA**

We previously generated an H5N1 virus with mutation K432E in the 2SBS of NA (H5N1<sub>432E</sub>) [5] to analyze the importance of the 2SBS for NA catalytic activity and virus replication. This mutation, which reduced catalytic activity of NA on multivalent, but not monovalent substrates [5], resulting from reduced receptor binding via the 2SBS (S1 Fig), rapidly reverted back to wild type NA (432K)[5]. This observation prompted us to examine the effect of mutation K432E in NA on the HA-NA balance of H5N1 virus. To this end, we used a recently established BLI assay [20, 24](Fig 1A), in which sensors were coated with recombinant soluble lysosomal-associated membrane glycoprotein 1 (LAMP1) receptors that carry several sialoglycans (receptor loading). The sensors were subsequently loaded with virus particles in the presence of the NA inhibitor oseltamivir-carboxylate (OC) [Virus association (+OC)], after which we determined the rate of NA-activity-dependent dissociation in the absence of OC [NA-driven dissociation (-OC)] . The virus self-elution rate (NA-driven dissociation normalized to the virus association level) is a reflection of the HA-NA balance where, for instance, viruses containing HA with low receptor-binding affinity or NA with high catalytic activity are released faster than viruses that bind stronger and/or have less active NA proteins [24]. Comparison of wild type H5N1 (H5N1 WT) and H5N1<sub>432E</sub> viruses carrying the same H5 protein, showed that mutation K432E in NA disturbs the HA-NA balance as it resulted in slower virion self-elution (Fig 1A).

In our previous work, revertant E432K was readily obtained upon passaging of H5N1<sub>432E</sub> [5]. To restore the altered HA-NA balance, compensatory mutations in HA may also suffice to compensate for substitution K432E in NA. Therefore, recombinantly generated H5N1 WT and H5N1<sub>432E</sub> viruses were serially passaged on MDCK cells. Each virus was generated twice by reverse genetics and passaged in triplicate series at low multiplicity of infection (MOI 0.001)(Fig 1B). After each passage, viral RNA was extracted and HA and NA genes were sequenced. For H5N1<sub>432E</sub>, back mutation E432K was observed in three out of the six passage series. In two series this was combined with mutation S223N in H5 (S227N according to H3 numbering) (S1 Table; Fig 2A). Mutation H125N in H5 (H129N according to H3 numbering) was observed in the other three series after only one passage (S1 Table; Fig 1B). Upon passaging, substitution H125N was, however, lost in all these series concomitantly with the appearance of A156T in H5 (A160T according to H3 numbering) (S1 Table; Fig 1B). Sequencing results of different passages of H5N1<sub>432E</sub> are shown in S2 Fig. Much fewer mutations (requiring at least four passages) were obtained upon passaging of H5N1 WT (S2 Table, Fig 1B). For five passage series of H5N1 WT, substitution A156T was observed in H5, while in one series additional mutation A156S was detected. No mutations were observed in NA upon passaging of H5N1 WT (S2 Table).

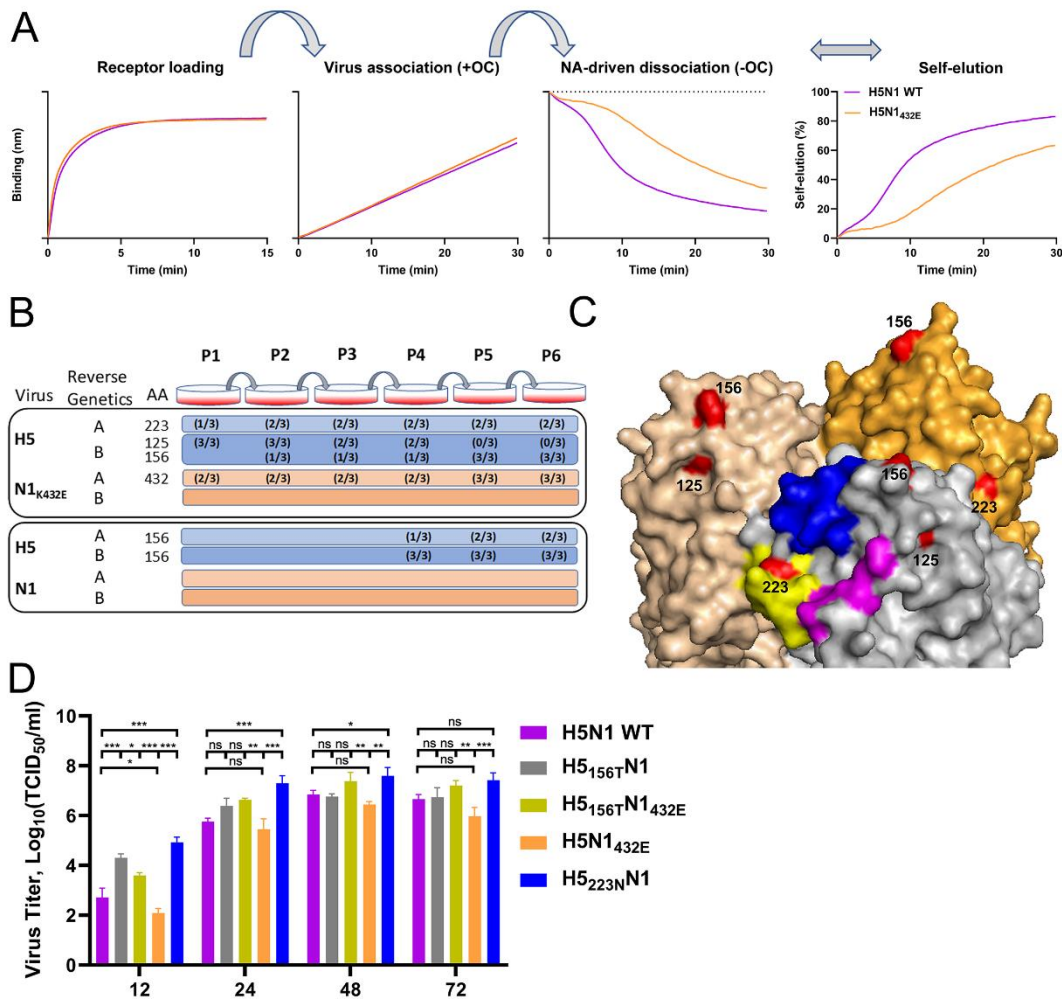


**Fig 1. Mutation of the 2SBS affects the HA-NA balance of H5N1 virus and selects for mutations in HA.** (A) Streptavidin-containing BLI sensors were loaded with biotinylated LAMP1, generating the receptor loading curve (Receptor loading). LAMP1 contains more  $\alpha 2,3$  than  $\alpha 2,6$  SIAs [20]. Subsequently, sensors were dipped into solution containing H5N1 or H5N1<sub>432E</sub> viruses (for a list of the virus stocks used see S3 Table) and the NA inhibitor oseltamivir-carboxylate (OC), resulting in a virus association curve [Virus association (+OC)]. Viruses were loaded to a similar loading level. NA-driven virus dissociation was observed when OC was removed by 3 short (5 s) washes [NA-driven dissociation (-OC)]. A virion self-elution graph was generated by normalizing virus dissociation to the virus association level in the presence of OC (Self-elution). A representative experiment out of three performed is shown. (B) Overview of the HA and NA mutations that were detected upon passaging of H5N1<sub>432E</sub> and H5N1 viruses. For an elaborate overview see S1 Table and S2 Table. Viruses were generated twice by reverse genetics (indicated by A and B), after which they were each passaged in triplicate. Amino acid (AA) positions of mutations in HA (H125N, A156S/T, S223N) and NA (E432K)

are indicated. Numbers between brackets indicate the occurrence of these mutations in the triplicate passage series. Mutation S223N was always detected in combination with E432K, which restored the 2SBS. Mutation at position 125 was followed by mutation at position 156, after which the mutation at position 125 disappeared from the population. Mutation at position 156 was also observed after several passages in H5N1 virus. (C) Surface representation of the crystal structure of the H5 trimer from A/Vietnam/1194/04 (H5N1) (PDB ID: 2IBX; [29]) was depicted using Pymol software. Head domains are shown. The three structural elements of the RBS are colored in blue (190-helix), yellow (220-loop) and magenta (130-loop). Residues in HA that are mutated during passaging of H5N1 viruses are shown in red and numbered. (D) MDCK-II cells were infected (n=3) with the indicated viruses (see S3 Table for details) at multiplicity of infection of 0.001 TCID<sub>50</sub> units per cell. The virus titer in the cell culture supernatants at the indicated times post infection was determined by limiting dilution followed by calculation of the TCID<sub>50</sub> titers. Standard deviations are indicated. Significant differences were analyzed by One-way ANOVA using Graphpad (\*, P<0.05; \*\*, P<0.01; \*\*\*, P<0.001; n.s., not significant).

Two of the observed HA mutations are located in (S223N; in the 220 loop) or close to (H125N; proximal of the 130 loop) the RBS of H5 (Fig 1C). Substitutions A156T and A156S, generating a N-linked glycosylation site (NXS/T; S3 Fig), are located at the tip of the head domain as confirmed by an increased electrophoretic mobility of recombinant soluble H5 proteins with substitution A156T (S4 Fig). In conclusion, mutation of the 2SBS in H5N1 rapidly selects for mutations in NA that restore the 2SBS and/or for mutations in HA located in or close to the RBS or resulting in the addition of a glycan chain to the HA head domain.

The selection of the mutations in HA suggests that viruses carrying these mutations are more fit and replicate more efficiently in MDCK cells. To analyze the effect of these HA mutations in more detail, we determined virus growth curves on MDCK cells. All mutant viruses reached higher titers than their respective parental viruses at the early time point (Fig 1D). Differences in viral titers were smaller at the later time points. Also the two parental viruses (H5N1 WT and H5N1<sub>432E</sub>) obtained significantly differed titers at the early time point, indicating that a disturbance of the HA-NA balance of H5N1 virus, resulting in slower virion self-elution as determined by BLI, negatively affects virus replication.

**Effect of compensatory mutations in HA on receptor binding and virion-self-elution**

Mutations in the H5 head domain may affect receptor binding and therefore HA-NA balance. We expressed recombinant soluble H5 proteins carrying the different mutations (H5<sub>223N</sub>, H5<sub>125N</sub>, and H5<sub>156T</sub>) and analyzed their receptor binding properties. Each of the three mutations negatively affected the H5 protein binding rate to an avian-type synthetic glycan (3'SLNLN; NeuAc $\alpha$ 2-3Gal $\beta$ 1-4GlcNAc $\beta$ 1-3Gal $\beta$ 1-4GlcNAc) as observed using BLI (Fig 2A and 2D). The effect of the different mutations on receptor binding was also analyzed in the context of virus particles by using BLI, by analyzing the initial binding rate of virions to the sensor surface in the presence of NA inhibitor OC similarly as described previously [24]. In this analysis, virions carrying the same NA protein (either the wildtype or the 432E NA) were compared. Substitutions S223N and A156T resulted in significantly lower initial binding rates (Fig 2B and 2E). As virus stocks carrying 125N in the absence of wildtype 125H were not obtained (S2 Fig and S1 Table), we determined the initial binding rate of virus stocks containing both 125H and 125N in HA as determined by sequence analysis (H5<sub>125H/N</sub>N1<sub>432E</sub>). The initial binding rate observed for these latter virus stocks did not differ compared to H5N1<sub>432E</sub> (Fig 2E). In short, mutations at position 223 and 156 in H5 result in reduced HA-receptor binding in both assays used. The mutation at position 125 also affected receptor binding, which was only observed when using recombinant H5 protein.

Subsequently, we analyzed the effect of the mutations in H5 on the HA-NA balance by analyzing virion self-elution from LAMP1-coated sensors (Fig 2C and 2F) similarly as described above (Fig 1). Virus with substitution S223N in H5 (H5<sub>223N</sub>N1) displayed much faster self-elution than parental H5N1<sub>432E</sub> virus. This self-elution was even faster than H5N1 WT virus, carrying the same NA (Fig 2C). Similarly, viruses carrying mutations at position 156 (H5<sub>156T</sub>N1<sub>432E</sub>) or 125 (H5<sub>125H/N</sub>N1<sub>432E</sub>) eluted much faster than virus carrying a wild type H5 combined with the same NA (H5N1<sub>432E</sub>) (Fig 2F). The faster elution observed for H5<sub>125H/NN</sub>1<sub>432E</sub> virus is likely due to 125N as the H5N1<sub>432E</sub> virus that carries 125H (and is otherwise identical in HA and NA) showed slower self-elution. The faster self-elution of H5<sub>223N</sub>N1 and H5<sub>156T</sub>N1<sub>432E</sub> compared to their respective parental virus is consistent with the higher titers of these two viruses on MDCK cells. We conclude that the mutations in HA affect the HA-NA balance as they cause faster virion self-elution from a receptor-coated surface as a result of reduced HA-receptor binding.

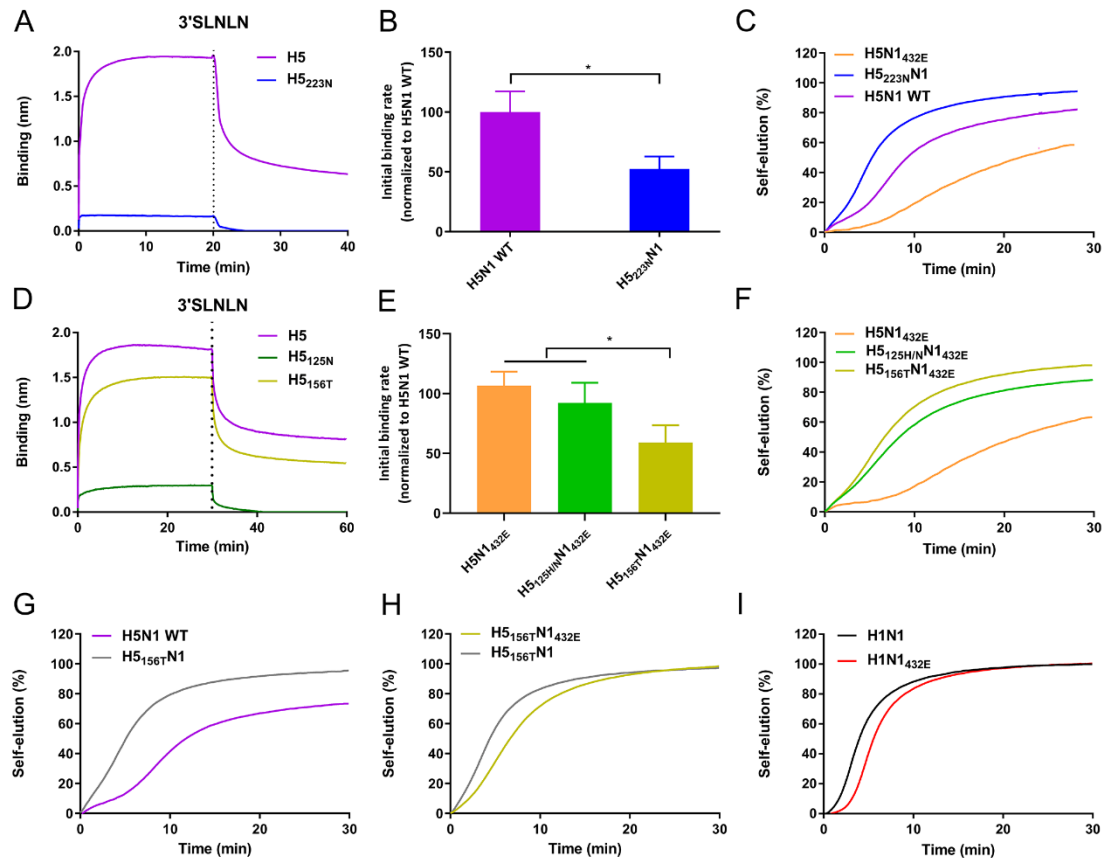


**Fig 2. Mutations in HA restore the HA-NA balance.** (A and D) Association and subsequent dissociation of indicated H5 proteins complexed with antibodies to and from 3'SLNLN-coated sensors. (B and E) Relative initial binding rates per virus particle ( $v_{obs}=dB/dT$ ) for LAMP1-coated sensors were determined for H5N1 and H5N1 mutant viruses ( $H5_{223N}N1$ ,  $H5_{156T}N1_{432E}$ ,  $H5_{125H/N}N1_{432E}$ , and  $H5N1_{432E}$ ) as described previously [20, 24] and graphed normalized to H5N1. Means of three independent experiments are graphed, standard deviations are shown. The relative initial binding rate per virus particle corresponds to the steepness of the initial part of binding curves (as show in Fig 1) normalized for virus particle numbers. (C and F) NA-driven self-elution of H5N1 and H5N1 mutant viruses from LAMP1-coated sensors was analyzed similarly as described in the legend to Fig 1. (G and H) NA-driven self-elution of H5N1 and H5N1 mutant viruses ( $H5_{156T}N1$  and  $H5_{156T}N1_{432E}$ ) from LAMP1-coated sensors. (I) Self-elution of H1N1 and  $H1N1_{432E}$  viruses from LAMP1-coated sensors. Representative experiments out of 2-3 performed are shown.



### **The importance of the 2SBS for virion self-elution depends on HA binding avidity**

The A156T mutation in HA was obtained in 5 out of 6 replicates in H5N1 WT, although more passages were required as for H5N1<sub>432E</sub> (Fig 1B, S1 Table and S2 Table). We therefore also compared the influence of this mutation on virion self-elution using H5N1 WT and H5<sub>156T</sub>N1 viruses. Again, the additional N-glycan in the head domain resulted in faster virion self-elution (Fig 2G). The selection of this mutation thus indicates that the HA-NA balance of H5N1 WT, which is presumably well adapted to replication in chickens, is not optimal for virus replication in MDCK cells, although this virus appears less off-balance than H5N1 with a mutated 2SBS (H5N1<sub>432E</sub>)(Fig 1A). The selection of H5<sub>223N</sub>N1 virus, which eluted even faster than H5N1 WT virus (Fig 2C), upon passaging of H5N1<sub>432E</sub> is in agreement herewith. In some passage series, viruses were selected with mutations in HA without restoration of the 2SBS in NA. We therefore also analyzed the importance of the 2SBS on virion self-elution when NA was combined with a weaker binding H5<sub>156T</sub> protein (Fig 2H). As expected, H5<sub>156T</sub>N1 virus eluted somewhat faster than H5<sub>156T</sub>N1<sub>432E</sub>, however, the importance of the 2SBS for self-elution was clearly smaller than when NA was combined with H5 lacking the additional glycan (compare Fig 1A and 2H). This prompted us to also analyze virus self-elution of H1N1 and H1N1<sub>432E</sub> viruses, in which the same H5N1-derived N1 (with or without K432E substitution) is paired with HA of H1N1 strain PR8 (Fig 2I). Recombinant H1 protein displays reduced receptor binding when compared to H5 (S5 Fig). These H1N1 viruses were genetically stable [5] and passaging did not result in compensatory mutations. Virus with a functional 2SBS (H1N1) eluted somewhat faster than virus with a mutated 2SBS (H1N1<sub>432E</sub>)(Fig 2I), but again the difference between these two viruses was much smaller when compared to viruses carrying a much stronger-binding H5 (Fig 1A). We conclude that the contribution of the 2SBS to the HA-NA balance is smaller when viruses contain a weaker-binding HA.

### **The effect of compensatory mutations in HA on receptor binding specificity**

The S223N mutation in H5 has been shown by some, but not by other studies to increase binding to human-type receptors [25-30]. We therefore studied to what extent the compensatory mutations in H5 affected receptor-binding specificity in the virus used in this study. To this end, we analyzed the initial binding rates of the viruses to BLI sensors (Fig 3A-B) coated with avian- (3'SLNLN; NeuA $\alpha$ 2-3Gal $\beta$ 1-4GlcNAc $\beta$ 1-3Gal $\beta$ 1-4GlcNAc) or human-type (6'SLNLN; NeuA $\alpha$ 2-6Gal $\beta$ 1-4GlcNAc $\beta$ 1-3Gal $\beta$ 1-4GlcNAc) receptors. The viruses displayed similar initial binding rates to 3'SLNLN (Fig 3A), but differed in their ability to bind 6'SLNLN (Fig 3B). Severely reduced binding to 6'SLNLN for H5<sub>125H/N</sub>N<sub>1432E</sub> and H5<sub>156T</sub>N<sub>1432E</sub> viruses was observed when compared to the control virus H5N1<sub>432E</sub> with the same NA (Fig 3B). The relative receptor-binding specificity did not appear to be affected, however, by S223N (compare H5<sub>223N</sub>N1 and H5N1 WT; Fig 3A-B). Although the S223N mutation did not increase binding to 6'SLNLN in the BLI assay, this mutation may positively affect binding to other

glycans containing  $\alpha$ 2,6-linked SIAs. Therefore, we probed the receptor specificity of H5N1 WT and H5<sub>223N</sub>N1 viruses using glycan array analysis. Both viruses preferred binding to branched glycans containing multiple LacNAc repeats capped with  $\alpha$ 2,3-linked SIAs (Fig 3C-3E). The H5<sub>223N</sub>N1, but not the H5N1 WT virus, displayed binding to the same glycans capped with  $\alpha$ 2,6-linked SIAs. Of note, antibody-complexed recombinant soluble H5 proteins, which are often used in glycan array analysis only bound to avian-type receptors (S6 Fig). We conclude that the S223N mutation results in increased binding to human-type receptors, which can only be observed for specific receptors and when using virus particles.

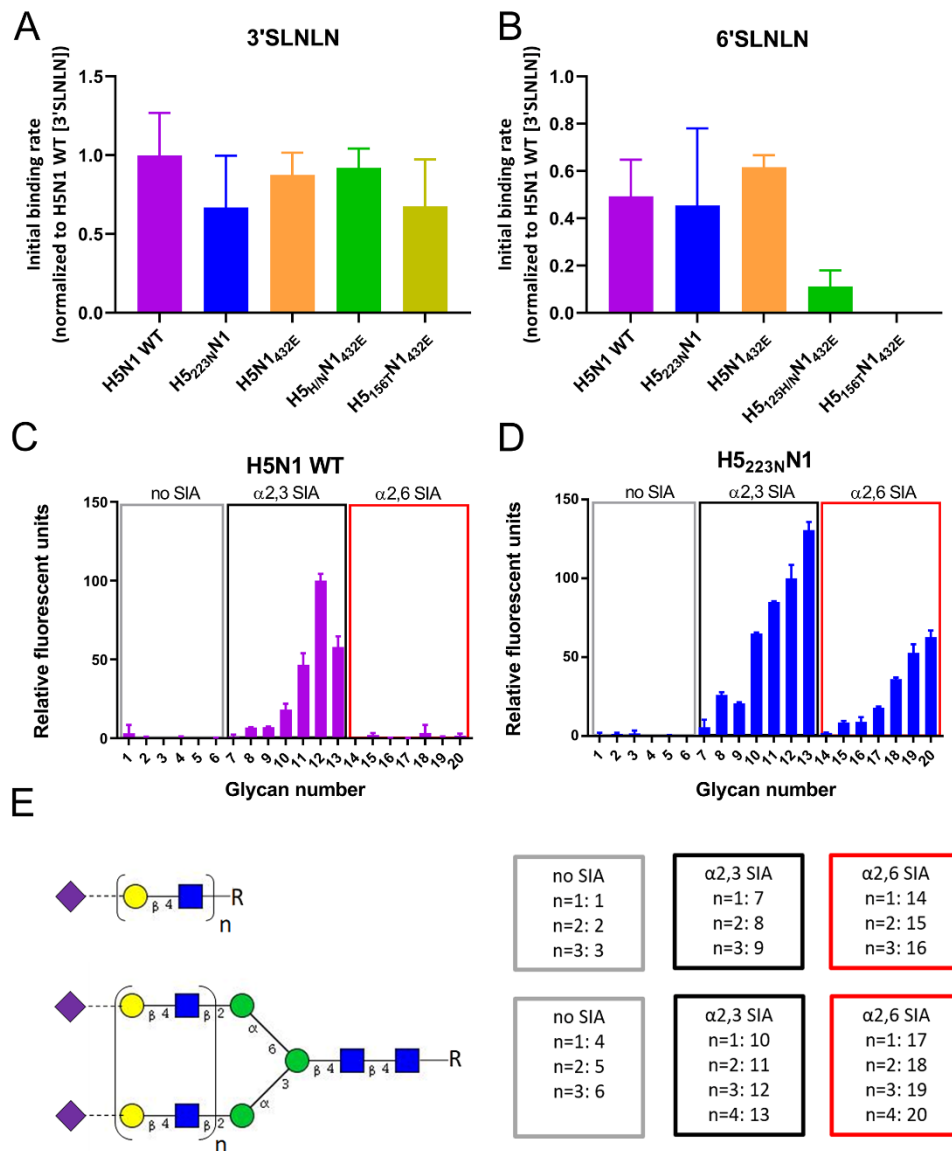


**Fig 3. Mutation in HA affect virus receptor-binding specificity.** (A and B) Initial binding rates of different H5N1 viruses for 3'SLNLN- (A) and 6'SLNLN- (B) coated sensors were determined as described previously [20, 24] and graphed normalized to the initial binding rate of H5N1 WT virus to

3'SLNLN. Means of three experiments are shown, standard deviations are indicated. (C and D) Glycan microarray analysis of the receptor binding specificities of H5N1 and H5<sub>223N</sub>N1 viruses. The relative fluorescent units normalized to glycan number 12 are graphed. The mean signals and standard deviations are shown for each glycan. The numbering of the glycans corresponds to the numbering of the glycans shown in (E). (E) Overview of the synthetic glycans printed on the microarray. Linear or branched glycans contain either no SIA,  $\alpha$ 2,3 SIA or  $\alpha$ 2,6 SIA and differ in their number of LAcNAc (*N*-acetylglucosamine [*Gal* $\beta$ 1-4*GlcNAc*]) repeats, indicated by *n*. Purple diamonds; SIA, yellow circles; *Gal*, blue squares; *GlcNAc*, green circles; *Man*.

Based on these results, we predicted that virus containing the S223N mutation should self-elute more slowly than its wild type counterpart from glycoprotein receptors containing high amounts of  $\alpha$ 2,6-linked SIAs. To test this hypothesis, we made use of recombinant LAMP1 containing increased levels of  $\alpha$ 2,6 SIA (6'LAMP1) by co-expression of human beta-galactoside alpha-2,6-sialyltransferase 1 (ST6*Gal*1). The presence of increased and decreased amounts of  $\alpha$ 2,6 and  $\alpha$ 2,3 SIAs on 6'LAMP1 compared to 'standard' LAMP1 was confirmed by binding of lectins specific for  $\alpha$ 2,6 (SNA) or  $\alpha$ 2,3 (MALI) SIAs (Fig 4A and 4B). As predicted, H5<sub>223N</sub>N1 eluted much slower from 6'LAMP1-coated sensor compared to H5N1 WT (Fig 4C), in contrast to results obtained for these viruses with LAMP1 (Fig 2C). As a control, we analyzed the self-elution of H5<sub>156T</sub>N1<sub>432E</sub> and H5<sub>125H/N</sub>N1<sub>432E</sub> viruses from 6'LAMP1. In agreement with the reduced binding to 6'SLNLN (Fig 3A), these viruses exhibited faster self-elution compared to H5N1<sub>432E</sub> (Fig 4D).

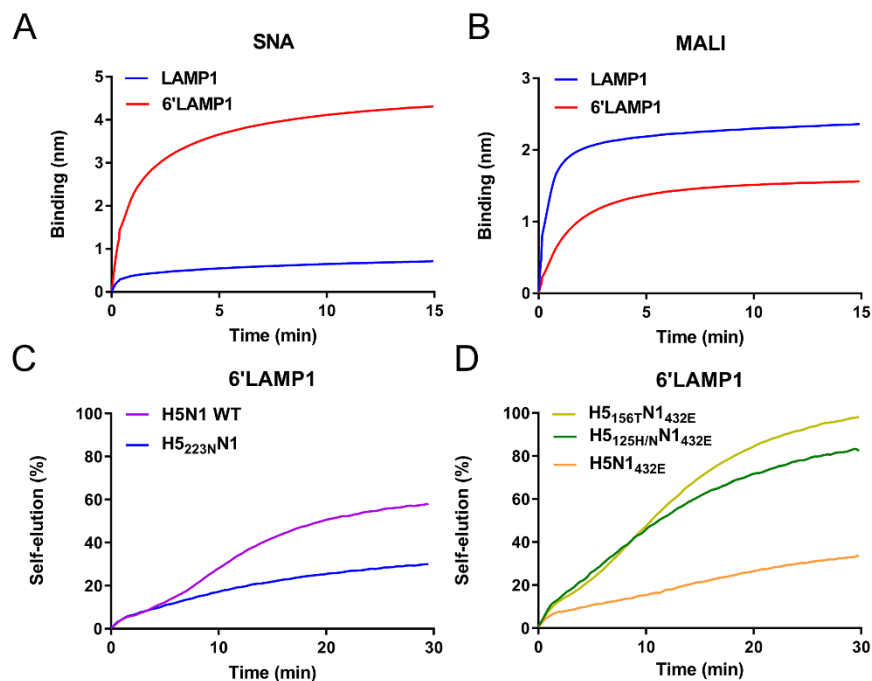


**Fig 4. Mutation S223N in HA negatively affects self-elution from LAMP1 containing increased levels of  $\alpha$ 2,6 SIAs (6'LAMP1).** (A and B) LAMP1 and 6'Lamp1 were analyzed for their attached glycans by BLI analysis of lectin binding to sensors coated with these glycoproteins as described previously [20]. (A) Binding of SNA, which is specific for SIA $\alpha$ 2,6Gal $\beta$ 1,4GlcNAc oligosaccharide abundantly present on N-linked glycans. (B) Binding of MAL I, which is specific for SIA $\alpha$ 2,3Gal $\alpha$ 1,4GlcNAc oligosaccharide abundantly present on N-linked glycans. We conclude that 6'LAMP1 contains increased levels of  $\alpha$ 2,6 SIAs and decreased levels of  $\alpha$ 2,3 SIAs. (C and D) NA-driven self-elution from 6'LAMP-coated sensors was analyzed for the indicated viruses (same stocks and amounts as used in in Fig 2) as described in the legend to Fig 1. Representative experiments out of 2-3 performed are shown. Mutation S223N results in faster self-elution from LAMP1 (Fig 2C), while elution from 6'LAMP is decreased.

### **Selection of compensatory mutations in field viruses upon mutation of the 2SBS**

Our results indicate that mutation of the 2SBS may drive the selection of mutations in HA that reduce the avidity of HA-receptor binding and may affect HA receptor-binding specificity. The 2SBS in NA is highly conserved in avian IAVs with notable exceptions in H9N2 viruses [3]. Current H9N2 viruses, which are the most abundant IAVs found in poultry, also contain a mutated 2SBS accompanied by several mutations in HA that were reported to increase binding to human-type receptors (e.g. E190A/V, Q226L) [3, 31]. To determine the order, in which these mutations in NA and HA appeared in H9N2 viruses, phylogenetic analysis, using Nextstrain analytic and visualization tools (<https://nextstrain.org>)[32](Fig 5), was employed. The similar topology of the HA and NA gene trees marks the coevolution of these genes in the distinct clades indicated by different colors in Fig 5. Key mutations affecting the 2SBS of NA and the RBS of HA, occurring along the trunk of the trees, are indicated to show that mutations in the 2SBS occur just prior to the branchpoint (B) at the origin of the Chinese/East Asian and the West/South Asian and African clades. On the contrary, mutations in or near the RBS of HA occur after branchpoint B independently in both clades. Mutations in the first and second loop of the 2SBS include amino acid substitutions at positions known to interact with SIA (S367N/K and N400S) [17, 18]. Substitutions in the RBS of HA occur at positions known to affect receptor specificity (E190A/V and Q226L)[3, 31], accompanied in the West Asian clade by the gain (A160S) and subsequent loss (N158S) of a glycosylation site at the tip of the HA head domain. Of note, the Chinese/East Asian clade also acquired a mutation at the extremely conserved base of the RBS (H183N), which is expected to affect the receptor-binding properties of HA. In conclusion, mutations in the 2SBS of H9N2 NA preceded selection of mutations in HA that decrease and increase binding to avian- and human-type receptors, respectively.

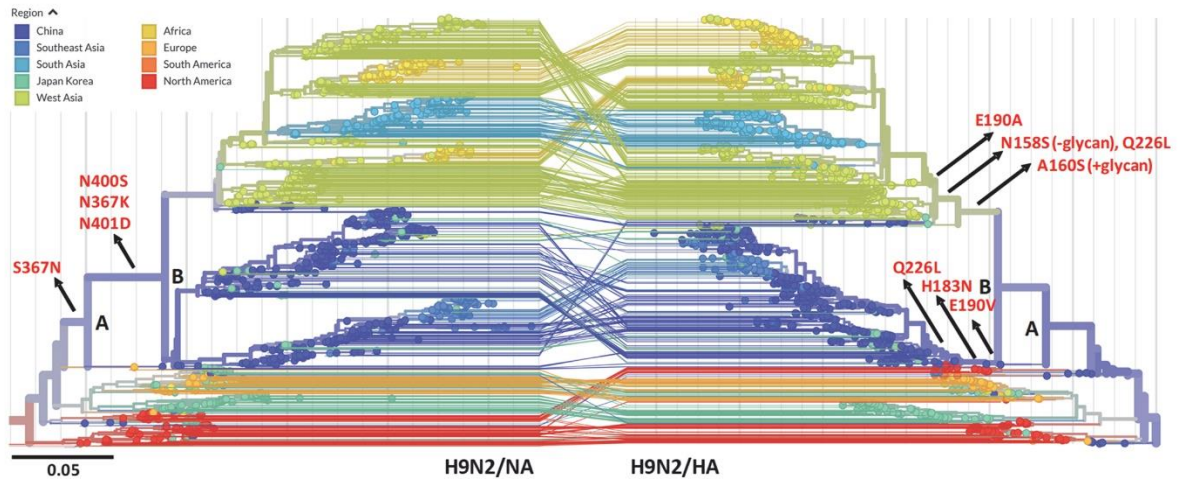


**Fig 5. Mutation of the 2SBS in N2 precedes mutation of the RBS in H9 of H9N2 field strains.** Phylogenetic trees of full-length NA and HA sequences of H9N2 viruses between 1970 and 2019 were generated using Nextstrain (<https://nextstrain.org>) [32]. Viruses are colored according to geographic location. NA (left) and HA (right) trees have a similar overall topology. Two corresponding branch points in the NA and HA trees are indicated by letters (A and B). Mutations in the 2SBS of NA or in HA that affect receptor binding are indicated, as well as the parts of the trunk of the trees to which they belong. Lines connecting HA and NA genes of the same isolate are shown. N2 and H3 numbering is used. Residue numbers shown for HA, correspond to residue number +8 in Nextstrain.

## Discussion

We here show that mutation of the 2SBS in H5N1 NA, resulting in reduced NA activity, disturbs the HA-NA balance of virions, particularly when NA is accompanied by a strong-binding HA. Passaging such viruses rapidly resulted in the selection of mutations in NA and/or HA that restore the HA-NA balance providing further evidence for the importance of a precisely tuned balance for optimal replication and for an important role of the 2SBS therein. Mutations in HA, which resulted in higher virus titers particularly at early time points, reduced receptor-binding avidity either because they affect the RBS directly (S223N and H125N) [25-28, 33], or by resulting in an additional glycan in the head domain that possibly sterically hinders access to the RBS [34-37]. The additional glycan was eventually also observed upon passaging of H5N1 WT virus. Apparently, also the wild type virus used in this study did not display an HA-NA balance optimal for replication in MDCK cells, although its particular balance presumably allows efficient replication in chickens. When the 2SBS-positive/negative N1 proteins were combined with H1 of PR8 virus, genetically stable viruses were obtained [5], which is explained by the absence or presence of a functional 2SBS being much less critical for the HA-NA balance when NA is combined with a weak-binding HA. This also explains why H5N1 viruses with a mutated 2SBS did not repair their 2SBS after obtaining H125N or the additional glycan in the head domain. In agreement herewith, for H3N2 viruses we previously showed that the importance of the 2SBS for the HA-NA balance and virus replication depends on the receptor-binding properties of HA with which NA is combined. A human H3-containing virus replicated faster when it contained a 2SBS-negative N2 rather than a 2SBS-positive N2. The opposite was observed for an avian H3-containing virus [20].

As H5 prefers binding to avian-type receptors, mutations in HAs, upon disruption of the 2SBS, are primarily selected on their ability to reduce binding to these receptors. Mutation S223N, however, simultaneously resulted in increased binding to human-type receptors. This mutation has previously been observed in H5N1 viruses isolated from humans [25, 38] and has been shown by some, but not by other studies to increase binding to human-type receptors [25-30]. Differences in human-type receptor-binding abilities for N223-containing HAs may be explained by different genetic backgrounds (e.g. absence or presence of a glycan at position 160) and/or experimental assays used. The H5N1 virus that acquired N223 in this study displays increased binding to several, but not all, human-type receptors using glycan array analysis, while this was not observed when recombinant H5 protein was used. Apparently, low multivalency of antibody-HA complexes compared to virus particles prevented detection of low-affinity binding to human-type receptors. Thus, low affinity receptors may be missed when performing glycan array analyses with recombinant proteins rather than viruses [12]. Our glycan array data are corroborated by the reduced self-elution of virus with the

S223N mutation from a LAMP1 glycoprotein containing increased levels of  $\alpha$ 2,6 SIAs, as stronger HA binding will reduce self-elution. The other mutations that were selected upon passaging (H125N and A156T) did not result in enhanced binding to human-type receptors, but decreased binding to those even more so than to avian-type receptors. Thus, upon mutation of the 2SBS, mutations in HA are selected because they decrease binding to  $\alpha$ 2,3 SIAs. Concomitantly, these mutations can affect binding to human-type receptors either positively or negatively.

It is well established that all human viruses contain substitutions in the RBS of HA (e.g. Q226L) that increase binding to  $\alpha$ 2,6-linked SIAs and reduce binding to  $\alpha$ 2,3-linked SIAs, when compared to avian viruses [1, 2, 39-41]. In addition, the 2SBS, which is highly conserved in NA of avian viruses, is invariably lost in all human (pandemic) viruses [5, 16, 18, 20, 23]. Apparently, this particular combination of HA and NA features results in a HA-NA balance that allows optimal replication and spread in humans. Different scenarios might be envisioned by which avian viruses adapt their HA-NA balance to become pandemic viruses. On the one hand, mutations in HA, obtained e.g. when replicating in the new human host, may precede those in NA. The altered receptor-binding properties of HA may subsequently select for mutations in the 2SBS to obtain an optimal balance for replication in humans. Alternatively, avian viruses may also first acquire mutations in the 2SBS of NA, which may subsequently drive mutations in the RBS of HA that decrease receptor binding to avian-type receptors and accidentally increase binding to human-type receptors. The resulting viruses may more easily jump to humans, where the HA-NA balance may be adjusted further by additional mutations. Too few sequences are available of clinical isolates to conclude which scenario occurred in 1918 or 1957. In this study, we provide experimental evidence that disturbance of the 2SBS of NA may indeed select for mutations in HA that alter its receptor-binding properties, resulting in increased binding to human-type receptors. The plausibility of this scenario is supported by phylogenetic analyses that indicate that also for avian H9N2 viruses mutations in the 2SBS preceded, and may have driven, selection of mutations in the RBS of HA that reduce binding to avian-type receptors and increase binding to human-type receptors, and that may increase the zoonotic potential of these viruses. A similar scenario also appears to apply for novel H7N9 viruses, as a mutation in the 2SBS, albeit not a SIA-contact residue, that affected receptor binding and catalytic activity preceded a mutation in the RBS in HA (Q226L) [4], which reduced binding to avian-type receptors and increased binding to human-type receptors [2, 39, 42]. What drives mutation of the generally highly conserved 2SBS in NA of these avian viruses remains elusive, but might be related to adaptation of these viruses to a another avian host. Regardless, these observations warrant more detailed attention to the evolution of NA in avian viruses in relation to altered receptor-binding properties of these viruses.

## Materials and Methods

**Recombinant viruses.** Recombinant viruses were generated in the background of A/Puerto Rico/8/34 H1N1 (PR8 H1N1) by means of reverse genetics, using PR8 plasmids provided by Drs Hoffmann and Webster (St. Jude Children's Research Hospital, Memphis) as described [43, 44]. Recombinant H1N1 and H5N1 viruses contain the NA gene (GenBank accession no. BAM85820.1) from A/duck/Hunan/795/2002(H5N1) combined with either the HA gene of PR8 (7+1 virus) or its cognate HA gene (Accession number CY028963; 6+2 virus) [5]. The 2SBS in NA was mutated by replacing the AAA codon encoding K432 in wild type N1 by the GAG codon encoding E432 in N1<sub>432E</sub>. The nucleotide sequence encoding the wild-type multi-basic amino-acid sequence in H5 was modified to encode a low-pathogenic cleavage site as described previously [44]. The recombinant viruses were rescued in MDCK-II (ATCC) cells.

**Passaging of recombinant viruses and sequence analysis of HA and NA genes.** After rescue of the viruses in MDCK-II cells, the virus stocks were immediately used in the passage experiments. Viruses were passaged on MDCK-II cells at a multiplicity of infection (MOI) of 0.001 tissue culture infectious dose 50 (TCID<sub>50</sub>) per cell. After about 44hpi, cells culture media of infected cells were harvested and titers were determined by endpoint titration in MDCK-II cells. For each passage, viral RNA was extracted from cell culture media of infected cells with NucleoSpin® RNA virus kit (Macherey-Nagel) according to the manufacturer's instructions and converted to cDNA using SuperScript III Reverse Transcriptase (Invitrogen) with random Hexamers (Invitrogen). HA and NA sequences were amplified using the Q5 High-Fidelity DNA Polymerase (NEB) using specific primers (HA: forward: 5'-ATGGAGAAAATAGTGCTTCTTCTTG CAA-3', reverse: 5'-TTCTGCATTGTAACGATCCATTGGA-3'; NA: forward: 5'-TGAATCCAAATCAGAAGATAATAACCATCG-3', reverse: 5'-GTCAATGGTGAATGGCAACTCAGCA-3'). PCR products were size-separated using agarose gel electrophoresis and purified by NucleoSpin® Gel and PCR Clean-upkit (Macherey-Nagel) following manufacturer's instructions and then analyzed by Sanger sequencing (Macrogen).

**Expression of recombinant proteins.** Human-codon optimized cDNAs encoding the H1 ectodomain of A/Puerto Rico/8/34/Mount Sinai (H1N1)(GenBank accession no. AF389118.1 ) or H5 ectodomain of A/duck/Hunan/795/2002(H5N1) (GenBank accession no. CY028963.1) were cloned into pFRT or pCD5 expression plasmids as described previously [45]. Expression plasmids carrying the H5 S223N, H125N and A156T were made by using site directed mutagenesis. Human-codon optimized recombinant soluble N1 expression constructs were described previously [5]. Expression constructs encoding full length N1 were obtained by replacement of the signal sequence-, Strep tag- and Tetrabrachion tetramerization domain-encoding cDNAs in these constructs with cDNA encoding the



N-terminal part of N1 (cytoplasmic tail, transmembrane domain and part of the stalk domain). Generation of pCAGGs vector containing codon-optimized glycoprotein LAMP1 ectodomain-encoding cDNAs genetically fused to sequences encoding a Fc-tag, for Protein-A based purification, and a Bap tag [46], for binding to octet sensors, was described previously [24]. Generation of a pCAGGs vector encoding antibody Fi6v3 [47], was performed similarly as described previously [48]. HA plasmids were transfected into HEK293S GnTI(-) [49, 50] cells, while NA, Fi6 and LAMP1 expression plasmids were transfected into HEK293T (ATCC) cells, using polyethylenimine (PolyScience) [51]. An expression vector encoding BirA ligase was cotransfected with the LAMP1-coding vectors, and an expression vector encoding human ST6Gal1 was also included to get 6'LAMP1 [24]. Five days post transfection, cell culture media containing soluble HA, NA and glycoproteins were harvested and purified using Streptactin- or protein A- containing beads [24, 51]. Purified HA and NA were quantified by quantitative densitometry of GelCode Blue (Thermo Fisher Scientific)-stained protein gels additionally containing bovine serum albumin (BSA) standards. The signals were imaged and analyzed with an Odyssey imaging system (LI-COR). N1-containing VLPs released into the cell culture media upon expression of full length N1 were harvested after 3 days post-transfection. The amount of N1 in these preparations was determined by performing a MUNANA assay using limiting dilutions of the VLP preparations similarly as described previously for N2 [20].

**Biolayer interferometry (BLI) assays.** BLI assays were performed using the Octet RED348. All the experiments were performed in Dulbecco's phosphate buffered saline (PBS) with Calcium and Magnesium (Lonza) at 30 °C and with plates shaking at 1000 rpm. Streptavidin sensors were loaded to saturation unless indicated otherwise with biotinylated synthetic glycans 3'SLNLN, 6'SLNLN, LNLN, or with LAMP1 or 6'LAMP1 glycoproteins. Synthetic glycans were synthesized at the Department of Chemical Biology and Drug Discovery, Utrecht University, Utrecht, the Netherlands and the Complex Carbohydrate Research Center, University of Georgia, Athens, USA [52]. The virus binding and self-elution assays were performed as described previously [20, 24]. Virus particle numbers were determined by Nanoparticle tracking analysis as described previously [20]. Virus binding was monitored by moving receptor-loaded sensors to wells containing virus and OC (kindly provided by Roche). Relative initial binding rates ( $v_{\text{obs}}=dB/dT$ ) per virus particle, which quantifies virus binding affinity, were calculated similarly as previously described [20, 24]. For analysis of NA-driven dissociation, viruses were loaded to same level in the presence of OC prior to the dissociation in the absence of OC. OC was removed by three short (5s) washes of the sensor in PBS. BLI assays with recombinant H5 proteins were carried out as described previously [53]. In short, similar amount of HA proteins complexed with strepMabClassic-HRP (IBA; 2:1 molar ratio) were applied in the HA binding assay. Binding was analyzed for 20 mins, followed by a dissociation phase in PBS. The kinetic

NA activity assay was performed as described previously [20, 24]. In brief, sensors loaded with synthetic glycans were incubated in buffer containing N1 in the absence or presence of Erythrina cristagalli lectin (ECA; Vector Labs) or ECA alone. ECA binding to sensors coated with 3'SLNLN or 6'SLNLN is a measure for SIA cleavage from these receptors by NA. Differential sialylation of LAMP1 and 6'LAMP was analyzed by incubation of glycoprotein-coated sensors with 80 µg/mL Sambucus nigra elderberry bark lectin (SNA; Vector Labs) or with 80 µg/mL Maackia Amurensis Lectin I (MAL I; Vector Labs).

**Glycan array analysis.** The 100 µM synthetic compounds in sodium phosphate buffer (250 mM, pH 8.5) were printed on activated glass slides (Nexterion Slide H, Schott Inc) by piezoelectric non-contact printing (sciFLEXARRAYER S3, Scienion Inc) with a drop volume of ~400 pL and 1 drop per spot at 50 % relative humidity [54]. Compounds were printed as replicates of 6, with 32x25 spots per subarray and 24 subarrays (3x8) per slide. After overnight incubation in a saturated NaCl chamber (75% relative humidity), the remaining activated esters were quenched with ethanolamine (50 mM) in TRIS (100 mM, pH 9.0). Next, slides were rinsed with DI water, dried by centrifugation, and stored in a desiccator at RT. To validate printing, sub-arrays were incubated at RT with 50 µL mixtures of 10 µg/mL biotinylated lectins from Vector Labs (ECA, MAL II, and SNA) and 5 µg/mL Streptavidin-AlexaFluor635 (ThermoFisher Scientific) in TSM binding buffer (20 mM Tris Cl, pH 7.4, 150 mM NaCl, 2 mM CaCl<sub>2</sub>, 2 mM MgCl<sub>2</sub>, 0.05% Tween, 1% BSA) for 1 h followed by 4 successive washes of the whole slide with 1 time TSM wash buffer (20 mM Tris Cl, pH 7.4, 150 mM NaCl, 2 mM CaCl<sub>2</sub>, 2 mM MgCl<sub>2</sub>, 0.05% Tween-20), 1 time TSM buffer (20 mM Tris Cl, pH 7.4, 150 mM NaCl, 2 mM CaCl<sub>2</sub>, 2 mM MgCl<sub>2</sub>), 2 times DI water with each 10 min soak time. Recombinant HAs (H5, H5<sub>156T</sub>, H5<sub>125N</sub>, H5<sub>223N</sub>) were precomplexed at 50 µg/mL with StrepMAB-Classic (12.5 µg/mL; IBA) and goat anti-mouse IgG H&L-AlexaFluor647 (6.25 µg/mL; Abcam) in 50 µL TSM binding buffer. After incubation on ice for 30 min, the mixtures were added to the sub-arrays for 90 min. Washes were performed as described above for the plant lectins. Similarly as for the HAs, virus stocks (H5N1 and H5<sub>223N</sub>N1) were precomplexed with Fi6v3 antibody (5 µg/mL) and anti-human IgG-Cy3 (5 µg/mL; Jackson) in the presence of OC (10 µM). All wash steps were performed in the presence of OC (10 µM). Washed arrays were dried by centrifugation and immediately scanned for fluorescence on a GenePix 4000 B microarray scanner (Molecular Devices). The detection gain was adjusted to avoid saturation of the signal. The data were processed with GenePix Pro 7 software and further analyzed using our home written Microsoft Excel macro. After removal of the lowest and highest value of the 6 replicates, the mean fluorescent intensities (corrected for mean background) and standard deviations were calculated (n=4). Data were fitted using Prism software (GraphPad Software, Inc).

## Acknowledgments

We thank Roche for kindly providing OsC and Olav de Leeuw for technical assistance.

## References

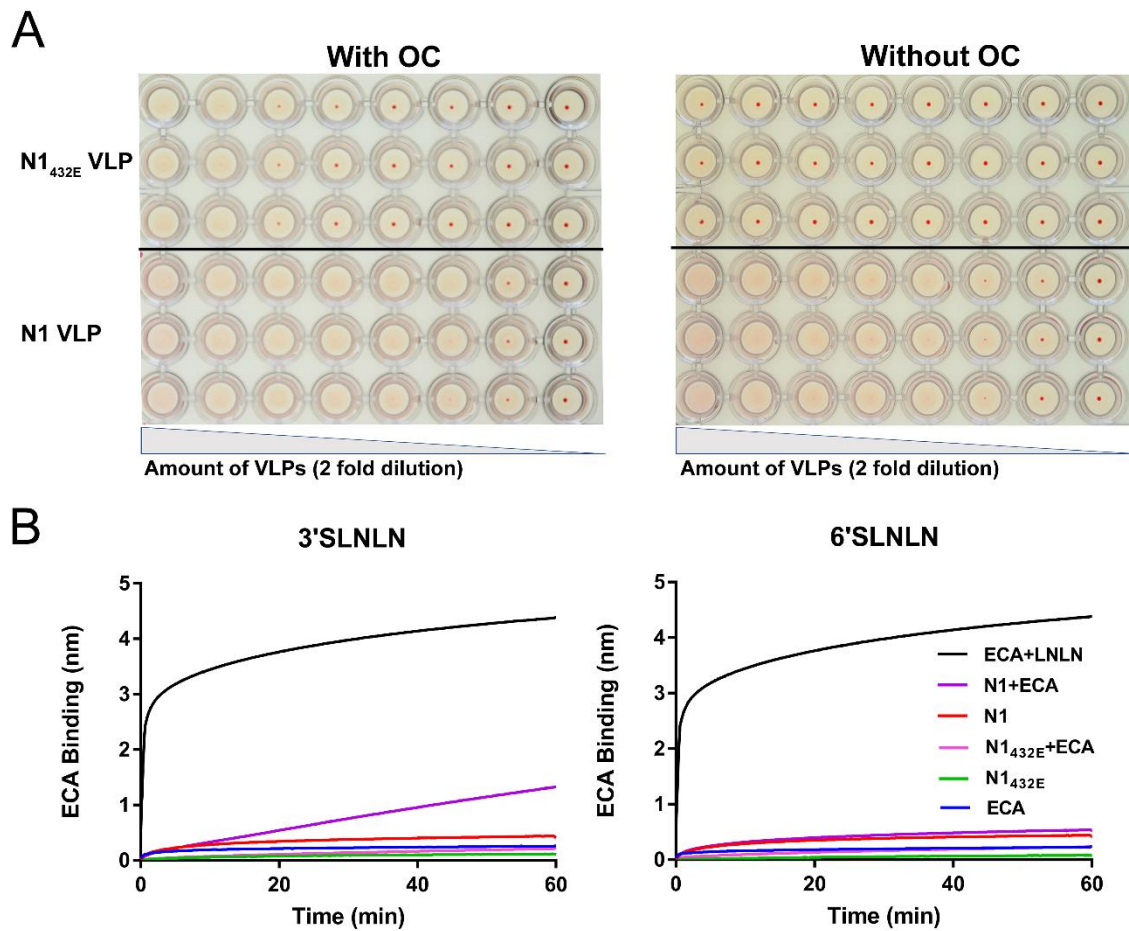
1. Matrosovich M, Tuzikov A, Bovin N, Gambaryan A, Klimov A, Castrucci MR, et al. Early alterations of the receptor-binding properties of H1, H2, and H3 avian influenza virus hemagglutinins after their introduction into mammals. *J Virol.* 2000;74(18):8502-12. Epub 2000/08/23. doi: 10.1128/jvi.74.18.8502-8512.2000. PubMed PMID: 10954551; PubMed Central PMCID: PMC116362.
2. Watanabe T, Kiso M, Fukuyama S, Nakajima N, Imai M, Yamada S, et al. Characterization of H7N9 influenza A viruses isolated from humans. *Nature.* 2013;501(7468):551-5. Epub 2013/07/12. doi: 10.1038/nature12392. PubMed PMID: 23842494; PubMed Central PMCID: PMC3891892.
3. Matrosovich MN, Krauss S, Webster RG. H9N2 influenza A viruses from poultry in Asia have human virus-like receptor specificity. *Virology.* 2001;281(2):156-62. Epub 2001/03/30. doi: 10.1006/viro.2000.0799. PubMed PMID: 11277689.
4. Dai M, McBride R, Dortmans J, Peng W, Bakkers MJG, de Groot RJ, et al. Mutation of the Second Sialic Acid-Binding Site, Resulting in Reduced Neuraminidase Activity, Preceded the Emergence of H7N9 Influenza A Virus. *J Virol.* 2017;91(9). Epub 2017/02/17. doi: 10.1128/jvi.00049-17. PubMed PMID: 28202753; PubMed Central PMCID: PMC5391454.
5. Du W, Dai M, Li Z, Boons G-J, Peeters B, van Kuppeveld FJM, et al. Substrate Binding by the Second Sialic Acid-Binding Site of Influenza A Virus N1 Neuraminidase Contributes to Enzymatic Activity. *Journal of virology.* 2018;92(20):e01243-18. doi: 10.1128/JVI.01243-18. PubMed PMID: 30089692.
6. Air GM. Influenza neuraminidase. *Influenza and other respiratory viruses.* 2012;6(4):245-56. Epub 11/16. doi: 10.1111/j.1750-2659.2011.00304.x. PubMed PMID: 22085243.
7. McAuley JL, Gilbertson BP, Trifkovic S, Brown LE, McKimm-Breschkin JL. Influenza Virus Neuraminidase Structure and Functions. *Frontiers in microbiology.* 2019;10:39-. doi: 10.3389/fmicb.2019.00039. PubMed PMID: 30761095.
8. Baum LG, Paulson JC. The N2 neuraminidase of human influenza virus has acquired a substrate specificity complementary to the hemagglutinin receptor specificity. *Virology.* 1991;180(1):10-5. Epub 1991/01/01. doi: 10.1016/0042-6822(91)90003-t. PubMed PMID: 1984642.
9. Xu R, Zhu X, McBride R, Nycholat CM, Yu W, Paulson JC, et al. Functional balance of the hemagglutinin and neuraminidase activities accompanies the emergence of the 2009 H1N1 influenza pandemic. *J Virol.* 2012;86(17):9221-32. doi: 10.1128/JVI.00697-12. PubMed PMID: 22718832; PubMed Central PMCID: PMC3416152.
10. Byrd-Leotis L, Cummings RD, Steinhauer DA. The Interplay between the Host Receptor and Influenza Virus Hemagglutinin and Neuraminidase. *Int J Mol Sci.* 2017;18(7). Epub 2017/07/18. doi: 10.3390/ijms18071541. PubMed PMID: 28714909; PubMed Central PMCID: PMC5536029.
11. Ward MJ, Lycett SJ, Avila D, Bollback JP, Leigh Brown AJ. Evolutionary interactions between haemagglutinin and neuraminidase in avian influenza. *BMC Evol Biol.* 2013;13:222. Epub 2013/10/10. doi: 10.1186/1471-2148-13-222. PubMed PMID: 24103105; PubMed Central PMCID: PMC3854068.
12. de Vries E, Du W, Guo H, de Haan CAM. Influenza A Virus Hemagglutinin-Neuraminidase-Receptor Balance: Preserving Virus Motility. *Trends Microbiol.* 2019. Epub 2019/10/21. doi: 10.1016/j.tim.2019.08.010. PubMed PMID: 31629602.
13. de Graaf M, Fouchier RA. Role of receptor binding specificity in influenza A virus transmission and pathogenesis. *Embo j.* 2014;33(8):823-41. Epub 2014/03/29. doi: 10.1002/embj.201387442. PubMed PMID: 24668228; PubMed Central PMCID: PMC4194109.

14. Peng W, de Vries RP, Grant OC, Thompson AJ, McBride R, Tsogtbaatar B, et al. Recent H3N2 Viruses Have Evolved Specificity for Extended, Branched Human-type Receptors, Conferring Potential for Increased Avidity. *Cell Host Microbe*. 2017;21(1):23-34. Epub 2016/12/27. doi: 10.1016/j.chom.2016.11.004. PubMed PMID: 28017661; PubMed Central PMCID: PMC5233592.
15. Imai M, Kawaoka Y. The role of receptor binding specificity in interspecies transmission of influenza viruses. *Curr Opin Virol*. 2012;2(2):160-7. Epub 2012/03/27. doi: 10.1016/j.coviro.2012.03.003. PubMed PMID: 22445963; PubMed Central PMCID: PMC5605752.
16. Uhlenendorff J, Matrosovich T, Klenk HD, Matrosovich M. Functional significance of the hemadsorption activity of influenza virus neuraminidase and its alteration in pandemic viruses. *Arch Virol*. 2009;154(6):945-57. Epub 2009/05/22. doi: 10.1007/s00705-009-0393-x. PubMed PMID: 19458903; PubMed Central PMCID: PMC2691527.
17. Varghese JN, Colman PM, van Donkelaar A, Blick TJ, Sahasrabudhe A, McKimm-Breschkin JL. Structural evidence for a second sialic acid binding site in avian influenza virus neuraminidases. *Proc Natl Acad Sci U S A*. 1997;94(22):11808-12. Epub 1997/10/29. doi: 10.1073/pnas.94.22.11808. PubMed PMID: 9342319; PubMed Central PMCID: PMC23599.
18. Sun X, Li Q, Wu Y, Wang M, Liu Y, Qi J, et al. Structure of influenza virus N7: the last piece of the neuraminidase "jigsaw" puzzle. *J Virol*. 2014;88(16):9197-207. Epub 2014/06/06. doi: 10.1128/jvi.00805-14. PubMed PMID: 24899180; PubMed Central PMCID: PMC4136277.
19. Lai JC, Garcia JM, Dyason JC, Bohm R, Madge PD, Rose FJ, et al. A secondary sialic acid binding site on influenza virus neuraminidase: fact or fiction? *Angew Chem Int Ed Engl*. 2012;51(9):2221-4. Epub 2012/01/28. doi: 10.1002/anie.201108245. PubMed PMID: 22281708.
20. Du W, Guo H, Nijman VS, Doedt J, van der Vries E, van der Lee J, et al. The 2nd sialic acid-binding site of influenza A virus neuraminidase is an important determinant of the hemagglutinin-neuraminidase-receptor balance. *PLOS Pathogens*. 2019;15(6):e1007860. doi: 10.1371/journal.ppat.1007860.
21. Kobasa D, Rodgers ME, Wells K, Kawaoka Y. Neuraminidase hemadsorption activity, conserved in avian influenza A viruses, does not influence viral replication in ducks. *J Virol*. 1997;71(9):6706-13. Epub 1997/09/01. PubMed PMID: 9261394; PubMed Central PMCID: PMC191950.
22. Benton DJ, Wharton SA, Martin SR, McCauley JW. Role of Neuraminidase in Influenza A(H7N9) Virus Receptor Binding. *J Virol*. 2017;91(11). Epub 2017/03/31. doi: 10.1128/jvi.02293-16. PubMed PMID: 28356530; PubMed Central PMCID: PMC5432883.
23. Gambaryan AS, Matrosovich MN. What adaptive changes in hemagglutinin and neuraminidase are necessary for emergence of pandemic influenza virus from its avian precursor? *Biochemistry (Mosc)*. 2015;80(7):872-80. Epub 2015/11/07. doi: 10.1134/s000629791507007x. PubMed PMID: 26542001.
24. Guo H, Rabouw H, Slomp A, Dai M, van der Vegt F, van Lent JWM, et al. Kinetic analysis of the influenza A virus HA/NA balance reveals contribution of NA to virus-receptor binding and NA-dependent rolling on receptor-containing surfaces. *PLoS Pathog*. 2018;14(8):e1007233. doi: 10.1371/journal.ppat.1007233. PubMed PMID: 30102740; PubMed Central PMCID: PMC6107293.
25. Gambaryan A, Tuzikov A, Pazynina G, Bovin N, Balish A, Klimov A. Evolution of the receptor binding phenotype of influenza A (H5) viruses. *Virology*. 2006;344(2):432-8. doi: <https://doi.org/10.1016/j.virol.2005.08.035>.
26. Chen L-M, Blixt O, Stevens J, Lipatov AS, Davis CT, Collins BE, et al. In vitro evolution of H5N1 avian influenza virus toward human-type receptor specificity. *Virology*. 2012;422(1):105-13. doi: <https://doi.org/10.1016/j.virol.2011.10.006>.
27. Ayora-Talavera G, Shelton H, Scull MA, Ren J, Jones IM, Pickles RJ, et al. Mutations in H5N1 influenza virus hemagglutinin that confer binding to human tracheal airway epithelium. *PLoS One*. 2009;4(11):e7836. Epub 2009/11/20. doi: 10.1371/journal.pone.0007836. PubMed PMID: 19924306; PubMed Central PMCID: PMC2775162.

28. Hoffmann E, Lipatov AS, Webby RJ, Govorkova EA, Webster RG. Role of specific hemagglutinin amino acids in the immunogenicity and protection of H5N1 influenza virus vaccines. *Proc Natl Acad Sci U S A*. 2005;102(36):12915-20. Epub 2005/08/25. doi: 10.1073/pnas.0506416102. PubMed PMID: 16118277; PubMed Central PMCID: PMC1200312.
29. Yamada S, Suzuki Y, Suzuki T, Le MQ, Nidom CA, Sakai-Tagawa Y, et al. Haemagglutinin mutations responsible for the binding of H5N1 influenza A viruses to human-type receptors. *Nature*. 2006;444(7117):378-82. Epub 2006/11/17. doi: 10.1038/nature05264. PubMed PMID: 17108965.
30. Xiong X, Xiao H, Martin SR, Coombs PJ, Liu J, Collins PJ, et al. Enhanced human receptor binding by H5 haemagglutinins. *Virology*. 2014;456-457:179-87. Epub 2014/06/04. doi: 10.1016/j.virol.2014.03.008. PubMed PMID: 24889237; PubMed Central PMCID: PMC4053833.
31. Neumann G, Kawaoka Y. Transmission of influenza A viruses. *Virology*. 2015;479-480:234-46. doi: <https://doi.org/10.1016/j.virol.2015.03.009>.
32. Hadfield J, Megill C, Bell SM, Huddleston J, Potter B, Callender C, et al. Nextstrain: real-time tracking of pathogen evolution. *Bioinformatics*. 2018;34(23):4121-3. doi: 10.1093/bioinformatics/bty407.
33. Watanabe Y, Arai Y, Daidoji T, Kawashita N, Ibrahim MS, El-Gendy EE-DM, et al. Characterization of H5N1 Influenza Virus Variants with Hemagglutinin Mutations Isolated from Patients. *mBio*. 2015;6(2):e00081-15. doi: 10.1128/mBio.00081-15.
34. Baigent SJ, McCauley JW. Glycosylation of haemagglutinin and stalk-length of neuraminidase combine to regulate the growth of avian influenza viruses in tissue culture. *Virus Research*. 2001;79(1):177-85. doi: [https://doi.org/10.1016/S0168-1702\(01\)00272-6](https://doi.org/10.1016/S0168-1702(01)00272-6).
35. Matrosovich M, Zhou N, Kawaoka Y, Webster R. The surface glycoproteins of H5 influenza viruses isolated from humans, chickens, and wild aquatic birds have distinguishable properties. *Journal of virology*. 1999;73(2):1146-55. PubMed PMID: 9882316.
36. Herfst S, Schrauwen EJ, Linster M, Chutinimitkul S, de Wit E, Munster VJ, et al. Airborne transmission of influenza A/H5N1 virus between ferrets. *Science*. 2012;336(6088):1534-41. Epub 2012/06/23. doi: 10.1126/science.1213362. PubMed PMID: 22723413; PubMed Central PMCID: PMC4810786.
37. Xiong X, Coombs PJ, Martin SR, Liu J, Xiao H, McCauley JW, et al. Receptor binding by a ferret-transmissible H5 avian influenza virus. *Nature*. 2013;497(7449):392-6. doi: 10.1038/nature12144.
38. Guo F, Li Y, Yu S, Liu L, Luo T, Pu Z, et al. Adaptive Evolution of Human-Isolated H5Nx Avian Influenza A Viruses. *Frontiers in Microbiology*. 2019;10(1328). doi: 10.3389/fmicb.2019.01328.
39. Dortmans JC, Dekkers J, Wickramasinghe IN, Verheije MH, Rottier PJ, van Kuppeveld FJ, et al. Adaptation of novel H7N9 influenza A virus to human receptors. *Sci Rep*. 2013;3:3058. Epub 2013/10/29. doi: 10.1038/srep03058. PubMed PMID: 24162312; PubMed Central PMCID: PMC3808826.
40. Connor RJ, Kawaoka Y, Webster RG, Paulson JC. Receptor Specificity in Human, Avian, and Equine H2 and H3 Influenza Virus Isolates. *Virology*. 1994;205(1):17-23. doi: <https://doi.org/10.1006/viro.1994.1615>.
41. Rogers GN, Paulson JC, Daniels RS, Skehel JJ, Wilson IA, Wiley DC. Single amino acid substitutions in influenza haemagglutinin change receptor binding specificity. *Nature*. 1983;304(5921):76-8. doi: 10.1038/304076a0.
42. Xu R, de Vries RP, Zhu X, Nycholat CM, McBride R, Yu W, et al. Preferential recognition of avian-like receptors in human influenza A H7N9 viruses. *Science*. 2013;342(6163):1230-5. Epub 2013/12/07. doi: 10.1126/science.1243761. PubMed PMID: 24311689; PubMed Central PMCID: PMC3954636.
43. Hoffmann E, Krauss S, Perez D, Webby R, Webster RG. Eight-plasmid system for rapid generation of influenza virus vaccines. *Vaccine*. 2002;20(25-26):3165-70. Epub 2002/08/07. PubMed PMID: 12163268.
44. Peeters B, Reemers S, Dortmans J, de Vries E, de Jong M, van de Zande S, et al. Genetic versus antigenic differences among highly pathogenic H5N1 avian influenza A viruses: Consequences

- for vaccine strain selection. *Virology*. 2017;503:83-93. Epub 2017/01/31. doi: 10.1016/j.virol.2017.01.012. PubMed PMID: 28135661.
45. Cornelissen LAHM, de Vries RP, de Boer-Luijtz EA, Rigter A, Rottier PJM, de Haan CAM. A single immunization with soluble recombinant trimeric hemagglutinin protects chickens against highly pathogenic avian influenza virus H5N1. *PLoS one*. 2010;5(5):e10645-e. doi: 10.1371/journal.pone.0010645. PubMed PMID: 20498717.
46. Predonzani A, Arnoldi F, Lopez-Requena A, Burrone OR. In vivo site-specific biotinylation of proteins within the secretory pathway using a single vector system. *BMC Biotechnol*. 2008;8:41. Epub 2008/04/22. doi: 10.1186/1472-6750-8-41. PubMed PMID: 18423015; PubMed Central PMCID: PMC2373293.
47. Corti D, Voss J, Gamblin SJ, Codoni G, Macagno A, Jarrossay D, et al. A neutralizing antibody selected from plasma cells that binds to group 1 and group 2 influenza A hemagglutinins. *Science*. 2011;333(6044):850-6. Epub 2011/07/30. doi: 10.1126/science.1205669. PubMed PMID: 21798894.
48. Rigter A, Widjaja I, Versantvoort H, Coenjaerts FE, van Roosmalen M, Leenhouts K, et al. A protective and safe intranasal RSV vaccine based on a recombinant prefusion-like form of the F protein bound to bacterium-like particles. *PLoS One*. 2013;8(8):e71072. Epub 2013/08/21. doi: 10.1371/journal.pone.0071072. PubMed PMID: 23951084; PubMed Central PMCID: PMC3741363.
49. Reeves PJ, Callewaert N, Contreras R, Khorana HG. Structure and function in rhodopsin: High-level expression of rhodopsin with restricted and homogeneous N-glycosylation by a tetracycline-inducible *N*-acetylglucosaminyltransferase I-negative HEK293S stable mammalian cell line. *Proceedings of the National Academy of Sciences*. 2002;99(21):13419. doi: 10.1073/pnas.212519299.
50. de Vries RP, de Vries E, Bosch BJ, de Groot RJ, Rottier PJM, de Haan CAM. The influenza A virus hemagglutinin glycosylation state affects receptor-binding specificity. *Virology*. 2010;403(1):17-25. doi: <https://doi.org/10.1016/j.virol.2010.03.047>.
51. Dai M, Guo H, Dortmans JC, Dekkers J, Nordholm J, Daniels R, et al. Identification of Residues That Affect Oligomerization and/or Enzymatic Activity of Influenza Virus H5N1 Neuraminidase Proteins. *J Virol*. 2016;90(20):9457-70. Epub 2016/08/12. doi: 10.1128/jvi.01346-16. PubMed PMID: 27512075; PubMed Central PMCID: PMC5044851.
52. Broszeit F, Tzarum N, Zhu X, Nemanichvili N, Eggink D, Leenders T, et al. N-Glycolylneuraminic Acid as a Receptor for Influenza A Viruses. *Cell Reports*. 2019;27(11):3284-94.e6. doi: <https://doi.org/10.1016/j.celrep.2019.05.048>.
53. Guo H, de Vries E, McBride R, Dekkers J, Peng W, Bouwman KM, et al. Highly Pathogenic Influenza A(H5Nx) Viruses with Altered H5 Receptor-Binding Specificity. *Emerg Infect Dis*. 2017;23(2):220-31. Epub 2016/11/22. doi: 10.3201/eid2302.161072. PubMed PMID: 27869615; PubMed Central PMCID: PMC5324792.
54. Gagarinov IA, Li T, Wei N, Sastre Torano J, de Vries RP, Wolfert MA, et al. Protecting-Group-Controlled Enzymatic Glycosylation of Oligo-N-Acetylglucosamine Derivatives. *Angew Chem Int Ed Engl*. 2019;58(31):10547-52. Epub 2019/05/21. doi: 10.1002/anie.201903140. PubMed PMID: 31108002.
55. Gagarinov IA, Li T, Wei N, Sastre Toraño J, de Vries RP, Wolfert MA, et al. Protecting-Group-Controlled Enzymatic Glycosylation of Oligo-N-Acetylglucosamine Derivatives. *Angewandte Chemie International Edition*. 2019;58(31):10547-52. doi: 10.1002/anie.201903140.

## Supporting information



**S1 Fig. Detailed analysis of the importance of K432E mutation in NA on receptor binding and activity of recombinant proteins.** (A) Hemagglutination assays were carried out using virus-like particle (VLP) preparations containing similar amounts of N1 protein similarly as described previously [20]. In short, VLPs were harvested from cells expressing full-length N1 proteins. Similar amounts of NA activity as determined using the monovalent substrate MUNANA were used in the analysis. Serial twofold dilutions of the VLPs were incubated in triplicate with equal volumes of 0.5% human erythrocytes at 4°C for 2 h in the presence or absence of OC. Red dots at the bottom of the wells indicate hemagglutination negative wells. N1 displayed a much higher hemagglutinating activity than N1432E. In the absence of OC, the difference in hemagglutination was even larger (S1A Fig), presumably because the receptor density on the red blood cells is decreased by NA activity and a much higher receptor density is needed for hemagglutination with N1432E than with N1 (B) Analysis of NA enzymatic activity by BLI kinetic assay was performed similarly as described previously [20]. Briefly, streptavidin biosensors were coated with biotinylated synthetic glycans (3'SLNLN, 6'SLNLN or LNLN). Subsequently, the sensors were incubated in buffer containing 4 µg recombinant soluble N1 or N1432E in the absence or presence of 8 µg ECA or ECA alone. ECA binding to sensors coated with



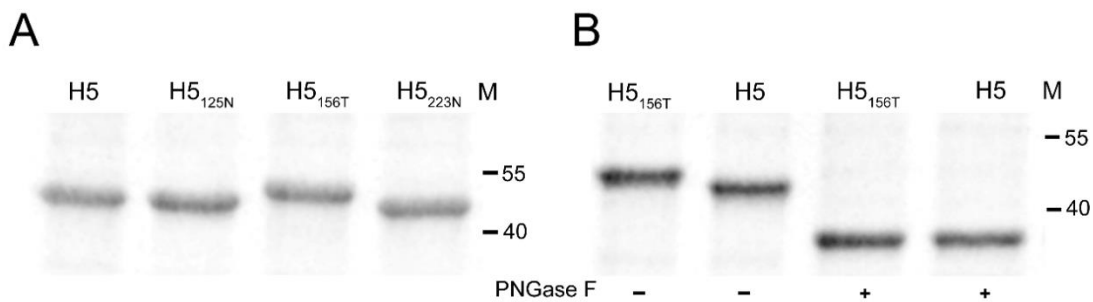


```

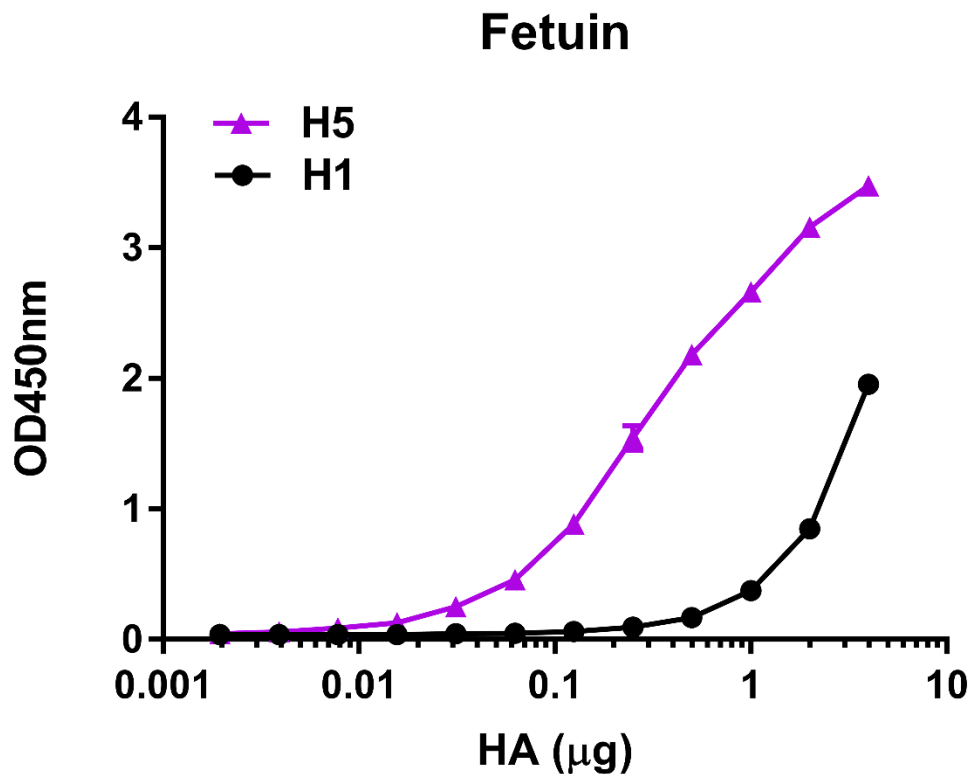
DQICIGYHANNSTEQVDTIMEKNVTVTTHAQDILEKTHNGKLCDDLGVKPLILRDCSVAGW 60
LLGNPMDEFINVPESYIVEKANPANDLCYPGNFNDYEEKHLLSRINHFEDIQIIPKS 120
125 130-loop * 156 *
SWSDHEASSGVSSACPYQGKSSFFRNVVWLIKNSAYPTIKRSYNNNTNQEDLLVLWGIHH 180
190-helix * 220-loop 223
PNDAAEQTRLYQNPTTYISVGTSTLNQRLVPKIATRSKVNGQSRMEFFWTILKPNDAIN 240
FESNGNFIAPAYAYKIVKKGDSAIMKSELEYGNCNTKQTPMGAINSSMPFHNIHPLTIG 300
ECPKYVKSNRLVLATGLRNSLQRERRRKRGLFGAIAGFIEGGWQGMVDGWYGYHHSNEQ 360
GSGYAADKESTQKAIDGVTNKVNSIIDKMNTQFEAVGREFNNLERRIENLNKKMEDGFLD 420
VWTYNAELLVLMENERTLDFHDSNVKNLYDKVRLQLRDNAKELGNGCFEFYHKCDNECME 480
SIRNGTYNYPQYSEEARLKREEISGVKLE

```

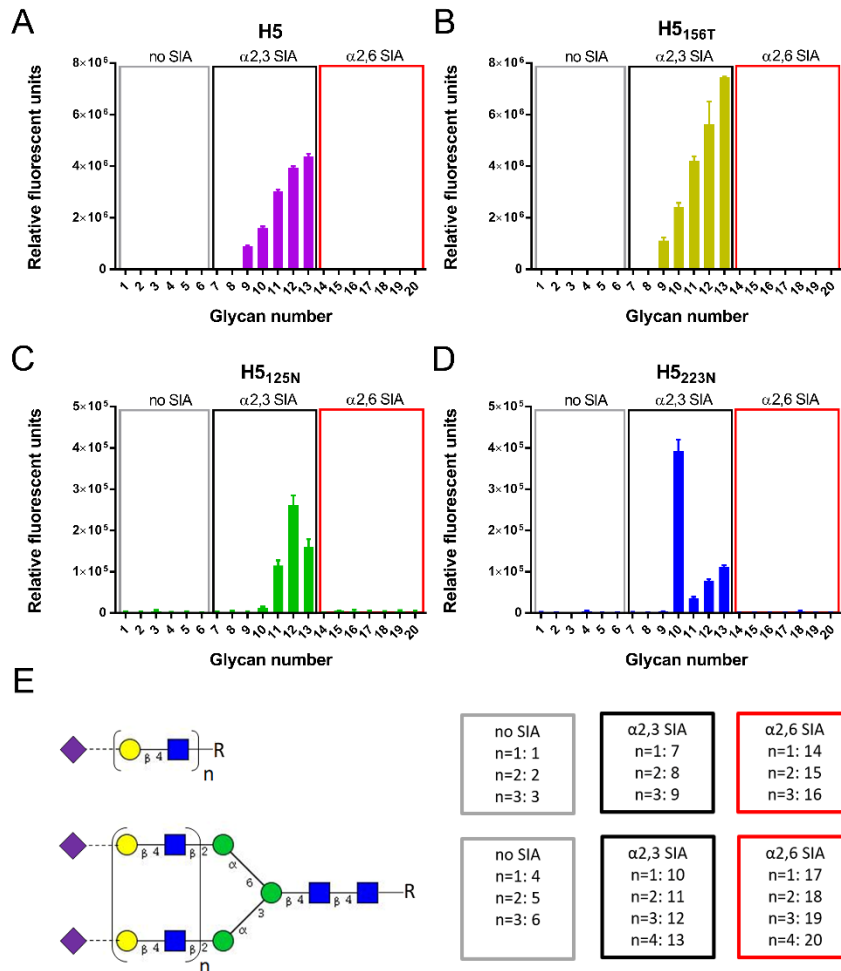
**S3 Fig. Sequence of H5.** Sequence of H5 protein of A/duck/Hunan/795/2002(H5N1) used in this study is shown. Residues that were mutated in this study are colored magenta (H125N, A156T and S223N). Amino acids of the three structural elements (130-loop, 190-helix, 220-loop) of RBD are shown in yellow. The four conserved, structurally-important amino acids of RBS are labelled with asterisks. Mutations A156T and A156S result in a N-glycosylation consensus sequence (NXS/T, X is any amino acid except P).



**S4 Fig. Glycosylation of recombinant HAs.** (A) Recombinant soluble H5 proteins expressed in HEK293S GnTI(-) were analyzed by gel electrophoresis followed by GelCode Blue staining. H5<sub>156T</sub> runs at a higher position in the gel than the other H5 proteins. (B) After (mock) treatment of H5 with PNGase F, the recombinant soluble H5 and H5<sub>156T</sub> proteins were examined by gel electrophoresis and GelCode Blue staining. The difference in electrophoretic mobility of the H5 proteins is lost upon removal of the N-glycans with PNGase F, indicating that H5<sub>156T</sub> contains an additional N-glycan side chain compared to H5. The position in the gel of relevant molecular weight markers is shown on the right side of the gels.



**S5 Fig. Receptor-binding avidity of H1 and H5 proteins.** Binding of HA to fetuin was analyzed using a fetuin solid phase binding assay as described previously [45, 53]. Briefly, purified, soluble trimeric HAs were precomplexed with strepMabClassic-HRP and rabbit- $\alpha$ -mouse-HRP (4:2:1 molar ratio) prior to incubation of limiting dilutions on the fetuin-coated (100 $\mu\text{g}/\text{ml}$  fetuin per well) 96-well Nunc MaxiSorp plates. After one hour incubation at room temperature, HA binding was subsequently determined using tetramethylbenzidine substrate (TMB, bioFX) in ELISA reader EL-808 (BioTEK) by measuring the optical density at 450 nm (OD450), which corresponds to binding of HA to fetuin. Standard deviations ( $n=3$ ) are indicated. H5 displayed a much higher receptor-binding avidity than H1. Low level expression of H1 precluded a BLI-based assay as shown in Fig 2A, for which high levels of HA are needed.



**S6 Fig. Glycan microarray with recombinant soluble H5 proteins.** Glycan microarray analysis was used to determine the receptor binding specificities of recombinant soluble H5 (A), H5156T (B), H5125N (C) and H5223N (D). All the HAs were precomplexed with antibodies against the Strep tag and goat anti-mouse IgG H&L (Alexa Fluor 647) similarly as described previously [52, 55]. The mean signals and standard deviations are shown for each glycan. The numbering of the glycans corresponds to the numbering of the glycans shown in (E). (E) Overview of the synthetic glycans printed on the microarray. Linear or branched glycans contain either no SIA,  $\alpha$ 2,3 SIA or  $\alpha$ 2,6 SIA and differ in their number of LACNAc (N-acetyllactosamine [Gal $\beta$ 1-4GlcNAc]) repeats, indicated by n. Purple diamonds; SIA, yellow circles; Gal, blue squares; GlcNAc, green circles; Man.

**S1 Table. Sequence analysis of 2SBS-negative H5N1<sub>432E</sub> virus upon passaging**

H5N1 2SBS- (432E )									
Reverse genetics	Passaging series	Protein	Parental	Passage 1	Passage 2	Passage 3	Passage 4	Passage 5	Passage 6
<b>A</b>	<b>1</b>	HA	223S	223 S/N	223 N	223 N	223 N	223 N	223 N
		NA	432E	432 E/K	432 K	432 K	432 K	432 K	432 K
	<b>2</b>	HA	223S		223 N	223 N	223 N	223 N	223 N
		NA	432E		432 K	432 K	432 K	432 K	432 K
	<b>3</b>	HA	223S						
		NA	432E					432 E/K	432 E/K
<b>B</b>	<b>1</b>	HA	125H 156A	125 H/N	125 H/N	125 H/N	125 H/N	156 A/T	156 T
		NA	432E						
	<b>2</b>	HA	125H 156A	125 H/N	125 H/N 156 A/T	156 A/T	156 A/T	156 T	156 T
		NA	432E						
	<b>3</b>	HA	125H 156A	125 H/N	125 H/N	125 H/N	125 H/N	156 A/T	156 T
		NA	432E						

**S2 Table. Sequence analysis of 2SBS-positive H5N1<sub>432K</sub> virus upon passaging**

H5N1 2SBS+ (432K )									
Reverse genetics	Passaging series	Protein	Parental	Passage 1	Passage 2	Passage 3	Passage 4	Passage 5	Passage 6
<b>A</b>	<b>1</b>	HA	156A				156 A/T	156 A/T	156 T
		NA	432K						
	<b>2</b>	HA	156A						
		NA	432K						
	<b>3</b>	HA	156A					156 A/T	156 T
		NA	432K						
<b>B</b>	<b>1</b>	HA	156A				156 A/T	156 T	156 T
		NA	432K						
	<b>2</b>	HA	156A				156 S/T	156 S/T	156 S/T
		NA	432K						
	<b>3</b>	HA	156A				156 T	156 T	156 T
		NA	432K						

**S3 Table. Overview of virus stocks used**

Figure	Virus	Passage series	Passage number	Table
<b>1A</b>	H5N1 WT	A2	P3	S2
	H5N1 <sub>432E</sub>	A3	P3	S1
<b>1D</b>	H5N1 WT	A2	P2	S2
	H5 <sub>156T</sub> N1	B1	P5	S2
	H5 <sub>156T</sub> N1 <sub>432E</sub>	B2	P5	S1
	H5N1 <sub>432E</sub>	A3	P2	S1
	H5 <sub>223N</sub> N1	A1	P4	S1
<b>2B/C</b>	H5N1 WT	A2	P3	S2
	H5 <sub>223N</sub> N1	A1	P4	S1
	H5N1 <sub>432E</sub>	A3	P3	S1
<b>2E/F</b>	H5 <sub>156T</sub> N1 <sub>432E</sub>	B2	P5	S1
	H5 <sub>125H/N</sub> N1 <sub>432E</sub>	B1	P3	S1
	H5N1 <sub>432E</sub>	A3	P3	S1
<b>2G</b>	H5N1 WT	A2	P3	S2
	H5 <sub>156T</sub> N1	B3	P5	S2
<b>2H</b>	H5 <sub>156T</sub> N1	B3	P5	S2
	H5 <sub>156T</sub> N1 <sub>432E</sub>	B2	P5	S1
<b>3A</b>	H5 <sub>223N</sub> N1	A1	P4	S1
	H5N1 WT	A2	P3	S2
	H5 <sub>125H/N</sub> N1 <sub>432E</sub>	B1	P3	S1
	H5N1 <sub>432E</sub>	A3	P3	S1
	H5 <sub>156T</sub> N1 <sub>432E</sub>	B2	P5	S1
<b>3C</b>	H5N1 WT	A2	P3	S2
<b>3D</b>	H5 <sub>223N</sub> N1	A1	P5	S1



## Chapter 5

# Analysis of pandemic influenza A (H1N1) virus neuraminidase evolution reveals entanglement of different phenotypic characteristics

Meiling Dai<sup>1</sup>#, Wenjuan Du<sup>1</sup>#, Carles Martínez-Romero<sup>2</sup>, Tim Leenders<sup>3</sup>, Tom Wennekes<sup>3</sup>, Guus F. Rimmelzwaan<sup>4</sup>, Frank J.M. van Kuppeveld<sup>1</sup>, Ron A.M. Fouchier<sup>5</sup>, Adolfo Garcia-Sastre<sup>2</sup>, Erik de Vries<sup>1</sup>, Cornelis A.M. de Haan<sup>1</sup>\*

1. Virology Division, Department of Infectious Diseases & Immunology, Faculty of Veterinary Science, Utrecht University, Yalelaan 1, 3584CL Utrecht, the Netherlands.
2. Department of Microbiology, Icahn School of Medicine at Mount Sinai, New York, New York, USA.
3. Department of Chemical Biology and Drug Discovery, Faculty of Science, Utrecht University, Universiteitsweg 99, 3584 CG Utrecht, the Netherlands
4. Research Center for Emerging Infections and Zoonoses, University of Veterinary Medicine, Bünteweg 17, 30559 Hannover, Germany
5. Department of Viroscience, Erasmus medical Center, Rotterdam, the Netherlands

@ present address: Commonwealth Scientific and Industrial Research Organisation (CSIRO), Australian Centre for Disease Preparedness (ACDP). East Geelong, VIC 3219, Australia

#: These authors contributed equally.

***(Submitted).***

## **Abstract**

The influenza A virus (IAV) neuraminidase (NA) is essential for virion release from cells and decoy receptors and an important target of antiviral drugs and antibodies. Adaptation to a new host sialome as well as escape from the host immune system are forces driving the selection of mutations in the NA gene. Phylogenetic analysis shows that until 2015 sixteen mutations in NA became fixed in the virus population after introduction in the human population of the pandemic IAV H1N1 (H1N1pdm09) in 2009. The accumulative effect of these mutations, in the order in which they appeared, was analyzed using recombinant proteins and viruses in combination with different functional assays. The results indicate that NA activity did not evolve to a single optimum but rather fluctuated within a certain bandwidth. Furthermore, antigenic and enzymatic properties of NA are intertwined, with several residues affecting multiple properties. For example, substitution K432E in the second sialic acid binding site, next to the catalytic site, was shown to affect catalytic activity, substrate specificity and the pH optimum for maximum activity. Selection of this mutation might have been driven by antigenic escape from the host immune response. We propose that the entanglement of NA phenotypes may be an important determining factor in the evolution of NA.



## Introduction

Influenza viruses (IAVs) are human respiratory pathogens that cause seasonal epidemics and occasional pandemics. Pandemics can occur when an animal IAVs cross the host species barrier and are efficiently spread between humans. In subsequent years, these viruses give rise to seasonal epidemics with significant disease and mortality. The only IAV pandemic of the 21<sup>st</sup> century started in April 2009 and was caused by a novel swine-origin H1N1 IAV (H1N1pdm09) [1]. This first influenza pandemic in the genomics era allows us to follow the evolution of a pandemic IAV spreading in the human population in detail. This evolution may entail selection of mutations in viral proteins driven by adaptation to the new host and selective pressure by the host immune system.

IAV particles contain two glycoproteins, the hemagglutinin (HA) receptor-binding and fusion protein and the neuraminidase (NA) protein, which has receptor-destroying activity. Both proteins are important determinants of host tropism, pathogenesis and transmission and prime targets of the host immune system. HAs of avian viruses preferentially bind to sialic acids (SIAs) linked to the proximal galactose by an  $\alpha$ 2,3 bond (avian-type receptor) [2, 3]. Human IAVs, including the H1N1pdm09 virus, preferentially bind  $\alpha$ 2,6-linked SIAs (human-type receptor), which are abundantly present on epithelial cells of the human upper respiratory tract [4, 5]. The IAV neuraminidase (NA) protein cleaves SIAs from glycoproteins and glycolipids. The NA protein thereby facilitates release of progeny virions from infected cells and decoy receptors (e.g. in mucus) and prevents virus self-aggregation [6]. Several studies indicate that a functional balance between HA binding and NA cleavage is important for maintaining optimal virus replication as well as transmission across different host species [7-14]. Knowledge of the molecular details of the HA-NA balance, and particularly the role of NA herein, however, are still largely lacking.

The NA protein is a type II membrane-anchored glycoprotein that forms homotetramers. The NA ectodomain contains a thin stalk and a globular head domain containing a six-bladed beta-propeller structure. SIA cleavage is mediated by the active site located in NA head domain [15]. The NA active site is composed of several highly conserved catalytic residues that directly contact the SIA substrate as well as structural residues that stabilize catalytic residues in place [16, 17]. The NA protein of H1N1pdm09 preferentially cleaves  $\alpha$ 2,3- over  $\alpha$ 2,6-linked SIAs [9, 12, 18, 19] with an optimal pH range of 5.5–6.5 [17, 20].  $\text{Ca}^{2+}$  is required for NA catalytic activity and thermostability [17] and three  $\text{Ca}^{2+}$ -binding sites have been identified for the NA protein of H1N1pdm09 [21]. NA catalytic activity for multivalent substrates is enhanced by the presence of a 2<sup>nd</sup> SIA binding site (2SBS)[12-14, 21-23], a shallow pocket composed of three surface loops located adjacent to the active site [24]. The 2SBS of N1, N2 and N9 proteins preferably binds  $\alpha$ 2,3-linked sialosides [12, 13, 23]. Five of the six SIA-

contact residues in the 2SBS identified by structural analysis of the N9 protein [24] are highly conserved among the NAs of avian IAVs, but this conservation is lost in the N1 and N2 proteins of human seasonal IAVs [12, 13, 22, 24, 25], including the H1N1pdm09 virus. In agreement herewith, the N1 proteins of H1N1pdm09 and seasonal human H1N1 IAVs display severely reduced binding to  $\alpha$ 2,3-sialyllactose compared to their avian counterparts as determined by saturation-transfer difference (STD) NMR [26].

The NA protein is an important target for antiviral drugs and antibodies contributing to protection against influenza [27-33]. The phenotypic evolution of NA of H1N1pdm09 in the human population is not well studied even though understanding evolution of NA-directed immunity may contribute to the design of better IAV vaccines [34]. Possibly alterations of NA activity are linked to changes in antigenicity just as has been observed for HA [35, 36]. Analysis of antigenic drift of H1N1pdm09 N1 suggests a role for substitutions at position 386, 390 and 432 in antigenicity changes [31, 37]. These residues have been shown to be important for the binding of monoclonal antibodies [31, 38-41]. However, the effect of most of these substitutions on NA enzymatic activity is not known, even while this probably plays an important role in their selection. In the current study we studied evolution of H1N1pdm09 N1 activity and antigenicity and analyzed to what extent different phenotypic properties of NA are intertwined. Therefore, we performed phylogenetic analysis of H1N1pdm09 NA sequences deposited between 2009 and 2015 and analyzed the accumulative effect of those mutations that became fixed in the virus population, in the order in which they appeared, using different functional assays. Our results indicate that NA functionality fluctuates within a certain bandwidth and does not evolve to obtain maximum activity. Furthermore, several substitutions were shown to affect several phenotypic characteristics of NA, including enzymatic activity and antigenicity. Of note, we identified an important role for the residue at position 432 in the 2SBS adjacent to the catalytic site as substitution of this residue was shown to affect multiple aspects of NA activity as well as antigenicity. The entanglement of NA phenotypes is proposed to be an important determining factor in the evolution of this protein.

## Results

### Evolution and expression of NA of H1N1pdm09 from 2009 until 2015

To get more insight into the phenotypic evolution of NA of H1N1pdm09 virus, we first reconstructed the evolutionary path of NA starting with the emergence of the H1N1pdm09 virus in April 2009 by generating a NA phylogenetic tree (Fig 1). Analysis of the different NA gene sequences revealed that sixteen amino acid substitutions (N248D, V106I, N369K, V241I, N44S, I106V, N200S, I321V, I34V/K432E, N386K, L40I, I314M, and V13I/V264I/N270K) became fixed in the virus population (Fig 1 and Table 1). For some substitutions (I34V/K432E and V13I/V264I/N270K) the order in which they were acquired could not be resolved. The location of these substitutions in the NA, (excluding the substitutions located in the transmembrane domain or the stalk region (V13I, I34V, L40I and N44S), the structure of which is not resolved) is shown in Fig 2. Although some substitutions are located relatively close to the active site (N200S, N248D, V241I, and K432E), none of them involves catalytic or framework residues [16, 17] (Fig 2). Substitutions N369K and K432E are located in the 2SBS at positions known to interact with SIA according to a N9 crystal structure [24]. The other residues, except the residue at position 106, are scattered across the surface of the NA head domain. Of note, N386K and N44S disrupt or generate a potential N-glycosylation site, respectively. Residue 386 is also part of a Ca<sup>2+</sup>-binding site, while residue 106 is located close to the subunit interfaces and to the Ca<sup>2+</sup>-binding site located at the 4-fold axis [20, 50, 51].

To evaluate the phenotypic changes in NA functionality associated with these mutations, they were introduced into recombinant soluble tetrameric versions of H1N1pdm09 NA [12] (starting at position 42) in accumulative order according to the phylogenetic analysis (Table 1). Viruses carrying these NA proteins are indicated in Fig 1, while a NA alignment is shown in S1 Fig. The NA proteins are abbreviated with two letters that refer to the location and two digits that refer to the year of isolation. In addition, we made a recombinant NA protein containing the I314M substitution in the background of the WI/13 NA protein. As this mutation is found in combination with other (non-fixed) mutations, this NA protein is referred to as WI/13-314.

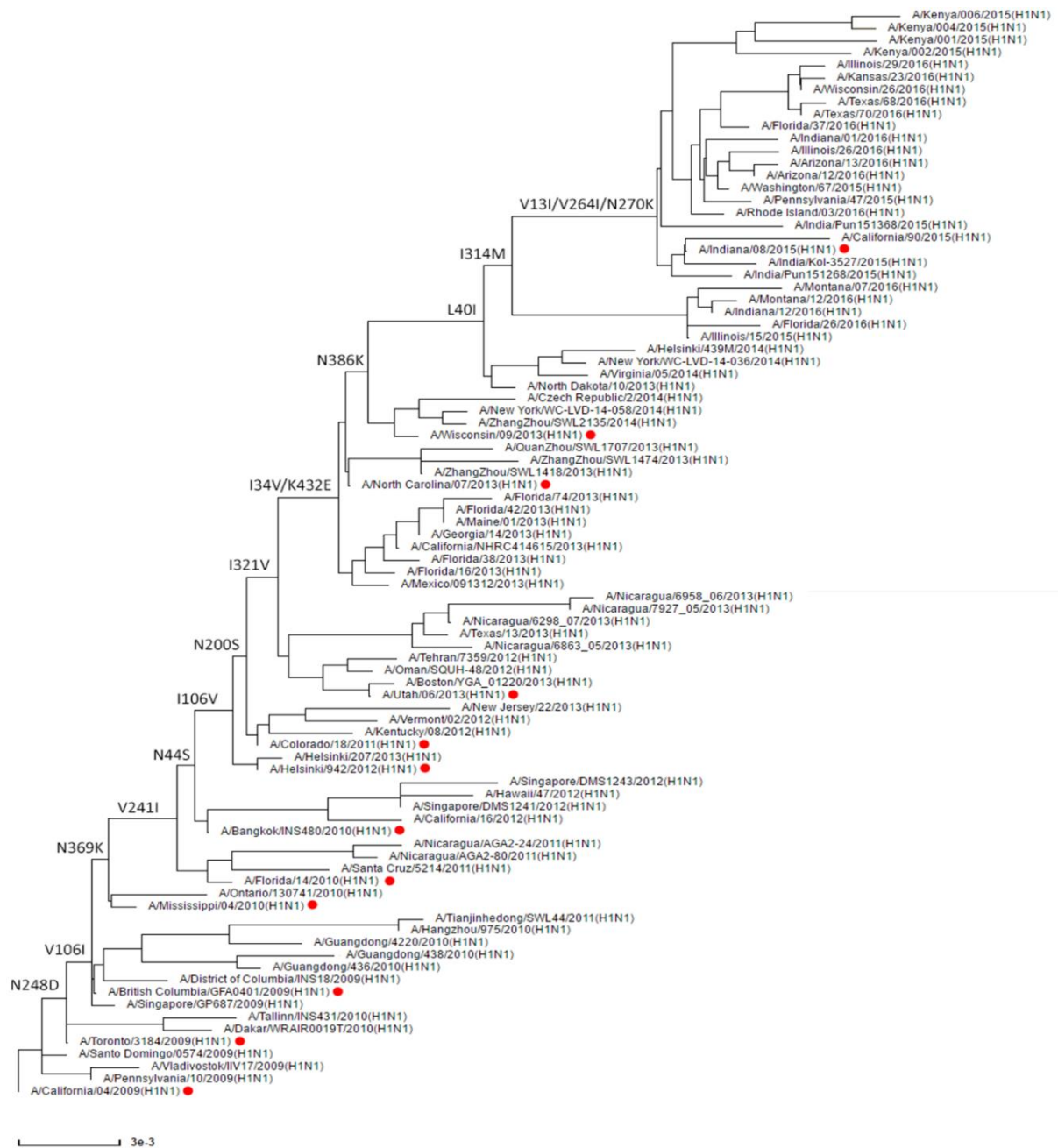


**Fig 1. Phylogenetic analysis of H1N1pdm09 N1 proteins from 2009 until 2015.** All full-length and unique N1 protein sequences of H1N1pdm09 were downloaded from the NCBI database and used to construct a N1 gene guide-tree, which was used to select N1 sequences representing all main branches of the tree. The selected N1 genes were used to construct a summary-tree of similar topology as the guide-tree. The N1 tree is rooted by the A/California/04/2009 isolate. Substitutions specified on the tree backbone indicate specific protein mutations that became fixed in the virus population. Red dots indicate virus isolates, the NA proteins of which only contain the indicated substitutions and were expressed in this study. An alignment of these proteins is shown in S1 Fig, while the mutations are also indicated in Table 1.

**Table 1. NA proteins analyzed**

Abbreviation	Isolate <sup>a</sup>	Mutation(s) introduced <sup>b</sup>	All mutations relative to A/California/04/2009
CA/09	A/California/04/2009		
TO/09	A/Toronto/3184/2009	N248D	N248D
BC/09	A/British Columbia/GFA0401/2009	V106I	N248D+V106I
MS/10	A/Mississippi/04/2010	N369K	N248D+V106I+N369K
FL/10	A/Florida/14/2010	V241I	N248D+V106I+N369K+V241I
BK/10	A/Bangkok/INS480/2010	N44S	N248D+V106I+N369K+N44S+V241I
HS/12	A/Helsinki/942/2012	I106V	N248D+V106I+N369K+N44S+V241I+I106V
CO/11	A/Colorado/18/2011	N200S	N248D+V106I+N369K+N44S+V241I+I106V+N200S
UT/13	A/Utah/06/2013	I321V	N248D+V106I+N369K+N44S+V241I+I106V+N200S+I321V
NC/13	A/North Carolina/07/2013	K432E	N248D+V106I+N369K+N44S+V241I+I106V+N200S+I321V+K432E
WI/13	A/Wisconsin/09/2013	N386K	N248D+V106I+N369K+N44S+V241I+I106V+N200S+I321V+K432E+N386K
WI/13-314		I314M	N248D+V106I+N369K+V241I+N44S+I106V+N200S+I321V+K432E+N386K+I314M
IN/15	A/Indiana/08/2015	V264I+N270K	N248D+V106I+N369K+V241I+N44S+I106V+N200S+I321V+K432E+N386K+I314M+V264I+N270K

<sup>a</sup> Virus isolates carrying NA proteins identical to those analyzed in this study are indicated. These isolates correspond to the isolates indicated with the red dots in Fig. 1.

<sup>b</sup> Mutation(s) introduced relative to the precursor virus are indicated.

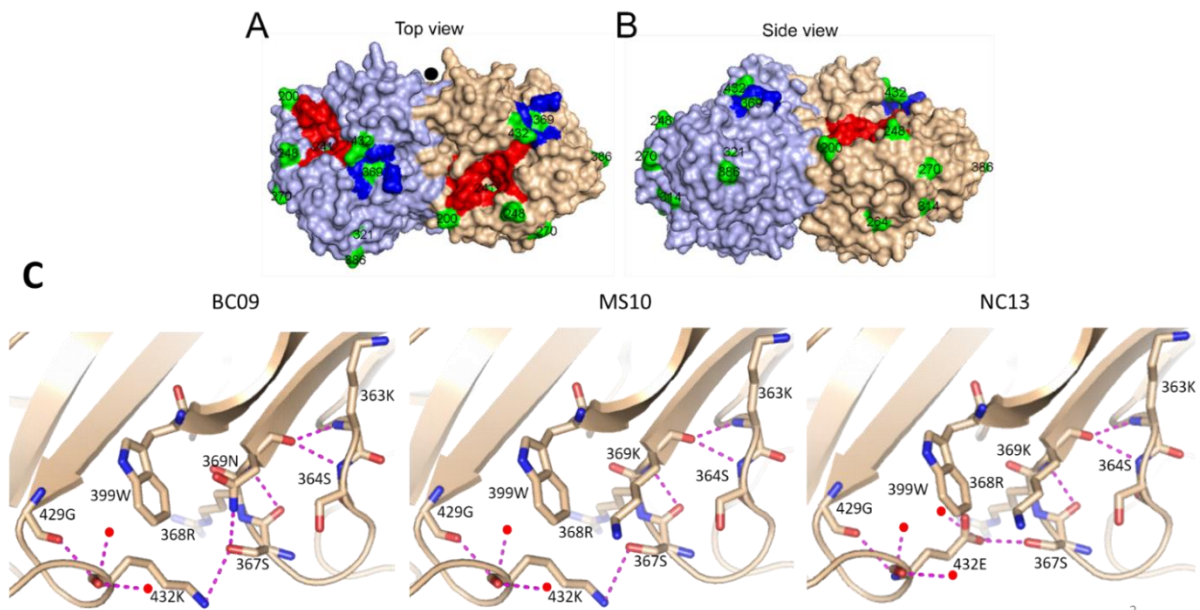


**Fig 2. Structural analysis of the N1 proteins.** Top (A) and side (B) views of the structure of the NA protein from A/California/04/2009 (PDB 3NSS) generated with PyMol software [21]. The NA active site and the 2nd SIA-binding site are colored red and blue. The amino acids in the NA head domain, substitution of which is indicated in Fig 1 and which became fixed in the population, are colored green and their numbering is indicated. V241I is located underneath the active site but doesn't belong to the catalytic or framework residues. K432E and N369K are located in the 2SBS. The residue at position 106 is not visible in this surface representation. The black circle indicates the fourfold symmetry axis. The substitutions are also indicated in the alignment shown in S1 Fig and in Table 1. (C) Close ups of the structures of the indicated NAs are shown in cartoon representation with the indicated amino acids shown as sticks (oxygen in red, nitrogen in blue). Water molecules are shown as red spheres and hydrogen bonds as dashed lines.

### **Cleavage of monovalent substrates**

While humans only synthesize N-Acetylneuraminic acid (Neu5Ac)-containing sialoglycan receptors, swine in addition also express N-Glycolylneuraminic acid (Neu5Gc) [52]. As substitutions in NA may result from adaptation of the H1N1pdm09 virus to the human SIA-receptor repertoire, the enzymatic properties of NA were analyzed using monovalent substrates that either represent Neu5Ac; (MUNANA) or Neu5Gc (MUNGNA). The specific activity (activity/amount of protein) of the NAs for Neu5Ac-containing substrate gradually increased to a 1.5- to 2-fold higher level by the cumulative addition of NA substitutions (Fig 3A). None of the NAs displayed significantly altered specific activity compared to their precursor protein. After introduction of the K432E mutation (NC/13) an increased  $K_m$  value (i.e. decreased substrate affinity) was observed using the MUNANA substrate (Fig 3B). This higher  $K_m$  value was maintained in the other proteins containing this substitution. All NA proteins displayed the same ratio of specific activities comparing MUNANA to MUNGNA substrates, with the exception again of the NA proteins containing the K432E mutation, which were consistently decreased in their ability to cleave MUNGNA (Fig 3C).

The ability of NA to cleave sialosides at low pH during virus entry has been shown to enhance virus replication in vitro [53, 54] and was suggested to contribute to the spread of pandemic viruses [20, 54]. Hence, we analyzed the enzymatic activity of the NA proteins at pH 4.6 compared to the activity at the routinely used pH 6.0 using the MUNANA assay. NA activity at pH 4.6 was relatively low for the proteins with K432 (CA/09-UT/13) and high for the proteins containing E432 (NC/13, WI/13 and WI/13-314) (Fig 3D). Thus, the K432E substitution (introduced in NC/13) has a positive effect on catalytic activity at low pH. As several substitutions are located at or close to  $Ca^{2+}$ -binding sites known to be important for thermal stability [51, 55-57], we analyzed the thermostability of NA activity by incubating NA at 50°C for 5 min in the absence or presence of EDTA after which the

activity was measured using the MUNANA assay (S2 Fig). The results indicate that residues 106 and 369 are determinants of  $\text{Ca}^{2+}$ -dependent thermostability. Mutations that affected  $\text{Ca}^{2+}$ -dependent thermostability did not affect the relative activity of the NA at low pH and *vice versa*.

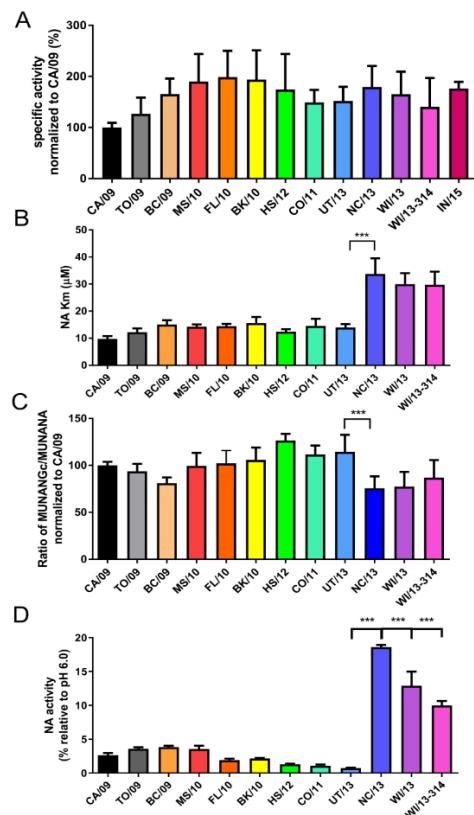


**Fig 3. Activity of H1N1pdm09 NA proteins using monovalent substrates.** (A) Specific activity of indicated NA proteins using the substrate MUNANA is graphed normalized to the specific activity of CA/09 NA. (B) Km values of the indicated NA proteins for MUNANA. (C) Ratio of the specific activity of the indicated NA proteins using the Neu5Gc-containing MUNGNA and the Neu5Ac-containing MUNANA (MUNGNA/MUNANA) graphed normalized to that of CA/09 NA. (D) The activity of the different NA proteins was determined at pH 4.6 using the MUNANA assay and graphed relative to the activity at pH 6.0. The graphs represent the mean of 2-6 independent experiments performed in triplicate. Error bars indicate standard deviations. (A-D) For each NA protein, significant differences relative to its precursor NA are indicated (\* $P < 0.05$ , \*\*  $P < 0.01$ , \*\*\*  $P < 0.001$ ).

### Cleavage of multivalent substrates

The enzymatic activity of the different NAs was analyzed with the glycoproteins fetuin and transferrin as a substrate using ELLAs described previously [12, 23]. The multivalent presentation of glycans on fetuin and transferrin resembles the *in vivo* presentation of SIAs on cell surface attached glycoproteins in contrast to the soluble monovalent substrates used above. Fetuin contains mono-

bi-, and triantennary glycans with  $\alpha$ 2,3- and  $\alpha$ 2,6-linked SIAs [58]. Transferrin contains two biantennary N-linked glycan chains with only  $\alpha$ 2,6-linked SIAs [59, 60]. Cleavage of SIAs from fetuin and transferrin by serially diluted NA was quantified by lectin binding in two ways, using either increase of ECA binding or decrease of MALI or SNA binding as a readout. ECA specifically recognizes glycans containing terminal Gal $\beta$ 1-4GlcNAc, which become exposed upon desialylation of N-linked sugars [61]. MALI and SNA specifically bind  $\alpha$ 2,3- or  $\alpha$ 2,6-linked SIAs, respectively [62, 63]. Despite small differences between different fetuin-lectin combinations (Fig 4), the results consistently show a positive effect of the N369K substitution (introduced in MS10) and a large negative effect of the K432E mutation (introduced in NC/13) on the cleavage of  $\alpha$ 2,3- and  $\alpha$ 2,6-linked SIA from fetuin. The other consistent effect was the modestly increased specific activity resulting from the N386K substitution (introduced in WI/13). No positive effect of the N369K substitution was observed when transferrin was used as substrate, while the negative effect of the K432E substitution was much smaller and not significantly different (Fig 4B and D). In contrast, the positive effect of the N386K mutation was still observed when transferrin was used (Fig 4B). N386K results in the loss of a putative glycosylation site (S1 Fig). Gel-electrophoretic analysis of NC/13 and WI/13 proteins, differing only at position 386 (S3 Fig) indicated, however, that the N386 residue is not modified by the addition of a N-glycan.



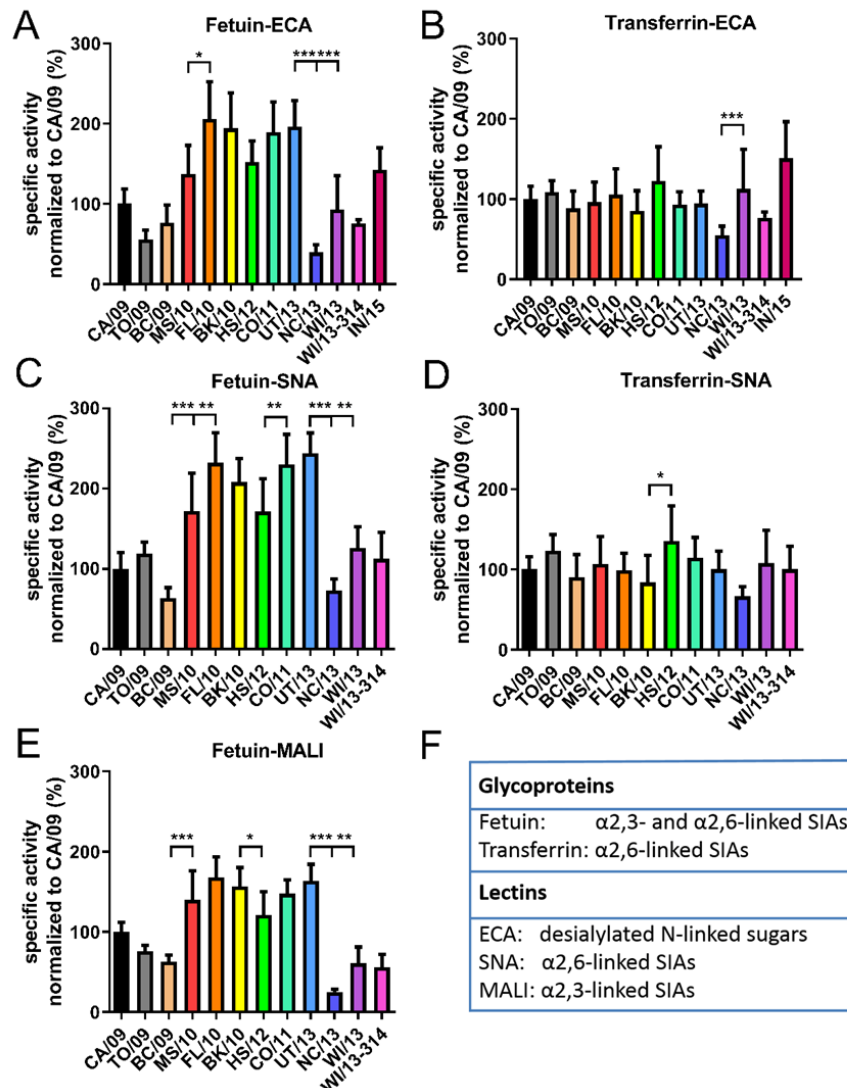


**Fig 4. Specific activity of H1N1pdm09 NA proteins for multivalent substrates.** Specific activity of indicated H1N1pdm09 NA proteins was determined by ELLA using different glycoprotein-lectin combinations: (A) fetuin-ECA, (B) transferrin-ECA, (C) fetuin-SNA, (D) transferrin-SNA, and (E) fetuin-MALI and graphed normalized to that of NA CA/09. (F) Information about the fetuin, transferrin and the binding preference of lectins used in this study. Means of at least three independent experiments performed in duplicate/triplicate are shown. Standard deviations are indicated. For each NA protein, significant differences relative to its precursor protein are indicated (\* $P < 0.05$ ; \*\* $P < 0.01$ ; \*\*\* $P < 0.001$ ).

Previously, we showed that increased cleavage of multivalent substrates correlated with increased binding of NA to glycans via the 2SBS to  $\alpha$ 2,3-linked SIAs [12, 13, 23] whereas activity on monovalent substrates was not affected. Here, the substitutions at position 369 and 432, located in the 2SBS of the N1 protein, only affect the specific activity when the multivalent substrate fetuin (Fig 4A) was

used, but not when soluble monovalent MUNANA (Fig 3A) or transferrin, which only contains  $\alpha$ 2,6-linked SIAs (Fig 4B), was used (note that the 2SBS binds much better to  $\alpha$ 2,3-linked SIAs). Therefore, we also analyzed the hemagglutinating ability of membrane vesicles containing UT/13 (with K432) and NC/13 NA (with E432) as described previously [13] (S4 Fig). Both proteins did not display hemagglutinating activity, in contrast to an avian N1, indicating a very low avidity for the interaction of NA of H1N1pdm09 with sialosides via the 2SBS regardless of the identity of the residue at position 432. Still, considering the effect of mutations in the 2SBS when using fetuin ( $\alpha$ 2,3-linked SIAs) in the ELLA assay (Fig 4A), we conclude that a very weak interaction of  $\alpha$ 2,3-linked SIAs with 2SBS contributes to NA activity on multivalent substrates.

### Effect of N1 mutations on virus replication and NA activity of virions

To investigate the effect of the substitutions in NA in the context of virus particle, five recombinant viruses were generated in the background of A/California/04/2009 pdmH1N1. These viruses, which contain either CA/09, MS/10, UT/13, NC/13 and IN/15 NA, only differ in their NA genome segments. The replication of these viruses in human bronchial epithelial cells (NHBE) and MDCK cells was assessed (Fig 5). Three viruses produced similar virus titers as CA/09 virus, whereas IN/15 virus titers were somewhat lower at early timepoints.

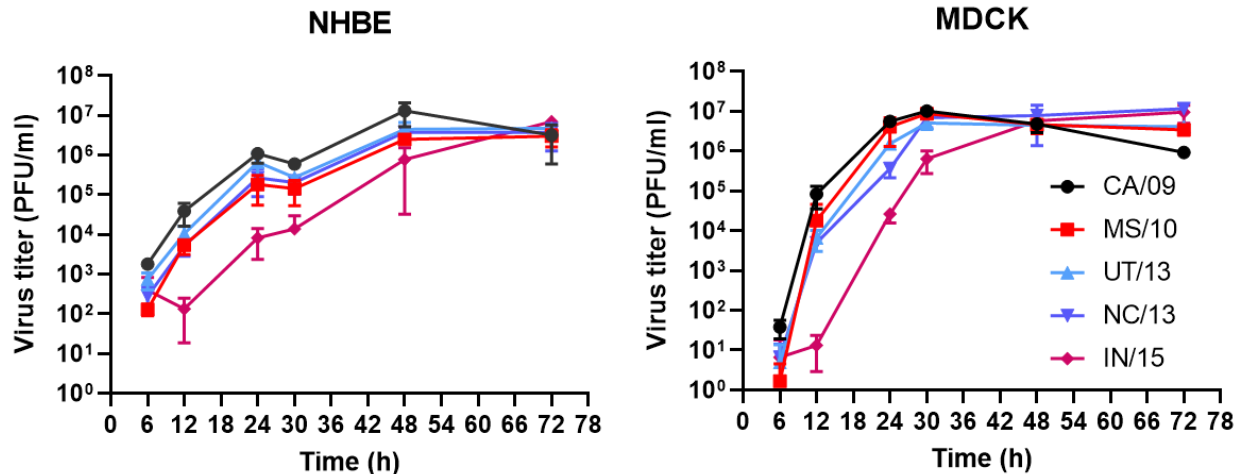


**Fig 5. Replication kinetics of recombinant H1N1 viruses.** NHBE (A) and MDCK cells (B) were infected with recombinant H1N1 viruses carrying different NA proteins at MOI 0.1 and 0.001, respectively. Virus in the cell culture supernatants at the indicated times post infection was harvested and titrated on MDCK cells, and the titers were expressed as PFU/ml.

Using a recently established biolayer interferometry (BLI)-based kinetic assay [13, 49], the contribution of the different NAs to the HA-NA balance of virus particles was determined by analyzing NA-driven virion self-elution. For viruses carrying the same HA, kinetics of self-elution are determined by NA enzymatic activity of virions. Sensors coated with  $\alpha$ 2,6-sialylated glycoprotein (6'LAMP1) were loaded to equal levels with the different recombinant viruses in the presence of the NA inhibitor oseltamivir-carboxylate (OC), after which NA-driven virion self-elution in the absence of OC was monitored (Fig 6A and 6B). Viruses carrying CA/09 NA displayed the fastest self-elution. Mutations in NA reduced virion self-elution, which was slowest for NC/13 virus. Additional substitutions in IN/15 increased virion-self elution again (Fig 6A and 6B). As the different self-elution rates did not correlate with the catalytic activities of the recombinant proteins (Fig 3 and 4 and S5 Fig), we analyzed the incorporation of the different NAs into virus particles, by analyzing the MUNANA activity per virus particle (Fig 6C). The enzymatic activity per virus particle correlated well with the virion dissociation rate (Fig 6D). As the five N1 proteins do not differ much in their MUNANA activity (Fig 3A), we conclude that the difference in MUNANA activity per virus particle particularly results from differential incorporation of NA into particles. To check whether the difference in NA incorporation was due to reduced intracellular NA trafficking and cell surface expression, the enzymatic activity of cell surface and intracellular full-length NA was quantified by using the MUNANA assay. The results indicate that the different NAs appear positively affect in their cell surface expression compared to CA/09 (Fig 6E). Although the cell surface expression of NA appeared to inversely correlate with the incorporation into virus particles, this correlation was not significant (S5 Fig). The different NAs displayed a similar ratio of cell surface/intracellular enzymatic activity indicating that intracellular trafficking was not negatively affected (Fig 6F). Apparently, reduced incorporation of the different NAs compared to CA/09 NA does not result from reduced intracellular trafficking and cell surface expression.

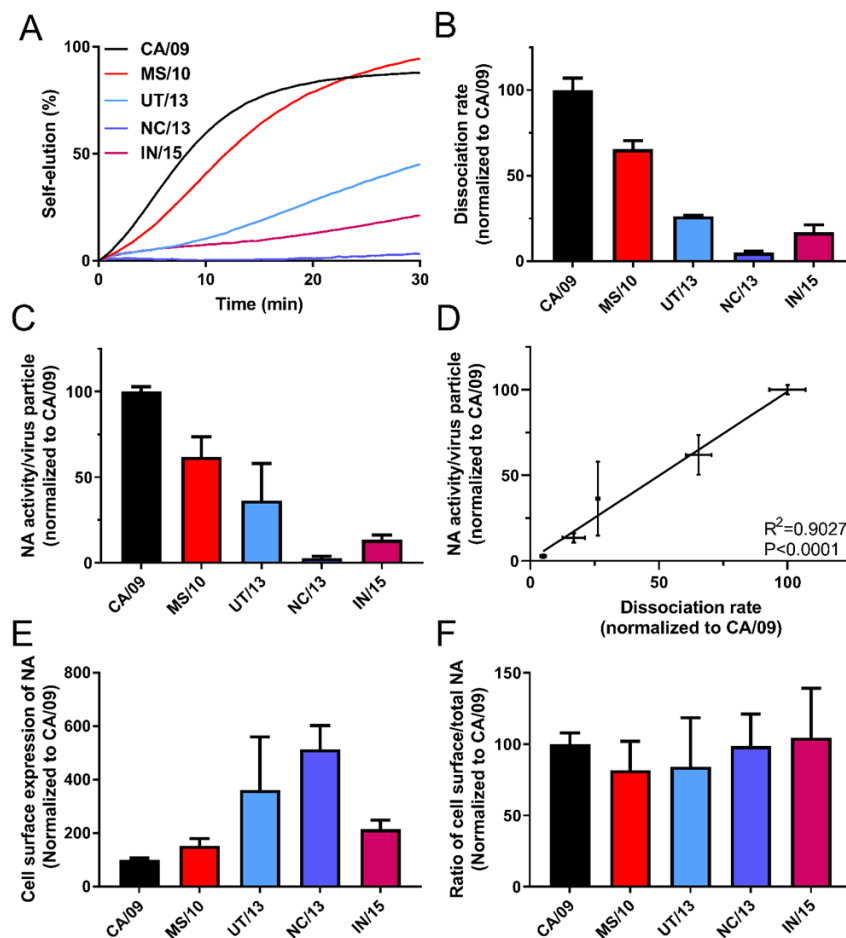
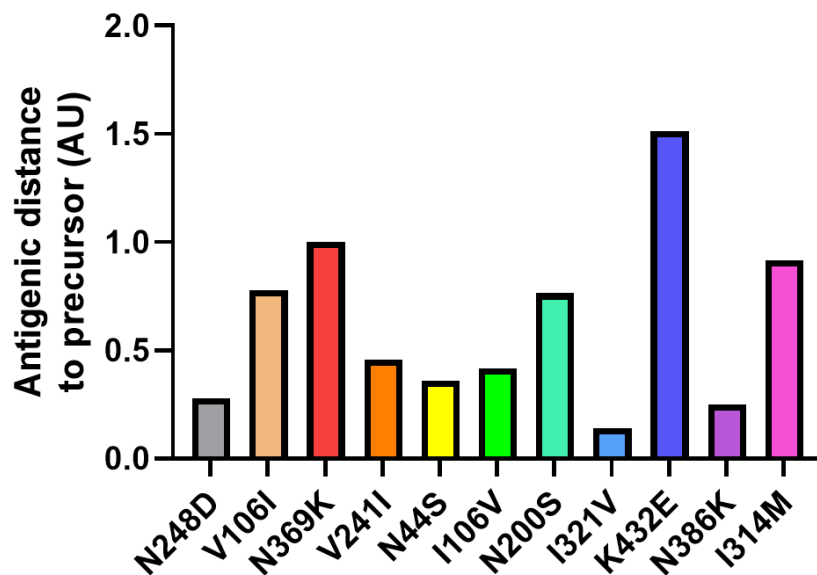


**Fig 6. NA enzymatic activity of recombinant viruses.** (A) Recombinant viruses were allowed to bind to similar levels to sensors containing 6'LAMP1 in the presence of OC. After removal of OC by short washes, virion self-elution in the absence of OC was monitored. Dissociation of virus particles was normalized to the virus association levels in the presence of OC. A representative experiment out of three performed is shown. (B) The slope of virus dissociation curve (shown in A) was calculated and normalized to that of the CA/09 virus. (C) NA activity in virus preparations was analyzed using the MUNANA assay. NA activity per virion is graphed relative to CA/09 virus (N=3). (D) Correlation between NA activity per virus particle shown in C and virus dissociation rate shown in B as determined using Graphpad Software. (E) Enzymatic activity of cell surface-expressed NAs using the MUNANA assay. (F) Ratio of cell surface expressed NA/total cell-associated NA was determined by using the MUNANA assay. All results represent the mean of three independent experiments. Standard deviations are indicated.

### Antigenicity of N1 proteins

Substitutions in NA may be selected because of their effect on NA antigenicity. The antigenic properties of the different NAs were tested by performing NA inhibition ELLAs (S1 Table) using recombinant soluble NA proteins in combination with a panel of ferret antisera (S1 Table). Generally, the ferret sera raised against the early viruses (from 2009) displayed the highest titers against the NAs from the early viruses, while the reciprocal effect was observed for the ferret serum raised against the 2015 virus. Based on the results shown in S1 Table, an antigenic map was generated (S6 Fig) and the antigenic change resulting from each mutation was determined (Fig 7). The largest antigenic change resulted from the K432E substitution introduced in NC13. The N369K substitution, which locates in the 2SBS just as K432E, also had a relatively large effect on NA antigenicity.



(AU)= antigenic units, corresponds to 2-fold dilution

**Fig 7. Antigenic distance of NA relative to its precursor NA.** For each NA protein, the antigenic distance relative to its precursor NA based on the antigenic map shown in S5 Fig is graphed. AU; antigenic unit, corresponds to a 2-fold serum dilution.

## Discussion

In this study we analyzed the genetic and phenotypic evolution of H1N1pdm09 NA starting with the emergence of H1N1pdm09 virus in 2009 until 2015. NA activity fluctuated with time within a certain bandwidth rather than to evolve to a distinct optimum. NAs in viruses from 2013-2015 display a rather similar enzymatic activity as NA from an early 2009 virus. Apparently, H1N1pdm09 NA was already well adapted to its human host at the beginning of the pandemic, similarly as we concluded earlier for HA [64].

None of the substitutions that became fixed in NA involve catalytic or framework residues, in agreement with these residues being extremely conserved in all NA genotypes [16, 17]. Of the several mutations that are located relatively close to the active site (N200S, N248D, V241I, and K432E), only K432E had a clear effect on NA catalytic activity. While the specific activity of NA for MUNANA was not affected by this mutation, it increased the  $K_m$  value for MUNANA, decreased cleavage of a NeuGc substrate and resulted in a more active NA at low pH. Residue 432 locates in the 2SBS of NA at a position immediately adjacent to the catalytic site. It interacts via hydrogen bonds with S367, which is an immediate neighbor of the catalytic site residue R368 (Fig 2). Mutation K432E, which resulted in the formation of two additional hydrogen bonds with water molecules, may therefore indirectly affect the catalytic site (Fig 2). Substitutions at positions 248 and 106 that were previously reported to increase low pH activity of NA [20], only had minor effects on low pH activity in our assays. Mutation of residue 106, together with substitution of residue 369, affected  $Ca^{2+}$ -dependent thermostability of NA, in agreement with findings of a recent study [51].

NAs of most avian IAVs contain a functional 2SBS that, by binding to  $\alpha$ 2,3-linked sialosides, contributes to catalytic activity on multivalent substrates [12, 13, 23]. NA of H1N1pdm09 contains, just as all NAs of human IAVs, mutations of SIA-contact residues in the 2SBS. Thus, CA/09 carries an N at position 369 rather than S, which is found in N1 of avian viruses [12, 22]. This N residue was subsequently replaced by K in MS/10 NA, which results in loss of a hydrogen bond with the SIA-contact residue S367 (Fig. 2). Somewhat later, K at position 432 was replaced by E in NC/13. N369K increased, while K432E decreased cleavage of fetuin containing  $\alpha$ 2,3-linked SIAs, but not of monovalent substrates or of transferrin containing only  $\alpha$ 2,6-linked SIAs. The altered cleavage exclusively of sialosides on fetuin corresponds with the preferred binding of NA via its 2SBS to  $\alpha$ 2,3-linked SIAs [12, 13, 43] although for this N1 it may be very weak as we were not able to demonstrate SIA binding via the 2SBS directly. We conclude that low affinity binding of the 2SBS of N1 of H1N1pdm09 to  $\alpha$ 2,3-linked SIAs can contribute to the catalytic activity of NA. In agreement herewith, previous studies demonstrated binding of H1N1pdm09 NA to SIA via the 2SBS by Brownian dynamics

simulation [65] and STD-NMR [26], which was, however, with a much lower affinity than for N1 of avian viruses. Of note, the negative effect of K432E on cleavage of multivalent substrates was partly compensated by N386K, which resulted in the loss of a N-glycosylation consensus sequence. While the loss of an N-glycan may explain increased NA activity for multivalent substrates by providing better access to the catalytic site, we did not find proof for the addition of a N-glycan to this site. The positive effect of N386K may therefore rather be explained by its localization in a  $\text{Ca}^{2+}$ -binding site [50].

Mutations in NA were shown to affect the sialidase activity of virions, which particularly resulted from reduced incorporation into virions. As CA/09 and MS/10 only differ in their ectodomains (N248D, V106I and N369K), mutations in this domain apparently are sufficient to affect NA incorporation into virions. The other NAs contain beside mutations in the NA ectodomain (e.g. K432E) additional mutation(s) in their transmembrane (proximal) regions, which may affect their incorporation. Reduced incorporation did not result from the NAs being defective in intracellular trafficking and cell surface expression. Mutations in NA rather resulted in increased cell surface expression levels similarly as observed previously [45]. Whether these mutations affect NA incorporation to the same extent when combined with their cognate HAs, remains to be determined. Of note, reduced sialidase activity of virions did not appear to affect virus replication much, as virus containing NC/13 replicated with similar kinetics as CA/09-containing virus. While well balanced HA and NA activities are important for efficient replication [8-11, 13], the low receptor-binding avidity of CA/09 HA [66] may preclude the necessity for high sialidase activity of virions in our assays, similarly as was observed previously for other IAVs [12, 14, 67].

Immune pressure is known to be a major driving force in IAV evolution. Most substitutions observed in H1N1pdm09 NA are located at the cell surface and several of them in or close to antigenic sites (e.g. positions 248, 369 and 432) [29, 31, 37, 39, 40, 68]. Analysis of NA antigenicity using a recombinant protein approach in combination with polyclonal ferret sera revealed a relatively large effect of mutations in the 2SBS (N369K and K432E). N369K was previously reported to abolish binding of monoclonal antibody HF5 to CA/09 NA, suggesting that it is part of an epitope that may also be targeted by human NA-specific antibodies [39]. Antigenic analysis of NA using H1N1pdm09 viruses also suggested an important role for residue 432 in antigenic drift [37], while K432 was shown to be crucial for the binding of several monoclonal antibodies [31, 69, 70]. The intertwinement of NA phenotypic properties, as exemplified by K432E affecting both NA activity and antigenicity, may be an important determining factor in NA evolution. Because of the multiple effects of K432E on NA activity, it may require a receptive background for its selection. Evolution of H1N1pdm09 is furthermore also likely influenced by the importance of a functional HA-NA balance [6]. Thus,

changes in NA activity and antigenicity, e.g. resulting from K432E, may subsequently drive compensatory mutations in NA (such as N386K) but also in HA. Vice versa, mutations in HA may also drive the selection of mutations in NA. Clearly, more research is needed to fully understand the complex functional interplay between HA and NA and the consequences thereof for antigenic evolution.



## Materials and Methods

**Phylogenetic analysis.** All full-length and unique NA sequences of A(H1N1)pdm09 viruses in the NCBI database were downloaded (from 2009 until 2015). NA gene trees were constructed by using the PHYLIP neighbor-joining algorithm with the F84 distance matrix. This tree was used as a guide-tree to select NA sequences representing all main branches of the tree. The selected NA genes were used to construct a summary-tree of similar topology as the guide-tree. This unrooted N1 tree has been displayed in Fig 1 with A/California/04/2009 at the base.

**Cell lines.** The Human Embryonic Kidney 293T (HEK293) cell line and the Madin-Darby Canine Kidney cell line were obtained from the American Type Culture Collection (ATCC) and cultured in Dulbecco's modified Eagle's medium (Thermo Fisher Scientific) supplemented with 10% fetal bovine serum (FBS) (Thermo Fisher Scientific), 100 IU/ml Penicillin, 100 µg/ml Streptomycin and 0.25 µg/ml Amphotericin B (Corning Antibiotic-Antimycotic Solution), at 37°C and 5% CO<sub>2</sub>. Normal human bronchial epithelial (NHBE) cells (Lonza, CC-2540 Lot# 630564) were isolated from a 16-year-old Caucasian female and were differentiated in an air-liquid interface following manufacturer's instructions (Lonza, CC-4175) at 37°C and 5% CO<sub>2</sub>.

**NA expression and purification.** Human codon-optimized NA ectodomain (amino acids.42–469; N1 numbering)-encoding cDNAs (Genscript, USA) of A/California/04/2009(H1N1) (GenBank accession no. ACP41107.1, referred to as CA/09) and A/Wisconsin/09/2013(H1N1) (GenBank accession no. AGV29183.1, referred to as WI/13) were cloned into a pFRT expression plasmid (Thermo Fisher Scientific) fused to sequences coding for an N-terminal signal sequence derived from *Gaussia* luciferase, a double Strep-tag for affinity purification (One-STREP; IBA GmbH), and a *Staphylothermus marinus* Tetrabrachion tetramerization domain, similarly as described previously [12]. Mutations of interest (Table 1) were introduced into the NA genes by using the Q5 Site-Directed Mutagenesis Kit (New England Biolabs) and confirmed by sequencing. For full-length NA constructs, corresponding NA transmembrane domains were added to the soluble NA-encoding sequences by replacing the terminal signal sequence, strep-tag and Tetrabrachion tetramerization domain using conventional cloning. Recombinant soluble NA proteins were expressed by transfection of HEK293T cells with NA-encoding plasmids and purified using Strep-tactin beads (IBA), similarly as described previously [12]. Quantification of the purified proteins was performed by comparative coomassie gel staining using standard BSA samples (Sigma-Aldrich) with known concentrations as a reference.

**NA enzymatic assays using soluble NA tetramers.** The activity of serially-diluted recombinant soluble NA proteins against monovalent substrates was determined by using a fluorometric assay similarly as described before (35) using either 2'-(4-methylumbelliferyl)- $\alpha$ -D-N-acetylneuraminic acid (MUNANA;

Sigma-Aldrich) or 2'-(4-methylumbelliferyl)- $\alpha$ -D-N-glycolylneuraminic acid (MUNGNA; [42]) as substrate. When indicated NA samples were incubated at 50°C in the absence or presence of 1mM Ethylenediaminetetraacetic acid (EDTA; Sigma-Aldrich) prior to incubation with MUNANA to determine NA thermostability. The MUNANA assay was also performed in 0.1 M citrate reaction buffer (at pH 6.0 or 4.6 ). NA kinetic analysis was performed to determine the  $K_m$  values (substrate binding affinity) of the NA proteins, similarly as described previously [43].

Activity of the recombinant soluble NA proteins towards multivalent glycoprotein substrates was analyzed using a previously described enzyme-linked lectin assay (ELLA) [23, 44]. Briefly, fetuin- or transferrin-coated (both from Sigma-Aldrich) 96-well plates were incubated with serial dilutions of recombinant soluble NA proteins in reaction buffer (50mM Tris/HCl, 4mM CaCl<sub>2</sub>, pH 6.0). After overnight incubation at 37°C, plates were washed and incubated with biotinylated lectins Erythrina Cristagalli Lectin (ECA), Sambucus Nigra Lectin (SNA) or Maackia Amurensis Lectin I (MAL I) (all from Vector Laboratories). The binding of ECA, PNA, SNA and MALI was detected using horseradish peroxidase (HRP)-conjugated streptavidin (Thermo Fisher Scientific) and tetramethylbenzidine substrate (TMB, BioFX) in an ELISA reader EL-808 (BioTEK) reading the OD at 450 nm. Both for the fluorometric assay and the ELLA, the data were fitted by non-linear regression using the Prism 6.05 software (Graph Pad). The resulting curves were used to determine the amount of NA protein corresponding to half maximum activity or lectin binding. The inverse of this amount is a measure for specific activity (activity/amount of protein) and is graphed relative to other NA proteins.

**NA enzymatic assays using virions and cell-associated proteins.** NA activity per virus particle was determined by MUNANA assay as described above. The number of virus particles was determined by Nanoparticle tracking analysis (NTA) using a NanoSight NS300 instrument (Malvern), similarly as described previously [13]. Each virus preparation was analyzed by NTA twice and mean values were used. NA activity of cell-associated proteins was also determined using the MUNANA assay, similarly as described previously [45]. Briefly, HEK293T cells, transfected with equal amounts of full-length NA-encoding expression plasmids were treated with trypsin-EDTA for 2 mins at 72 hours post transfection, followed by the addition of 10% fetal calf serum to neutralize the trypsin. Subsequently, cells were collected by centrifugation for 5 mins at 1500 rpm followed by three time washes with Dulbecco's phosphate buffered saline (PBS). The MUNANA assay was performed in PBS containing 1mM Ca<sup>2+</sup> to determine the activity of NA at the cell surface. To determine the total cell NA activity, 0.1% triton was added to the reaction buffer.

**Antigenic analysis of NA.** Inhibition of NA activity by the ferret sera was measured by enzyme-linked lectin assay (ELLA) as described previously with modifications [23, 46]. Ferret sera were raised either

against a classical swine H1N1 strain (A/NL/386/86), H1N1pdm09 vaccine strain (A/California/007/09) or several other H1N1pdm09 viruses isolated in the Netherlands (S1 Table). Serial dilutions of ferret sera were mixed with purified NA protein diluted in reaction buffer (50mM Tris/HCl, 4mM CaCl<sub>2</sub>, pH 6.0). The mixture was transferred to 96-well plates coated with 2.5 µg/ml fetuin (Sigma-Aldrich) and incubated at 37°C for 2 h. After extensive washing, the plates were incubated with biotinylated ECA (1.25 µg/ml; Vector Laboratories) at RT for 1 h. The amount of ECA binding was determined as described above. The anti-NA ELLA titers of the sera correspond to the dilutions at which 50% of maximal NA enzyme activity was achieved as determined by nonlinear regression analysis (Graph Pad Prism 6.05). The antigenic relatedness was calculated [47] using mean titers of 2-3 experiments performed in duplicate/triplicate. Calculated distances between proteins and sera correlated well with distances on the 2D map (R<sup>2</sup>=0,8671), allowing us to determine antigenic distances between NA proteins by measuring distances on the 2D map.

**Plasmid-based viral rescue and propagation.** Specific nucleotide substitutions in the A/California/04/2009 Neuraminidase (NA) coding sequence were added to match the sequence of the NA of A/Mississippi/04/2010 (MS10), A/North Carolina/07/2013 (NC13), A/Utah/06/2013 (UT13) and A/Indiana/08/2015 (IN15) strains (Table 1). This was achieved using the Quickchange Mutagenesis kit (Agilent) or by generating specific synthesized oligonucleotides using the GeneArt Strings DNA fragments platform (Thermo Fisher Scientific, Waltham, MA) and subcloning into pDZ vectors. Standard reverse genetics were used to rescue each individual virus in a A/California/04/2009 (Cal09) backbone, as previously described [48]. Lipofectamine 2000 (Thermo Fisher Scientific, Waltham, MA) was used to transfect a co-culture of HEK293T and MDCK cells with seven ambisense pDZ plasmids, each one encoding for a segment of the virus, and using the specific pDZ vector containing either the Cal09 NA or the modified NA cDNAs. Transfected cells were incubated for 72 hours at 37°C in a 5% CO<sub>2</sub> incubator. Cell culture supernatants containing influenza virions were collected. Final stocks of each recombinant virus were achieved after plaque purification and infecting fresh MDCK cells (80% confluence) with a 1:100 dilution of the purified plaque and incubated at 37°C for 48 hours in Minimum Essential Medium Eagle (MEM) (Thermo Fisher Scientific) supplemented with 1µg/ml of TPCK trypsin (Sigma-Aldrich). Viral titers were determined by plaque assay and by hemagglutination assays using a suspension of 5% turkey red blood cells in PBS. Absence of defective interfering particles was confirmed by comparing hemagglutination activity versus viral titers and complete genome sequencing was obtained using the Illumina miSeq platform to confirm nucleotide substitutions and absence of unexpected changes in the sequence.

**IAV infections.** MDCK cells were inoculated with virus preparations in PBS supplemented with 0.3% Bovine Serum Albumin (BSA) (Gemini) in triplicates. After one hour of incubation at room

temperature, cells were washed with DMEM supplemented with 10% FBS to remove the unbound virus. Cells were incubated in MEM supplemented with 0.3% BSA and 1 µg/ml (MDCK cells) of TPCK-trypsin at 37°C in a 5% CO<sub>2</sub> incubator. When indicated, cell culture supernatants were sampled at different time points to assess viral replication by standard plaque assay technique using MDCK cells. NHBE cells were incubated with the viral inoculum in PBS on the apical surface. After one hour of incubation at 37°C, 5% CO<sub>2</sub>, viral inoculum was removed, and the apical surface was washed twice with PBS to remove unbound virus. Cells were incubated without the presence of TPCK-trypsin at 37°C in 5% CO<sub>2</sub>. When indicated, cell culture supernatants were sampled at different time points to assess viral replication by standard plaque assay technique using MDCK cells.

**Analysis of NA activity using biolayer interferometry (BLI).** BLI assays were performed using Octet RED348 as described previously [13, 49]. All the experiments were performed in PBS with Calcium and Magnesium (Lonza) at 30 °C and with plates shaking at 1000 rpm. Streptavidin sensors were loaded to saturation with recombinant soluble lysosomal-associated membrane glycoprotein 1 (LAMP1) co-expressed with human  $\alpha$ -2,6-sialyltransferase 1 (ST6Gal1) to increase levels of  $\alpha$ 2,6 sialylated glycans (6'LAMP1; [14]). Receptor-loaded sensors were subsequently moved to wells containing viruses to perform virus binding in the presence of NA inhibitor oseltamivir carboxylate (OC; kindly provided by Roche). Amounts of virus stocks used were adjusted so that similar binding levels were obtained and thus that similar numbers of virus particles were captured on the sensors. After 3 short (5s) washes in PBS to remove OC, NA-driven dissociation was monitored in the absence of OC.

**Statistical analysis.** The mean values of 2-6 experiments performed in duplicate/triplicate are graphed. All statistical analyses were performed by one-way analysis of variance (ANOVA) using Tukey's multiple comparisons test (Graph Pad Prism 6.05). The level of significance was expressed as \* $P$ <0.05, \*\*  $P$ <0.01, \*\*\*  $P$ <0.001.

### **Acknowledgements**

M.D. and W.D were supported by grants from the Chinese Scholarship Council. C.A.M.d.H. was supported by the Dutch Ministry of Economic Affairs, Agriculture, and Innovation, within the Castellum Project "Zoonotic Avian Influenza". RF and AGS were supported by NIAID/NIH contract HHSN272201400008C. The funders had no role in study design, data collection and analysis, decision to publish, or preparation of the manuscript.

## References

1. Neumann G, Noda T, Kawaoka Y. Emergence and pandemic potential of swine-origin H1N1 influenza virus. *Nature*. 2009;459(7249):931-9. doi: 10.1038/nature08157.
2. Shinya K, Ebina M, Yamada S, Ono M, Kasai N, Kawaoka Y. Influenza virus receptors in the human airway. *Nature*. 2006;440(7083):435-6. doi: 10.1038/440435a.
3. van Riel D, Munster VJ, de Wit E, Rimmelzwaan GF, Fouchier RAM, Osterhaus ADME, et al. H5N1 Virus Attachment to Lower Respiratory Tract. *Science*. 2006;312(5772):399. doi: 10.1126/science.1125548.
4. Stevens J, Blixt O, Glaser L, Taubenberger JK, Palese P, Paulson JC, et al. Glycan Microarray Analysis of the Hemagglutinins from Modern and Pandemic Influenza Viruses Reveals Different Receptor Specificities. *Journal of Molecular Biology*. 2006;355(5):1143-55. doi: <https://doi.org/10.1016/j.jmb.2005.11.002>.
5. Chandrasekaran A, Srinivasan A, Raman R, Viswanathan K, Raguram S, Tumpey TM, et al. Glycan topology determines human adaptation of avian H5N1 virus hemagglutinin. *Nature Biotechnology*. 2008;26(1):107-13. doi: 10.1038/nbt1375.
6. de Vries E, Du W, Guo H, de Haan CAM. Influenza A Virus Hemagglutinin–Neuraminidase–Receptor Balance: Preserving Virus Motility. *Trends in Microbiology*. 2020;28(1):57-67. doi: <https://doi.org/10.1016/j.tim.2019.08.010>.
7. de Wit E, Munster VJ, van Riel D, Beyer WEP, Rimmelzwaan GF, Kuiken T, et al. Molecular Determinants of Adaptation of Highly Pathogenic Avian Influenza H7N7 Viruses to Efficient Replication in the Human Host. *Journal of Virology*. 2010;84(3):1597. doi: 10.1128/JVI.01783-09.
8. Yen H, Liang C, Wu C, Forrest HL, Ferguson A, Choy K, et al. Hemagglutinin–neuraminidase balance confers respiratory-droplet transmissibility of the pandemic H1N1 influenza virus in ferrets. *Proceedings of the National Academy of Sciences*. 2011;108(34):14264. doi: 10.1073/pnas.1111000108.
9. Xu R, Zhu X, McBride R, Nycholat CM, Yu W, Paulson JC, et al. Functional Balance of the Hemagglutinin and Neuraminidase Activities Accompanies the Emergence of the 2009 H1N1 Influenza Pandemic. *Journal of Virology*. 2012;86(17):9221. doi: 10.1128/JVI.00697-12.
10. Gambaryan AS, Matrosovich MN. What adaptive changes in hemagglutinin and neuraminidase are necessary for emergence of pandemic influenza virus from its avian precursor? *Biochemistry (Moscow)*. 2015;80(7):872-80. doi: 10.1134/S000629791507007X.
11. Gaymard A, Le Briand N, Frobert E, Lina B, Escuret V. Functional balance between neuraminidase and haemagglutinin in influenza viruses. *Clinical Microbiology and Infection*. 2016;22(12):975-83. doi: 10.1016/j.cmi.2016.07.007.
12. Du W, Dai M, Li Z, Boons G-J, Peeters B, van Kuppeveld FJM, et al. Substrate Binding by the Second Sialic Acid-Binding Site of Influenza A Virus N1 Neuraminidase Contributes to Enzymatic Activity. *Journal of virology*. 2018;92(20):e01243-18. doi: 10.1128/JVI.01243-18. PubMed PMID: 30089692.
13. Du W, Guo H, Nijman VS, Doedt J, van der Vries E, van der Lee J, et al. The 2nd sialic acid-binding site of influenza A virus neuraminidase is an important determinant of the hemagglutinin-neuraminidase-receptor balance. *PLOS Pathogens*. 2019;15(6):e1007860. doi: 10.1371/journal.ppat.1007860.
14. Du W, Wolfert MA, Peeters B, van Kuppeveld FJM, Boons G-J, de Vries E, et al. Crosstalk between the receptor-binding properties of influenza A virus hemagglutinin and neuraminidase drives their co-evolution. *PLOS Pathogens*. 2020:(submission).
15. Colman PM. Influenza virus neuraminidase: structure, antibodies, and inhibitors. *Protein Sci*. 1994;3(10):1687-96. doi: 10.1002/pro.5560031007. PubMed PMID: 7849585.
16. Burmeister WP, Ruigrok RW, Cusack S. The 2.2 Å resolution crystal structure of influenza B neuraminidase and its complex with sialic acid. *EMBO J*. 1992;11(1):49-56. PubMed PMID: 1740114.

17. Air GM. Influenza neuraminidase. *Influenza and Other Respiratory Viruses*. 2012;6(4):245-56. doi: 10.1111/j.1750-2659.2011.00304.x.
18. Garcia J-M, Lai JCC, Haselhorst T, Choy KT, Yen H-L, Peiris JSM, et al. Investigation of the binding and cleavage characteristics of N1 neuraminidases from avian, seasonal, and pandemic influenza viruses using saturation transfer difference nuclear magnetic resonance. *Influenza and other respiratory viruses*. 2014;8(2):235-42. Epub 2013/09/30. doi: 10.1111/irv.12184. PubMed PMID: 24118862.
19. Gerlach T, Kühling L, Uhlenhorff J, Laukemper V, Matrosovich T, Czudai-Matwisch V, et al. Characterization of the neuraminidase of the H1N1/09 pandemic influenza virus. *Vaccine*. 2012;30(51):7348-52. doi: <https://doi.org/10.1016/j.vaccine.2012.09.078>.
20. Takahashi T, Song J, Suzuki T, Kawaoka Y. Mutations in NA That Induced Low pH-Stability and Enhanced the Replication of Pandemic (H1N1) 2009 Influenza A Virus at an Early Stage of the Pandemic. *PLOS ONE*. 2013;8(5):e64439. doi: 10.1371/journal.pone.0064439.
21. Li Q, Qi J, Zhang W, Vavricka CJ, Shi Y, Wei J, et al. The 2009 pandemic H1N1 neuraminidase N1 lacks the 150-cavity in its active site. *Nature Structural & Molecular Biology*. 2010;17(10):1266-8. doi: 10.1038/nsmb.1909.
22. Uhlenhorff J, Matrosovich T, Klenk H-D, Matrosovich M. Functional significance of the hemadsorption activity of influenza virus neuraminidase and its alteration in pandemic viruses. *Arch Virol*. 2009;154(6):945-57. Epub 2009/05/21. doi: 10.1007/s00705-009-0393-x. PubMed PMID: 19458903.
23. Dai M, McBride R, Dortmans JCFM, Peng W, Bakkers MJG, de Groot RJ, et al. Mutation of the Second Sialic Acid-Binding Site, Resulting in Reduced Neuraminidase Activity, Preceded the Emergence of H7N9 Influenza A Virus. *Journal of virology*. 2017;91(9):e00049-17. doi: 10.1128/JVI.00049-17. PubMed PMID: 28202753.
24. Varghese JN, Colman PM, van Donkelaar A, Blick TJ, Sahasrabudhe A, McKimm-Breschkin JL. Structural evidence for a second sialic acid binding site in avian influenza virus neuraminidases. *Proceedings of the National Academy of Sciences*. 1997;94(22):11808. doi: 10.1073/pnas.94.22.11808.
25. Kobasa D, Rodgers ME, Wells K, Kawaoka Y. Neuraminidase hemadsorption activity, conserved in avian influenza A viruses, does not influence viral replication in ducks. *Journal of virology*. 1997;71(9):6706-13. PubMed PMID: 9261394.
26. Lai JCC, Garcia J-M, Dyason JC, Böhm R, Madge PD, Rose FJ, et al. A Secondary Sialic Acid Binding Site on Influenza Virus Neuraminidase: Fact or Fiction? *Angewandte Chemie International Edition*. 2012;51(9):2221-4. doi: 10.1002/anie.201108245.
27. Cardoso FM, Ibañez LI, Van den Hoecke S, De Baets S, Smet A, Roose K, et al. Single-domain antibodies targeting neuraminidase protect against an H5N1 influenza virus challenge. *Journal of virology*. 2014;88(15):8278-96. Epub 2014/05/14. doi: 10.1128/JVI.03178-13. PubMed PMID: 24829341.
28. Schotsaert M, Ysenbaert T, Smet A, Schepens B, Vanderschaeghe D, Stegalkina S, et al. Long-Lasting Cross-Protection Against Influenza A by Neuraminidase and M2e-based immunization strategies. *Scientific Reports*. 2016;6(1):24402. doi: 10.1038/srep24402.
29. Gilchuk IM, Bangaru S, Gilchuk P, Irving RP, Kose N, Bombardi RG, et al. Influenza H7N9 Virus Neuraminidase-Specific Human Monoclonal Antibodies Inhibit Viral Egress and Protect from Lethal Influenza Infection in Mice. *Cell Host & Microbe*. 2019;26(6):715-28. doi: <https://doi.org/10.1016/j.chom.2019.10.003>.
30. Zhu X, Turner HL, Lang S, McBride R, Bangaru S, Gilchuk IM, et al. Structural Basis of Protection against H7N9 Influenza Virus by Human Anti-N9 Neuraminidase Antibodies. *Cell Host & Microbe*. 2019;26(6):729-38. doi: <https://doi.org/10.1016/j.chom.2019.10.002>.
31. Rijal P, Wang BB, Tan TK, Schimanski L, Janesch P, Dong T, et al. Broadly Inhibiting Antineuraminidase Monoclonal Antibodies Induced by Trivalent Influenza Vaccine and H7N9 Infection in Humans. *Journal of Virology*. 2020;94(4):e01182-19. doi: 10.1128/JVI.01182-19.

32. Stadlbauer D, Zhu X, McMahon M, Turner JS, Wohlbold TJ, Schmitz AJ, et al. Broadly protective human antibodies that target the active site of influenza virus neuraminidase. *Science*. 2019;366(6464):499. doi: 10.1126/science.aay0678.
33. Monto AS, Petrie JG, Cross RT, Johnson E, Liu M, Zhong W, et al. Antibody to Influenza Virus Neuraminidase: An Independent Correlate of Protection. *The Journal of Infectious Diseases*. 2015;212(8):1191-9. doi: 10.1093/infdis/jiv195.
34. Krammer F, Fouchier RAM, Eichelberger MC, Webby RJ, Shaw-Saliba K, Wan H, et al. NAction! How Can Neuraminidase-Based Immunity Contribute to Better Influenza Virus Vaccines? *mBio*. 2018;9(2):e02332-17. doi: 10.1128/mBio.02332-17.
35. Li Y, Bostick DL, Sullivan CB, Myers JL, Griesemer SB, StGeorge K, et al. Single Hemagglutinin Mutations That Alter both Antigenicity and Receptor Binding Avidity Influence Influenza Virus Antigenic Clustering. *Journal of Virology*. 2013;87(17):9904. doi: 10.1128/JVI.01023-13.
36. Hensley SE, Das SR, Bailey AL, Schmidt LM, Hickman HD, Jayaraman A, et al. Hemagglutinin Receptor Binding Avidity Drives Influenza A Virus Antigenic Drift. *Science*. 2009;326(5953):734. doi: 10.1126/science.1178258.
37. Gao J, Couzens L, Burke DF, Wan H, Wilson P, Memoli MJ, et al. Antigenic Drift of the Influenza A(H1N1)pdm09 Virus Neuraminidase Results in Reduced Effectiveness of A/California/7/2009 (H1N1pdm09)-Specific Antibodies. *mBio*. 2019;10(2):e00307-19. doi: 10.1128/mBio.00307-19.
38. Yasuhara A, Yamayoshi S, Kiso M, Sakai-Tagawa Y, Koga M, Adachi E, et al. Antigenic drift originating from changes to the lateral surface of the neuraminidase head of influenza A virus. *Nature Microbiology*. 2019;4(6):1024-34. doi: 10.1038/s41564-019-0401-1.
39. Jiang L, Fantoni G, Couzens L, Gao J, Plant E, Ye Z, et al. Comparative Efficacy of Monoclonal Antibodies That Bind to Different Epitopes of the 2009 Pandemic H1N1 Influenza Virus Neuraminidase. *Journal of virology*. 2015;90(1):117-28. doi: 10.1128/JVI.01756-15. PubMed PMID: 26468531.
40. Wan H, Yang H, Shore DA, Garten RJ, Couzens L, Gao J, et al. Structural characterization of a protective epitope spanning A(H1N1)pdm09 influenza virus neuraminidase monomers. *Nat Commun*. 2015;6:6114. doi: 10.1038/ncomms7114. PubMed PMID: 25668439.
41. Job ER, Schotsaert M, Ibañez LI, Smet A, Ysenbaert T, Roose K, et al. Antibodies Directed toward Neuraminidase N1 Control Disease in a Mouse Model of Influenza. *Journal of Virology*. 2018;92(4):e01584-17. doi: 10.1128/JVI.01584-17.
42. Broszeit F, Tzarum N, Zhu X, Nemanichvili N, Eggink D, Leenders T, et al. N-Glycolylneuraminic Acid as a Receptor for Influenza A Viruses. *Cell Rep*. 2019;27(11):3284-94. doi: 10.1016/j.celrep.2019.05.048. PubMed PMID: 31189111.
43. Dai M, Guo H, Dortmans JCFM, Dekkers J, Nordholm J, Daniels R, et al. Identification of Residues That Affect Oligomerization and/or Enzymatic Activity of Influenza Virus H5N1 Neuraminidase Proteins. *Journal of virology*. 2016;90(20):9457-70. doi: 10.1128/JVI.01346-16. PubMed PMID: 27512075.
44. Lambré CR, Terzidis H, Greffard A, Webster RG. An enzyme-linked lectin assay for sialidase. *Clinica Chimica Acta*. 1991;198(3):183-93. doi: [https://doi.org/10.1016/0009-8981\(91\)90352-D](https://doi.org/10.1016/0009-8981(91)90352-D).
45. Butler J, Hooper KA, Petrie S, Lee R, Maurer-Stroh S, Reh L, et al. Estimating the fitness advantage conferred by permissive neuraminidase mutations in recent oseltamivir-resistant A(H1N1)pdm09 influenza viruses. *PLoS pathogens*. 2014;10(4):e1004065. doi: 10.1371/journal.ppat.1004065. PubMed PMID: 24699865.
46. Couzens L, Gao J, Westgeest K, Sandbulte M, Lugovtsev V, Fouchier R, et al. An optimized enzyme-linked lectin assay to measure influenza A virus neuraminidase inhibition antibody titers in human sera. *Journal of Virological Methods*. 2014;210:7-14. doi: <https://doi.org/10.1016/j.jviromet.2014.09.003>.
47. Smith DJ, Lapedes AS, de Jong JC, Bestebroer TM, Rimmelzwaan GF, Osterhaus ADME, et al. Mapping the Antigenic and Genetic Evolution of Influenza Virus. *Science*. 2004;305(5682):371. doi: 10.1126/science.1097211.

48. Fodor E, Devenish L, Engelhardt OG, Palese P, Brownlee GG, García-Sastre A. Rescue of Influenza A Virus from Recombinant DNA. *Journal of Virology*. 1999;73(11):9679.
49. Guo H, Rabouw H, Slomp A, Dai M, van der Vegt F, van Lent JWM, et al. Kinetic analysis of the influenza A virus HA/NA balance reveals contribution of NA to virus-receptor binding and NA-dependent rolling on receptor-containing surfaces. *PLOS Pathogens*. 2018;14(8):e1007233. doi: 10.1371/journal.ppat.1007233.
50. Xu X, Zhu X, Dwek RA, Stevens J, Wilson IA. Structural characterization of the 1918 influenza virus H1N1 neuraminidase. *Journal of virology*. 2008;82(21):10493-501. Epub 2008/08/20. doi: 10.1128/JVI.00959-08. PubMed PMID: 18715929.
51. Wang H, Dou D, Östbye H, Revol R, Daniels R. Structural restrictions for influenza neuraminidase activity promote adaptation and diversification. *Nature Microbiology*. 2019;4(12):2565-77. doi: 10.1038/s41564-019-0537-z.
52. Petterson S-O, Sivertsson R, Sjögren S, Svennerholm L. The sialic acids of hog pancreas. *Biochimica et Biophysica Acta*. 1958;28:444-5. doi: [https://doi.org/10.1016/0006-3002\(58\)90498-0](https://doi.org/10.1016/0006-3002(58)90498-0).
53. Suzuki T, Takahashi T, Guo C-T, Hidari KIPJ, Miyamoto D, Goto H, et al. Sialidase Activity of Influenza A Virus in an Endocytic Pathway Enhances Viral Replication. *Journal of Virology*. 2005;79(18):11705. doi: 10.1128/JVI.79.18.11705-11715.2005.
54. Takahashi T, Suzuki T. Low-pH Stability of Influenza A Virus Sialidase Contributing to Virus Replication and Pandemic. *Biological and Pharmaceutical Bulletin*. 2015;38(6):817-26. doi: 10.1248/bpb.b15-00120.
55. Chong AKJ, Pegg MS, von Itzstein M. Influenza virus sialidase: effect of calcium on steady-state kinetic parameters. *Biochimica et Biophysica Acta (BBA) - Protein Structure and Molecular Enzymology*. 1991;1077(1):65-71. doi: [https://doi.org/10.1016/0167-4838\(91\)90526-6](https://doi.org/10.1016/0167-4838(91)90526-6).
56. Burmeister WP, Cusack S, Ruigrok RWH. Calcium is needed for the thermostability of influenza B virus neuraminidase. *Journal of General Virology*. 1994;75(2):381-8. doi: <https://doi.org/10.1099/0022-1317-75-2-381>.
57. Smith BJ, Huyton T, Joosten RP, McKimm-Breschkin JL, Zhang J-G, Luo CS, et al. Structure of a calcium-deficient form of influenza virus neuraminidase: implications for substrate binding. *Acta Crystallographica Section D*. 2006;62(9):947-52. doi: doi:10.1107/S0907444906020063.
58. Baenziger JU, Fiete D. Structure of the complex oligosaccharides of fetuin. *Journal of Biological Chemistry*. 1979;254(3):789-95.
59. Studies on glycoconjugates. LXIV. Complete structure of two carbohydrate units of human serotransferrin. *FEBS Letters*. 1975;50(3):296-9. doi: 10.1016/0014-5793(75)90053-8.
60. von Bonsdorff L, Tölö H, Lindeberg E, Nyman T, Harju A, Parkkinen J. Development of a Pharmaceutical Apotransferrin Product for Iron Binding Therapy. *Biologicals*. 2001;29(1):27-37. doi: <https://doi.org/10.1006/biol.2001.0273>.
61. Wu AM, Wu JH, Tsai M-S, Yang Z, Sharon N, Herp A. Differential affinities of Erythrina cristagalli lectin (ECL) toward monosaccharides and polyvalent mammalian structural units. *Glycoconjugate Journal*. 2007;24(9):591-604. doi: 10.1007/s10719-007-9063-y.
62. Geisler C, Jarvis DL. Letter to the Glyco-Forum: Effective glycoanalysis with Maackia amurensis lectins requires a clear understanding of their binding specificities. *Glycobiology*. 2011;21(8):988-93. doi: 10.1093/glycob/cwr080.
63. Shibuya N, Goldstein IJ, Broekaert WF, Nsimba-Lubaki M, Peeters B, Peumans WJ. The elderberry (*Sambucus nigra* L.) bark lectin recognizes the Neu5Ac(alpha 2-6)Gal/GalNAc sequence. *Journal of Biological Chemistry*. 1987;262(4):1596-601.
64. de Vries RP, de Vries E, Martínez-Romero C, McBride R, van Kuppeveld FJ, Rottier PJM, et al. Evolution of the hemagglutinin protein of the new pandemic H1N1 influenza virus: maintaining optimal receptor binding by compensatory substitutions. *Journal of virology*. 2013;87(24):13868-77. Epub 2013/10/09. doi: 10.1128/JVI.01955-13. PubMed PMID: 24109242.
65. Sung JC, Van Wynsberghe AW, Amaro RE, Li WW, McCammon JA. Role of secondary sialic acid binding sites in influenza N1 neuraminidase. *J Am Chem Soc*. 2010;132(9):2883-5. doi: 10.1021/ja9073672. PubMed PMID: 20155919.



66. de Vries RP, de Vries E, Moore KS, Rigter A, Rottier PJM, de Haan CAM. Only two residues are responsible for the dramatic difference in receptor binding between swine and new pandemic H1 hemagglutinin. *J Biol Chem*. 2011;286(7):5868-75. Epub 2010/12/20. doi: 10.1074/jbc.M110.193557. PubMed PMID: 21173148.
67. Baigent SJ, McCauley JW. Glycosylation of haemagglutinin and stalk-length of neuraminidase combine to regulate the growth of avian influenza viruses in tissue culture. *Virus Research*. 2001;79(1):177-85. doi: [https://doi.org/10.1016/S0168-1702\(01\)00272-6](https://doi.org/10.1016/S0168-1702(01)00272-6).
68. Wan H, Gao J, Xu K, Chen H, Couzens LK, Rivers KH, et al. Molecular basis for broad neuraminidase immunity: conserved epitopes in seasonal and pandemic H1N1 as well as H5N1 influenza viruses. *Journal of virology*. 2013;87(16):9290-300. Epub 2013/06/19. doi: 10.1128/JVI.01203-13. PubMed PMID: 23785204.
69. Malby RL, Tulip WR, Harley VR, McKimm-Breschkin JL, Laver WG, Webster RG, et al. The structure of a complex between the NC10 antibody and influenza virus neuraminidase and comparison with the overlapping binding site of the NC41 antibody. *Structure*. 1994;2(8):733-46. doi: [https://doi.org/10.1016/S0969-2126\(00\)00074-5](https://doi.org/10.1016/S0969-2126(00)00074-5).
70. Tulip WR, Varghese JN, Laver WG, Webster RG, Colman PM. Refined crystal structure of the influenza virus N9 neuraminidase-NC41 Fab complex. *Journal of Molecular Biology*. 1992;227(1):122-48. doi: [https://doi.org/10.1016/0022-2836\(92\)90687-F](https://doi.org/10.1016/0022-2836(92)90687-F).

Supplementary Figures

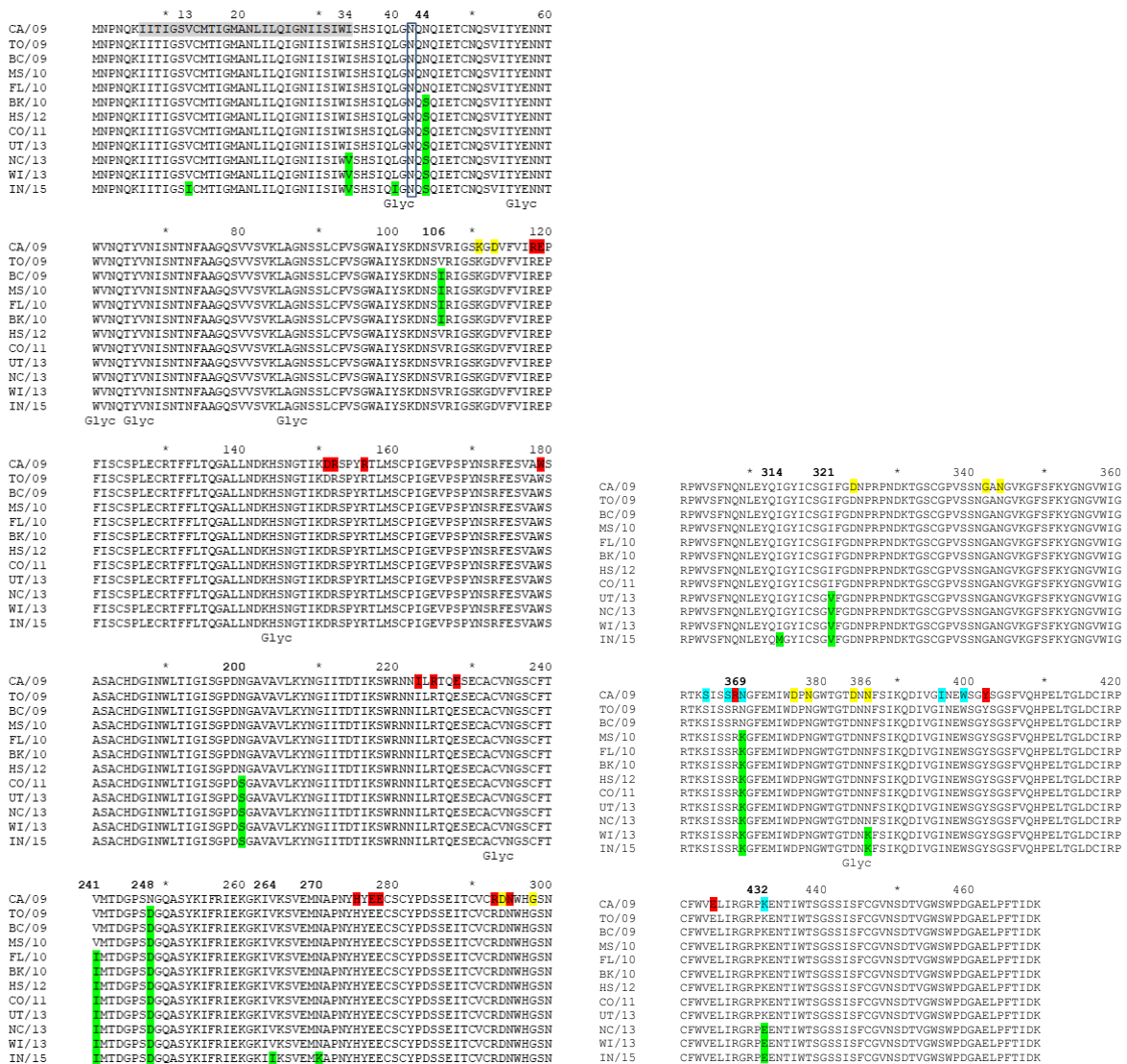


**Fig S1. Alignment of NA of npH1N1.** Alignment of the N1 proteins analyzed in this study. Differences between the different proteins are highlighted in green. Active site residues (including both residues that have direct interaction with the substrate and framework residues that stabilize the catalytic site) are indicated in red (1). Residues that form the Ca<sup>2+</sup> binding sites (site 1: positions 111 and 113, site 2: positions 293, 297, 324, 345 and 347, site 3: positions 376, 379, 384, and 386) are indicated in yellow (2). Residues corresponding to residues in the N9 protein that have direct interaction with SIA in the 2nd SIA-binding site are in highlighted in blue (3). The transmembrane domain is indicated in grey, while N-glycosylation sites are indicated by “Glyc”. NA starting residue of the recombinant soluble NA proteins is indicated by the blue rectangle (N42).

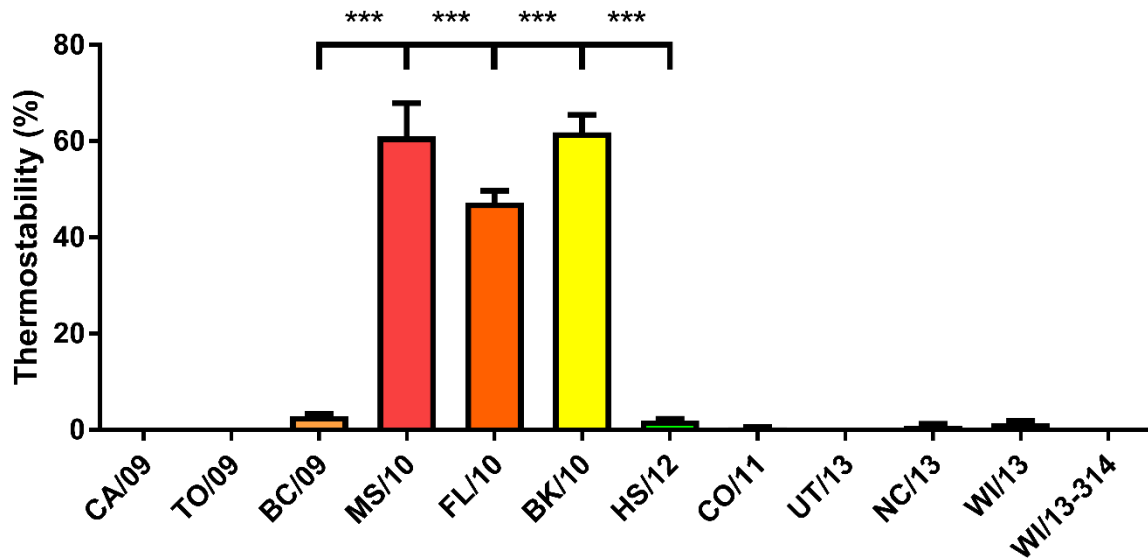


**Fig S2.  $Ca^{2+}$ -dependent thermostability of H1N1pdm09 NAs.**  $Ca^{2+}$ -dependent thermostability was analyzed by determining the NA activity using the MUNANA assay after heating NA samples for 5 min at 50°C in buffer lacking  $Ca^{2+}$  and containing EDTA. Values are graphed relative to unheated controls. Representative experiments performed in triplicate are shown. For each NA protein, significant differences relative to its precursor protein are indicated (\* $P < 0.05$ ; \*\* $P < 0.01$ ; \*\*\* $P < 0.001$ ).

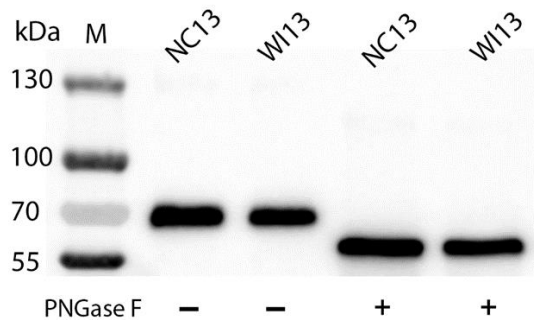


**Fig S3. N-glycosylation of H1N1pdm09 NAs.** (A) Recombinant soluble NC/13 and WI/13 proteins expressed in HEK293S GnT1(-) were analyzed by gel electrophoresis followed by Western blotting using an antibody against the Strep tag (StrepMabClassic-HRP [IBA]). NC/13 and WI/13 run at a similar position in the gel before and after PNGase F treatment, which removes N-glycans, indicating that N386 residue is not modified by the addition of a N-glycan in NC/13. The position on the gel of the relevant molecular weight markers is shown on the left side of the gels.

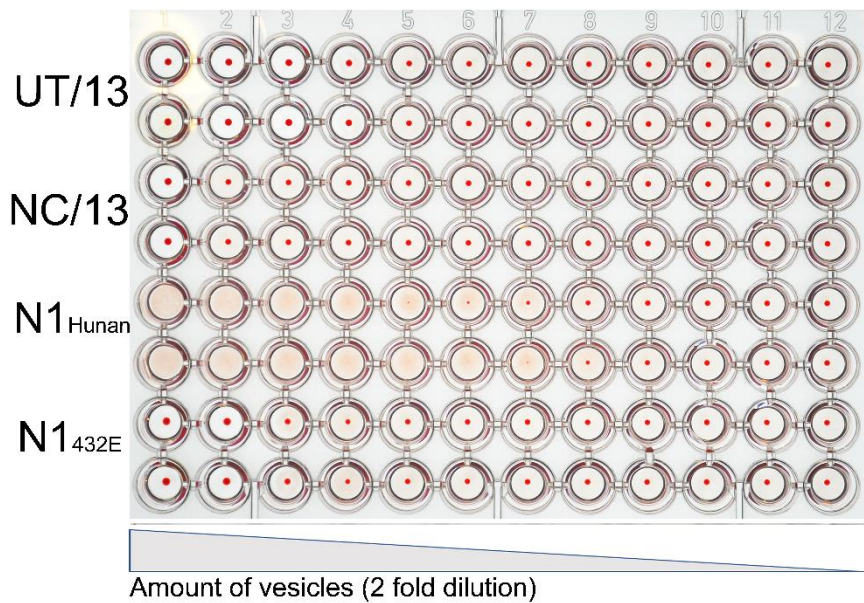


**Fig S4. Hemagglutination assay of NA membrane vesicles.** Hemagglutination assays were performed with membrane vesicles containing similar amounts of either the indicated H1N1pdm09 NAs or NAs (N1<sub>Hunan</sub> and N1<sub>432E</sub>) from H5N1 viruses [14] similarly as described previously [13]. The N1 proteins from H5N1 viruses serve as positive and negative controls [12]. Two fold serial dilutions of the vesicles were incubated with equal volumes of 0.5% human erythrocytes at 4°C for 2 h in the presence of OC. Red dots at the bottom of the wells indicate absence of hemagglutination. A representative experiment (out of three performed) is shown.

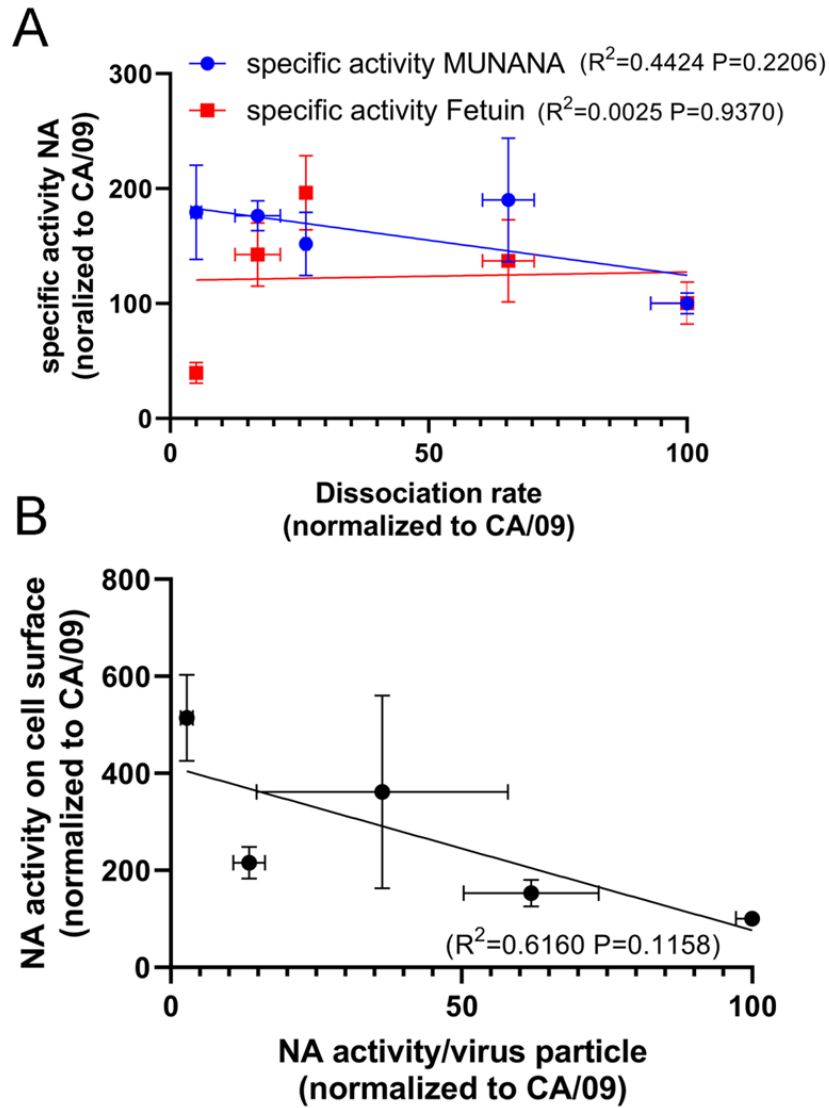


**Fig S5. Correlation between NA activities of proteins and viruses.** A) Correlation between specific activities of NA as determined using MUNANA (Fig 3A) or ELLA (Fig 4A; Fetuin-ECA combination) and virus self-elution (Fig 6B). B) Correlation between NA activity on the cell surface (Fig 6E) and NA activity per virus particle (Fig 6C).

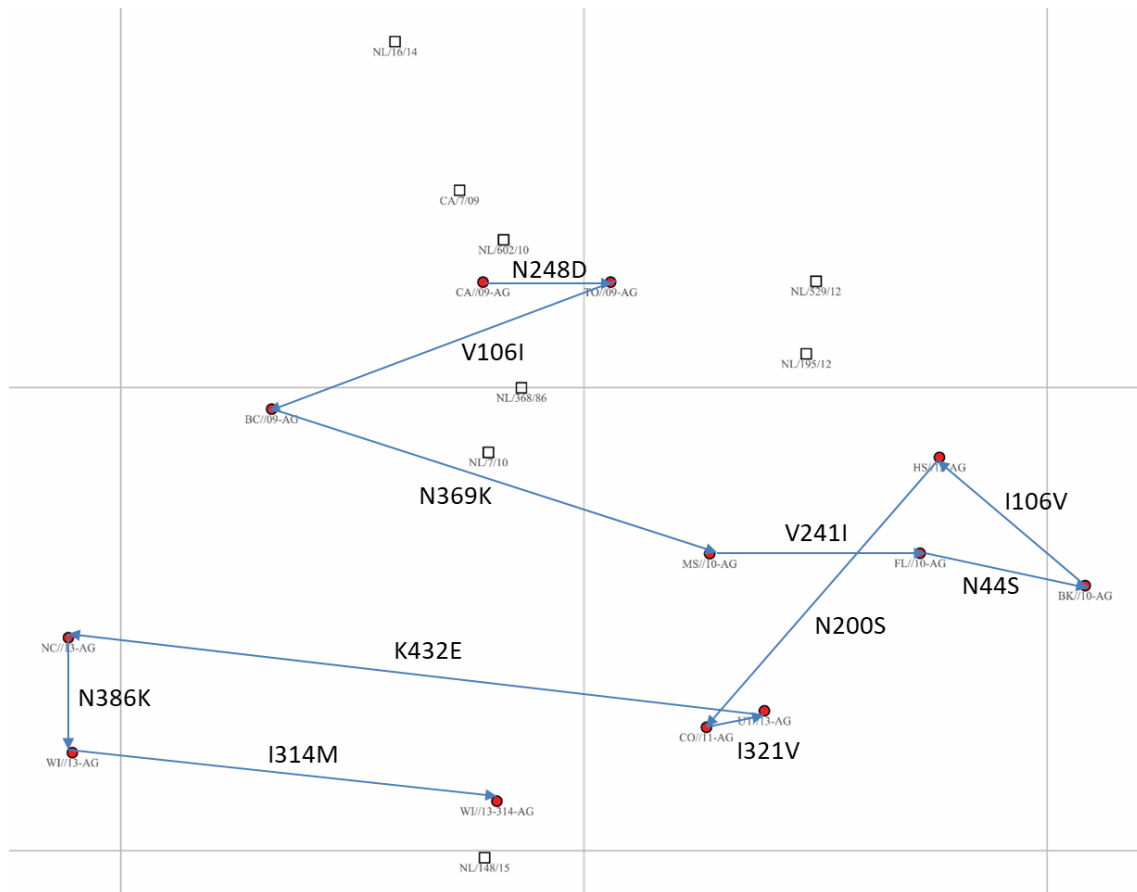


**Fig S6. H1N1pdm09 NA antigenic map.** Inhibition of NA activity of recombinant NA proteins by the ferret sera was measured by ELLA (S1 Table). The antigenic relatedness was calculated [47] using mean titers of 2-3 experiments performed in duplicate/triplicate. Distances between proteins (red dots) and sera (rectangles) in the map correlated well with the respective raw ELLA NI titers ( $R^2=0,8671$ ), indicating that the 2D map is a good representation of the data and can be used to extrapolate antigenic distances between the NAs. Antigenic distances between NAs shown in Fig. 7 were determined by measuring distances between NAs on the 2D map. Antigenic distances obtained with recombinant NA proteins appear smaller than those obtained with virus preparations [37]. Substitutions in NA relative to the precursor protein (Table 1) are indicated, arrows indicate the evolutionary track according to the phylogenetic tree shown in Fig. 1.

S1 Table NA inhibition titer determined by ELLA

Antigen <sup>a</sup>	Ferret sera raised against <sup>b</sup>							
	A/NL/386/86	A/CA/007/09	A/NL/602/09	A/NL/007/10	A/NL/195/12	A/NL/529/12	A/NL/016/14	A/NL/148/15
CA/09	7,78 <sup>c</sup>	8,44	8,00	8,00	8,90	8,69	8,92	7,08
TO/09	7,55	8,12	7,97	7,64	9,19	9,66	8,81	7,22
BC/09	7,27	7,85	7,12	7,69	8,18	8,58	7,90	6,78
MS/10	7,76	7,35	7,13	7,41	8,79	8,86	7,38	7,14
FL/10	7,07	7,14	7,00	7,24	8,73	8,87	7,08	6,77
BK/10	6,60	6,90	6,52	6,85	8,48	8,71	6,84	6,61
HS/12	6,67	7,13	6,88	7,17	9,24	9,38	7,13	6,98
CO/11	7,04	7,13	6,78	7,35	8,55	8,71	7,08	7,72
UT/13	6,86	7,07	6,84	7,16	8,58	8,86	7,21	7,66
NC/13	7,09	7,09	7,04	7,36	7,12	7,52	7,18	7,12
WI/13	6,66	6,86	6,71	6,96	7,25	7,65	7,25	7,33
WI/13-314	6,39	7,25	6,52	7,42	8,03	8,62	7,64	8,19





## **Interlude**

**Tuning influenza A virus HA-NA balance to the receptor repertoire**

---

The hemagglutinin (HA) - neuraminidase (NA) balance of influenza A virus (IAV) is important for virus replication and transmission and probably is an important host tropism determinant that needs to be adapted to the sialoglycan repertoire of a specific host species. An optimally tuned HA-NA balance should sustain efficient cell entry and release as well as virus mobility through the heavily sialylated mucus layer. The development of novel assays to assess the kinetics of virus binding and release, such as biolayer interferometry [1] and live imaging [2], allows a more detailed analysis of this balance in relation to (decoy) receptors. In this thesis the HA-NA balance was particularly studied using biolayer interferometry using synthetic glycans and a limited number of glycoproteins. It will be of interest to perform these analyses with an extended repertoire of (decoy) receptors, including mucus preparations, to firmly establish the importance of the HA-NA balance in relation to host tropism. The HA-NA-receptor balance and its importance for virion mobility is discussed in detail in **chapter 6**.

HA-NA balance and virion mobility are likely affected by virion morphology and the distribution of HA and NA on these particles. Lab strains generally have a spherical or slightly elongated appearance while very long filaments are often observed for clinical isolates [3]. We did not take differences in virion morphology into account when evaluating the HA-NA balance of virus particles. Analysis of the importance of filamentous morphology is complicated when using clinical isolates as these usually contain both types of particles, which are difficult to separate. In addition, filamentous particles are very unstable and easily damaged by freeze thawing [4]. Nevertheless, filamentous morphology in combination with NA being localized to the virion poles was shown to be important for directionality of virion mobility on/through mucus by performing single particle analysis [5].

The HA-NA balance needs to be adjusted upon a host tropism change, to adapt to the novel host sialome, but also when mutations accumulate in HA and/or NA as a result of antigenic drift, which may affect the functionality of these proteins. Antigenic drift of HA is predominantly associated with mutations in or close to the receptor-binding site of HA, which may affect receptor-binding properties in HA [6, 7]. Other mutations in the HA genome segment that are expected to affect the HA-NA balance include mutations that affect RNA and protein expression levels, glycosylation, folding, trimerization, intracellular transport and incorporation of HA in virus particles.

The HA-NA balance can obviously also be affected by alterations in NA. These may include mutations in the catalytic site of NA. The catalytic site of NA is, however, highly conserved among all IAV subtypes. Mutations in the NA catalytic site, which negatively affect catalytic activity, are only associated with the development of resistance against NA inhibitors [8, 9]. Deletions in the NA stalk domain are also known to affect the HA-NA balance. A shortened NA stalk resulting in reduced NA activity in virus particles, is often observed in viruses adapted to replication in chickens [10, 11]. Mutations in the NA

genome segment that affect expression, glycosylation, folding, oligomerization [12], intracellular transport, Ca<sup>2+</sup> binding and virion incorporation (**chapter 5**) of this protein may also affect the HA-NA balance. Finally, the HA-NA balance can also be affected by mutations in the second sialic acid-binding site (2SBS) in NA as is shown in **chapters 2-5** and discussed in detail in **chapter 7**.

## Reference

1. Guo H, Rabouw H, Slomp A, Dai M, van der Vegt F, van Lent JWM, et al. Kinetic analysis of the influenza A virus HA/NA balance reveals contribution of NA to virus-receptor binding and NA-dependent rolling on receptor-containing surfaces. *PLoS Pathog.* 2018;14(8):e1007233-e. doi: 10.1371/journal.ppat.1007233. PubMed PMID: 30102740.
2. Sakai T, Nishimura SI, Naito T, Saito M. Influenza A virus hemagglutinin and neuraminidase act as novel motile machinery. *Scientific Reports.* 2017;7(1):45043. doi: 10.1038/srep45043.
3. Dadonaite B, Vijaykrishnan S, Fodor E, Bhella D, Hutchinson EC. Filamentous influenza viruses. *Journal of General Virology.* 2016;97(8):1755-64. doi: <https://doi.org/10.1099/jgv.0.000535>.
4. Hirst JC, Hutchinson EC. Single-particle measurements of filamentous influenza virions reveal damage induced by freezing. *J Gen Virol.* 2019;100(12):1631-40. doi: 10.1099/jgv.0.001330. PubMed PMID: 31553305.
5. Vahey MD, Fletcher DA. Influenza A virus surface proteins are organized to help penetrate host mucus. *Elife.* 2019;8:e43764. doi: 10.7554/eLife.43764. PubMed PMID: 31084711.
6. Koel BF, Burke DF, Bestebroer TM, van der Vliet S, Zondag GCM, Vervaet G, et al. Substitutions Near the Receptor Binding Site Determine Major Antigenic Change During Influenza Virus Evolution. *Science.* 2013;342(6161):976-9. doi: 10.1126/science.1244730.
7. Hensley SE, Das SR, Bailey AL, Schmidt LM, Hickman HD, Jayaraman A, et al. Hemagglutinin Receptor Binding Avidity Drives Influenza A Virus Antigenic Drift. *Science.* 2009;326(5953):734. doi: 10.1126/science.1178258.
8. Tamura D, DeBiasi RL, Okomo-Adhiambo M, Mishin VP, Campbell AP, Loechelt B, et al. Emergence of Multidrug-Resistant Influenza A(H1N1)pdm09 Virus Variants in an Immunocompromised Child Treated With Oseltamivir and Zanamivir. *The Journal of Infectious Diseases.* 2015;212(8):1209-13. doi: 10.1093/infdis/jiv245.
9. Gulati S, Smith DF, Air GM. Deletions of neuraminidase and resistance to oseltamivir may be a consequence of restricted receptor specificity in recent H3N2 influenza viruses. *Virol J.* 2009;6:22-. doi: 10.1186/1743-422X-6-22. PubMed PMID: 19216793.
10. Li J, Dohna Hz, Cardona CJ, Miller J, Carpenter TE. Emergence and Genetic Variation of Neuraminidase Stalk Deletions in Avian Influenza Viruses. *PLOS ONE.* 2011;6(2):e14722. doi: 10.1371/journal.pone.0014722.
11. Long JS, Benfield CT, Barclay WS. One-way trip: Influenza virus' adaptation to gallinaceous poultry may limit its pandemic potential. *BioEssays.* 2015;37(2):204-12. doi: 10.1002/bies.201400133.
12. da Silva DV, Nordholm J, Madjo U, Pfeiffer A, Daniels R. Assembly of subtype 1 influenza neuraminidase is driven by both the transmembrane and head domains. *J Biol Chem.* 2013;288(1):644-53. Epub 11/13. doi: 10.1074/jbc.M112.424150. PubMed PMID: 23150659.



## Chapter 6

# Influenza A virus hemagglutinin–neuraminidase–receptor balance: preserving virus motility

Erik de Vries<sup>1</sup>, Wenjuan Du<sup>1</sup>, Hongbo Guo<sup>1</sup>, Cornelis A.M. de Haan<sup>1</sup>

<sup>1</sup> Virology Division, Department of Infectious Diseases and Immunology, Faculty of Veterinary Medicine, Utrecht, University, Yalelaan 1, 3584 CL Utrecht, the Netherlands

## **Abstract**

Influenza A viruses (IAVs) occasionally cross the species barrier and adapt to novel host species. This requires readjustment of the functional balance of the sialic acid receptor-binding hemagglutinin (HA) and the receptor-destroying neuraminidase (NA) to the sialoglycan-receptor repertoire of the new host. Novel techniques have revealed mechanistic details of this HA–NA–receptor balance, emphasizing a previously underappreciated crucial role for NA in driving the motility of receptor-associated IAV particles. Motility enables virion penetration of the sialylated mucus layer as well as attachment to, and uptake into, underlying epithelial cells. As IAVs are essentially irreversibly bound in the absence of NA activity, the fine-tuning of the HA–NA–receptor balance rather than the binding avidity of IAV particles *per se* is an important factor in determining host species tropism.

### Receptor binding of Influenza A Virus

Influenza A viruses (IAVs) infect birds and mammals. Aquatic birds constitute the natural host reservoir of IAVs. Occasionally, these enveloped, negative-strand RNA viruses (Fig. 1) cross the host species barrier and become established as viruses of humans or other mammals (e.g. porcine, equine and canines). Their host tropism is determined by an interplay between different viral proteins and host factors that is crucial for efficient replication and transmission within a species. Host tropism switches require adaptation of IAV proteins to host factors of the novel host species. The IAV envelope carries trimeric hemagglutinin (HA) that binds to sialic acid (SIA) receptors and its functional antagonist, the tetrameric receptor-destroying neuraminidase (NA) (Fig. 1 and 2). 18 HA (H1-18) and 11 NA (N1-11) subtypes have been identified [1, 2]. All combinations of H1-16 and N1-9 have been found in wild waterfowl IAVs [3]. Currently, H1N1 and H3N2 viruses are circulating in the human population. The question is not if, but when a new animal IAV will manage to breach the host range barrier and cause the next influenza pandemic.

The receptor-binding properties of HA, a well-established host tropism determinant, need to change in order for an avian virus to evolve into a human virus. Avian viruses prefer binding to SIAs attached to cell-surface associated glycan chains via an  $\alpha$ 2,3-linkage, while human viruses preferentially bind  $\alpha$ 2,6-linked sialic acids [4, 5]. A switch from  $\alpha$ 2,3 to  $\alpha$ 2,6 binding specificity requires several mutations in HA [6-8]. However, the situation is a little more complex. HA proteins do not bind with similar affinity to every sialoside containing appropriately linked SIAs. Internal sugars and their linkages also affect the HA-receptor binding specificity [9, 10]. Also, the  $\alpha$ 2,6/ $\alpha$ 2,3 dichotomy is not absolute. Several H1N1 [11,12] and H3N2 [13] human viruses have been reported to also bind avian-type  $\alpha$ 2,3 receptors whereas avian IAVs of several genotypes bind to  $\alpha$ 2,6 receptors [14-17], although none of the latter have (yet) breached the host range barrier. Once established as a human virus, the receptor binding properties further evolve with time presumably in conjunction with antigenic drift [18] that predominantly occurs at positions surrounding the receptor binding site [19, 20]. As a consequence, successful human IAVs can acquire rather different HA binding properties [13, 21, 22]. Considering the functional antagonism of HA and NA, it seems likely that not the receptor binding properties of HA alone determine host tropism, but that the activities of HA and NA need to be well balanced in relation to the host receptor repertoire for optimal viral fitness. Novel developments with respect to this HA-NA-receptor balance are the main focus of this review [for previous reviews on this topic see 23-27].

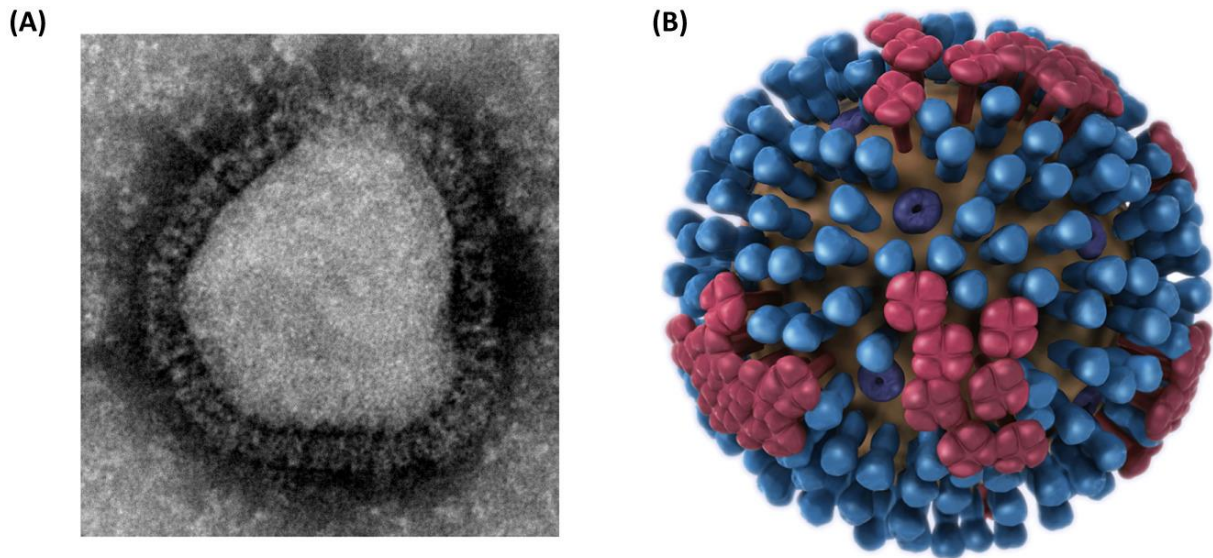


**Figure 1. IAV particle.** A) Electron micrograph of negatively-stained A/Netherlands/602/2009 (H1N1) virus particle (picture kindly provided by Jan van Lent, Laboratory of Virology, Wageningen University and Research). The virion has a diameter of approximately 100 nm. B) Graphical representation of a generic IAV particle (Centre for Disease Control and Prevention, National Centre for Immunization and Respiratory Diseases). HA trimers are shown in blue, NA tetramers in red and M2 ion channels in purple. The lipid envelope has a brownish colour. Virions display more HA trimers than NA tetramers. NA tetramers may be evenly distributed on the virion surface or be present in a patch-like distribution [88, 89, 128].

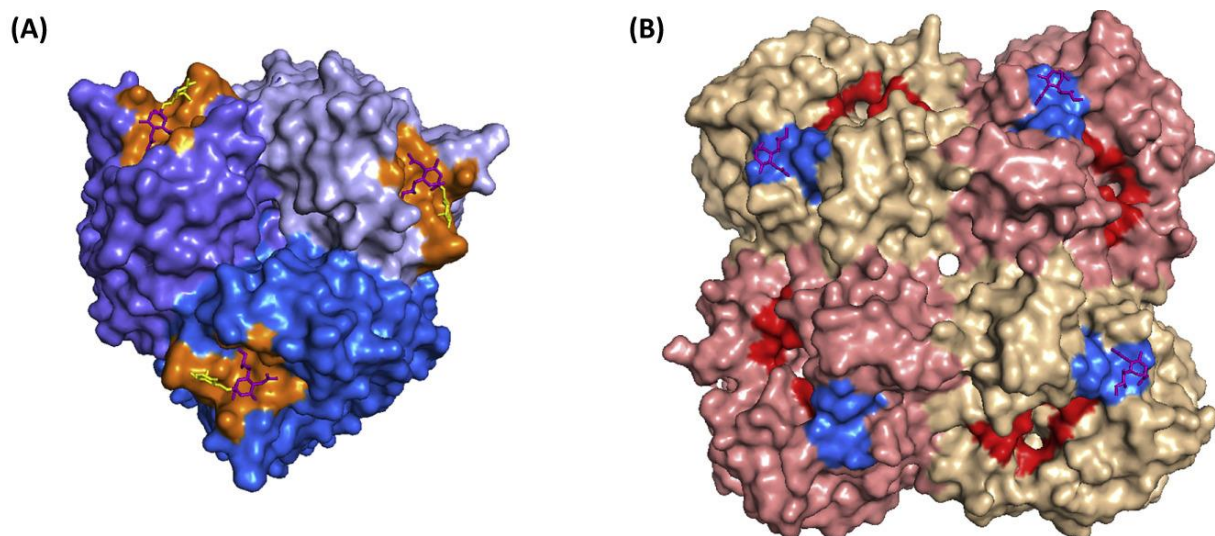




**Figure 2. Structure of HA and NA.** A) Top view of a HA trimer (H3; PDB 6BKM, [129]) in a surface representation. The receptor binding site is coloured orange. The SIA and galactose residues in the receptor binding sites are shown in a stick representation coloured purple and yellow, respectively. B) Top view of a NA tetramer (N2; PDB 4H53, [130]) in a surface representation. The SIA contact residues in the catalytic site and 2<sup>nd</sup> SIA-binding site (2SBS) in each protomer are coloured red and blue, respectively. SIA residues in the 2SBS are shown in a stick representation (purple).

### HA-NA-Receptor Balance

We define the HA-NA balance as the balance between the activities of HA and NA on the full, highly diverse, spectrum of functional and decoy receptors present on cells and mucus. Multivalent IAV-receptor binding by low affinity interactions of several HA trimers with sialosides [28, 29] enables a dynamic binding mode. Individual HA-SIA interactions ( $K_D \sim 1\text{-}20\text{ mM}$ ) [30, 31] are rapidly formed and broken without causing dissociation of the virus but providing access of NA to temporarily free SIAs. Sialidase activity by NA results in reduced SIA-receptor density which drives virus movement, as first demonstrated by microscopy [32], and ultimately causes dissociation [33, 34]. Functionally balanced HA and NA activities are traditionally considered to be important for efficient release of newly assembled virus particles [35, 36]. They are also essential, however, in enabling virus penetration of the heavily sialylated mucus layer overlaying the epithelial cells (Fig. 3), and in supporting virus interactions with host cell receptors that result in endocytic uptake (Fig. 4) as is described in more detail below.

The HA-NA balance is likely tuned to the receptor repertoire IAV encounters in a specific host species. Cells expose a dense layer of sialylated glycans attached to proteins and lipids (Fig. 3). Whether binding to specific sialoglycoproteins or -lipids is required for endocytic uptake and infection is not known. IAVs appear to preferentially bind to N-linked glycans on proteins [37] but these are not absolutely essential for host cell entry in vitro [38]. Functional receptors that are required for cell entry may be restricted to specific sialoglycan chains, as well as the proteins or lipids to which they are attached. For example, the voltage-dependent  $\text{Ca}^{2+}$  channel Cav1.2 was proposed as an IAV entry receptor [39]. IAV entry was inhibited by  $\text{Ca}^{2+}$  channel blockers, however, knockdown of Cav1.2 decreased the number of IAV-infected cells only two-fold. Other specific membrane proteins of which the specific sialylation state affected IAV entry have been described including fibronectin [40] and PDGF- $\beta$  [41]. It can also not be excluded that cells present decoy receptors that will have a negative effect on endocytic uptake although no such molecules have been described so far. The sialoside-rich mucus layer definitely acts as a decoy for IAV. The soluble mucins herein are elongated proteins (longer than 100 nm with an average radius of gyration of  $\sim 150\text{ nm}$ ;) [42], densely covered with short O-glycans forming a gel-like barrier to diverse pathogens (Fig. 3;

reviewed in [43]). Mucus also contains large numbers of potentially sialylated exosomes that may function as a decoy [44]. Thus, the sialoglycan repertoire of a host has a complex constitution and distribution of decoy and functional receptors. It varies between species [45-48] and therefore a species-specific HA-NA balance is potentially restricting crossing of the species-barrier by IAV.

The restoration of a functional HA-NA-receptor balance by the selection of mutations in either HA or NA in response to an inhibitory decoy receptor was first shown 36 years ago [49]. Since then the reassortment of HA and NA genome segments from different viruses has frequently been shown to attenuate the resulting viruses. Acquisition of mutations in HA or NA after reassortment [50-51] or upon an otherwise disturbed balance [52-55] has been shown to restore fitness and the requirement of a functional HA-NA-receptor balance is widely accepted now [reviewed in 23-27]. At the molecular level this HA-NA-receptor balance is, however, not well established. This is in part due to a biased focus on HA, but mainly because suitable assays for directly assessing the dynamics of virion-receptor interactions in presence of NA activity are lacking. Studies using recombinant HA and NA proteins and monovalently-displayed substrates are informative but HA binding and NA sialidase activity inevitably occur at the multivalent configuration encountered at the virus-cell interface. Receptor-binding and sialidase-activity properties should therefore also be studied in the context of virus particles. Recently developed assays using biolayer interferometry (BLI) [33, 56-58] or fluorescence imaging microscopy [32, 59] allowed direct analysis of the dynamics of virus-receptor interactions. Initial interactions of virus particles with a receptor-coated surface are often short lived [59], presumably because they are driven by 1-2 HA-SIA binding events, each of which is rapidly formed and broken resulting from its very low affinity ( $K_D \sim 1-20$  mM). However, absence of NA activity also enabled virtually irreversible binding, as a result of multivalent HA-receptor interactions, to either a receptor-coated surface [33] or laterally mobile sialoglycolipid receptors embedded in a supported lipid bilayer [59]. Multivalent HA-receptor interactions, combined with NA activity, induced virus movement on a receptor-coated surface [32, 33, 60] until receptor density was decreased to an extent that allows virion elution [33]. Virus attached to sialoglycolipid receptors in a supported lipid bilayer were also shown to move by lateral diffusion of the attached sialoglycolipids in an NA-independent fashion [59]. Virion self-elution from a receptor-coated surface depended on the receptor-binding and -sialidase activity properties of HA and NA as well as on receptor density and identity [33, 34]. The inferred speed of virus motility on a surface and the self-elution rate thus depend on the HA-NA-receptor balance governing the dynamics of virus-glycan interactions.

IAV cross-species transmission likely requires adjustment of the HA-NA-receptor balance as the sialoglycan repertoire differs between species [45-48]. Within the human host, changes in HA and NA

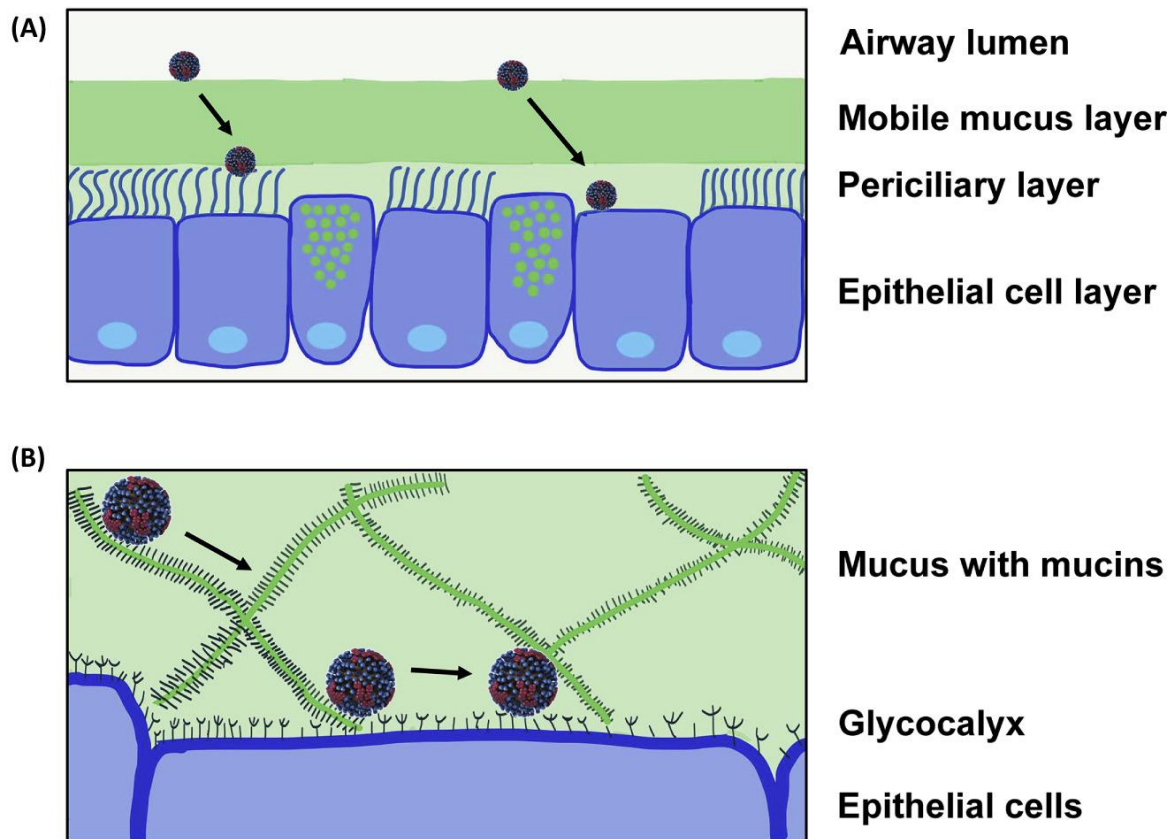


**Figure 3. IAV particles penetrate the mucus layer of the respiratory tract.** A) IAV particles need to penetrate a gel-like mobile mucus layer as well as a brush-like periciliary layer to reach the underlying epithelial cells. The gel-like mobile mucus layer contains soluble mucins MUC5AC/5B, while the periciliary layer is occupied by membrane-spanning mucins and large mucopolysaccharides that are tethered to cilia, microvilli, and epithelial cell surface [108]. Ciliated and non-ciliated cells are shown, as well as mucus-producing goblet cells. B) Upon association of IAV particles to the mucus layer, they are continuously in a receptor-bound state. In presence of mucus, inhibition of NA activity inhibits infection *in vitro* [43, 94-96]. The dynamics of IAV-receptor interactions allow the particles to move through the mucus layer in a NA-dependent manner [60, 97]. We speculate that virions are rolling over heavily-sialylated, elongated mucin molecules, until they reach the sialylated glycocalyx of the epithelial cells.

activity resulting from antigenic drift may require functional coadaptation of HA and NA to restore the balance. This may be achieved by tuning the receptor (fine-)specificity and affinity of HA [61] and the activity of NA. Of note, all NA proteins preferentially cleave avian- over human-type receptors, although NA of human viruses cleave human type receptors relatively more efficiently [62, 63]. One way to modulate NA activity is by mutation of the catalytic site which is, however, extremely

conserved between avian and human viruses. Mutations in the active site are primarily observed upon development of resistance against NAIs [64-67]. As an exception, recent human H3N2 viruses that depend on NA rather than HA for hemagglutination were recently shown to carry HA proteins with very weak receptor binding properties and NA with presumed low activity due to a mutation in the catalytic site [68]. NA-dependent hemagglutination could also be observed upon passaging of H3N2 viruses on MDCK cells [69]. NA proteins with relatively low catalytic activity (low  $k_{cat}$ ) were recently shown by BLI to contribute to the virion-receptor binding rate [33, 57], which seems logic considering the relatively lower  $K_D$  of NA than of HA for binding to sialosides [70].

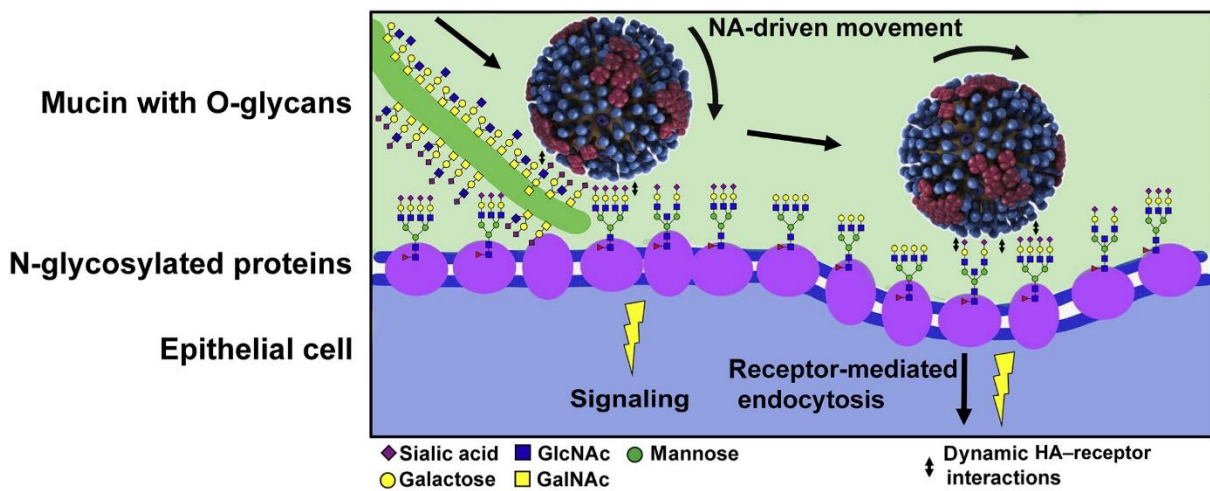


**Figure 4. Dynamics of IAV-receptor interactions at the mucus-cell interface.** IAV particles are dynamically interacting with SIA receptors present on O-glycans (present in high density on mucins) and on N-glycans (particularly present on the cell surface). Low affinity HA-SIA interactions [30, 31] are rapidly formed and broken, thereby allowing NA access to these receptors. Upon local receptor destruction resulting from SIA cleavage, virions move to a higher receptor density-containing vicinity. This NA-dependent movement likely occurs in the mucus layer [60, 97], but possibly also on the cell surface [32]. Binding of IAV particles to sialylated cell surface receptors results in their (transient) clustering and activation, thereby inducing signalling events that trigger the uptake of IAV particle via receptor-mediated endocytosis [110-112].

NA carries a second SIA binding site (2SBS) adjacent to the catalytic site (Fig. 2) which is highly conserved in most avian, but not in (pandemic) human viruses [34, 63, 71-73]. The 2SBS of N9 preferentially binds to avian type receptors [34, 63, 74] and enhances cleavage of SIAs from multivalent receptor surfaces carrying these receptors. Binding via the 2SBS presumably enhances sialidase activity by bringing NA closer to its substrate and is functionally reminiscent to the lectin binding sites present in many glycosidases. The 2SBS may contribute to the virus-receptor binding rate in addition to HA [34, 57] and the active site of NAs with low catalytic activity [33, 57, 75].

Altogether, this presents a range of options for fine-tuning the HA/NA/receptor balance that includes three receptor-binding sites (HA and two on NA) and a cleavage site (NA), all organized in an oligomeric (trimeric; HA, tetrameric; NA) configuration (Fig. 2). The loss of a functional 2SBS in NA of human IAVs might have evolved as a functional prerequisite for restoring the functional balance in response to the new  $\alpha$ 2,6-linked human receptor repertoire that was encountered upon zoonotic transfer. Alternatively, the 2SBS may have lost its functional role in human IAVs and therefore have become apt to antigenic variation. Despite the general view that the primary change in adapting to a new host receptor repertoire takes place in HA, followed by further adaptations in NA this is not the exclusive order of events. In the recently emerged H7N9 avian viruses mutation of the 2SBS, reducing binding to avian receptors, preceded the acquisition of the infamous Q226L mutation in HA which increased binding to human-type receptors [74]. Also in H9N2 avian viruses, mutation of the 2SBS is often found in company with the Q226L mutation in HA [76].

Additional mechanisms for tuning the HA-NA-receptor balance have been described. Changes in the length of the NA stalk domain usually (with some exceptions [77, 78]) do not change the NA activity of a virus particle on soluble monomeric substrates or of the isolated NA protein. However, a shortened stalk affects virus replication *in vivo* and NA activity on multivalent substrates in the context of the viral particle *in vitro* [79, 80], thereby for instance reducing virus self-elution from erythrocytes. Steric hindrance by HA was suggested to limit access of a retracted NA head domain to SIA receptors on the cell surface [81]. Several reports have demonstrated that altered stalk length differentially affects replication in different hosts emphasizing the importance of the HA-NA-receptor balance on host specificity [82-84]. A shorter stalk is considered to be an adaptation of IAVs originating from the intestinal tract of waterfowl to the respiratory tract of chicken [reviewed by [85, 86]. Also, virus particle morphology could have an impact on the HA-NA-receptor balance. In contrast to the mainly spherical morphology of laboratory adapted IAVs harvested from *in vitro* cell cultures, clinical isolates often contain filamentous IAVs [reviewed in 87] displaying an asymmetric surface distribution of HA and NA [60, 88-90] that may affect the HA-NA-receptor balance. Furthermore, mutations that affect intracellular transport and oligomerization of HA and NA [91, 92] could affect their ratio and distribution.

### Getting In

Transmission of respiratory IAVs to a new host occurs by the airborne route via respiratory droplets or aerosols as well as by direct contact with mucosal secretions [93]. The site of primary infection (intranasal, tracheal, lung) may affect pathogenicity but at all entry sites it is inevitable that virus particles are rapidly deposited on the mucosal surface and bind to mucins densely covered with sialylated O-linked glycans (Fig. 4). Inhibition of NA activity in presence of mucus inhibits infection in

vitro [43, 94-96] probably because under these conditions virus particles are not able to penetrate the mucus layer [97]. As outlined above, the HA-NA-receptor balance is critical for the interaction dynamics with a SIA receptor-coated surface. It is the NA activity that drives virus rolling/motility on such a receptor-coated substrate [32, 33] which needs to be sufficiently cleared of receptors by NA activity before the virus can dissociate [33]. Considering the presence of the enormous amount of SIA receptors on mucins (reviewed by [98]) relative to the small number of IAV particles required for starting an infection [99-101], we consider that dissociation of virus particles from the highly organized mucus structure is not likely. Instead, we and others [32, 33, 60] propose that NA activity will locally decrease the receptor density and the resulting SIA gradient will drive virus movement to areas of higher concentration. The first microscopic studies on IAV motility have identified NA activity-driven directional motility of spherical IAV particles on fetuin-coated glass slides [32]. Crawling as well as gliding motility (movement over short and longer distances respectively) were observed. Variation in length of alternating phases of strong and weak attachment of the virus particles, dependent on the HA-NA-receptor balance, were proposed to give rise to the two mechanisms of motion [32]. Others have studied the motility of filamentous IAVs (up to 1  $\mu\text{m}$  in length) on fetuin-coated surfaces and in mucus gels [60]. Filamentous IAVs appeared to move with higher directionality than the spherical particles studied in [32] when NA displayed a polarized distribution, restricted to one pole, on the viral filaments. The NA-rich pole functioned as an outboard engine propelling the filament forwards. Directionality was lost when NA was randomly distributed. Remarkably, filamentous Influenza C virus (ICV) particles, which carry their receptor-binding site and receptor-destroying activity in a single hemagglutinin-esterase-fusion (HEF) protein also displayed highly directional motion on a mucus-coated substrate [102] which was less obvious for spherical ICV particles. Thus, receptor cleavage in combination with rapid receptor exchange on individual receptor binding sites may be a general driving force for the motion of viruses belonging to different classes on different substrates as for instance also proposed for  $\beta$ -coronaviruses [103] which harbour an hemagglutinin esterase that evolved from ICV HEF. Given the observed directionality of movement on sialylated substrates, we hypothesize that mucins are not merely IAV decoy receptors but actually support rapid directional transfer of virus particles through a viscous mucus layer. Movement of particles through mucus will obviously depend on the HA-NA-receptor balance. Too strong binding by HA in combination with an NA with low sialidase activity has been shown to slow down the speed of virus rolling in vitro [32-34] while particle morphology and HA-NA distribution affect directionality [60, 102].

Upon crossing the viscous maze-like mucus layer rich in soluble mucins, further penetration of a watery periciliary layer (PCL) is required in order to attach to sites on membranes of epithelial cells

resulting in endocytic entry. The PCL, from which soluble mucins are excluded, is formed by the cilia and microvilli that protrude from the membranes of ciliated cells, and the mucin-secreting goblet cells and serous cells, respectively [104]. These are the major cell types of the mammalian upper respiratory tract that face the mucus layer and of which at least ciliated and goblet cells can be infected by IAVs [105-107]. The narrow space (< 200 nm) in between the cilia, filled with a glycocalyx composed of sialylated membrane-tethered mucins and other glycoconjugates, is impenetrable for beads >40nm by diffusion [108]. Thus, entry of >100nm diameter IAV particles by endocytosis, which is likely to occur only at base of these protrusions, requires the type of active transport that could be provided by NA activity-driven rolling over sialylated substrates and will be dependent on the HA-NA-receptor balance. It cannot be excluded that IAV primarily enters cells at regions where cilia density is less, for instance at cell-cell borders, but also in this case it is crucial that the relative small number of particles that start a new infection do not become trapped in between cilia.

Once in close contact with the surface of the cell body, the virus needs to bind (enigmatic) functional receptors that allow/induce endocytic uptake. IAV entry has been shown to proceed by clathrin-mediated endocytosis (CME) as well as macropinocytosis (MP) [reviewed in 109]. Both entry routes fully depend on sialylated cell-surface receptors [110]. The latter was shown to require signalling by receptor tyrosine kinases (RTKs). Several different RTKs are involved and their effects may be redundant as well as additive [110, 111]. CME of IAVs does not follow the ubiquitous route of surfing into preformed clathrin-coated pits but is characterized by the *de novo* formation of a clathrin coat at sites where virus particles have become immobilized [112]. Such a process requires, yet undefined, transmembrane signalling as well as fixation at a spot by stable binding to (clustered) receptors. Many eukaryotic signalling receptors are heavily decorated with (sialylated) N-linked glycans. N-linked glycans have been shown to be important, but not absolutely required, for IAV entry. Especially in cells lacking sialylated N-glycans decoy receptors were shown to interfere with entry [38]. We speculate that weak binding to O-glycans on mucins may not only be needed to move through the mucus layer but also to allow transfer of virions to higher affinity receptors at the cell-surface, which may be N-linked glycans in particular. Multiantennary N-linked glycans containing multiple LacNAc repeats were, by structural modelling, suggested to associate simultaneously with two RBSs in single HA trimers of H3N2 viruses isolated since the 1990s. The HA proteins of these viruses display high avidity for such glycans and do not bind to short LacNAc antennae as analysed by glycan array analysis [21].

Of note, binding receptors and signalling receptors at entry spots supporting CME or MP are not necessarily the same entities as multivalent IAV particles can engage multiple different receptors simultaneously. Viruses bind to cell surfaces displaying heterologous sialoglycan receptors, enabling

hetero-multivalent virion-cell interactions that will affect the HA-NA-receptor balance and the dynamics of virus-receptor interactions in ways that have not been explored yet. Cell-cell interaction studies have shown that short-lived interactions can lead to signalling and it has been suggested that these weak interactions can be enabled by higher affinity interactions involving receptors that do not signal [113-115]. The same may hold true for weak interactions between virus and cell surface signalling receptors. Glycan arrays have so far mainly been employed for screening the binding of recombinant HA proteins. This approach focusses on identification of high avidity binders whereas identification of low affinity receptors necessarily relies on the highly multivalent binding mode of virions as used in BLI [33, 57, 58]. Indeed the occasional use of virus particles on glycan arrays has shown its potential to identify a broader spectrum receptors than by recombinant proteins [11, 13, 101]. For instance, in contrast to the high specificity of recombinant HA of H7N9 for avian-type receptors [117] the corresponding H7N9 virus particles were shown to bind human- and avian-type receptors to similar levels [15]. Viruses could in theory move/roll in a HA-NA-receptor balance-dependent mode over the cell surface. However, this type of motility does not seem to be as crucial as for penetrating the mucus layer as NA inhibitors have only a moderate effect on virus entry *in vitro* in a watery buffer of low protein content [38, 96]. Possibly, under these conditions, IAV particles attach to abundantly present and highly mobile sialylated membrane protein receptors that surf with their cargo through the fluid lipid membrane over the cell surface. In the absence of NA activity viruses do not roll [32, 33], but, because of the high  $K_D$  of single HA-SIA interaction, we expect them to display NA activity-independent wobbling “on the spot”, which enables the virus particle to exchange bound receptors with closely adjoining receptors. Combined with surfing such a mechanism may still allow the virus to recruit functional receptors required for entry.

### **Getting Out, and In Again**

The crucial role for NA at the end of the infection cycle, when newly assembled particles at the cell surface are released from cells has been abundantly documented. NA activity results in destruction of receptors that are otherwise bound by HA, both on the cell surface and on mucus. No release/aggregation of virus particles is observed when NA activity is blocked [35, 118] showing the crucial function of NA in producing infectious progeny. NA sialidase activity is probably not required at the site of particle assembly per se, but expression of NA rather results in a cell surface devoid of sialosides, which also prevents superinfection [119]. Subsequent spreading of an infection differs from a primary infection in particle numbers (much higher [120]) and location (directly at the epithelial cell surface) and may have a different requirement for the HA-NA-receptor balance. Particles that are assembled are often spherical, but those of clinical isolates may also be filamentous [reviewed in [87, 121]. Very long filamentous particles are particularly easily observed when cell



associated [121 and references therein], but may be more labile than spherical particles when released from cells [122]. The filamentous particle phenotype is lost upon passaging in vitro, mostly resulting from mutations in M1, while this phenotype is maintained or may even be regained upon passaging in vivo [87, 123] thereby suggesting an important, yet to be established, role for such particles in vivo. Filamentous particles may serve to efficiently spread from cell to cell when these cells are covered with a mucus layer. Alternatively, filamentous particles may be able to penetrate the mucus layer towards the luminal side and thereby be important for transmission. Of note, association of virus particles with mucus was shown to enhance particle stability in aerosols and thereby transmissibility [124, 125]. Likely, there is also an important role for the HA-NA-receptor balance in this respect, as before infecting a new host, virus particles need to dissociate from these mucus molecules.

### **Concluding Remarks and Future Perspectives**

Historically, identification of IAV receptors has mostly focussed on the identification of receptors with high avidity for HA despite the frequent demonstration of efficiently replicating IAVs that carry HAs with almost undetectable sialoglycan binding. At the same time, there has been a longstanding awareness of the requirement for an optimal HA-NA balance which, in simple terms, was defined as the need for matching HA affinities and NA activities in order to assure prevention of virions being trapped by decoy receptors but allowing binding to functional receptors on the cell surface. Only recently, the use of techniques that allow real-time detection of the dynamic interaction between IAV particles and receptor-coated surfaces, in the presence of NA activity, has permitted quantification of this balance. By multivalent interactions (avidity), HAs with low or relatively high binding affinity all support essentially irreversible virus binding to polyvalent receptor surfaces, as encountered in the mucus layer and on the cell surface, leading to the assumption that IAV particles are continuously in a receptor-bound state. It is the NA activity which, in conjunction with the  $K_D$  of monomeric HA-receptor interactions, enables virus motility on such surfaces and thereby assures efficient penetration of the mucus layer and migration over the cell surface to an, as yet undefined, spot that permits (signalling-induced) virus entry. Further development of microscopy and BLI-based techniques should help to answer numerous questions that address the basic principles of the HA-NA-receptor balance and its role in IAV-receptor interaction dynamics.

Clearly, this balance needs to be addressed in respect to the highly heterogeneous receptor repertoire that is encountered within a host. The use of recombinant glycoproteins in BLI is a step forward and recent developments in binding cells to BLI sensors [126] have opened opportunities to directly examine virus-cell interactions by this technique. This should provide a quantitative description of species-specific IAV-host balance in order to understand which adaptations are

required for crossing the species-barrier. While not only the cell surface but also the mucus layer likely poses a selective barrier [43, 127], their composition and interaction with IAV currently receives too little attention (see Outstanding Questions). Ultimately, studying the HA-NA-(decoy)receptor balance of viruses from different hosts and the adjustment thereof by mutations in HA and NA should have predictive value in linking naturally occurring amino acid substitutions to the potential of IAVs for altering their host range.

## Highlights

- Functional properties of the IAV HA and NA proteins need to be balanced to allow penetration of the heavily sialylated mucus layer, attachment to and endocytic uptake into underlying epithelial cells, and efficient spread of progeny virions.
- The HA-NA-receptor balance is readjusted upon cross-species transmission as the sialoglycan repertoire differs between species. This adjustment is achieved via mutations in the receptor binding site of HA, but may also be achieved by adaptation of the receptor-binding and -sialidase activity properties of NA.
- IAVs are continuously in a receptor-bound state, which is highly dynamic resulting from multivalent, low affinity HA-SIA interactions combined with NA activity and which allows virion movement on a receptor-containing surface.
- Novel technological developments allow detailed kinetic analysis of the HA-NA-receptor balance.

## Outstanding Questions Box

- The HA-NA-receptor balance of different viruses adapted to different (as well as to the same) host species remains to be determined. In view of the plethora of (decoy) receptors that viruses encounter *in vivo*, it is not yet known which (combinations of) receptors are best suited to perform these analyses. In order to directly compare the HA-NA-balance of different viruses, the same receptors need to be used.
- Is the functional HA-NA-receptor balanced required for efficient replication in and transmission between specific host species a very narrow balance, or is the required balance not so strict?
- It is not known whether the functional HA-NA-receptor balances of different viruses adapted to different host species are distinct or (partly) overlapping. Does an overlapping HA-NA-receptor balance window provide an increased opportunity for cross-species transmission?
- Do IAVs need to bind to specific functional receptors on host cells to initiate infection? How large is the repertoire of functional receptors and what is their redundancy?
- To what extent does mucus from different host species differ in sialoglycan makeup and to what extent does the mucus layer function as a host range barrier? Does mucus function as a barrier at all for a well-adapted virus, or may it even enhance virus infection by helping viruses to reach the underlying epithelial cells?
- To what extent should we take into account that IAV particles are continuously in a receptor-bound state *in vivo* when we study the ability of antibodies or molecules to interfere with HA or NA functions *in vitro*?

## Glossary

**Affinity:** Affinity indicates how tightly a ligand binds to a protein and is commonly described by the dissociation constant  $K_D$  (the ligand concentration at which half of the protein binding sites are occupied at equilibrium). We refer to affinity with respect to the interaction of a single HA protomer with a receptor.

**Avidity:** Avidity refers to the accumulated strength of multiple individual binding interactions as they occur for example when a virion displaying multiple HA trimers interacts with a receptor-coated surface.

**Biolayer interferometry (BLI):** BLI is a label-free technology, based on an optical analytical technique, for measuring biomolecular interactions on a biosensor surface.

**Clathrin-mediated endocytosis (CME):** CME is a process by which a cells internalizes extracellular components via inward budding of the plasma membrane. These inward buds are assembled with the help of clathrin molecules.

**Glycan array:** Glycan arrays contain (synthetic) oligosaccharides immobilised on a solid support in a microarray format. They can be used for high-throughput analysis of protein-glycan interactions.

**Macropinocytosis (MP):** Endocytosis process that results in the uptake of liquid material by cells from their external environment via heterogeneously sized intracellular vesicles called macropinosomes.

**Multivalent binding:** Multivalent binding refers to binding between two entities via multiple binding sites (e.g. virus particle and cell surface/mucin).

**N-linked glycan:** Oligosaccharide attached to an asparagine residue of a protein. N-glycosylation is a co-translational process that occurs in the endoplasmic reticulum. N-glycans are modified during transport of proteins along the secretory pathway. The final structure of N-linked glycans is determined by the protein and the cell in which it is expressed and varies across species.

**O-linked glycan:** O-linked glycosylation is the attachment of a sugar molecule to serine or threonine residues in a protein. O-glycosylation is a post-translational modification. After addition of the initial sugar, other sugars can be attached. In general O-glycans are shorter and less complex than N-glycans. Mucins contain many O-glycans.

**Receptor tyrosine kinase (RTK):** RTKs are transmembrane-containing tyrosine kinases that are cell surface receptors for growth factors, cytokines, and hormones. Extracellular ligand binding will typically cause receptor di/oligomerization, which activates the receptor thereby propagating a signal through the plasma membrane.

**Sialic acid (SIA):** SIA is a nine carbon saccharide that generally occupies a terminal position of an oligosaccharide (referred to as sialoglycan). SIAs are generally attached to a penultimate galactose via an  $\alpha 2,3$ - or an  $\alpha 2,6$ -linkage.

## References

- 1 Bouvier, N.M. and Palese, P. (2008) The biology of influenza viruses. *Vaccine* 26 (Suppl. 4), D49–D53
- 2 Wu, Y. et al. (2014) Bat-derived influenza-like viruses H17N10 and H18N11. *Trends Microbiol.* 22, 183–191
- 3 Rejmanek, D. et al. (2015) Evolutionary Dynamics and Global Diversity of Influenza A Virus. *J. Virol.* 89, 10993–11001
- 4 Matrosovich, M. et al. (2000) Early alterations of the receptor-binding properties of H1, H2, and H3 avian influenza virus hemagglutinins after their introduction into mammals. *J. Virol.* 74, 8502–8512
- 5 Rogers, G.N. et al. (1983) Receptor determinants of human and animal influenza virus isolates: differences in receptor specificity of the H3 hemagglutinin based on species of origin. *Virology* 127, 361–373
- 6 Shi, Y. et al. (2014) Enabling the 'host jump': structural determinants of receptor-binding specificity in influenza A viruses. *Nat Rev Microbiol.* 12, 822–831
- 7 de Graaf, M. and Fouchier R.A. (2014) Role of receptor binding specificity in influenza A virus transmission and pathogenesis. *EMBO J.* 33, 823–841
- 8 de Vries, R.P. et al. (2017) Three mutations switch H7N9 influenza to human-type receptor specificity. *PLoS Pathog.* 13, e1006390
- 9 Gambaryan, A. et al. (2005) Receptor specificity of influenza viruses from birds and mammals: new data on involvement of the inner fragments of the carbohydrate chain. *Virology* 334, 276–283
- 10 Stevens, J. et al. (2006) Structure and receptor specificity of the hemagglutinin from an H5N1 influenza virus. *Science* 312, 404–410
- 11 Liu, Y. et al. (2010) Altered receptor specificity and cell tropism of D222G hemagglutinin mutants isolated from fatal cases of pandemic A(H1N1) 2009 influenza virus. *J Virol.* 84, 12069–12074
- 12 Childs, R.A. et al. (2009) Receptor-binding specificity of pandemic influenza A (H1N1) 2009 virus determined by carbohydrate microarray. *Nat Biotechnol.* 9, 797–799
- 13 Gulati, S. et al. (2013) Human H3N2 Influenza Viruses Isolated from 1968 To 2012 Show Varying Preference for Receptor Substructures with No Apparent Consequences for Disease or Spread. *PLoS ONE* 8, e66325
- 14 Belser, J.A. et al. (2013) Pathogenesis and transmission of avian influenza A (H7N9) virus in ferrets and mice. *Nature* 501, 556–559
- 15 Watanabe, T. et al. (2013) Characterization of H7N9 influenza A viruses isolated from humans. *Nature* 501, 551–555
- 16 Stevens, J. et al. (2008) Recent avian H5N1 viruses exhibit increased propensity for acquiring human receptor specificity. *J Mol Biol.* 381, 1382–1394
- 17 Peacock, T.P. et al. (2017) Variability in H9N2 haemagglutinin-receptor-binding preference and the pH of fusion. *Emerg Microbes Infect.* 6, e11
- 18 Hensley, S. et al. (2009) Receptor binding avidity drives influenza A virus antigenic drift. *Science* 326, 734–736
- 19 Koel, B.F. et al. (2013) Substitutions near the receptor binding site determine major antigenic change during influenza virus evolution. *Science.* 342, 976–979
- 20 Koel, B.F. et al. (2015) Identification of amino acid substitutions supporting antigenic change of influenza A(H1N1)pdm09 viruses. *J Virol.* 89, 3763–3775
- 21 Peng, W. et al. (2017) Specificity for Extended, Branched Human-type Receptors, Conferring Potential for Increased Avidity. *Cell Host Microbe* 21
- 22 Lin, Y.P. et al. (2012) Evolution of the receptor binding properties of the influenza A(H3N2) hemagglutinin. *Proc Natl Acad Sci USA* 109, 21474–21579
- 23 Wagner, R. et al. (2002) Functional balance between haemagglutinin and neuraminidase in influenza virus infections. *Rev. Med. Virol.* 12, 159–166

- 24 McAuley, J.L. et al. (2019) Influenza Virus Neuraminidase Structure and Functions. *Front Microbiol.* 10, e00039
- 25 Kosik, I. and Yewdell, J.W. (2019) Influenza Hemagglutinin and Neuraminidase: Yin-Yang Proteins Coevolving to Thwart Immunity. *Viruses* 11, e346
- 26 Gaymard, A. et al. (2016) Functional balance between neuraminidase and haemagglutinin in influenza viruses. *Clin Microbiol Infect.* 22, 975-983
- 27 Byrd-Leotis, L. et al. (2017) The Interplay between the Host Receptor and Influenza Virus Hemagglutinin and Neuraminidase. *Int J Mol Sci.* 18, e1541
- 28 Sauter, N.K. et al. (1989) Hemagglutinins from two influenza virus variants bind to sialic acid derivatives with millimolar dissociation constants: a 500-MHz proton nuclear magnetic resonance study. *Biochemistry* 28, 8388-8396
- 29 Takemoto, D.K. et al. (1996) Surface plasmon resonance assay for the binding of influenza virus hemagglutinin to its sialic acid receptor. *Virology* 217, 452-458
- 30 Fei, Y. et al. (2015) Characterization of Receptor Binding Profiles of Influenza A Viruses Using An Ellipsometry-Based Label-Free Glycan Microarray Assay Platform. *Biomolecules* 5, 480-498
- 31 Xiong, X. et al. (2018) Receptor binding by a ferret-transmissible H5 avian influenza virus. *Nature* 497, 392-396
- 32 Sakai, T et al. (2017) Influenza A virus hemagglutinin and neuraminidase act as novel motile machinery. *Sci Rep.* 7, e45043
- 33 Guo, H. et al. (2018) Kinetic analysis of the influenza A virus HA/NA balance reveals contribution of NA to virus-receptor binding and NA-dependent rolling on receptor-containing surfaces. *PLoS Pathog.* 14, e1007233
- 34 Du, W. et al. (2019) The 2nd sialic acid-binding site of influenza A virus neuraminidase is an important determinant of the hemagglutinin-neuraminidase-receptor balance. *PLoS Path.* In press
- 35 Palese, P. et al. (1974) Characterization of temperature sensitive influenza virus mutants defective in neuraminidase. *Virology* 61, 397-410
- 36 Basak, S. et al. (1985) Sialic acid is incorporated into influenza hemagglutinin glycoproteins in the absence of viral neuraminidase. *Virus Res.* 2, 61-68
- 37 Chu, V.C. et al. (2004) Influenza virus entry and infection require host cell N-linked glycoprotein. *Proc Natl Acad Sci U S A.* 101, 18153-18158
- 38 de Vries, E. et al. (2012) Influenza A virus entry into cells lacking sialylated N-glycans. *Proc Natl Acad Sci U S A.* 109, 7457-7462
- 39 Fujioka, Y. et al. (2018) A Sialylated Voltage-Dependent Ca<sup>2+</sup> Channel Binds Hemagglutinin and Mediates Influenza A Virus Entry into Mammalian Cells. *Cell Host Microbe* 23, 809-818
- 40 Leung, H.S. (2012) Entry of influenza A Virus with a  $\alpha$ 2,6-linked sialic acid binding preference requires host fibronectin. *J Virol.* 86, 10704-10713
- 41 Vrijens, P. (2019) Influenza virus entry via the GM3 ganglioside-mediated platelet-derived growth factor receptor-signalling pathway. *J Gen Virol.* 100, 583-601
- 42 Kesimer, M. et al. (2010) Unpacking a gel-forming mucin: a view of MUC5B organization after granular release. *Am J Physiol Lung Cell Mol Physiol.* 298, L15-22
- 43 Zanin, M. et al. (2016) The Interaction between Respiratory Pathogens and Mucus. *Cell Host Microbe* 19, 159-168
- 44 Kesimer, M. et al. (2015) Physical characterization and profiling of airway epithelial derived exosomes using light scattering. *Methods* 87, 59-63
- 45 Lakdawala, S.S. et al. (2015) The soft palate is an important site of adaptation for transmissible influenza viruses. *Nature* 526, 122-125
- 46 Jia, N. et al. (2014) Glycomic characterization of respiratory tract tissues of ferrets: implications for its use in influenza virus infection studies. *J Biol Chem.* 289, 28489-28504
- 47 Chan, R.W. et al. (2013) Infection of swine ex vivo tissues with avian viruses including H7N9 and correlation with glycomic analysis. *Influenza Other Respir Viruses.* 6, 1269-1282
- 48 Walther, T. et al. (2013) Glycomic analysis of human respiratory tract tissues and correlation with influenza virus infection. *PLoS Pathog.* 9, e1003223

- 49 Rogers, G.N. et al. (1983) Differential sensitivity of human, avian, and equine influenza A viruses to a glycoprotein inhibitor of infection: selection of receptor specific variants. *Virology* 131, 394-408
- 50 Kaverin, N.V. et al. (1998) Post-reassortment changes in influenza A virus hemagglutinin restoring HA-NA functional match. *Virology* 244, 315-321
- 51 Kaverin, N.V. et al. (2000) Intergenic HA-NA interactions in influenza A virus: postreassortment substitutions of charged amino acid in the hemagglutinin of different subtypes. *Virus Res.* 66, 123-129
- 52 Mitnaul, L.J. et al. (2000) Balanced hemagglutinin and neuraminidase activities are critical for efficient replication of influenza A virus. *J Virol.* 74, 6015-6020
- 53 Hughes, M.T. et al. (2001) Adaptation of influenza A viruses to cells expressing low levels of sialic acid leads to loss of neuraminidase activity. *J Virol.* 75, 3766-3770
- 54 Hughes, M.T. et al. (2000) Influenza A viruses lacking sialidase activity can undergo multiple cycles of replication in cell culture, eggs, or mice. *J Virol.* 74, 5206-5212
- 55 Xu, R. et al. (2012) Functional balance of the hemagglutinin and neuraminidase activities accompanies the emergence of the 2009 H1N1 influenza pandemic. *J Virol.* 86, 9221-9232
- 56 Xiong, X. et al. (2014) Enhanced human receptor binding by H5 haemagglutinins. *Virology* 457, 179-187
- 57 Benton, D.J. et al. (2017) Role of Neuraminidase in Influenza A(H7N9) Virus Receptor Binding. *J Virol.* 91, e02293-16
- 58 Benton, D.J. et al. (2015) Biophysical measurement of the balance of influenza a hemagglutinin and neuraminidase activities. 290, 6516-6521
- 59 Müller, M. et al. (2019) Mobility-Based Quantification of Multivalent Virus-Receptor Interactions: New Insights Into Influenza A Virus Binding Mode. *Nano Lett.* 19, 1875-1882
- 60 Vahey, M.D. and Fletcher, D.A. (2019) Influenza A virus surface proteins are organized to help penetrate host mucus. *Elife* 8, e43764
- 61 Ji, Y. et al. (2017) New insights into influenza A specificity: an evolution of paradigms. *Curr Opin Struct Biol.* 44, 219-231
- 62 Baum, L.G. and Paulson, J.C. (1991) The N2 neuraminidase of human influenza virus has acquired a substrate specificity complementary to the hemagglutinin receptor specificity. *Virology* 180, 10-15
- 63 Du, W. et al. (2018) Substrate Binding by the Second Sialic Acid-Binding Site of Influenza A Virus N1 Neuraminidase Contributes to Enzymatic Activity. *J Virol.* 92, e01243-18
- 64 Gulati, S. et al. (2009) Deletions of neuraminidase and resistance to oseltamivir may be a consequence of restricted receptor specificity in recent H3N2 influenza viruses. *Virol. J.* 22, e1743
- 65 Eshaghi, A. et al. (2015) Multiple influenza A (H3N2) mutations conferring resistance to neuraminidase inhibitors in a bone marrow transplant recipient. *Antimicrob. Agents Chemother.* 58, 7188-7197
- 66 Tamura, D. et al. (2015) Emergence of Multidrug-Resistant Influenza A(H1N1)pdm09 Virus Variants in an Immunocompromised Child Treated With Oseltamivir and Zanamivir. *J Infect Dis.* 212, 1209-1213
- 67 van der Vries, E. (2010) Emergence of a multidrug-resistant pandemic influenza A (H1N1) virus. *N Engl J Med.* 363, 1381-1382
- 68 Mögling, R. et al. (2017) Neuraminidase-mediated haemagglutination of recent human influenza A(H3N2) viruses is determined by arginine 150 flanking the neuraminidase catalytic site. *J Gen Virol.* 98, 1274-1281
- 69 Mohr, P.G. et al. (2015) The neuraminidases of MDCK grown human influenza A(H3N2) viruses isolated since 1994 can demonstrate receptor binding. *Virol J.* 67, s12985
- 70 Reiter-Scherer, V. et al. (2019) Force Spectroscopy Shows Dynamic Binding of Influenza Hemagglutinin and Neuraminidase to Sialic Acid. *Biophys J.* 116, 1037-1048
- 71 Sung, J.C. et al. (2010) Role of secondary sialic acid binding sites in influenza N1 neuraminidase. *J Am Chem Soc.* 132, 2883-2885

- 72 Varghese, J.N. et al. (1997) Structural evidence for a second sialic acid binding site in avian influenza virus neuraminidases. *Proc Natl Acad Sci U S A* 94, 11808-11812
- 73 Uhlenendorff, J. et al. (2009) Functional significance of the hemadsorption activity of influenza virus neuraminidase and its alteration in pandemic viruses. *Arch Virol.* 154, 945-957
- 74 Dai, M. et al. (2017) Mutation of the Second Sialic Acid-Binding Site, Resulting in Reduced Neuraminidase Activity, Preceded the Emergence of H7N9 Influenza A Virus. *J Virol.* 91, e00049
- 75 Hiono, T. et al. (2016) Amino acid residues at positions 222 and 227 of the hemagglutinin together with the neuraminidase determine binding of H5 avian influenza viruses to sialyl Lewis, X. et al. *Arch Virol.* 161, 307-316
- 76 Matrosovich, M.N. et al. (2001) H9N2 influenza A viruses from poultry in Asia have human virus-like receptor specificity. *Virology* 281, 156-162
- 77 Durrant, J. D. et al. (2016) Microsecond molecular dynamics simulations of influenza neuraminidase suggest a mechanism for the increased virulence of stalk-deletion mutants. *J. Phys. Chem. B* 120, 8590–8599
- 78 Zanin, M., Duan, S., Wong, S. S., Kumar, G., Baviskar, P., Collin, E., et al. (2017). An amino acid in the stalk domain of N1 neuraminidase is critical for enzymatic activity. *J. Virol.* 91, e00868–e00916
- 79 Els, M. C. et al. (1985) An 18-amino acid deletion in an influenza neuraminidase. *Virology* 142, 241–247
- 80 Castrucci, M. R., and Kawaoka, Y. (1993). Biologic importance of neuraminidase stalk length in influenza A virus. *J. Virol.* 67, 759–764
- 81 Baigent, S. J., and McCauley, J. W. (2001). Glycosylation of haemagglutinin and stalk-length of neuraminidase combine to regulate the growth of avian influenza viruses in tissue culture. *Virus Res.* 79, 177–185
- 82 Matsuoka, Y. et al. (2009) Neuraminidase stalk length and additional glycosylation of the hemagglutinin influence the virulence of influenza H5N1 viruses for mice. *J. Virol.* 83, 4704–4708
- 83 Blumenkrantz, D. et al. (2013) The short stalk length of highly pathogenic avian influenza H5N1 virus neuraminidase limits transmission of pandemic H1N1 virus in ferrets. *J. Virol.* 87, 10539–10551
- 84 Hoffmann, T. W. et al. (2012) Length variations in the NA stalk of an H7N1 influenza virus have opposite effects on viral excretion in chickens and ducks. *J. Virol.* 86, 584–588
- 85 Long, J.S. et al. (2015) One-way trip: influenza virus' adaptation to gallinaceous poultry may limit its pandemic potential. *Bioessays* 37, 204-212
- 86 Li, J. et al. (2011) Emergence and genetic variation of neuraminidase stalk deletions in avian influenza viruses. *PLoS One* 6, e14722
- 87 Badham, M.D and Rossman, J.S. (2016) Filamentous Influenza Viruses. *Curr Clin Microbiol Rep.* 3, 155-161
- 88 Harris, A. et al. (2006) Influenza virus pleiomorphy characterized by cryoelectron tomography. *Proc. Natl. Acad. Sci. USA* 103, 19123-19127
- 89 Calder, L.J. et al. (2010) Structural organization of a filamentous influenza A virus. *Proc Natl Acad Sci U S A* 107, 10685–10690
- 90 Rossman, J.S. and Lamb, R.A. (2011) Influenza virus assembly and budding. *Virology* 411. 229-236
- 91 Hensley, S.E. (2011) Influenza A virus hemagglutinin antibody escape promotes neuraminidase antigenic variation and drug resistance. *PLoS ONE* 6, e15190
- 92 Das, S.R. (2013) Defining influenza A virus hemagglutinin antigenic drift by sequential monoclonal antibody selection. *Cell Host Microbe* 13, 314–323
- 93 Kutter, J.S. et al. (2018) Transmission routes of respiratory viruses among humans. *Curr Opin Virol.* 28, 142-151
- 94 Matrosovich, M.N. et al. (2004) Neuraminidase is important for the initiation of influenza virus infection in human airway epithelium. *J Virol.* 78, 12665-12667
- 95 Cohen, M. et al. (2015) Notable Aspects of Glycan-Protein Interactions. *Biomolecules* 5, 2056-2072



- 96 Cohen, M. et al. (2013) Influenza A penetrates host mucus by cleaving sialic acids with neuraminidase. *Virology* 510, 321
- 97 Yang, X. et al. (2014) A beneficiary role for neuraminidase in influenza virus penetration through the respiratory mucus. *PLoS One* 9, e110026
- 98 Duncan, G.A. et al. (2016) The Mucus Barrier to Inhaled Gene Therapy *Mol Ther.* 24, 2043-2053
- 99 Varble, A. et al. (2014) Influenza A virus transmission bottlenecks are defined by infection route and recipient host. *Cell Host & Microbe* 16, 691–700
- 100 Poon, L.L. et al. (2016) Quantifying influenza virus diversity and transmission in humans. *Nature Genetics* 48, 195–200
- 101 Sobel Leonard, A. et al. (2017) Transmission bottleneck size estimation from pathogen deep-sequencing data, with an application to human influenza A virus. *J. Virol.* 91, e00171-17
- 102 Sakai, T. et al. (2018) Unique Directional Motility of Influenza C Virus Controlled by Its Filamentous Morphology and Short-Range Motions. *J Virol.* 92, e01522-17
- 103 Tortorici, M.A. et al. (2019) Structural basis for human coronavirus attachment to sialic acid receptors. *Nat Struct Mol Biol.* 26, 481-489
- 104 Bals, R. (1997) Cell types of respiratory epithelium: morphology, molecular biology and clinical significance. *Pneumologie* 51,142-149
- 105 Ibricevic, A. et al (2006) Influenza virus receptor specificity and cell tropism in mouse and human airway epithelial cells. *J Virol.* 80, 7469-7480
- 106 Davis, A.S. et al. (2015) Validation of normal human bronchial epithelial cells as a model for influenza A infections in human distal trachea. *J Histochem Cytochem.* 63, 312-328
- 107 Chan, R.W. et al., (2013) Use of ex vivo and in vitro cultures of the human respiratory tract to study the tropism and host responses of highly pathogenic avian influenza A (H5N1) and other influenza viruses. *Virus Res.* 178, 133-145
- 108 Button, B. et al. (2012) A periciliary brush promotes the lung health by separating the mucus layer from airway epithelia. *Science* 337, 937-41
- 109 Edinger, T.O. et al. (2014) Entry of influenza A virus: host factors and antiviral targets. *J Gen Virol.* 95, 263-277
- 110 de Vries, E. et al. (2011) Dissection of the influenza A virus endocytic routes reveals macropinocytosis as an alternative entry pathway. *PLoS Pathog.* 7, e1001329
- 111 Eierhoff, T. et al. (2010) The epidermal growth factor receptor (EGFR) promotes uptake of influenza A viruses (IAV) into host cells. *PLoS Pathog.* 6, e1001099
- 112 Rust, M.J. et al. (2004) Assembly of endocytic machinery around individual influenza viruses during viral entry. *Nat Struct Mol Biol.* 11, 567-573
- 113 Davis, S.J. et al. (1998) The role of charged residues mediating low affinity protein-protein recognition at the cell surface by CD2. *Proc Natl Acad Sci U S A.* 95, 5490-4
- 114 Wright, G.J. (2009) Signal initiation in biological systems: the properties and detection of transient extracellular protein interactions. *Mol Biosyst.* 5, 1405-12
- 115 Lever, M. et al. (2014). Phenotypic models of T cell activation. *Nat Rev Immunol.* 14, 619-629
- 116 Gulati, S. et al. (2014) Glycan array analysis of influenza H1N1 binding and release. *Cancer Biomark.* 14, 43-53
- 117 Xu, R. et al. (2013) Preferential recognition of avian-like receptors in human influenza A H7N9 viruses. *Science* 342, 1230-1235
- 118 Hinshaw V. S. et al. (1983) Altered tissue tropism of human-avian reassortant influenza viruses. *Virology* 128:260–263
- 119 Huang, I.C. (2008) Influenza A virus neuraminidase limits viral superinfection. *J Virol.* 82, 4834-4843
- 120 Jacobs, N.T. (2019) Incomplete influenza A virus genomes occur frequently but are readily complemented during localized viral spread. *Nat Commun.* 10, 3526
- 121 Dadonaite, B. et al. (2016) Filamentous influenza viruses. *J Gen Virol.* 97, 1755-1764

- 122 Rossman, J.S. et al.(2010) Influenza virus m2 ion channel protein is necessary for filamentous virion formation. *J Virol.* 84, 5078-8508
- 123 Seladi-Schulman, J. et al. (2013) Spherical influenza viruses have a fitness advantage in embryonated eggs, while filament-producing strains are selected in vivo. *J Virol.* 87, 13343-13353
- 124 Kormuth, K.A. et al. (2018) Influenza Virus Infectivity Is Retained in Aerosols and Droplets Independent of Relative Humidity. *J Infect Dis.* 218, 739-747
- 125 Thomas, Y.et al (2008) Survival of influenza virus on banknotes. *Appl Environ Microbiol.* 74, 3002-3007
- 126 Verzijl, D. et al, (2017) A novel label-free cell-based assay technology using biolayer interferometry. *Biosens Bioelectron.* 87, 388-395
- 127 Zanin, M. et al. (2015) Pandemic Swine H1N1 Influenza Viruses with Almost Undetectable Neuraminidase Activity Are Not Transmitted via Aerosols in Ferrets and Are Inhibited by Human Mucus but Not Swine Mucus. *J Virol.* 89, 5935-5948
- 128 Wasilewski, S. et al. (2012) Distribution of surface glycoproteins on influenza A virus determined by electron cryotomography. *Vaccine* 30, 7368–7373
- 129 Wu, N.C. et al. (2018) A complex epistatic network limits the mutational reversibility in the influenza hemagglutinin receptor-binding site. *Nat Commun.* 9, 1264
- 130 Vavricka, C.J. et al. (2013) Influenza neuraminidase operates via a nucleophilic mechanism and can be targeted by covalent inhibitors. *Nat Commun.* 4, 1491

## **Chapter 7**

**Second sialic acid-binding site of influenza A virus neuraminidase: binding receptors for efficient release**

## **Abstract**

Influenza A viruses (IAVs) are a major cause of human respiratory tract infections and cause significant disease and mortality. Human IAVs originate from animal viruses that breached the host species barrier. IAV particles contain sialoglycan receptor-binding haemagglutinin (HA) and receptor-destroying neuraminidase (NA) in their envelope. When IAV crosses the species barrier, the functional balance between HA and NA needs to be adjusted to the sialoglycan repertoire of the novel host species. Very little is known about the role of NA in host adaptation in contrast to the extensively studied HA. NA prevents virion aggregation and facilitates release of (newly assembled) virions from cell surfaces as well as from decoy receptors abundantly present in mucus. In addition to a highly conserved catalytic site, NA carries a second sialic acid binding site (2SBS). The 2SBS preferentially binds  $\alpha$ 2,3-linked sialic acids, and enhances activity of the neighboring catalytic site on multivalent substrates by bringing it in close contact with its substrate. In this way, the 2SBS significantly contributes to the HA-NA balance of virus particles and affects virus replication in an HA- and cell type-dependent manner. The 2SBS is highly conserved in all NA subtypes of avian IAVs, with some notable exceptions associated with changes in the receptor-binding specificity of HA and host tropism. Conservation of the 2SBS is lost in several viruses adapted to mammalian host species, including humans. Preservation or loss of the 2SBS is likely to be an important factor for (changes in) host tropism.

## Introduction

Sialoglycans are omnipresent at the surface of every cell type and therefore appear attractive attachment/entry receptors for viruses. Indeed, members of several virus families initiate cell infection by binding to cell surface sialoglycans, such as influenza viruses (IAVs), coronaviruses, picornaviruses, and paramyxoviruses (Thompson et al., 2019). Binding to sialoglycans comes at a cost, however, as the sheer abundance of these glycans makes it inherently difficult for viruses to bind their *bona fide* receptors as required for cell entry, and on the other hand to be released from cells at the end of the infection cycle. To solve this problem some enveloped viruses not only contain glycan-receptor binding properties, but also receptor-destroying activity carried in either a separate glycoprotein or an enzymatic domain genetically fused to the glycan-binding protein. These include neuraminidase (NA) proteins of influenza A and B viruses (IAV and IBVs), hemagglutinin-esterase fusion (HEF) proteins of influenza C and D viruses, hemagglutinin-esterase (HE) proteins of some coronaviruses (embecoviruses), and hemagglutinin–neuraminidase (HN) proteins of some paramyxoviruses.

Cleavage of sialoglycans has originally been recognized as being required for release of newly assembled virions and to prevent virion aggregation (Palese and Compans, 1976), but it is increasingly being appreciated that it also enables virion mobility through mucus layers containing heavily-sialylated mucin decoy receptors [reviewed by (de Vries et al., 2020)]. A functional balance between low affinity binding of individual attachment proteins to sialoglycans in combination with glycan-destroying activity is thought to enable these virions to move through environments with high concentrations of sialoglycans in search for their cell surface entry receptors.

IAVs are zoonotic pathogens that infect a broad range of host species, including humans, wild birds, poultry, pigs, horses, and marine mammals (Webster et al., 1992; Medina and García-Sastre, 2011). Aquatic birds are the natural host reservoir from which IAVs can jump to other host species. In humans IAVs cause seasonal epidemics resulting in major public health problems and a huge economic burden (Krammer et al., 2018). Occasional pandemics of influenza are caused by animal IAVs that managed to cross the host species barrier and adapt to humans (Taubenberger and Kash, 2010). In little more than 100 years, four of such pandemics have been recorded: H1N1 Spanish pandemic in 1918, H2N2 Asian pandemic in 1957, H3N2 Hong Kong pandemic in 1968, and H1N1 pandemic in 2009 (H1N1pdm09) (Edwin, 2006; Taubenberger and Kash, 2010). The H1N1 Spanish pandemic, which stands as the single most fatal event in human history, killed an estimated 50 million or more people (Johnson and Mueller, 2002). The other pandemics were less severe, resulting in much lower

casualties. In post-pandemic years, the pandemic viruses establish themselves in the human population and cause seasonal influenza, thereby usually replacing previous human IAV subtypes.

IAV particles contain two major surface glycoproteins: hemagglutinin (HA) and NA. HA, of which 16 subtypes exist in aquatic birds (H1-16), is responsible for virus binding to sialic acid (SIA) receptors on the cell surface and mediates virus-cell membrane fusion after endocytosis. The receptor-destroying enzyme NA, of which 9 subtypes are known in wild waterfowl (N1-9), cleaves SIA from glycosylated proteins and lipids. As HA and NA have apparent opposite functions and work in concert, a delicate balance between HA binding and NA cleavage is needed for efficient viral replication (Wagner et al., 2002; Gaymard et al., 2016; Byrd-Leotis et al., 2017; de Vries et al., 2020). For example, mutations in NA conferring resistance to antiviral drugs often result in reduced NA activity creating an altered HA-NA balance (Carr et al., 2002; Ives et al., 2002; Marjuki et al., 2015). The balance is subsequently restored by selecting for compensatory mutations in NA and/or HA that enhance NA activity (Bloom et al., 2010; Butler et al., 2014; Duan et al., 2014) or decrease HA binding affinity (Ginting et al., 2012).

The HA-NA balance of IAVs is probably highly adapted to the specific sialoglycan host repertoire and may constitute an important host tropism determinant (Chan et al., 2013; Walther et al., 2013; Lakdawala et al., 2015). When viruses cross the species barrier and encounter a novel sialoglycan repertoire in mucus and on the epithelial cell surface, the HA-NA balance of these viruses needs to be readjusted to allow efficient replication and intra- and inter-host spread. When avian IAVs cross the species barrier and adapt to humans, this is accompanied with a change in the receptor-binding preference of HA from SIAs connected to the penultimate galactose via  $\alpha$ 2,3- (avian-type receptors) to  $\alpha$ 2,6-linkage (human-type receptors) (Rogers and Paulson, 1983; Matrosovich et al., 2000). The mutations in the receptor-binding site of HA that cause this alteration have been extensively studied and characterized for different HA subtypes (de Graaf and Fouchier, 2014; Shi et al., 2014; de Vries et al., 2017). Compared to the well-documented HA, much less is known about the role of NA in host adaptation. Here, we review the available literature on a 2nd SIA binding site (2SBS) in NA, which is increasingly being recognized as an important determinant of NA enzymatic activity, HA-NA balance, virus replication and host tropism.

## **IAV NA**

NA is a type II glycoprotein, which forms tetramers of four identical polypeptides. Each protomer of about 470 amino acids harbors four distinct domains: the N-terminal cytoplasmic tail, the transmembrane region, the thin stalk and the catalytic head (**Figure 1**) [reviewed by (McAuley et al., 2019)]. Crystal structures of the box-shaped NA head domain have been determined for all IAV NA

subtypes (Burmeister et al., 1992; Russell et al., 2006; Xu et al., 2008; Li et al., 2010a; Sun et al., 2014). Each protomer forms a six-bladed propeller-like structure, with each blade having four antiparallel  $\beta$ -sheets that are stabilized by disulfide bonds and connected by loops of variable length (Varghese et al., 1983; McAuley et al., 2019). Each head domain contains a catalytic site with highly conserved residues that directly contact SIA and framework residues that keep the catalytic site in place. Close to the catalytic site NA contains a 2SBS (also referred to as hemadsorption site) with sialoglycan-binding properties (**Figure 1**) (Laver et al., 1984; Varghese et al., 1997).

The NA active site is highly conserved among all IAVs. Regardless whether NA is derived from an avian or human virus, it prefers cleavage of  $\alpha$ 2,3- over  $\alpha$ 2,6-linked sialosides. Human viruses, however, are generally more efficient in cleaving  $\alpha$ 2,6-linked SIAs than avian viruses (Baum and Paulson, 1991; Kobasa et al., 1999; Gambaryan and Matrosovich, 2015; Du et al., 2018). For example, N2 protein of human H2N2 and H3N2 viruses evolved an increased ability to cleave  $\alpha$ 2,6-linked SIAs, presumably to match the binding preference of HA. Increased cleavage of  $\alpha$ 2,6-linked SIAs was, however, not yet observed in the earliest pandemic H2N2 viruses (Baum and Paulson, 1991). The dual cleavage specificity of NA, i.e. the ability to cleave both  $\alpha$ 2,3- and  $\alpha$ 2,6-linked SIAs, appears to contrast the apparent clear receptor preference of HA of human viruses for  $\alpha$ 2,6 sialylated glycans and avian viruses for  $\alpha$ 2,3 sialylated glycans (Couceiro et al., 1993; Matrosovich et al., 1997; Matrosovich et al., 2007).

In contrast to the NA catalytic site, the stalk domain is subject to host species adaptation. Stalk deletions in several NA subtypes are regarded as a poultry adaptation of IAVs derived from aquatic birds (Li et al., 2011). Experimental studies showed that stalk truncations confer increased virulence in chickens (Munier et al., 2010), and interestingly also in mice (Zhou et al., 2009). All human pandemic and seasonal IAVs contain full length stalk domains. The length of the stalk domain has been shown to affect NA enzymatic activity of virus particles on multivalent receptor surfaces (Blumenkrantz et al., 2013). Deletions in the stalk result in lower enzymatic activity presumably by reducing access of the NA catalytic site to sialoglycan substrates (Baigent and McCauley, 2001). The role of the stalk domain in IAV replication and host tropism has been reviewed in detail elsewhere (Li et al., 2011; Long et al., 2015). Besides the stalk domain also the 2SBS displays host species adaptation. While the 2SBS is highly conserved in most avian IAVs it is invariably lost in human IAVs (Kobasa et al., 1997; Uhlenborff et al., 2009; Air, 2012; Du et al., 2018; Du et al., 2019), suggesting that the 2SBS plays an important role in the adaptation of IAV to humans as is discussed in more detail below.

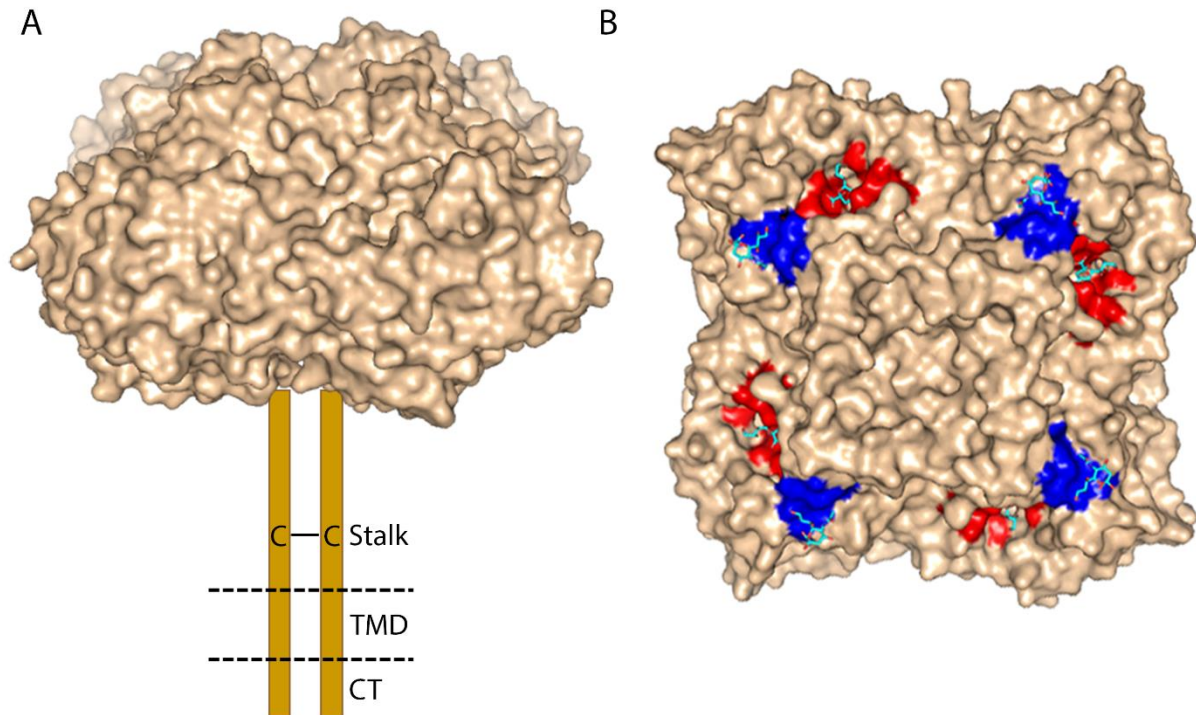


**Figure 1. NA structure.** (A) Schematic representation of NA structure. NA forms a homo-tetramer with four identical subunits. Each subunit contains a cytoplasmic tail (CT), transmembrane domain (TMD), stalk and head domain. Cys residues present in the stalk domain result in the formation of disulfide-bonds two protomers (C—C) (Air, 2012; McAuley et al., 2019). (B) Crystal structure of NA head domain (PDB ID: 1W20) shown in surface representation. The catalytic site and 2SBS bound with SIAs are colored red and blue, respectively. The SIA is shown as sticks (oxygen in red; nitrogen in blue; carbon in cyan). The figure is made by using Pymol.

### I) Structure of the 2SBS

Hemagglutinating activity of NA was first discovered in 1984 for N9 (Laver et al., 1984). In contrast to the NA catalytic activity the hemadsorption activity of NA was not inhibited by an NA inhibitor targeting the NA catalytic site. Amino acid residues responsible for hemadsorption were identified by sequencing monoclonal antibody escape mutants of N9 that had lost this activity (Webster et al., 1987) and led to the conclusion that enzymatic and hemadsorption activities of NA are associated with two separate sites on the head domain of N9. Hemagglutinating activity was acquired upon transfer of these amino acids by site-directed mutagenesis to an hemadsorption-negative N2 (Nuss and Air, 1991). Structural evidence for a 2SBS responsible for the hemadsorption activity of NA was obtained in 1997 by solving the crystal structure of N9 in complex with SIAs bound to both the catalytic site and the 2SBS (Varghese et al., 1997). While the catalytic site forms a deep pocket, the 2SBS forms a shallow pocket (**Figure 2**). Three loops – 370 loop (residues 366 to 373), 400 loop



(residues 399 to 404), and 430 loop (residues 430 to 433) – form the 2SBS and contain the SIA contacting residues: S367, S370, S372, N400, W403, and K432. These residues directly interact with SIA via hydrophobic interactions (W403) or the formation of hydrogen bonds (other residues). Until now, binding of SIA to the 2SBS has been demonstrated using X-ray crystallography for N2, N5, N6 and N9 (Varghese et al., 1997; Rudino-Pinera et al., 2004; Vavricka et al., 2013; Sun et al., 2014)(**Figure 2**) and by saturation-transfer difference (STD) NMR for N1 (Lai et al., 2012). Similar contacts between the 2SBS and SIA are observed for the different NAs as determined by X-ray crystallography, with exception of the residue at position 432, which only interacts with SIA in N9 (**Figure 2**). SIAs in the 2SBS and catalytic site adopt the chair and boat conformation, respectively (Sun et al., 2014). SIA bound to the receptor binding site of HA adopts the chair conformation as well (Shi et al., 2014). There is no direct interaction between the penultimate galactose residue and the 2SBS, which is different from HA-receptor binding where the galactose and N-acetylglucosamine residues in the sialoglycan also form critical interactions with the HA receptor binding site (Shi et al., 2014; Sun et al., 2014).

## II) Receptor-binding properties of the 2SBS

In early studies, the receptor-binding specificity of the 2SBS was analyzed using red blood cell binding assays. Hemadsorption by NA could be observed with erythrocytes from chicken and human origin, but not with equine, bovine or swine erythrocytes, suggesting that these latter erythrocytes do not contain sialoglycans that are recognized by the 2SBS (Kobasa et al., 1997). Equine, bovine and swine erythrocytes abundantly display N-glycolylneuraminic acid (Neu5Gc). Glycan array analysis indicated

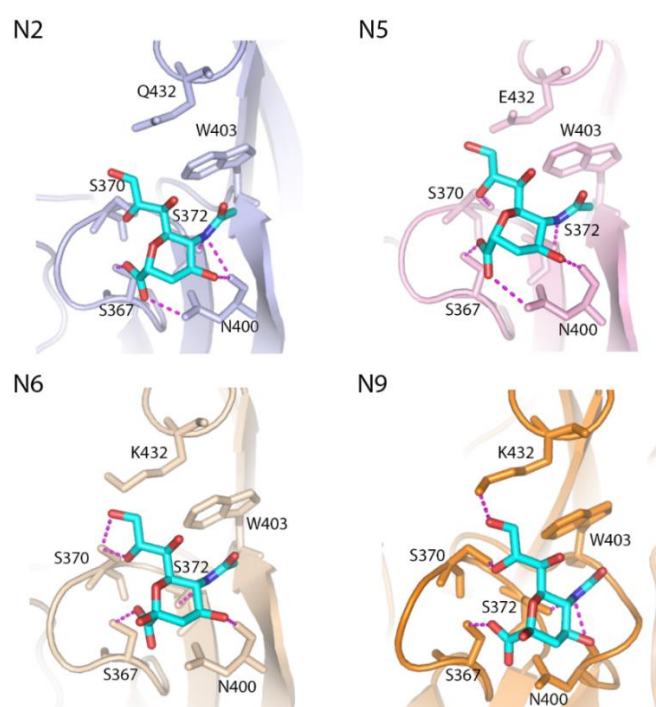


**Figure 2. Interaction of 2SBS with Neu5Ac.** The complex of the 2SBS with Neu5Ac for N2 (PDB ID: 4H53), N5 (PDB ID: 4QN5), N6 (PDB ID: 1W20) and N9 (PDB ID: 1MWE) is shown (Sun et al., 2014). Neu5Ac is shown as sticks (oxygen in red; nitrogen in blue; carbon in cyan). The numbering of residues in the 2SBS that directly contact with Neu5Ac is indicated (Note: W403 forms hydrophobic interactions with the Neu5Ac N-acetyl group). Hydrogen bonds are shown as dashed magenta lines. The figures are made by using Pymol.

that the 2SBS of N9 was able to bind to elongated sialoglycans containing Neu5Gc. This binding occurred, however, at lower efficiency than observed for sialoglycans containing N-acetylneuraminic acid (Neu5Ac), which is the SIA form that is found in humans and most avian species (Dai et al., 2017)(unpublished results). In other studies, erythrocytes that had been desialylated followed by linkage-type specific resialylation using  $\alpha$ 2,3- or  $\alpha$ 2,6-sialyltransferases were used to show that the 2SBS of N1 and N2 of avian viruses bound to  $\alpha$ 2,3- and  $\alpha$ 2,6-linked SIAs with similar efficiency (Hausmann et al., 1995; Uhlendorff et al., 2009). Cell-derived vesicles containing similar N1 or N2 proteins were shown by using biolayer interferometry (BLI), however, to exclusively bind to synthetic glycans containing  $\alpha$ 2,3-linked SIAs when blocking the NA catalytic site by NA inhibitor oseltamivir carboxylate (Du et al., 2018; Du et al., 2019). In agreement, as shown by glycan array analysis, N9 prefers binding to  $\alpha$ 2,3-linked sialosides, particularly bi- and triantennary glycans with multiple LacNAc repeats, whereas weak or no binding to  $\alpha$ 2,6-linked sialosides was observed (Dai et al., 2017). This discrepancy in the receptor-binding preference of the 2SBS is probably explained by the different methods used to analyze the receptor specificity of the 2SBS. A higher receptor density on erythrocytes compared to the BLI sensor surface might allow for binding of  $\alpha$ 2,6-linked SIAs. Alternatively, binding to resialylated erythrocytes might be affected by prior incomplete desialylation or by the absence of the catalytic site inhibitor oseltamivir carboxylate, which may enable binding via the catalytic site (Hausmann et al., 1995; Uhlendorff et al., 2009).

Interestingly, receptor binding via the 2SBS of N9 appeared more efficient than of avian N1, as recombinant soluble N9, but not N1, proteins complexed to lumazine synthase nanoparticles agglutinated human erythrocytes (Du et al., 2018). Glycan receptor-binding, including hemagglutination, could be demonstrated for N1, however, by displaying these proteins in vesicles or virus-like particles resulting in increased multivalency (Du et al., 2018; Du et al., 2020). Using STD-NMR, binding of  $\alpha$ 2,3-sialyllactose via the 2SBS was also observed for avian N1, which was much stronger than for N1 of H1N1pdm09 (Lai et al., 2012), in agreement with the presence and absence of hemagglutination activity of similar proteins when contained within virus-like particles (chapter 5). Mutations in all three loops of the 2SBS were shown to affect the receptor-binding properties of NA. These include mutations in both SIA-contact residues in the 370 loop (S367N for N2 and N9; S370L

for N1, N2 and N9; S372Y for N9) (Webster et al., 1987; Hausmann et al., 1995; Uhlendorff et al., 2009; Benton et al., 2017; Du et al., 2019) and the 400 loop (N400S for N2, N400K for N9; W403R for N2) (Webster et al., 1987; Uhlendorff et al., 2009) as well as some non-SIA contact residues (N369H for N1; A369D and T401A for N9) (Webster et al., 1987; Dai et al., 2017; Du et al., 2018). Also substitutions of residue K432, which is a SIA-contact residue in N9 but not N6 (**Figure 2**), in N1 (K432E) (Du et al., 2018) and N9 (K432N) (Webster et al., 1987), was shown to abolish (N1) or reduce (N9) the hemagglutination activity of the resulting NAs. Thus, NAs that differ in their 2SBS are likely to also differ in their receptor-binding properties.

### III) 2SBS and NA catalytic activity

Mutations in the 2SBS affect cleavage of SIAs from multivalent receptors such as glycoproteins or mucins much more than of monovalent substrates such as 2'-(4-Methylumbelliferyl)- $\alpha$ -D-N-acetylneuraminic acid (MUNANA) (chapter 5) (Uhlendorff et al., 2009; Benton et al., 2017; Dai et al., 2017; Du et al., 2018; Du et al., 2019; Du et al., 2020). 2SBS-positive N9 displayed a lower  $K_m$  value for fetuin, but not MUNANA, compared to a 2SBS-negative N9, while their  $k_{cat}$  values were similar (Benton et al., 2017). Mutations in all three receptor binding loops of the 2SBS for N1, N2 and N9 were shown to affect cleavage of multivalent substrates (Dai et al., 2017; Du et al., 2018; Du et al., 2019), indicating the importance of receptor binding by the 2SBS for cleavage by the catalytic site. In agreement herewith, glycan array analysis showed that glycans that were efficiently bound by the N9 2SBS were also cleaved efficiently (Dai et al., 2017). Cleavage of synthetic glycans immobilized on BLI sensors by N1 and N2 carrying a functional 2SBS was observed for  $\alpha$ 2,3- but not  $\alpha$ 2,6-linked sialoglycans, corresponding with their binding preference for  $\alpha$ 2,3-linked glycans (Du et al., 2018; Du et al., 2019). Likewise, cleavage of SIAs from fetuin, which contains both  $\alpha$ 2,3- and  $\alpha$ 2,6-linked sialosides, was generally much more affected by mutation of the 2SBS than cleavage of SIAs from transferrin, which only contains  $\alpha$ 2,6-linked sialosides (Dai et al., 2017; Du et al., 2018; Du et al., 2019; Du et al., 2020). Nevertheless, also for some multivalent substrates containing only  $\alpha$ 2,6-linked sialosides (modestly) altered cleavage of SIAs was observed upon mutation of the 2SBS (Uhlendorff et al., 2009; Dai et al., 2017; Du et al., 2018; Du et al., 2019; Du et al., 2020)(chapter 5), suggesting that the 2SBS may bind to some extent to these human-type receptors. Collectively, these studies indicate that mutations in the 2SBS resulting in enhanced or reduced catalytic activity against multivalent substrates primarily results from increased or reduced glycan-binding via the 2SBS rather than from direct effects of the substitutions in the 2SBS on the structure of the adjacent catalytic site.

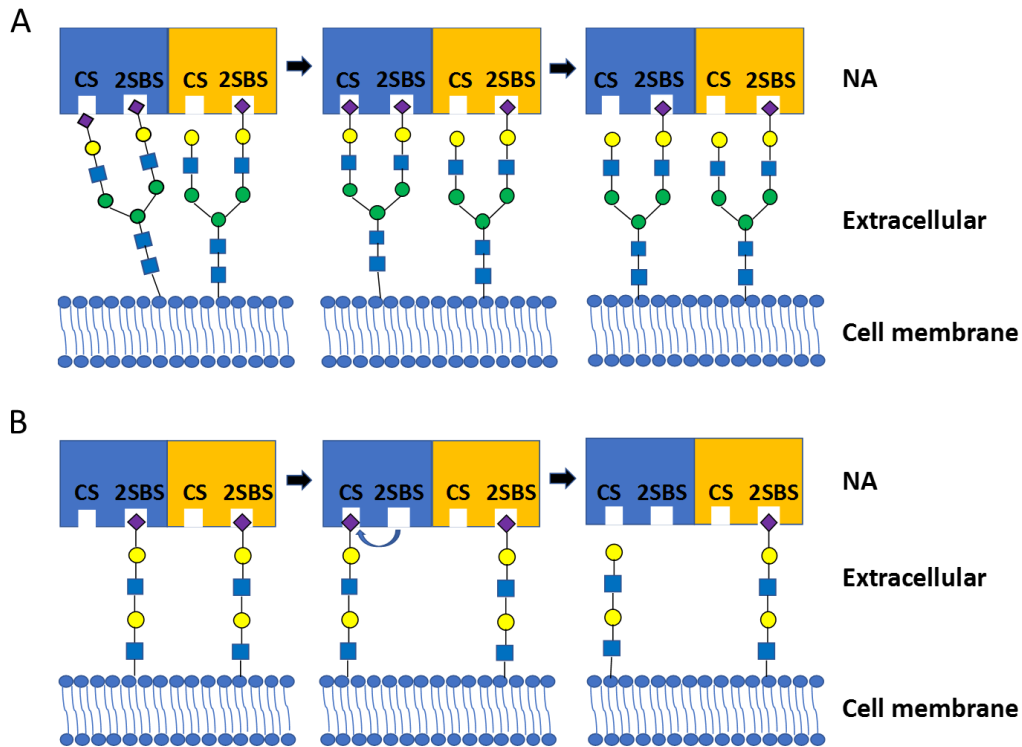


**Figure 3. Proposed models of the enhanced cleavage activity induced by the 2SBS.** (A) “Bind and trans-cleave” model: binding of the 2SBS to SIA on multivalent substrates brings adjacent SIA closer to the catalytic site (CS) in the same or another protomer, resulting in a higher cleavage efficiency. (B) “Bind and transfer” model: SIA receptors first bind to the 2SBS, after which they are transferred to the CS, resulting in enhanced cleavage of SIA by CS. Blue and yellow rectangle represent NAs. Purple diamond: Neu5Ac; yellow circle: galactose; green circle: mannose; blue square: N-acetylglucosamine.

Enhancement of NA catalytic activity by the 2SBS may be explained by a “bind and trans-cleave” model (Uhlendorff et al., 2009; Dai et al., 2017), in which the 2SBS recruits and keeps sialosides in close proximity of the catalytic site (**Figure 3A**). More recently, an alternative model was proposed (**Figure 3B**) (Durrant et al., 2020), in which the SIA receptors first bind the 2SBS before being transferred to the catalytic site, referred to as a “bind and transfer” mechanism. This latter model is based on Brownian dynamics simulations, which indicate that substrates bind faster to the 2SBS of avian NA than to the catalytic site (Sung et al., 2010; Amaro et al., 2018), and on chlorine anion distribution and the projection of the electrostatic potential onto the NA surface, which may indicate the existence of a path between the 2SBS and the catalytic site wide enough to allow movement of negatively charged SIAs (Durrant et al., 2020). Of note, cleavage of  $\alpha$ 2,6-linked SIAs by NA may be enhanced to a similar extent by a functional 2SBS as cleavage of  $\alpha$ 2,3-linked SIAs as long as the multivalent substrate (e.g. fetuin) also displays  $\alpha$ 2,3-linked sialosides preferred by the 2SBS (Du et al., 2019) (chapter 5). This result fits well with the “bind and trans-cleave” model but is more difficult

to reconcile with the “bind and transfer” model. In this latter model, enhanced cleavage of substrates would only be expected for those glycans that are bound by the 2SBS. Of note, enhancement of catalytic efficiency of glycoside hydrolases, by combining catalytic and glycan-binding domains, appears to be a common theme that is observed for most eukaryotic and bacterial NAs (Thobhani et al., 2003) as well as for other viral receptor-destroying enzymes, such as the HE protein of embecoviruses (Langereis et al., 2015; Bakkers et al., 2016).

#### **IV) Importance of the 2SBS for the HA-NA-receptor balance**

Uhlendorff and coworkers (Uhlendorff et al., 2009) showed that a functional 2SBS also contributes to catalytic activity of NA in the context of virions. H3N2 viruses that only differed in their 2SBS displayed identical hemagglutination activity but differed in the NA-driven disaggregation of the erythrocytes. Thus, virus with a non-functional 2SBS destroyed receptors on red blood cells more slowly than did its 2SBS-positive counterpart. Recent development of BLI-based assays to study virus-receptor interactions (Guo et al., 2018) allows for a more detailed analysis of the contribution of the 2SBS to the HA-NA-receptor balance. BLI enables analysis of virus binding by determining the initial binding rate of virus binding to a receptor-coated surface (Guo et al., 2018) or by analyzing the receptor density at which half maximum binding occurs (Benton et al., 2015). These assays are usually performed in the presence of inhibitors of the NA catalytic site. When NA activity is not (longer) inhibited, virus binding is followed by NA-driven virion mobility on the sensor surface, which finally results in virion self-elution when the receptor density is too low to sustain virion association (Guo et al., 2018). The rate at which viruses are released from the sensor surface reflects the HA-NA-receptor balance as it depends on the binding and cleavage characteristics of both HA and NA for the immobilized receptors.

Using BLI, the 2SBS was shown to contribute to receptor binding of virus particles in an HA- and receptor-dependent manner (Benton et al., 2017; Du et al., 2019). A functional 2SBS was shown to enhance H3N2 virion binding to synthetic glycans carrying  $\alpha$ 2,3- but not  $\alpha$ 2,6-linked SIAs, in agreement with the binding preference of the 2SBS. When combined with an H3 preferring binding to  $\alpha$ 2,6-linked SIAs, the 2SBS of N2 also enhanced binding to glycoprotein receptors LAMP1, carrying mostly N-glycans, and glycoporphin A, carrying mainly O-linked sugars. Enhanced binding to these glycoproteins was not observed when N2 was combined with an H3 that prefers binding to  $\alpha$ 2,3-linked SIAs (Du et al., 2019). The presence of a functional 2SBS was also shown to result in a lower receptor density at which half maximum virion binding was observed (Benton et al., 2017). The 2SBS is also a critical determinant of the HA-NA-receptor balance of virus particles as analyzed by BLI. 2SBS-positive viruses [H3N2 (Du et al., 2019), H5N1 and H1N1 (Du et al., 2020)] display faster self-elution from surfaces containing LAMP1 or glycoporphin A. Of note, the contribution of the 2SBS to

virion self-elution is larger when NA is combined with an HA that binds these receptors more strongly. Mutations that decreased HA-receptor binding avidity also decreased the contribution of the 2SBS to virion self-elution (Du et al., 2020). Apparently, a weaker-binding HA does not necessarily require a 2SBS-positive NA, with a higher enzymatic activity, for efficient self-elution.

#### **V) Influence of the 2SBS on virus replication**

Mutation of the 2SBS affects virus replication *in vitro* in an HA- and cell type-dependent manner. Several studies show that loss of a functional 2SBS negatively affected virus replication when NA was combined with HAs preferring binding to  $\alpha$ 2,3-linked sialoglycans [H1 (Du et al., 2018), H2 (Kobasa et al., 1997), H3 (Du et al., 2019), H5 (Du et al., 2018; Du et al., 2020)]. A recombinant virus, in which a 2SBS-negative N1 was combined with H5, rapidly reverted to a functional 2SBS, indicating the evolutionary advantage of a functional 2SBS for replication in cell culture *in vitro* (Du et al., 2018; Du et al., 2020). In contrast, a recombinant virus harboring the same NA and PR8 H1, which displays a lower receptor-binding avidity than H5, stably maintained the debilitating mutation in the 2SBS (Du et al., 2018; Du et al., 2020). These results indicate that the importance of the 2SBS for virus replication corresponds with its importance for the HA-NA balance, which is larger when NA is combined with a stronger binding HA.

An H3N2 virus with preferred avian-type receptor binding displayed reduced replication upon loss of a functional 2SBS in correspondence with its reduced virion self-elution. In contrast, absence of a functional 2SBS in N2 enhanced virus replication when combined with H3 from the 1968 pandemic virus, which prefers binding to  $\alpha$ 2,6-linked SIAs (Du et al., 2019). In this latter case, reduced virus replication and fuzzy plaques, resulting from the presence of many non-infected cells, corresponded with fast virion self-elution as determined by BLI. Possibly, high NA activity combined with low HA binding avidity tips the balance to premature virus dissociation from the cell surface before the virus can enter these cells. Replication in MDCK cells of a H3N9 recombinant virus carrying H3 from a human H3N2 virus from 2012, which displays reduced receptor binding to short human-type receptors (Lin et al., 2012; Gulati et al., 2013; Peng et al., 2017), was enhanced by the presence of a functional 2SBS in N9. No difference in virus propagation was observed, however, on MDCK cells with increased levels of  $\alpha$ 2,6-linked sialoglycans (Benton et al., 2017). Possibly, a functional 2SBS can enhance binding to cells when insufficient numbers of receptors are present. In summary, an optimal HA-NA balance appears to exist for virus replication *in vitro*, which is significantly influenced by the absence or presence of a functional 2SBS. The importance of a functional 2SBS in NA depends on HA binding affinity for the receptor repertoire that is present.

So far, only one study reported the importance of a functional 2SBS for virus replication *in vivo* (Kobasa et al., 1997). No difference in virus replication in ducks was reported for viruses with or without a 2SBS, although replication *in vitro* was reduced in the absence of the 2SBS. In this study, recombinant viruses were used containing HA and NA derived from different viruses. This may have resulted in a mismatched HA-NA combination, in which the presence of the 2SBS might be of minor influence. Alternatively, the virus acquired compensatory mutations in HA (discussed below) or a functional 2SBS may not be required for efficient replication, but rather for transmission between ducks. Clearly, additional studies are needed to demonstrate the importance of the 2SBS for IAV replication and possibly transmission *in vivo*.

#### VI) Conservation of the 2SBS in viruses from different host species

To visualize the conservation of the 2SBS of IAVs derived from different host species, we generated sequence logos of the three loops that constitute the 2SBS. The SIA-contact residues in the 370 and 400 loops are highly conserved in avian IAVs regardless of the NA subtype (**Figure 4**), with exception of residues at position 400 in N1 and 370 in N3. The presence of I400 in N1 might explain the reduced receptor binding of this NA compared to N9 (Du et al., 2018). The K432 SIA-contact residue in the 430 loop of N9 is conserved in some, but not in other NA subtypes. Mutation of K432 in N1 (Du et al., 2018) or N9 (Webster et al., 1987) negatively affected sialoglycan binding via the 2SBS. However, as avian N2 proteins carrying Q432 have a functional 2SBS (Uhlendorff et al., 2009; Du et al., 2019), a K at position 432 is not absolutely required for sialoglycan binding. Of note, N1 and N9 display some variations in non-SIA contact residues (positions 369 and 401), which may also affect the receptor-binding properties of NA (Dai et al., 2017; Du et al., 2018). Although so far a functional 2SBS has only been demonstrated for N1, N2, N5, N6 and N9, all other NA subtypes, with the exception of N3, display a high conservation in avian viruses of the SIA-contact residues in the 370 and 400 loops, indicating that a functional 2SBS is a highly conserved feature in most avian viruses.

The sequence logos of the 2SBS of N1 indicate that, while the SIA-contact residues are highly conserved in N1 protein of avian viruses, this conservation is invariably lost for both the seasonal (prior 2009) and the H1N1pdm09 viruses (**Figure 5**) (Uhlendorff et al., 2009; Du et al., 2018). Based on Brownian dynamics simulation, it was concluded that some of the key features of the 2SBS are retained in N1 of H1N1pdm09 (with N372 and K432), although this NA displayed a 16-fold reduced  $k_{on}$  compared to N1 from an avian virus (Sung et al., 2010). STD-NMR analyses confirmed that N1 of seasonal H1N1 virus (prior to 2009) and of H1N1pdm09 have some residual binding of  $\alpha$ 2,3-sialyllactose, which is much lower than for N1 of avian H5N1 virus (Lai et al., 2012). Interestingly, differential effects on the cleavage of monovalent and multivalent substrates indicates that N372K and K432E substitutions in NA of H1N1pdm09 increased and decreased receptor-binding via the

2SBS, respectively. This indicates that also low avidity binding via the 2SBS of H1N1pdm09 can contribute to catalytic activity (chapter 5). Receptor binding by N1 of H1N1pdm09 could not be detected in contrast to N1 of H5N1 (chapter 5).

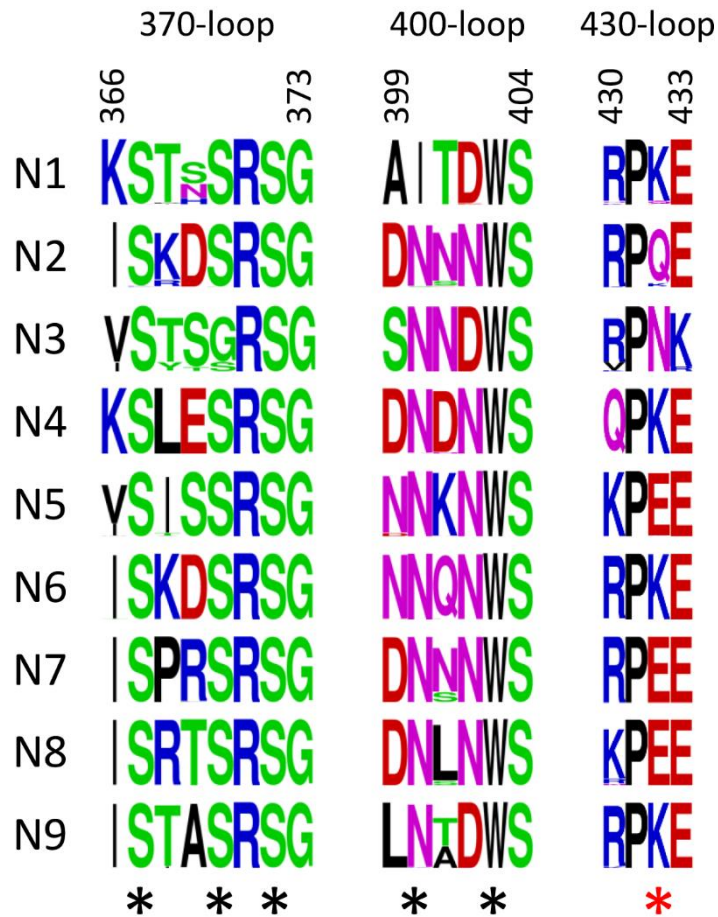


**Figure 4. Sequence logos of the 2SBS of avian N1-9.** Sequence logos were created for the three loops in the 2SBS: 370-loop (residues 366 to 373), 400-loop (residues 399 to 404) and 430-loop (residues 430 to 433) with the WebLogo program (<https://weblogo.berkeley.edu/logo.cgi>) (Crooks et al., 2004) using all sequences available for avian N1 to N9 on Influenza Research Database (<https://www.fludb.org/>). For N2, H9N2 viruses were excluded from the analysis. The overall height of the stack represents the sequence conservation at that position, while the height of the symbols within the stack indicates the relative frequency of each amino acid at that position. SIA contact residues are labelled with black asterisks. The red asterisk indicates an additional SIA contact residue in N9.

The role of the 2SBS in N1 of swine IAVs appears much more complex, as both in the classical and the Eurasian lineages, viruses/clades are present with and without a conserved 2SBS. Interestingly, the clade within the Eurasian lineage from which the N1 of H1N1pdm09 evolved has a conserved functional 2SBS, including the most closely-related N1 protein from a swine H1N1 virus isolated from



before 2009 that is present in the NCBI database (A/swine/Alsfeld/6673/2007(H1N1); GenBank: AZS66675.1). In contrast, closely related swine viruses isolated in Mexico in 2012 that form a sister lineage to H1N1pdm09 for HA and NA, and which do not result from a reverse zoonosis event, do contain the S372N mutation (Mena et al., 2016). Possibly, the mutation of the 2SBS was an important event in the emergence of H1N1pdm09. Just as in N1 of human viruses, the 2SBS of human H2N2 and H3N2 viruses is essentially invariably mutated. Again, these mutations involve both SIA-contact and non-contact residues (**Figure 5**) (Kobasa et al., 1997; Uhlenendorff et al., 2009; Du et al., 2019). The lack of conservation in the 2SBS of both N1 and N2 of human viruses indicates that a mutated 2SBS may be regarded as an adaptation to replication in, and transmission between, humans.

The 2SBS is highly conserved in N2 of avian HxN2 viruses, with the exception of H9N2 viruses, which display a large variability in (non-)contact residues (Matrosovich et al., 2001b; Aamir et al., 2007; Tombari et al., 2011; Naguib et al., 2017) (**Figure 5**). Avian H9N2 viruses are mainly (>80%) found in Galliformes species (chicken, turkey and quail), while other avian N2 viruses are circulating mainly in non-Galliformes species (>75%) (Du et al., 2019). Mutation of the 2SBS in the early 1980ies ([https://nextstrain.org/staging/flu/avian/h9n2/na?c=gt-NA\\_367](https://nextstrain.org/staging/flu/avian/h9n2/na?c=gt-NA_367)) may have contributed to the success of H9N2 viruses in Galliformes species. H3N2 viruses of dogs originated from avian H3N2 viruses and can now transmit between dogs and to cats (Song et al., 2008; Li et al., 2010b). The change in host tropism of these H3N2 viruses was accompanied with a S370L mutation in the 370 loop of the 2SBS (**Figure 5**). Equine H7N7 and H3N8 viruses also contain mutations in the 2SBS compared to their avian counterparts. All equine H7N7 viruses contain substitution S370L, while approximately half of the equine H3N8 viruses contain N400D. The conservation of some of the non-SIA-contacts is also less strict in the equine viruses. All H3N8 dog viruses, which originate from equine H3N8 viruses, contain D400 in the 2SBS. Notably, while N3 proteins of avian viruses do not have a strict conservation of the SIA-contact residue S370, this residue is strictly conserved in H16N3 gull viruses. Although founder effects can sometimes not be excluded, the repeated correlation between the preservation and loss of the 2SBS and adaptation to a certain host species is indicative of an important role for the 2SBS in host tropism (changes).

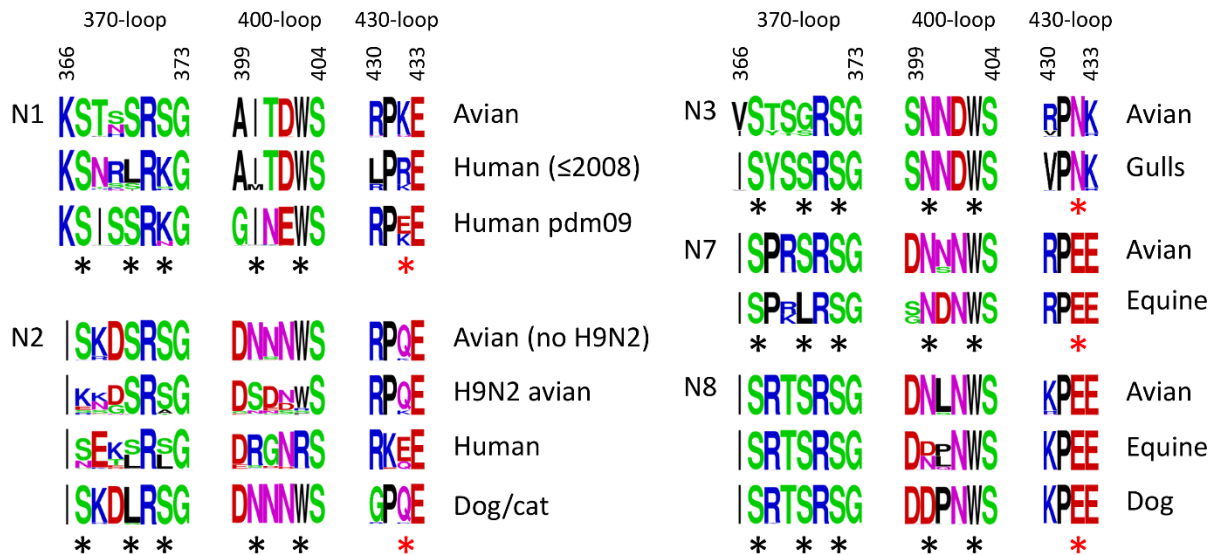


**Figure 5. Sequence logos of the 2SBS of NA proteins from viruses that infect different species.** Sequence logos were generated for the three loops that constitute the 2SBS similarly as described in the legend to Figure 4. All NA sequences available for viruses infecting different species from the Influenza Research Database (<https://www.fludb.org/>) were used. For N1 of human viruses, sequences were limited to sequences prior to 2009 [seasonal H1N1 virus; Human (<2009)] or between 2010-2016 (H1N1pdm09; (Human pdm09). For N2 of human viruses, sequences were limited to sequences prior to 2012. SIA contact residues are labelled with black asterisks. The red asterisk indicates an additional SIA contact residue in N9.

### VII) Interplay between HA, NA and (decoy) sialoglycans

Perhaps not surprisingly in view of the interplay between HA and NA, mutations in the 2SBS are often accompanied with mutations in HA that affect its receptor-binding properties. This, as mentioned above, holds true for the human N1- and N2-containing viruses, in which NAs with a mutated 2SBS (**Figure 5**) are associated with HA proteins that prefer binding to human-type receptors (Rogers and Paulson, 1983; Matrosovich et al., 2000; de Graaf and Fouchier, 2014; Shi et al., 2014). Likewise, loss of the 2SBS in canine H3N2 and H3N8 viruses is for both subtypes accompanied with a W222L mutation in the receptor-binding site of H3 (Yang et al., 2013; Wen et al., 2018). Canine H3 proteins predominantly bind to  $\alpha$ 2,3-linked sialosides, but display higher binding avidity to fucosylated and sulfated glycan receptors and glycans with Neu5Gc moieties compared to precursor avian and equine HAs lacking this mutation (Yang et al., 2013; Collins et al., 2014; Wen et al., 2018). Similarly, equine H7N7 viruses not only carried NA with a mutated 2SBS, but also contained HA that preferentially bound to  $\alpha$ 2,3-linked Neu5Gc, in contrast to avian H7-containing viruses which prefer binding to Neu5Ac-containing sialoglycans (Gambaryan et al., 2012; Broszeit et al., 2019). N3 proteins of gull viruses, which have a conserved 2SBS, always team up with H16 proteins, which appear to differ in

their receptor-binding properties from HAs that are combined with N3 proteins containing G370 found in other avian species (Gambaryan et al., 2018).

Two scenarios can be envisioned via which IAVs acquire mutations in both the receptor-binding sites of HA and NA. The first scenario is that mutations in HA precede and drive mutations in NA. Thus, changes obtained in HA as an adaptation to the sialoglycan repertoire of a novel host species, may be followed by compensatory mutations in the 2SBS of NA. Such NA mutations may also serve to escape inhibitory molecules that may be present in the novel host species, e.g. in saliva (Iverson et al., 2017). An alternative scenario is that mutations in the 2SBS of NA may precede or drive compensatory mutations in HA, thereby facilitating a host tropism jump. Often it is unclear which protein mutated first due to a lack of sequences available. Thus, for pandemic H1N1 and H2N2 viruses from 1918 and 1957 it cannot be indisputably concluded whether the mutations in the receptor-binding site of HA, resulting in increased binding to human-type receptors and decreased binding to avian-type receptors, preceded or followed mutations in the 2SBS of NA. For some viruses, however, phylogenetic analysis indicates that mutation of the 2SBS preceded, and may have driven, mutations in HA that change its receptor-binding properties. Substitution T401A in NA of novel H7N9 viruses, known to decrease receptor binding via the 2SBS and NA catalytic activity, preceded the Q226L mutation that results in decreased binding to avian- and increased to human-type receptors (Dortmans et al., 2013; Shi et al., 2013; Dai et al., 2017; de Vries et al., 2017). Also for H9N2 viruses, mutations in the 2SBS of N2 preceded mutations in H9 (Du et al., 2020), including Q226L, known to affect the receptor-binding properties of H9 and to result in increased binding to human- and decreased binding to avian-type receptors (Matrosovich et al., 2001a; Neumann and Kawaoka, 2015). The plausibility of a scenario, in which mutations in the 2SBS drive acquisition of mutations in HA that alter its receptor-binding properties, was recently experimentally shown for H5N1 virus (Du et al., 2020). Passaging H5N1 viruses with a mutated 2SBS in cell culture rapidly resulted in the selection of mutations in NA that restored the 2SBS and/or in HA that reduced binding to avian-type receptors to compensate for the lowered NA activity. Of note, one of these mutations in HA (S223N) concomitantly increased binding to human-type receptors, similarly as observed for H7N9 and H9N2 field viruses. Probably also for H7N9 and H9N2 viruses, mutations that increased binding to human-type receptors were primarily selected for their negative effect on binding to avian-type receptors in order to restore the HA-NA balance after loss of a functional 2SBS.

## Outlook

A complex interplay exists between receptor-binding and -cleavage of IAV virions, which needs to be adapted to the sialoglycan repertoire of specific host species and is an important determinant of host tropism. As emphasized by this review, the precarious HA-NA-receptor balance that is required includes not only the receptor-destroying activity of NA, but also the receptor binding affinity of its 2SBS. This binding may affect virion binding to a receptor-containing surface but is also of critical importance for the catalytic activity of virions. Likewise, receptor-binding via HA was also shown to contribute to the catalytic activity of virions (Guo et al., 2018; Lai et al., 2019). To add to this complexity, receptor binding by the catalytic site of NA may also contribute to the initial binding rate of virions, which is more pronounced for a low activity NA (Lin et al., 2010; Mögling et al., 2017; Guo et al., 2018). The HA-NA-receptor balance needs adjustment when IAVs infect a novel host species, but is also continuously subjected to alterations and thus requires compensation when well-adapted viruses remain replicating in their favored host species due to antigenic drift. Antigenic drift in HA has been shown to be accompanied with altered receptor-binding properties (Smith et al., 2004; Hensley et al., 2009; Lin et al., 2012; Gulati et al., 2013; Koel et al., 2013; Peng et al., 2017). Likewise, antigenic drift in NA, e.g. resulting from mutations in the 2SBS, may also alter NA catalytic activity. That mutations in the 2SBS contribute to antigenic drift is indicated by such mutations abrogating the binding of several monoclonal antibodies (Webster et al., 1987; Tulip et al., 1992; Malby et al., 1994; Jiang et al., 2016; Rijal et al., 2020), while they also appear to affect inhibition of NA activity by polyclonal sera (Gao et al., 2019)(chapter 5). The entanglement of NA phenotypic properties, as exemplified by mutation of the 2SBS affecting both NA activity and antigenicity, may be an important determinant of NA evolution (chapter 5). Recently developed assays based on live imaging (Sakai et al., 2017; Vahey and Fletcher, 2019) or BLI analyses (Guo et al., 2018) enable researchers to study the (evolution of the) HA-NA-receptor balance of IAVs, and the contribution of the 2SBS thereto, in detail. Such kinetic assays are needed to understand the full complexity of IAV evolution, including links between HA-NA-receptor balance, host tropism, antigenic drift and the zoonotic potential of IAVs.

## References

- Aamir, U.B., Wernery, U., Ilyushina, N., and Webster, R.G. (2007). Characterization of avian H9N2 influenza viruses from United Arab Emirates 2000 to 2003. *Virology* 361(1), 45-55. doi: 10.1016/j.virol.2006.10.037.
- Air, G.M. (2012). Influenza neuraminidase. *Influenza and Other Respiratory Viruses* 6(4), 245-256. doi: 10.1111/j.1750-2659.2011.00304.x.
- Amaro, R.E., leong, P.U., Huber, G., Dommer, A., Steven, A.C., Bush, R.M., et al. (2018). A Computational Assay that Explores the Hemagglutinin/Neuraminidase Functional Balance Reveals the Neuraminidase Secondary Site as a Novel Anti-Influenza Target. *ACS Cent Sci* 4(11), 1570-1577. doi: 10.1021/acscentsci.8b00666.
- Baigent, S.J., and McCauley, J.W. (2001). Glycosylation of haemagglutinin and stalk-length of neuraminidase combine to regulate the growth of avian influenza viruses in tissue culture. *Virus Research* 79(1), 177-185. doi: [https://doi.org/10.1016/S0168-1702\(01\)00272-6](https://doi.org/10.1016/S0168-1702(01)00272-6).
- Bakkers, M.J.G., Zeng, Q., Feitsma, L.J., Hulswit, R.J.G., Li, Z., Westerbeke, A., et al. (2016). Coronavirus receptor switch explained from the stereochemistry of protein-carbohydrate interactions and a single mutation. *Proceedings of the National Academy of Sciences* 113(22), E3111. doi: 10.1073/pnas.1519881113.
- Baum, L.G., and Paulson, J.C. (1991). The N2 neuraminidase of human influenza virus has acquired a substrate specificity complementary to the hemagglutinin receptor specificity. *Virology* 180(1), 10-15. doi: [https://doi.org/10.1016/0042-6822\(91\)90003-T](https://doi.org/10.1016/0042-6822(91)90003-T).
- Benton, D.J., Martin, S.R., Wharton, S.A., and McCauley, J.W. (2015). Biophysical measurement of the balance of influenza a hemagglutinin and neuraminidase activities. *The Journal of biological chemistry* 290(10), 6516-6521. doi: 10.1074/jbc.M114.622308.
- Benton, D.J., Wharton, S.A., Martin, S.R., and McCauley, J.W. (2017). Role of Neuraminidase in Influenza A(H7N9) Virus Receptor Binding. *J Virol* 91(11). doi: 10.1128/JVI.02293-16.
- Bloom, J.D., Gong, L.I., and Baltimore, D. (2010). Permissive Secondary Mutations Enable the Evolution of Influenza Oseltamivir Resistance. *Science* 328(5983), 1272. doi: 10.1126/science.1187816.
- Blumenkrantz, D., Roberts, K.L., Shelton, H., Lycett, S., and Barclay, W.S. (2013). The Short Stalk Length of Highly Pathogenic Avian Influenza H5N1 Virus Neuraminidase Limits Transmission of Pandemic H1N1 Virus in Ferrets. *Journal of Virology* 87(19), 10539. doi: 10.1128/JVI.00967-13.
- Broszeit, F., Tzarum, N., Zhu, X., Nemanichvili, N., Eggink, D., Leenders, T., et al. (2019). N-Glycolylneuraminic Acid as a Receptor for Influenza A Viruses. *Cell reports* 27(11), 3284-3294.e3286. doi: 10.1016/j.celrep.2019.05.048.
- Burmeister, W.P., Ruigrok, R.W., and Cusack, S. (1992). The 2.2 Å resolution crystal structure of influenza B neuraminidase and its complex with sialic acid. *The EMBO journal* 11(1), 49-56.
- Butler, J., Hooper, K.A., Petrie, S., Lee, R., Maurer-Stroh, S., Reh, L., et al. (2014). Estimating the fitness advantage conferred by permissive neuraminidase mutations in recent oseltamivir-resistant A(H1N1)pdm09 influenza viruses. *PLoS pathogens* 10(4), e1004065-e1004065. doi: 10.1371/journal.ppat.1004065.
- Byrd-Leotis, L., Cummings, R.D., and Steinhauer, D.A. (2017). The Interplay between the Host Receptor and Influenza Virus Hemagglutinin and Neuraminidase. *International journal of molecular sciences* 18(7), 1541. doi: 10.3390/ijms18071541.
- Carr, J., Ives, J., Kelly, L., Lambkin, R., Oxford, J., Mendel, D., et al. (2002). Influenza virus carrying neuraminidase with reduced sensitivity to oseltamivir carboxylate has altered properties in vitro and is compromised for infectivity and replicative ability in vivo. *Antiviral Research* 54(2), 79-88. doi: [https://doi.org/10.1016/S0166-3542\(01\)00215-7](https://doi.org/10.1016/S0166-3542(01)00215-7).
- Chan, R.W.Y., Karamanska, R., Van Poucke, S., Van Reeth, K., Chan, I.W.W., Chan, M.C.W., et al. (2013). Infection of swine ex vivo tissues with avian viruses including H7N9 and correlation

- with glycomic analysis. *Influenza and Other Respiratory Viruses* 7(6), 1269-1282. doi: 10.1111/irv.12144.
- Collins, P.J., Vachieri, S.G., Haire, L.F., Ogradowicz, R.W., Martin, S.R., Walker, P.A., et al. (2014). Recent evolution of equine influenza and the origin of canine influenza. *Proceedings of the National Academy of Sciences* 111(30), 11175. doi: 10.1073/pnas.1406606111.
- Couceiro, J.N.S.S., Paulson, J.C., and Baum, L.G. (1993). Influenza virus strains selectively recognize sialyloligosaccharides on human respiratory epithelium; the role of the host cell in selection of hemagglutinin receptor specificity. *Virus Research* 29(2), 155-165. doi: [https://doi.org/10.1016/0168-1702\(93\)90056-S](https://doi.org/10.1016/0168-1702(93)90056-S).
- Crooks, G.E., Hon, G., Chandonia, J.-M., and Brenner, S.E. (2004). WebLogo: a sequence logo generator. *Genome research* 14(6), 1188-1190. doi: 10.1101/gr.849004.
- Dai, M., McBride, R., Dortmans, J., Peng, W., Bakkers, M.J.G., de Groot, R.J., et al. (2017). Mutation of the Second Sialic Acid-Binding Site, Resulting in Reduced Neuraminidase Activity, Preceded the Emergence of H7N9 Influenza A Virus. *J Virol* 91(9). doi: 10.1128/JVI.00049-17.
- de Graaf, M., and Fouchier, R.A.M. (2014). Role of receptor binding specificity in influenza A virus transmission and pathogenesis. *The EMBO Journal* 33(8), 823-841. doi: 10.1002/embj.201387442.
- de Vries, E., Du, W., Guo, H., and de Haan, C.A.M. (2020). Influenza A Virus Hemagglutinin-Neuraminidase-Receptor Balance: Preserving Virus Motility. *Trends in microbiology* 28(1), 57-67. doi: 10.1016/j.tim.2019.08.010.
- de Vries, R.P., Peng, W., Grant, O.C., Thompson, A.J., Zhu, X., Bouwman, K.M., et al. (2017). Three mutations switch H7N9 influenza to human-type receptor specificity. *PLOS Pathogens* 13(6), e1006390. doi: 10.1371/journal.ppat.1006390.
- Dortmans, J.C.F.M., Dekkers, J., Wickramasinghe, I.N.A., Verheije, M.H., Rottier, P.J.M., van Kuppeveld, F.J.M., et al. (2013). Adaptation of novel H7N9 influenza A virus to human receptors. *Scientific Reports* 3(1), 3058. doi: 10.1038/srep03058.
- Du, W., Dai, M., Li, Z., Boons, G.-J., Peeters, B., van Kuppeveld, F.J.M., et al. (2018). Substrate Binding by the Second Sialic Acid-Binding Site of Influenza A Virus N1 Neuraminidase Contributes to Enzymatic Activity. *Journal of virology* 92(20), e01243-01218. doi: 10.1128/JVI.01243-18.
- Du, W., Guo, H., Nijman, V.S., Doedt, J., van der Vries, E., van der Lee, J., et al. (2019). The 2nd sialic acid-binding site of influenza A virus neuraminidase is an important determinant of the hemagglutinin-neuraminidase-receptor balance. *PLoS Pathog* 15(6), e1007860. doi: 10.1371/journal.ppat.1007860.
- Du, W., Wolfert, M.A., Peeters, B., van Kuppeveld, F.J.M., Boons, G.-J., de Vries, E., et al. (2020). Crosstalk between the receptor-binding properties of influenza A virus hemagglutinin and neuraminidase drives their co-evolution. *PLOS Pathogens*.
- Duan, S., Govorkova, E.A., Bahl, J., Zaraket, H., Baranovich, T., Seiler, P., et al. (2014). Epistatic interactions between neuraminidase mutations facilitated the emergence of the oseltamivir-resistant H1N1 influenza viruses. *Nature Communications* 5(1), 5029. doi: 10.1038/ncomms6029.
- Durrant, J.D., Kochanek, S.E., Casalino, L., leong, P.U., Dommer, A.C., and Amaro, R.E. (2020). Mesoscale All-Atom Influenza Virus Simulations Suggest New Substrate Binding Mechanism. *ACS Cent Sci* 6(2), 189-196. doi: 10.1021/acscentsci.9b01071.
- Edwin, D.K. (2006). Influenza Pandemics of the 20th Century. *Emerging Infectious Disease journal* 12(1), 9. doi: 10.3201/eid1201.051254.
- Gambaryan, A.S., and Matrosovich, M.N. (2015). What adaptive changes in hemagglutinin and neuraminidase are necessary for emergence of pandemic influenza virus from its avian precursor? *Biochemistry (Moscow)* 80(7), 872-880. doi: 10.1134/S000629791507007X.
- Gambaryan, A.S., Matrosovich, T.Y., Boravleva, E.Y., Lomakina, N.F., Yamnikova, S.S., Tuzikov, A.B., et al. (2018). Receptor-binding properties of influenza viruses isolated from gulls. *Virology* 522, 37-45. doi: <https://doi.org/10.1016/j.virol.2018.07.004>.

- Gambaryan, A.S., Matrosovich, T.Y., Philipp, J., Munster, V.J., Fouchier, R.A.M., Cattoli, G., et al. (2012). Receptor-Binding Profiles of H7 Subtype Influenza Viruses in Different Host Species. *Journal of Virology* 86(8), 4370. doi: 10.1128/JVI.06959-11.
- Gao, J., Couzens, L., Burke, D.F., Wan, H., Wilson, P., Memoli, M.J., et al. (2019). Antigenic Drift of the Influenza A(H1N1)pdm09 Virus Neuraminidase Results in Reduced Effectiveness of A/California/7/2009 (H1N1pdm09)-Specific Antibodies. *mBio* 10(2), e00307-00319. doi: 10.1128/mBio.00307-19.
- Gaymard, A., Le Briand, N., Frobert, E., Lina, B., and Escuret, V. (2016). Functional balance between neuraminidase and haemagglutinin in influenza viruses. *Clin Microbiol Infect* 22(12), 975-983. doi: 10.1016/j.cmi.2016.07.007.
- Ginting, T.E., Shinya, K., Kyan, Y., Makino, A., Matsumoto, N., Kaneda, S., et al. (2012). Amino Acid Changes in Hemagglutinin Contribute to the Replication of Oseltamivir-Resistant H1N1 Influenza Viruses. *Journal of Virology* 86(1), 121. doi: 10.1128/JVI.06085-11.
- Gulati, S., Smith, D.F., Cummings, R.D., Couch, R.B., Griesemer, S.B., St. George, K., et al. (2013). Human H3N2 Influenza Viruses Isolated from 1968 To 2012 Show Varying Preference for Receptor Substructures with No Apparent Consequences for Disease or Spread. *PLOS ONE* 8(6), e66325. doi: 10.1371/journal.pone.0066325.
- Guo, H., Rabouw, H., Slomp, A., Dai, M., van der Vegt, F., van Lent, J.W.M., et al. (2018). Kinetic analysis of the influenza A virus HA/NA balance reveals contribution of NA to virus-receptor binding and NA-dependent rolling on receptor-containing surfaces. *PLoS pathogens* 14(8), e1007233-e1007233. doi: 10.1371/journal.ppat.1007233.
- Hausmann, J., Kretzschmar, E., Garten, W., and Klenk, H.-D. (1995). N1 neuraminidase of influenza virus A/FPV/Rostock/34 has haemadsorbing activity. *Journal of General Virology* 76(7), 1719-1728. doi: <https://doi.org/10.1099/0022-1317-76-7-1719>.
- Hensley, S.E., Das, S.R., Bailey, A.L., Schmidt, L.M., Hickman, H.D., Jayaraman, A., et al. (2009). Hemagglutinin Receptor Binding Avidity Drives Influenza A Virus Antigenic Drift. *Science* 326(5953), 734. doi: 10.1126/science.1178258.  
[https://nextstrain.org/staging/flu/avian/h9n2/na?c=gt-NA\\_367](https://nextstrain.org/staging/flu/avian/h9n2/na?c=gt-NA_367).
- Ives, J.A.L., Carr, J.A., Mendel, D.B., Tai, C.Y., Lambkin, R., Kelly, L., et al. (2002). The H274Y mutation in the influenza A/H1N1 neuraminidase active site following oseltamivir phosphate treatment leave virus severely compromised both in vitro and in vivo. *Antiviral Research* 55(2), 307-317. doi: [https://doi.org/10.1016/S0166-3542\(02\)00053-0](https://doi.org/10.1016/S0166-3542(02)00053-0).
- Ivinson, K., Deliyannis, G., McNabb, L., Grollo, L., Gilbertson, B., Jackson, D., et al. (2017). Salivary Blockade Protects the Lower Respiratory Tract of Mice from Lethal Influenza Virus Infection. *J Virol* 91(14). doi: 10.1128/JVI.00624-17.
- Jiang, L., Fantoni, G., Couzens, L., Gao, J., Plant, E., Ye, Z., et al. (2016). Comparative Efficacy of Monoclonal Antibodies That Bind to Different Epitopes of the 2009 Pandemic H1N1 Influenza Virus Neuraminidase. *Journal of Virology* 90(1), 117. doi: 10.1128/JVI.01756-15.
- Johnson, N.P., and Mueller, J. (2002). Updating the accounts: global mortality of the 1918-1920 "Spanish" influenza pandemic. *Bull Hist Med* 76(1), 105-115. doi: 10.1353/bhm.2002.0022.
- Kobasa, D., Kodihalli, S., Luo, M., Castrucci, M.R., Donatelli, I., Suzuki, Y., et al. (1999). Amino Acid Residues Contributing to the Substrate Specificity of the Influenza A Virus Neuraminidase. *Journal of Virology* 73(8), 6743.
- Kobasa, D., Rodgers, M.E., Wells, K., and Kawaoka, Y. (1997). Neuraminidase hemadsorption activity, conserved in avian influenza A viruses, does not influence viral replication in ducks. *Journal of virology* 71(9), 6706-6713.
- Koel, B.F., Burke, D.F., Bestebroer, T.M., van der Vliet, S., Zondag, G.C.M., Vervaet, G., et al. (2013). Substitutions Near the Receptor Binding Site Determine Major Antigenic Change During Influenza Virus Evolution. *Science* 342(6161), 976. doi: 10.1126/science.1244730.
- Krammer, F., Smith, G.J.D., Fouchier, R.A.M., Peiris, M., Kedzierska, K., Doherty, P.C., et al. (2018). Influenza. *Nature reviews. Disease primers* 4(1), 3-3. doi: 10.1038/s41572-018-0002-y.

- Lai, J.C.C., Garcia, J.-M., Dyason, J.C., Böhm, R., Madge, P.D., Rose, F.J., et al. (2012). A Secondary Sialic Acid Binding Site on Influenza Virus Neuraminidase: Fact or Fiction? *Angewandte Chemie International Edition* 51(9), 2221-2224. doi: 10.1002/anie.201108245.
- Lai, J.C.C., Karunarathna, H.M.T.K., Wong, H.H., Peiris, J.S.M., and Nicholls, J.M. (2019). Neuraminidase activity and specificity of influenza A virus are influenced by haemagglutinin-receptor binding. *Emerging Microbes & Infections* 8(1), 327-338. doi: 10.1080/22221751.2019.1581034.
- Lakdawala, S.S., Jayaraman, A., Halpin, R.A., Lamirande, E.W., Shih, A.R., Stockwell, T.B., et al. (2015). The soft palate is an important site of adaptation for transmissible influenza viruses. *Nature* 526(7571), 122-125. doi: 10.1038/nature15379.
- Langereis, Martijn A., Bakkens, Mark J.G., Deng, L., Padler-Karavani, V., Vervoort, Stephin J., Hulswit, Ruben J.G., et al. (2015). Complexity and Diversity of the Mammalian Sialome Revealed by Nidovirus Virolectins. *Cell Reports* 11(12), 1966-1978. doi: <https://doi.org/10.1016/j.celrep.2015.05.044>.
- Laver, W.G., Colman, P.M., Webster, R.G., Hinshaw, V.S., and Air, G.M. (1984). Influenza virus neuraminidase with hemagglutinin activity. *Virology* 137(2), 314-323. doi: [https://doi.org/10.1016/0042-6822\(84\)90223-X](https://doi.org/10.1016/0042-6822(84)90223-X).
- Li, J., Zu Dohna, H., Cardona, C.J., Miller, J., and Carpenter, T.E. (2011). Emergence and genetic variation of neuraminidase stalk deletions in avian influenza viruses. *PLoS one* 6(2), e14722-e14722. doi: 10.1371/journal.pone.0014722.
- Li, Q., Qi, J., Zhang, W., Vavricka, C.J., Shi, Y., Wei, J., et al. (2010a). The 2009 pandemic H1N1 neuraminidase N1 lacks the 150-cavity in its active site. *Nature Structural & Molecular Biology* 17(10), 1266-1268. doi: 10.1038/nsmb.1909.
- Li, S., Shi, Z., Jiao, P., Zhang, G., Zhong, Z., Tian, W., et al. (2010b). Avian-origin H3N2 canine influenza A viruses in Southern China. *Infection, genetics and evolution : journal of molecular epidemiology and evolutionary genetics in infectious diseases* 10(8), 1286-1288. doi: 10.1016/j.meegid.2010.08.010.
- Lin, Y.P., Gregory, V., Collins, P., Kloess, J., Wharton, S., Cattle, N., et al. (2010). Neuraminidase Receptor Binding Variants of Human Influenza A(H3N2) Viruses Resulting from Substitution of Aspartic Acid 151 in the Catalytic Site: a Role in Virus Attachment? *Journal of Virology* 84(13), 6769. doi: 10.1128/JVI.00458-10.
- Lin, Y.P., Xiong, X., Wharton, S.A., Martin, S.R., Coombs, P.J., Vachieri, S.G., et al. (2012). Evolution of the receptor binding properties of the influenza A(H3N2) hemagglutinin. *Proceedings of the National Academy of Sciences* 109(52), 21474. doi: 10.1073/pnas.1218841110.
- Long, J.S., Benfield, C.T., and Barclay, W.S. (2015). One-way trip: Influenza virus' adaptation to gallinaceous poultry may limit its pandemic potential. *BioEssays* 37(2), 204-212. doi: 10.1002/bies.201400133.
- Malby, R.L., Tulip, W.R., Harley, V.R., McKimm-Breschkin, J.L., Laver, W.G., Webster, R.G., et al. (1994). The structure of a complex between the NC10 antibody and influenza virus neuraminidase and comparison with the overlapping binding site of the NC41 antibody. *Structure* 2(8), 733-746. doi: [https://doi.org/10.1016/S0969-2126\(00\)00074-5](https://doi.org/10.1016/S0969-2126(00)00074-5).
- Marjuki, H., Mishin, V.P., Chesnokov, A.P., De La Cruz, J.A., Davis, C.T., Villanueva, J.M., et al. (2015). Neuraminidase Mutations Conferring Resistance to Oseltamivir in Influenza A(H7N9) Viruses. *Journal of Virology* 89(10), 5419. doi: 10.1128/JVI.03513-14.
- Matrosovich, M., Matrosovich, T., Uhlenendorff, J., Garten, W., and Klenk, H.-D. (2007). Avian-virus-like receptor specificity of the hemagglutinin impedes influenza virus replication in cultures of human airway epithelium. *Virology* 361(2), 384-390. doi: <https://doi.org/10.1016/j.virol.2006.11.030>.
- Matrosovich, M., Tuzikov, A., Bovin, N., Gambaryan, A., Klimov, A., Castrucci, M.R., et al. (2000). Early Alterations of the Receptor-Binding Properties of H1, H2, and H3 Avian Influenza Virus Hemagglutinins after Their Introduction into Mammals. *Journal of Virology* 74(18), 8502. doi: 10.1128/JVI.74.18.8502-8512.2000.



- Matrosovich, M.N., Gambaryan, A.S., Teneberg, S., Piskarev, V.E., Yamnikova, S.S., Lvov, D.K., et al. (1997). Avian Influenza A Viruses Differ from Human Viruses by Recognition of Sialyloligosaccharides and Gangliosides and by a Higher Conservation of the HA Receptor-Binding Site. *Virology* 233(1), 224-234. doi: <https://doi.org/10.1006/viro.1997.8580>.
- Matrosovich, M.N., Krauss, S., and Webster, R.G. (2001a). H9N2 Influenza A Viruses from Poultry in Asia Have Human Virus-like Receptor Specificity. *Virology* 281(2), 156-162. doi: <https://doi.org/10.1006/viro.2000.0799>.
- Matrosovich, M.N., Krauss, S., and Webster, R.G. (2001b). H9N2 influenza A viruses from poultry in Asia have human virus-like receptor specificity. *Virology* 281(2), 156-162. doi: [10.1006/viro.2000.0799](https://doi.org/10.1006/viro.2000.0799).
- McAuley, J.L., Gilbertson, B.P., Trifkovic, S., Brown, L.E., and McKimm-Breschkin, J.L. (2019). Influenza Virus Neuraminidase Structure and Functions. *Frontiers in Microbiology* 10(39). doi: [10.3389/fmicb.2019.00039](https://doi.org/10.3389/fmicb.2019.00039).
- Medina, R.A., and García-Sastre, A. (2011). Influenza A viruses: new research developments. *Nature Reviews Microbiology* 9(8), 590-603. doi: [10.1038/nrmicro2613](https://doi.org/10.1038/nrmicro2613).
- Mena, I., Nelson, M.I., Quezada-Monroy, F., Dutta, J., Cortes-Fernández, R., Lara-Puente, J.H., et al. (2016). Origins of the 2009 H1N1 influenza pandemic in swine in Mexico. *eLife* 5, e16777. doi: [10.7554/eLife.16777](https://doi.org/10.7554/eLife.16777).
- Mögling, R., Richard, M.J., Vliet, S.v.d., Beek, R.v., Schrauwen, E.J.A., Spronken, M.I., et al. (2017). Neuraminidase-mediated haemagglutination of recent human influenza A(H3N2) viruses is determined by arginine 150 flanking the neuraminidase catalytic site. *Journal of General Virology* 98(6), 1274-1281. doi: <https://doi.org/10.1099/jgv.0.000809>.
- Munier, S., Larcher, T., Cormier-Aline, F., Soubieux, D., Su, B., Guigand, L., et al. (2010). A Genetically Engineered Waterfowl Influenza Virus with a Deletion in the Stalk of the Neuraminidase Has Increased Virulence for Chickens. *Journal of Virology* 84(2), 940. doi: [10.1128/JVI.01581-09](https://doi.org/10.1128/JVI.01581-09).
- Naguib, M.M., Arafa, A.S., Parvin, R., Beer, M., Vahlenkamp, T., and Harder, T.C. (2017). Insights into genetic diversity and biological propensities of potentially zoonotic avian influenza H9N2 viruses circulating in Egypt. *Virology* 511, 165-174. doi: [10.1016/j.virol.2017.08.028](https://doi.org/10.1016/j.virol.2017.08.028).
- Neumann, G., and Kawaoka, Y. (2015). Transmission of influenza A viruses. *Virology* 479-480, 234-246. doi: <https://doi.org/10.1016/j.virol.2015.03.009>.
- Nuss, J.M., and Air, G.M. (1991). Transfer of the hemagglutinin activity of influenza virus neuraminidase subtype N9 into an N2 neuraminidase background. *Virology* 183(2), 496-504. doi: [https://doi.org/10.1016/0042-6822\(91\)90979-L](https://doi.org/10.1016/0042-6822(91)90979-L).
- Palese, P., and Compans, R.W. (1976). Inhibition of Influenza Virus Replication in Tissue Culture by 2-deoxy-2,3-dehydro-N-trifluoroacetylneuraminic acid (FANA): Mechanism of Action. *Journal of General Virology* 33(1), 159-163. doi: <https://doi.org/10.1099/0022-1317-33-1-159>.
- Peng, W., de Vries, R.P., Grant, O.C., Thompson, A.J., McBride, R., Tsogtbaatar, B., et al. (2017). Recent H3N2 Viruses Have Evolved Specificity for Extended, Branched Human-type Receptors, Conferring Potential for Increased Avidity. *Cell host & microbe* 21(1), 23-34. doi: [10.1016/j.chom.2016.11.004](https://doi.org/10.1016/j.chom.2016.11.004).
- Rijal, P., Wang, B.B., Tan, T.K., Schimanski, L., Janesch, P., Dong, T., et al. (2020). Broadly Inhibiting Antineuraminidase Monoclonal Antibodies Induced by Trivalent Influenza Vaccine and H7N9 Infection in Humans. *Journal of Virology* 94(4), e01182-01119. doi: [10.1128/JVI.01182-19](https://doi.org/10.1128/JVI.01182-19).
- Rogers, G.N., and Paulson, J.C. (1983). Receptor determinants of human and animal influenza virus isolates: Differences in receptor specificity of the H3 hemagglutinin based on species of origin. *Virology* 127(2), 361-373. doi: [https://doi.org/10.1016/0042-6822\(83\)90150-2](https://doi.org/10.1016/0042-6822(83)90150-2).
- Rudino-Pinera, E., Tunnah, P., Crennell, S.J., Webster, R.G., Laver, W.G., and Garman, E.F. (2004). The Crystal Structure of Type a Influenza Virus Neuraminidase of the N6 Subtype Reveals the Existence of Two Separate Neu5Ac Binding Sites. doi: <https://www.rcsb.org/structure/1w20>.
- Russell, R.J., Haire, L.F., Stevens, D.J., Collins, P.J., Lin, Y.P., Blackburn, G.M., et al. (2006). The structure of H5N1 avian influenza neuraminidase suggests new opportunities for drug design. *Nature* 443(7107), 45-49. doi: [10.1038/nature05114](https://doi.org/10.1038/nature05114).

- Sakai, T., Nishimura, S.I., Naito, T., and Saito, M. (2017). Influenza A virus hemagglutinin and neuraminidase act as novel motile machinery. *Scientific Reports* 7(1), 45043. doi: 10.1038/srep45043.
- Shi, Y., Wu, Y., Zhang, W., Qi, J., and Gao, G.F. (2014). Enabling the 'host jump': structural determinants of receptor-binding specificity in influenza A viruses. *Nature Reviews Microbiology* 12(12), 822-831. doi: 10.1038/nrmicro3362.
- Shi, Y., Zhang, W., Wang, F., Qi, J., Wu, Y., Song, H., et al. (2013). Structures and Receptor Binding of Hemagglutinins from Human-Infecting H7N9 Influenza Viruses. *Science* 342(6155), 243. doi: 10.1126/science.1242917.
- Smith, D.J., Lapedes, A.S., de Jong, J.C., Bestebroer, T.M., Rimmelzwaan, G.F., Osterhaus, A.D.M.E., et al. (2004). Mapping the Antigenic and Genetic Evolution of Influenza Virus. *Science* 305(5682), 371. doi: 10.1126/science.1097211.
- Song, D., Kang, B., Lee, C., Jung, K., Ha, G., Kang, D., et al. (2008). Transmission of avian influenza virus (H3N2) to dogs. *Emerging infectious diseases* 14(5), 741-746. doi: 10.3201/eid1405.071471.
- Sun, X., Li, Q., Wu, Y., Wang, M., Liu, Y., Qi, J., et al. (2014). Structure of influenza virus N7: the last piece of the neuraminidase "jigsaw" puzzle. *J Virol* 88(16), 9197-9207. doi: 10.1128/JVI.00805-14.
- Sung, J.C., Van Wynsberghe, A.W., Amaro, R.E., Li, W.W., and McCammon, J.A. (2010). Role of secondary sialic acid binding sites in influenza N1 neuraminidase. *Journal of the American Chemical Society* 132(9), 2883-2885. doi: 10.1021/ja9073672.
- Taubenberger, J.K., and Kash, J.C. (2010). Influenza virus evolution, host adaptation, and pandemic formation. *Cell host & microbe* 7(6), 440-451. doi: 10.1016/j.chom.2010.05.009.
- Thobhani, S., Ember, B., Siriwardena, A., and Boons, G.-J. (2003). Multivalency and the Mode of Action of Bacterial Sialidases. *Journal of the American Chemical Society* 125(24), 7154-7155. doi: 10.1021/ja029759w.
- Thompson, A.J., de Vries, R.P., and Paulson, J.C. (2019). Virus recognition of glycan receptors. *Current opinion in virology* 34, 117-129. doi: 10.1016/j.coviro.2019.01.004.
- Tombari, W., Nsiri, J., Larbi, I., Guerin, J.L., and Ghram, A. (2011). Genetic evolution of low pathogenicity H9N2 avian influenza viruses in Tunisia: acquisition of new mutations. *Virology journal* 8, 467-467. doi: 10.1186/1743-422X-8-467.
- Tulip, W.R., Varghese, J.N., Laver, W.G., Webster, R.G., and Colman, P.M. (1992). Refined crystal structure of the influenza virus N9 neuraminidase-NC41 Fab complex. *Journal of Molecular Biology* 227(1), 122-148. doi: [https://doi.org/10.1016/0022-2836\(92\)90687-F](https://doi.org/10.1016/0022-2836(92)90687-F).
- Uhlendorff, J., Matrosovich, T., Klenk, H.D., and Matrosovich, M. (2009). Functional significance of the hemadsorption activity of influenza virus neuraminidase and its alteration in pandemic viruses. *Arch Virol* 154(6), 945-957. doi: 10.1007/s00705-009-0393-x.
- Vahey, M.D., and Fletcher, D.A. (2019). Influenza A virus surface proteins are organized to help penetrate host mucus. *eLife* 8, e43764. doi: 10.7554/eLife.43764.
- Varghese, J.N., Colman, P.M., van Donkelaar, A., Blick, T.J., Sahasrabudhe, A., and McKimm-Breschkin, J.L. (1997). Structural evidence for a second sialic acid binding site in avian influenza virus neuraminidases. *Proceedings of the National Academy of Sciences of the United States of America* 94(22), 11808-11812. doi: 10.1073/pnas.94.22.11808.
- Varghese, J.N., Laver, W.G., and Colman, P.M. (1983). Structure of the influenza virus glycoprotein antigen neuraminidase at 2.9 Å resolution. *Nature* 303(5912), 35-40. doi: 10.1038/303035a0.
- Vavricka, C.J., Liu, Y., Kiyota, H., Sriwilaijaroen, N., Qi, J., Tanaka, K., et al. (2013). Influenza neuraminidase operates via a nucleophilic mechanism and can be targeted by covalent inhibitors. *Nature Communications* 4(1), 1491. doi: 10.1038/ncomms2487.
- Wagner, R., Matrosovich, M., and Klenk, H.-D. (2002). Functional balance between haemagglutinin and neuraminidase in influenza virus infections. *Reviews in Medical Virology* 12(3), 159-166. doi: 10.1002/rmv.352.

- Walther, T., Karamanska, R., Chan, R.W.Y., Chan, M.C.W., Jia, N., Air, G., et al. (2013). Glycomic Analysis of Human Respiratory Tract Tissues and Correlation with Influenza Virus Infection. *PLOS Pathogens* 9(3), e1003223. doi: 10.1371/journal.ppat.1003223.
- Webster, R.G., Air, G.M., Metzger, D.W., Colman, P.M., Varghese, J.N., Baker, A.T., et al. (1987). Antigenic structure and variation in an influenza virus N9 neuraminidase. *Journal of virology* 61(9), 2910-2916.
- Webster, R.G., Bean, W.J., Gorman, O.T., Chambers, T.M., and Kawaoka, Y. (1992). Evolution and ecology of influenza A viruses. *Microbiological reviews* 56(1), 152-179.
- Wen, F., Blackmon, S., Olivier, A.K., Li, L., Guan, M., Sun, H., et al. (2018). Mutation W222L at the Receptor Binding Site of Hemagglutinin Could Facilitate Viral Adaption from Equine Influenza A(H3N8) Virus to Dogs. *Journal of virology* 92(18), e01115-01118. doi: 10.1128/JVI.01115-18.
- Xu, X., Zhu, X., Dwek, R.A., Stevens, J., and Wilson, I.A. (2008). Structural Characterization of the 1918 Influenza Virus H1N1 Neuraminidase. *Journal of Virology* 82(21), 10493. doi: 10.1128/JVI.00959-08.
- Yang, G., Li, S., Blackmon, S., Ye, J., Bradley, K.C., Cooley, J., et al. (2013). Mutation tryptophan to leucine at position 222 of haemagglutinin could facilitate H3N2 influenza A virus infection in dogs. *The Journal of general virology* 94(Pt 12), 2599-2608. doi: 10.1099/vir.0.054692-0.
- Zhou, H., Yu, Z., Hu, Y., Tu, J., Zou, W., Peng, Y., et al. (2009). The Special Neuraminidase Stalk-Motif Responsible for Increased Virulence and Pathogenesis of H5N1 Influenza A Virus. *PLOS ONE* 4(7), e6277. doi: 10.1371/journal.pone.0006277.



## **Summary in English**

---

In **chapter 1**, an introduction to influenza A viruses (IAVs) is provided with particular attention to the hemagglutinin (HA) and neuraminidase (NA) proteins. IAVs infect a broad range of species including humans, wild birds, poultry, pigs, horses, dogs, and marine mammals. Aquatic birds are the natural reservoir of IAVs, in which infection is normally asymptomatic. Occasionally IAVs breach the species barrier to infect humans, which may result in a pandemic. Once established in the human population, IAVs cause seasonal epidemics. Both pandemics and seasonal epidemics pose a huge health and economic burden.

IAV particles contain two major glycoproteins: HA and NA. Until now sixteen HA and nine NA subtypes have been identified, all of which exist in aquatic birds. HA is responsible for binding to sialic acid (SIA) receptors present on glycoproteins and glycolipids. The linkage type of the SIA to the penultimate galactose is an important determinant of host specificity. Avian viruses prefer binding to  $\alpha$ 2,3-linked SIA, while the human viruses preferentially bind to  $\alpha$ 2,6-linked SIA. NA is a receptor-destroying enzyme and cleaves SIAs from sialoglycans, thereby preventing virion aggregation and facilitating release of (newly assembled) virions from cell surfaces as well as decoy receptors abundantly present in mucus. The balance between HA and NA is important for virus replication and transmission and needs to be adjusted to the sialoglycan repertoire of a specific host. NA carries, in addition to a highly conserved catalytic site, a second SIA binding site (2SBS) which is generally conserved in avian, but not in human, IAVs. In this thesis, we studied the importance of the 2SBS on NA enzymatic activity, HA-NA balance and virus replication.

In **chapter 2**, we analyzed the enzymatic activities of N1 derived from avian H5N1 and human H1N1 IAVs and analyzed the role of the 2SBS therein. All N1 proteins preferred cleavage of  $\alpha$ 2,3- over  $\alpha$ 2,6-linked SIAs even when their corresponding HA proteins displayed a strict preference for  $\alpha$ 2,6-linked SIAs, suggesting that the specificity of the NAs does not need to fully match that of the corresponding HAs. We furthermore showed that substitutions in the 2SBS affected NA activity against multivalent substrates, while cleavage of monovalent substrate was much less affected. These mutations included both SIA-contact and non-SIA-contact residues in all three loops of the 2SBS. In addition, mutation of the 2SBS was shown to affect virus replication *in vitro* when combined with HA of the lab strain PR8. When combined with HA of H5N1 virus, the mutated residue in the 2SBS rapidly reverted to restore a functional 2SBS. The results indicate that substrate binding via the 2SBS contributes to enhanced N1 catalytic activity and is important for virus replication.

In **chapter 3**, we investigated the receptor-binding specificity of the 2SBS of N2 and the role of this site in the HA-NA balance of virions. Avian-like N2, with a functional 2SBS, was more active than human N2, carrying a mutated 2SBS, on multivalent substrates containing  $\alpha$ 2,3-linked SIAs, corresponding with the binding-specificity of avian-like N2 for these receptors. Replacing the N2 of human viruses by an avian-like N2 resulted in decreased replication. When combined with avian-like HA, the avian-like N2 protein enhanced virus replication compared to the human N2 protein. We also found that the presence of a functional 2SBS affected virion-receptor binding and subsequent NA-dependent self-elution. The contribution of the 2SBS to virus-receptor interactions depended, in addition to its own receptor specificity, on the receptor-binding specificity of its accompanying HA. Based on these observations, we conclude that the 2SBS is a significant determinant of the HA-NA-receptor balance of virus particles.

In **chapter 4**, we show that mutations in the 2SBS of N1 can drive the selection of mutations in H5 that affect its receptor-binding properties. Mutation of the 2SBS of an avian H5N1 virus was shown to disturb the HA-NA balance and to negatively affect virus replication. Passaging of this 2SBS-negative H5N1 virus in cell culture selected for progeny with a restored HA-NA balance. These viruses obtained mutations in NA that restored a functional 2SBS and/or in HA that reduced binding of avian-type receptors. One specific HA mutation also increased binding of human-type receptors. Phylogenetic analyses of avian H9N2 IAVs shows that mutations in the 2SBS preceded mutations in HA that reduce binding to avian-type receptors and increase binding of human-type receptors. This order of events implies that mutations in the 2SBS of NA potentially can drive acquisition of mutations in HA that in addition to restoring the HA-NA balance confer increased binding to human type receptors, imposing increased zoonotic potential on such viruses.

In **chapter 5**, we studied the effects of NA mutations that became fixed in the virus population after the introduction of the pandemic IAV H1N1 in 2009 (H1N1pdm09) in humans. Phylogenetic analysis identified sixteen mutations that became fixed in the NA of H1N1pdm09 until 2015. Some mutations had multiple phenotypic effects on NA, including catalytic activity and antigenicity. NA activity fluctuated over time instead of having evolved to an optimal level. Substitution K432E in the 2SBS affected NA substrate specificity and the pH optimum for maximum activity but also antigenicity. Thus, selection of this mutation might have been driven by escape from the host immune response. We propose that the entanglement of enzymatic and antigenic NA phenotypes, is one determining factor in the evolution of NA.

After a short **interlude** on tuning of the IAV HA-NA balance by mutations in HA and/or NA, the importance of the HA-NA balance for virion mobility is discussed in **chapter 6**. Finally, in **chapter 7** the results and insights obtained within this thesis on the 2SBS are discussed and placed in the context of a complete overview of the literature on the 2SBS of IAV NA.





## **Nederlandse samenvatting**

---

In **hoofdstuk 1** wordt een inleiding tot influenza A virussen (IAV's) gegeven, waarin met name aandacht wordt gegeven aan de hemagglutinine (HA) en neuraminidase (NA) eiwitten. IAV's infecteren een breed scala aan soorten, waaronder mensen, wilde vogels, pluimvee, varkens, paarden, honden en zeezoogdieren. Watervogels zijn het natuurlijke reservoir van IAV's, waarin infectie normaal gesproken asymptomatisch is. Af en toe doorbreken IAV's de soortbarrière en infecteren mensen, wat kan leiden tot een pandemie. Eenmaal gevestigd in de menselijke populatie, veroorzaken IAV's seizoensgebonden epidemieën. Zowel pandemieën als seizoensgebonden epidemieën vormen een enorme last voor de gezondheidszorg en de economische.

IAV deeltjes bevatten twee belangrijke glycoproteïnen: HA en NA. Tot nu toe zijn zestien HA en negen NA subtypes geïdentificeerd, die allemaal voorkomen bij watervogels. HA is verantwoordelijk voor binding aan sialzuur (SIA) receptoren die aanwezig zijn op glycoproteïnen en glycolipiden. Het type koppeling van SIA aan de voorlaatste galactose is een belangrijke determinant van de gastheerspecificiteit van IAVs. Aviaire virussen geven de voorkeur aan binding aan  $\alpha 2,3$ -gebonden SIA, terwijl de menselijke virussen bij voorkeur binden aan  $\alpha 2,6$ -gebonden SIA. NA is een receptorvernietigend enzym en splitst SIA's van sialoglycanen, waardoor aggregatie van virionen wordt voorkomen en het vrijkomen van (nieuw gevormde) virionen van het celoppervlak en van SIA receptoren, die overvloedig aanwezig zijn in slijm, wordt mogelijk gemaakt. De balans tussen HA en NA is belangrijk voor virusrePLICATIE en overdracht en moet worden aangepast aan het sialoglycaan-repertoire van een specifieke host. NA heeft, naast een sterk geconserveerde katalytische plek, een tweede SIA bindingsplaats (2SBP) die over het algemeen geconserveerd is in aviaire, maar niet in menselijke, IAV's. In dit proefschrift hebben we het belang bestudeerd van de 2SBP op de NA enzymatische activiteit, HA-NA balans en virusrePLICATIE.

In **hoofdstuk 2** analyseerden we de enzymatische activiteiten van N1 eiwitten van aviaire H5N1 en menselijke H1N1 virussen en analyseerden we de rol van de 2SBP daarin. Alle N1 eiwitten gaven de voorkeur aan splitsing van  $\alpha 2,3$ - boven  $\alpha 2,6$ -gekoppelde SIA's, zelfs wanneer hun overeenkomstige HA eiwitten een strikte voorkeur vertoonden voor  $\alpha 2,6$  gekoppelde SIA's, wat suggereert dat de specificiteit van de NA's niet volledig hoeft overeen te komen met die van de bijbehorende HA's. We toonden verder aan dat substituties in de 2SBP van invloed is op de NA-activiteit tegen multivalente substraten, terwijl splitsing van monovalent substraat veel minder werd beïnvloed. Deze mutaties omvatten zowel SIA-contactresiduen als niet-SIA-contactresiduen in alle drie de lussen van de 2SBP. Bovendien bleek mutatie van de 2SBP de virusrePLICATIE in vitro te beïnvloeden in combinatie met HA van de laboratoriumstam PR8. In combinatie met HA van het H5N1-virus veranderde het gemuteerde residu in de 2SBP snel om daarbij een functionele 2SBP te herstellen. De resultaten geven aan dat substraatbinding via de 2SBP bijdraagt aan verhoogde N1-katalytische activiteit en belangrijk is voor virusrePLICATIE.

In **hoofdstuk 3** hebben we de receptorbindende specificiteit van de 2SBP van N2 en de rol van de 2SBP in de HA-NA-balans van virions onderzocht. N2, dat lijkt op N2 van aviaire virussen en een functionele 2SBP heeft, was actiever dan humaan N2, met een gemuteerde 2SBP, op multivalente substraten die  $\alpha 2,3$ -gebonden SIA's bevatten, wat overeenkomt met de bindingspecificiteit van dit N2 voor deze receptoren. Het vervangen van 2BSP-negatief N2 door een 2BSP-positief N2 verminderde virusrePLICATIE wanneer N2 gecombineerd werd met HA uit een menselijk virus. In combinatie met HA dat een vergelijkbare receptorbinding vertoont als HA uit vogelvirussen, had de aanwezigheid van een functionele 2BSP juist een positief effect op virusrePLICATIE. We ontdekten ook dat de aanwezigheid

van een functionele 2SBP de virion-receptorbinding en daaropvolgende NA-afhankelijke elutie beïnvloedde. De bijdrage van de 2SBP aan virus-receptor-interacties hing, naast zijn eigen receptorspecificiteit, af van de receptorbindende specificiteit van HA. Op basis van deze waarnemingen concluderen we dat de 2SBP een significante determinant is van de HA-NA-receptorbalans van virusdeeltjes.

In **hoofdstuk 4** laten we zien dat mutaties in de 2SBP van N1 tot de selectie van mutaties in H5 kunnen leiden die de receptorbindende eigenschappen van HA beïnvloeden. Mutatie van de 2SBP van een vogel H5N1 virus bleek het HA-NA balans te verstoren en de virusreproductie negatief te beïnvloeden. Passeren van dit 2SBP-negatieve H5N1-virus in celweek selecteerde voor nageslacht met een herstelde HA-NA balans. Deze virussen verkregen mutaties in NA die een functionele 2SBP herstelden en/of in HA die de binding van aviaire ( $\alpha$ 2,3-gekoppelde SIA) receptoren verminderden. Een specifieke HA-mutatie leidde tegelijkertijd ook tot meer binding van humane ( $\alpha$ 2,6-gekoppelde SIA) receptoren. Fylogenetische analyses van aviaire H9N2 IAV's laten zien dat mutaties in de 2SBP voorafgegaan zijn aan mutaties in HA die de binding aan aviaire receptoren verminderen en de binding van humane receptoren verhogen. Deze volgorde impliceert dat mutaties in de 2SBP van NA mogelijk de selectie van mutaties in HA kunnen stimuleren die, naast het herstellen van de HA-NA balans, tot een verhoogde binding aan humane receptoren leiden, waardoor dergelijke virussen een verhoogd zoönotisch potentieel hebben.

In **hoofdstuk 5** hebben we de effecten bestudeerd van NA-mutaties die in de viruspopulatie zijn gevonden na de introductie van de pandemische H1N1 IAV in 2009 (H1N1pdm09) in de humane populatie. Fylogenetische analyse leidde tot de identificatie van zestien mutaties die tot 2015 gefixeerd werden in NA van H1N1pdm09. Sommige mutaties hadden meerdere fenotypische effecten op NA, waaronder veranderingen in katalytische activiteit en antigeniciteit. NA-activiteit fluctueerde in de tijd in plaats van een bepaald optimaal niveau te bereiken. Substitutie K432E in de 2SBP beïnvloedde NA-substraatspecificiteit en het pH-optimum voor maximale activiteit maar ook de antigeniciteit. De selectie van deze mutatie kan dus zijn geselecteerd zijn doordat het leidde tot ontsnapping aan de immuunrespons van de gastheer. We stellen voor dat de verstrengeling van enzymatische en antigene NA-fenotypen een bepalende factor is in de evolutie van NA.

Na een kort **intermezzo** over afstemming van de IAV HA-NA balans door mutaties in HA en/of NA, wordt het belang van de HA-NA balans voor virion mobiliteit besproken in **hoofdstuk 6**. Ten slotte, worden in **hoofdstuk 7** de resultaten en inzichten verkregen binnen dit proefschrift over de 2SBP besproken en geplaatst in de context van een volledig overzicht van de literatuur over de 2SBP van IAV NA.



**Miscellaneous**

**Acknowledgements**

**Curriculum Vitae**

**List of publications**

---

## Acknowledgements

The four-year research journey as a PhD candidate in the Virology section of Utrecht University is an amazing and unforgettable experience. Without the help and support from many people along the way who deserve my thanks, I could not have made this thesis possible.

First of all, I would like to express my deep gratitude to my promoter, **Frank van Kuppeveld**, who gave me the chance to pursue my PhD in the Netherlands. I still remember how excited I was when you replied to my email in January 2016 saying that we could have an interview. Your attitude and passion for science inspired me a lot. Thank you very much for your input on our papers and my thesis; I have benefited a lot from your comments and corrections. Thanks a lot for your supervision and support. All my best wishes to you.

My sincere appreciation goes to my co-promoters and daily supervisors, **Xander de Haan** and **Erik de Vries**. I cannot imagine what my PhD life would have been like without your help. You are the most responsible supervisors I have met and working with you has been one of the luckiest things in my life. Before I started my PhD, I did not know what to expect. However, what I have achieved from my PhD is far beyond any initial expectations. This is all due to the help and support from you both. Dear **Xander**, your incredible enthusiasm and dedication to research impresses me. You are really a great role model for my research career. When things did not go to plan, you were always there to help me and to manage to reach new points, thus taking the project further. Every time I sent an email to you, you always responded as soon as possible, which made the communication much more efficient. You have enormous energy towards science. You have taught me how to analyze experimental data, how to present data and how to write scientifically. I really appreciate all of your great ideas, knowledge and patience during my PhD. You helped me a lot not only in science but also in my daily life. I was really moved when you picked me up at Schiphol airport at 10:30 pm. Thank you very much for everything you have done for me and all the best wishes for your career and family. Dear **Erik**, your great sense of humor made my whole PhD life anything but boring! You always made complicated data easier to understand and had creative ideas for the explanation of the data. I really appreciate all of your useful suggestions and kind help which made a huge difference to my PhD. Thanks a lot and I wish you a pleasant life and good health in the future.

Of course, many thanks should also go to other supervisors who gave me constructive suggestions during the Monday Morning meetings. **Berend Jan**, thank you for giving me the opportunity to do a post-doctoral position, which is a perfect connection to my PhD. **Raoul**, thanks for teaching me how to ice skate which was an exciting experience. **Herman**, thanks for providing blood for my hemagglutination assays.

During the last four years, I received enormous support and help from my friends and colleagues. **Hongbo**, thanks a lot for your company. You taught me practical skills in the lab. Every time after the work discussions, I always went to you if I had questions and you explained everything to me clearly. Thanks for your patience, time and advice. All the best wishes to you and little Junde. **Meiling**, thanks for teaching me practical skills in the lab. We also went shopping together, which was an unforgettable experience. Your contagious laugh and optimistic attitude for life encouraged me. All my best wishes to you and little Aila. **Wentao**, you are an elder brother to most of us in the lab. Thank you very much for everything you have done for me. I still remember the first day I arrived in

the Netherlands, you cooked soup for me and you showed me how to grocery shop here. You are always the first one I want to ask for help not only in daily life but also in science. You are so warm-hearted and willing to help which made such a difference to my whole PhD life. I really enjoyed discussing and sharing opinions with you. All my best wishes for your future research career and I believe you will be a great scientist in the future.

I also want to thank all our collaborators, **Mikhail Matrosovich, Ben Peeters, Margreet Wolfert, Geert-Jan Boons, Carles Martínez-Romero, Guus Rimmelzwaan, Ron Fouchier** and **Adolfo García-Sastre**, who provided us useful materials, performed wonderful experiments and gave us constructive suggestions. Thank you very much for your input to this thesis.

**Arno and Nancy**, thank you very much for your help. Without technical support, my work in the lab would have been much less efficient. Thanks for organizing the Christmas Dinner every year which were some of my most unforgettable memories that I have from living in the Netherlands.

**Erhard**, thanks for bringing the Nanoparticle Tracking Analysis (NTA) machine to our lab which plays an important role in my publications. **Malte**, I am grateful for all the help you provided for my experiments and of course the amazing cakes you made.

**Vera, Joline, Julia, Davide, Francien**, the hard-working bachelor and master students. Thanks a lot for your excellent work during your internships. I learnt a lot about the Dutch, Spanish and Italian cultures from you guys which was really interesting. **Joline**, I really appreciate your company during my PhD. Every time I needed help for my experiment, you were always glad to do that. All my best wishes for your future. **Davide**, thanks for your nice Italian snacks. **Francien**, thank you very much for giving me the present to celebrate the submission of my thesis. You are always so sweet and kind. I wish all of you a bright future and pleasant life.

**Erion and Maryam**, two of the most elegant and beautiful ladies in the lab. **Erion**, you are always willing to help me when I needed it. I enjoyed talking and sharing my opinions with you. You are so nice and sweet. I also enjoyed the amazing Korean food you made. Thanks very much for your support and help. I wish that you have your PhD defense soon. **Maryam**, my lovely officemate who provided me different kinds of snacks and helped me to settle down in the office.

I would like to thank all my officemates, **Floor, Hongbo, Joline, Liane, Vera, Mengying, Louisa and Jipke**. **Floor**, thanks for teaching me practical skills in the lab. **Liane**, it was a really nice experience to have you as my officemate. **Mengying**, you are an optimistic and a hard-working girl. I enjoyed every talk we had. It was a lot of fun to go shopping with you. I wish you get your PhD with huge success and many publications. **Louisa**, you are a highly organized girl with blue hair. It's joyful to talk and share experience with you. All my best wishes for your future.

**Yongtao**, thanks for your companionship and the fun you brought to me in the fourth year of my PhD. I appreciate that you organized the running group. The regular running every week is a good balance for me between life and work. You are also the delivery man who helped me to deliver the food from the Chinese shops. I wish that you also have many unforgettable memories in the Netherlands. **Chunyan**, I feel so lucky that we were colleagues during my PhD. We have known each other since our Bachelor course. It's a really long-lasting friendship from which I have benefited a lot. I still remember when you and your husband helped me to move my heavy luggage in the train station.

Not only for that, I really appreciate the amazing delicious Chinese food you have made. One of the happiest moments I have during my PhD is when I was enjoying the Chinese food you prepared. Thank you very much for your support and help. All my best wishes for your bright future. I wish you and Peifa (培发) a happy and pleasant life forever. **Tengfeng**, thanks for the tasty Chinese food you prepared. I wish you a happy life in Germany.

I would like to thank all my colleagues in the Virology section, **Ruben, Huib, Linda, Lisa, Ivy, Yifei, Shan, Anja Irina, Mirte, Tabitha, Martijn, Ieva, Chiara, Dan, Susanne, Brenda, Hendrik, Hilde, Jim, Fiona, Esther, Jeroen, Floor, Clasien, Yongle, Xinyi, Xiaoyao and Tony**. It was great working together with you, sharing ideas, and helping each other. **Linda and Floor**, thanks for organizing the Sinterklaas activities.

I want to sincerely thank the **China Scholarship Council (CSC)**, who financially supported me and provided such a great chance to study abroad for four years.

Life in the Netherlands over the past four years would never have been so colorful and exciting without my dearest friends. Thanks for bringing me so many joyful moments and wonderful experiences. **练慈师姐**, 很感谢有你陪伴的这博士 3 年, 因为你的存在, 我这枯燥的博士生活也有了许多值得怀念的回忆, 你的贴心和付出让我很感动, 和你的每一次吐槽和谈心都是那么的愉悦和放松。希望师姐早日找到属于自己的幸福, 在国内的生活一切顺利。**吕博(庆康)**, 你是我在来荷兰之前第一个认识的 UU 的朋友, 在办签证的时候, 当时一有问题都会问你。在来到荷兰以后, 当生活和实验需要什么东西的时候, 也会在第一时间找你, 感谢一直以来你对我帮助和支持。希望你能尽快取得博士学位, 生活越来越好。**梁博(建)**, 在荷兰能遇到你这么靠谱的朋友是多么值得庆幸的事情, 虽说我们的实验楼离得比较远, 平时交流没那么多。但是每次开会时的交流都是那么开心。希望你能实验顺利, 发好的文章, 早日实现自己理想和抱负。**一飞和赵珊**, 感谢你们组织的一起去旅游的机会, 祝福你们越来越好, 一切顺利。**盛杰师姐和昭举师兄**, 谢谢你们请我到你家吃火锅, 还给了我们很有用的家具, 怀念一起在 **Bilthoven** 住的日子。祝你们的科研和生活一切顺利。**欣悦**, 感谢你当时组织去你家聚餐, 让我认识了好多有意思的人。希望你能顺利拿到博士学位, 生活越来越好。**丁云**, 感谢你当时提供给我的免费车票, 祝贺你文章发表, 相信你的未来一定是一片光明。**文涛师兄, 建森师兄, 媛媛, 舒斐**, 有幸成为你们的室友, 谢谢你们平时对我的照顾和关心。**钟蔚, 静涵**, 谢谢你们美味的中餐, 祝你们越来越幸福。**小刚**, 每次和你的聊天都很愉快, 祝贺你文章的发表, 相信你一定会会有一个美好的未来。同样要感谢我在荷兰的其它好朋友, **徐阳, 谢媛, 张敏, 文静, 韦宣, Wewei, 霜霜师姐, 陈娜师姐**, 谢谢你们的陪伴, 祝你们一切顺利, 心想事成。

感谢在国内一直关心我的好朋友, **丹姐, 芳芳, 冬杰师姐, 王迪师兄, 王林柏, 大鹏, 阿奎, 孙雪**, 谢谢你们在我回国后对我的照顾, 你们一直是我坚强的后盾, 祝福你们越来越好。期待在国内与你们的重逢。

感谢我尊敬的硕士生导师, **刘长明** 研究员, 谢谢您在我硕士期间对我的指导和关心, 感谢您对我出国求学的大力支持和帮助。感谢 **危艳武** 老师, **黄立平** 师姐, **王一平** 师兄, **吴姐** 以及其它各位老师和师兄师姐师弟师妹们对我的照顾和鼓励。

感谢我最爱的爸爸妈妈, 哥哥嫂嫂们, 你们对我的爱让我感到无比的幸福。谢谢你们无私的支持和包容, 我爱你们, 希望你们永远开心快乐。感谢王先生的爱, 包容和支持。



## Curriculum Vitae

Wenjuan Du (杜文娟) was born on 10<sup>th</sup> September 1988 in Heze, Shandong Province, China. She grew up and attended primary, middle and high school in her hometown. In the fall of 2009, she was enrolled in the bachelor program of Veterinary Medicine at Shandong Agricultural University, China. In 2013, she started her master study at the Graduate School of Chinese Academy of Agricultural Sciences (CAAS), Beijing, China. One year later, she moved to Harbin to formally start her master research training at Harbin Veterinary Research Institute, CAAS, under the supervision of Prof. dr. Changming Liu. During her master, she mainly focused on the “Construction and immunogenicity of a recombinant pseudorabies virus expressing cap protein of porcine circovirus type 2”. In 2016, she got funding from China Scholarship Council, then she started her PhD at the department of Biomolecular Health Sciences, Utrecht University, the Netherlands. Under the supervision of Prof. Dr. Frank van Kuppeveld, Dr. Xander de Haan and Dr. Erik de Vries, she studied the role of the 2<sup>nd</sup> SIA-binding site of NA in the HA-NA balance of influenza a virus.

## List of publications

1. **Du W**, Wolfert M, Peeters B, van Kuppeveld F, Boons G, de Vries E, de Haan C. (2020) Mutation of the second sialic acid-binding site of influenza A virus neuraminidase drives compensatory mutations in hemagglutinin. *Plos Pathog.* e1008816.
2. de Vries E, **Du W**, Guo H, de Haan C. (2020) Influenza A Virus hemagglutinin–neuraminidase–receptor balance: preserving virus motility. *Trends in Microbiology.* 28(1):57-67.
3. Dai M, **Du W**, Martínez-Romero C, Leenders T, Wennekes T, Rimmelzwaan GF, van Kuppeveld F, Fouchier R, Garcia-Sastre A, de Vries E, de Haan C. (2020) Analysis of pandemic influenza A (H1N1) virus neuraminidase evolution reveals entanglement of different phenotypic characteristics. (Submitted).
4. **Du W**, Guo H, Nijman V, Doedt J, de Vries E, van der Lee J, Li Z, Boons G, van Kuppeveld F, de Vries E, Matrosovich M, de Haan C. (2019) The 2nd sialic acid-binding site of influenza A Virus neuraminidase is an important determinant of the hemagglutinin-neuraminidase-receptor balance. *Plos Pathog.* e1007860.
5. Lu W, **Du W**, Somovilla V, Yu G, Haksar D, de Vries E, Boons G, de Vries R, de Haan C, Pieters R. (2019) Enhanced inhibition of influenza A virus adhesion by di- and trivalent hemagglutinin inhibitors. *J Med Chem.* 62 (13), 6398-6404.
6. **Du W**, Dai M, Li Z, Boons G, Peeters B, van Kuppeveld F, de Vries E, de Haan C. (2018) Substrate binding by the second sialic acid-binding site of influenza A virus N1 neuraminidase contributes to enzymatic activity. *J Virol.* 92(20): e01243-18.
7. **Du W**, Wang Y, Huang L, Wei Y, Chen D, Sun J, Wu H, Feng L, Liu C. (2015) Characterization of monoclonal antibodies that recognize the amino- and carboxy-terminal epitopes of the pseudorabies virus UL42 protein. *Appl Microbiol Biotechnol.* 100(1):181-192